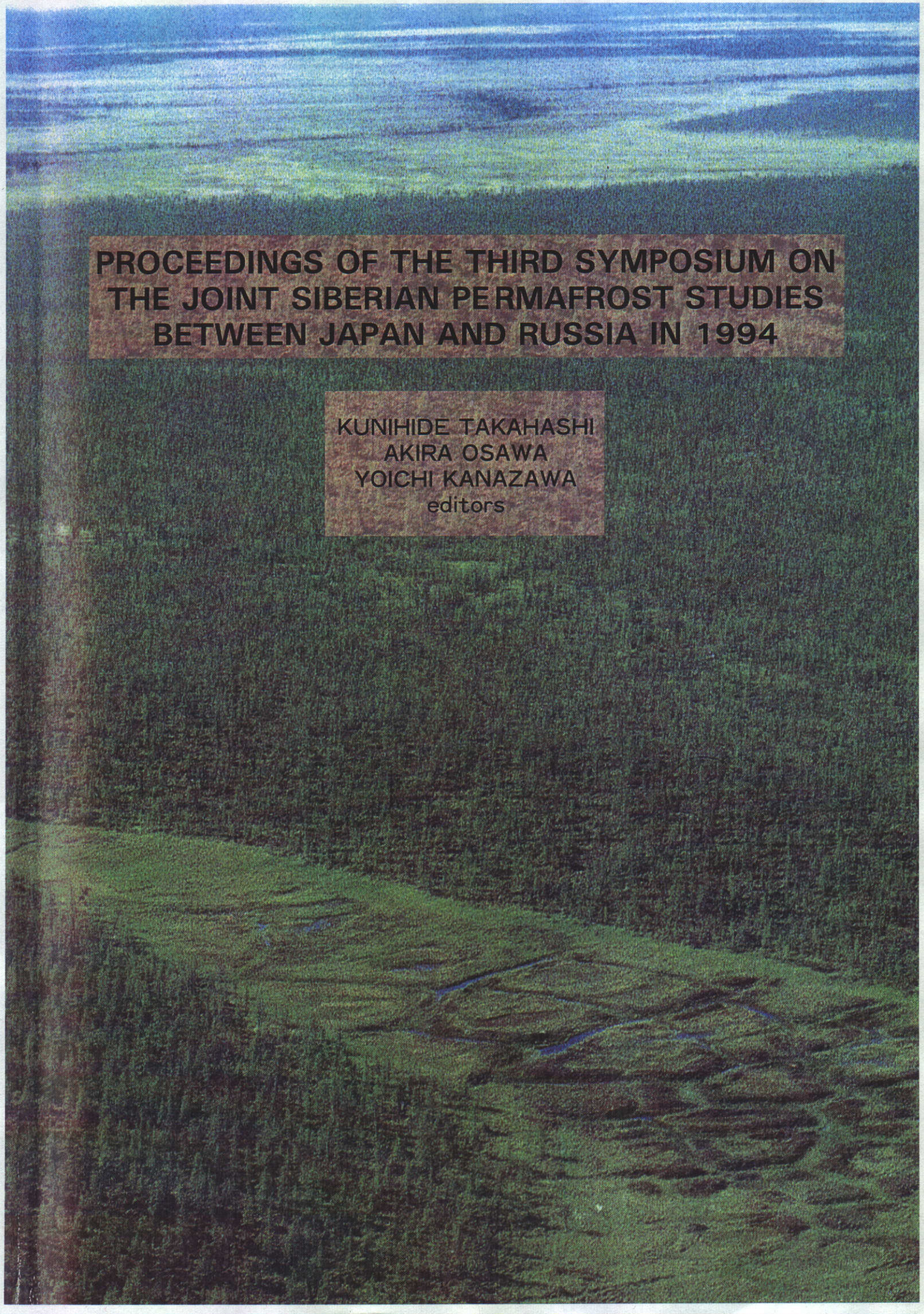

PROCEEDINGS OF THE THIRD SYMPOSIUM ON THE JOINT SIBERIAN PERMAFROST STUDIES BETWEEN JAPAN AND RUSSIA IN 1994

KUNIHIDE TAKAHASHI
AKIRA OSAWA
YOICHI KANAZAWA
editors

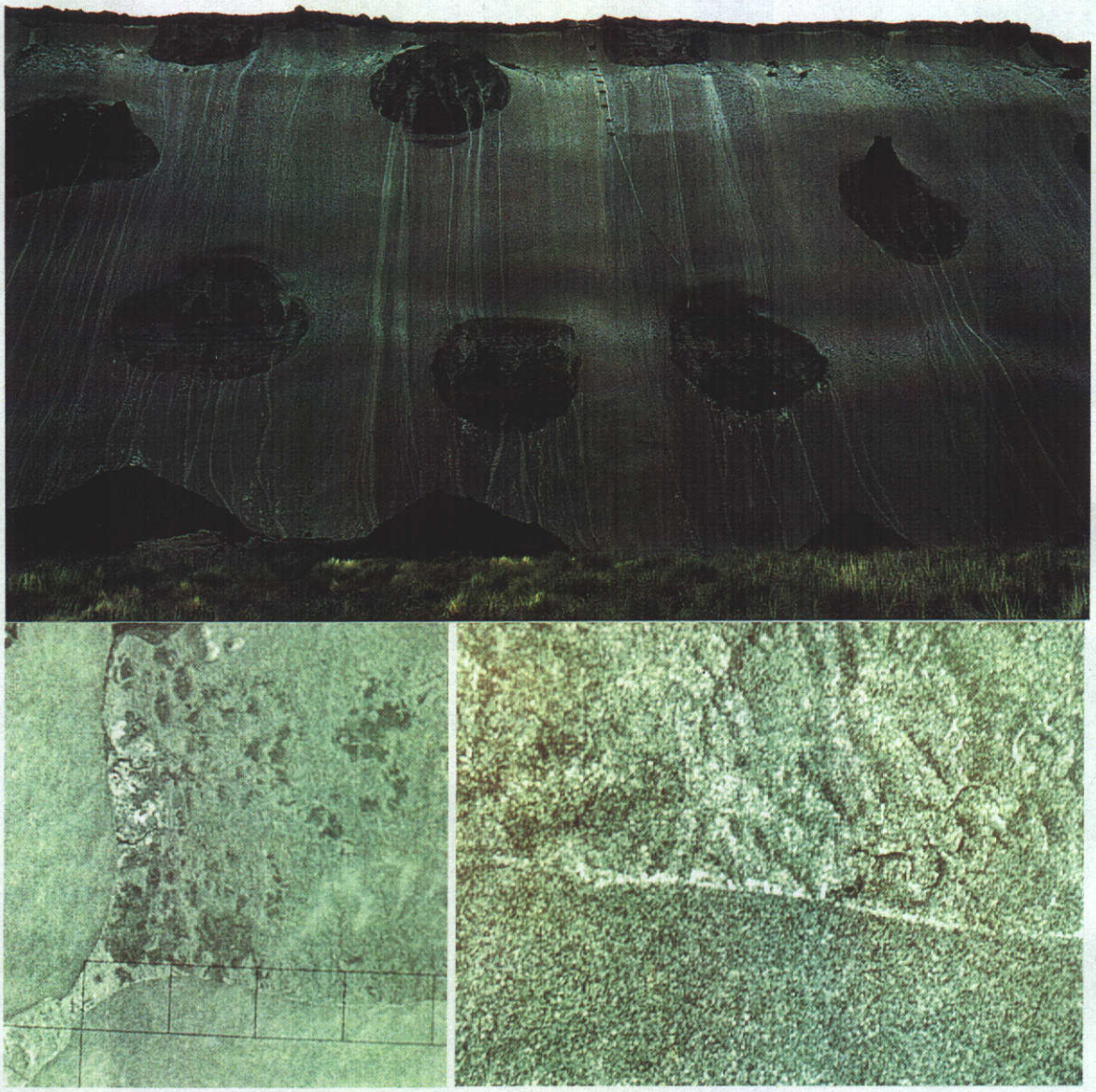

Counter clockwise from top of the page; Typical exposure of Edoma at Oiyagoskii Yar in eastern Siberia; Two shots of SAR Satellite images at Big Lhyavosky Island in eastern Siberia (NOAA), where Edoma exposures can be seen as white lines along the shore.

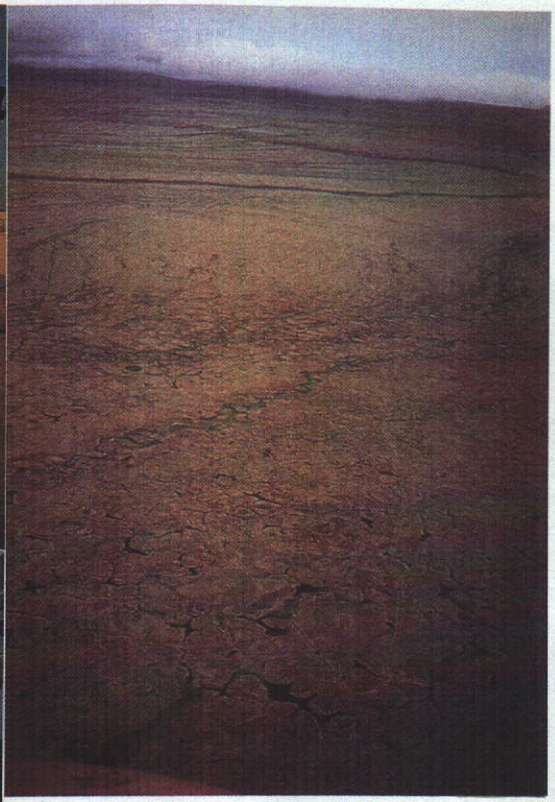

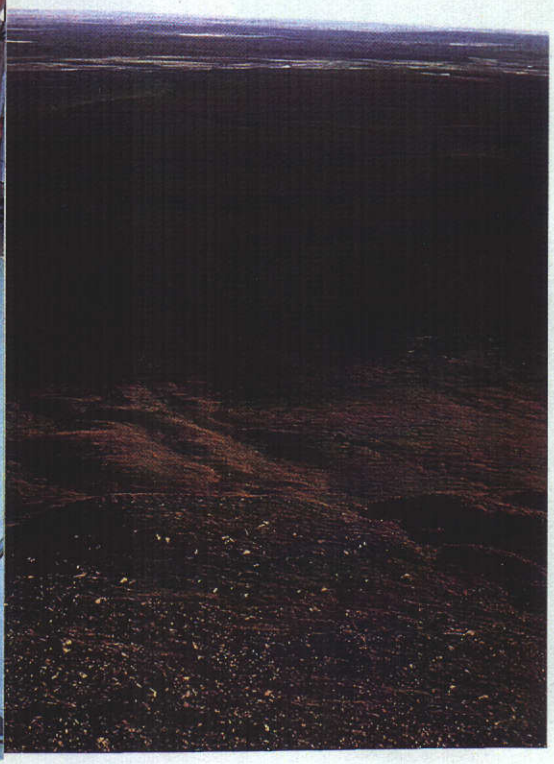

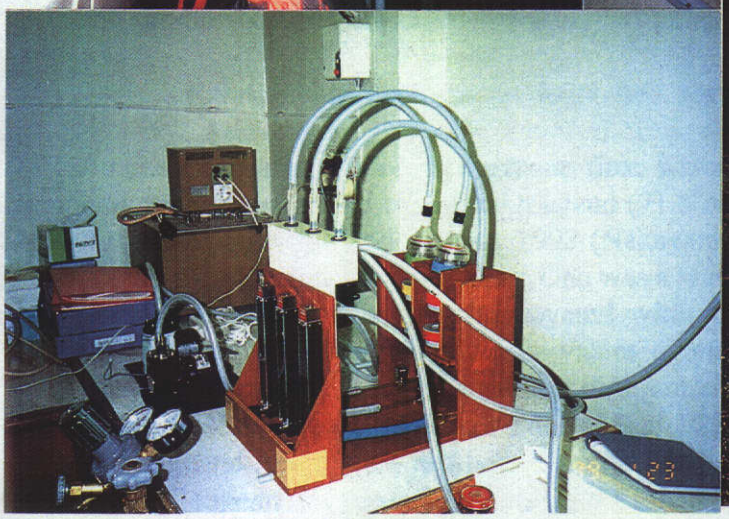

Counter clockwise from top left corner; Aircraft Dornier 228 used by Yazawa et al. for measurement of CO_2 and testing of an altrasonic anemometer; Instruments and scientists on board Dornier 228; Gass aerosol sampling set-up for measurements of atmospheric pollutants in Yakutsk by Ohta et al.; Airborn measurement of methane and CO_2 was conducted over the landscape of mountains, taiga, and wetlands seen in the background; Tundra is an important area of methane emission in eastern Siberia.

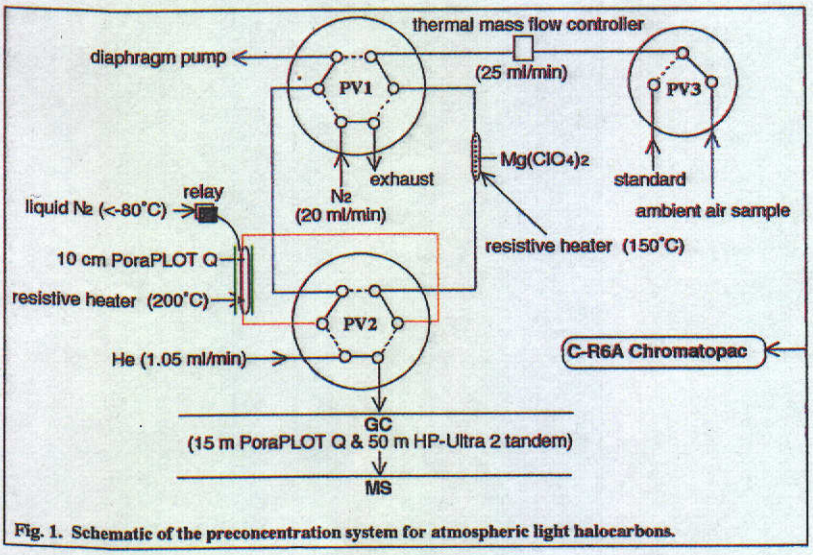

Fig. 1. Schematic of the preconcentration system for atmospheric light halocarbons.

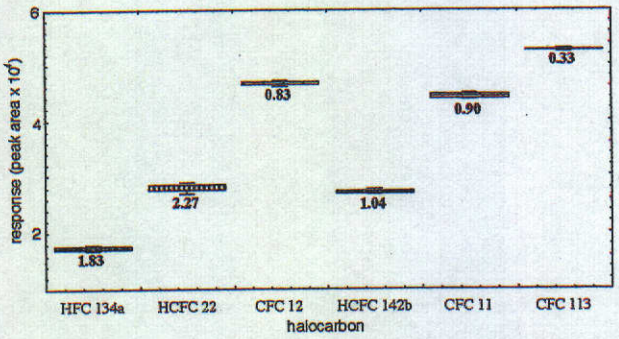

Fig. 2. Reproducibility of response of selected light halocarbons (respective RSD indicated) obtained from 12 standard runs.

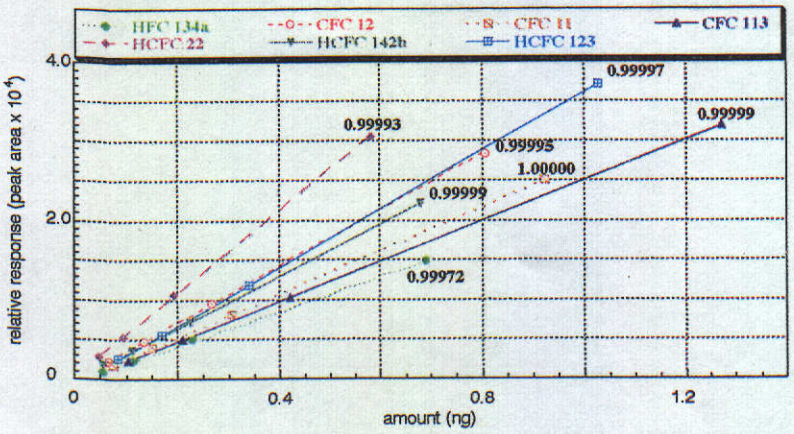

Fig. 3. Halocarbon standard for analysis of Moscow and Siberian samples.

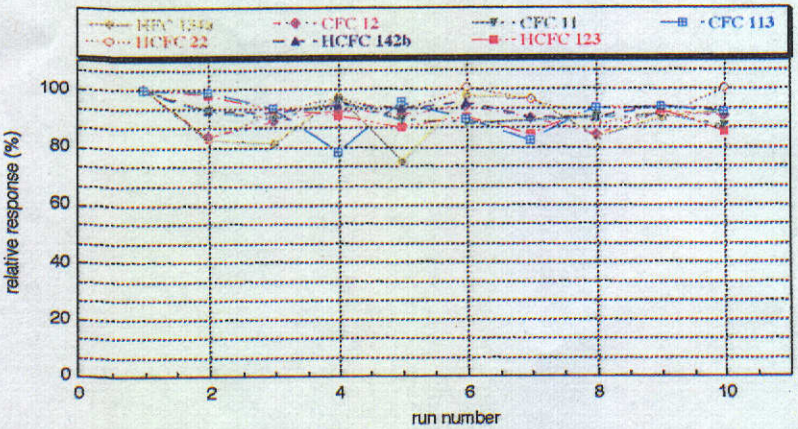

Fig. 4. Instrument response to standard gases ran at intervals of sample analysis.

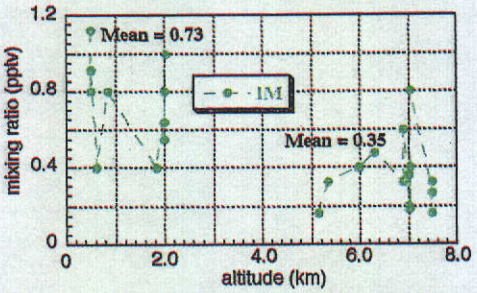

Fig. 5. Altitudinal variation of iodomethane.

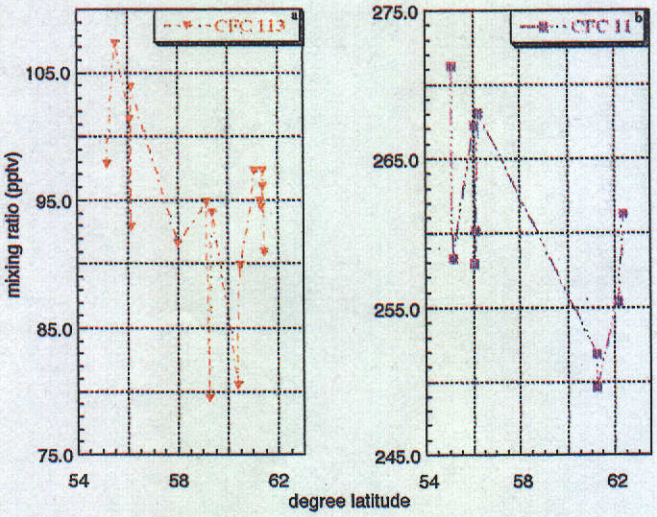

Fig. 6. Latitudinal (spanning Moscow and Siberia) variation of CFC 113 and CFC11.

[a]high altitude (5.0 to 7.5 km) and sub-zero (-11 to -28°C) temperature levels.

[b]low altitude (0.5 to 2.0 km) and above zero (3 to 18°C) temperature levels.

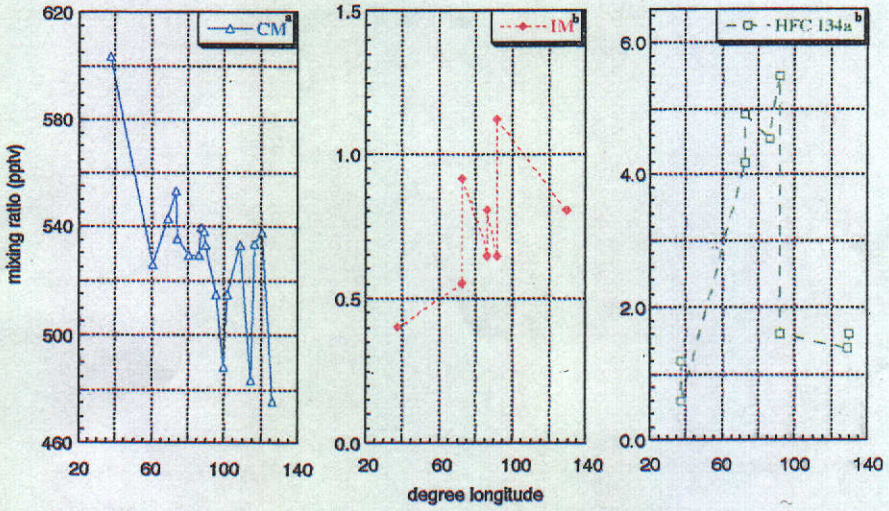

Fig. 7. Longitudinal (spanning Moscow and Siberia) variation of halocarbons.

[a]high altitude (5.0 to 7.5 km) and sub-zero (-11 to -28°C) temperature levels.

[b]low altitude (0.5 to 2.0 km) and above zero (3 to 18°C) temperature levels.

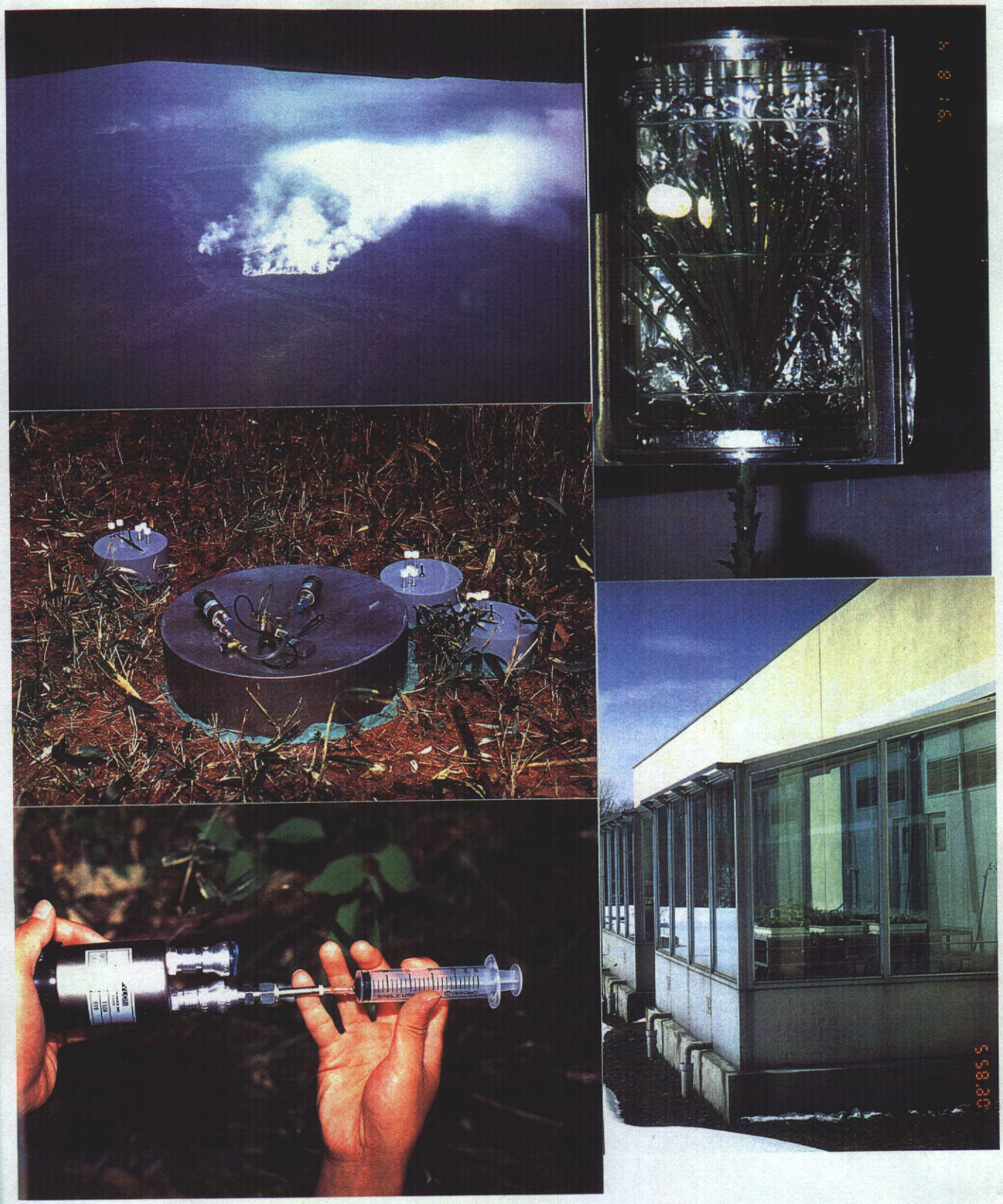

Counter clockwise from top left corner; Natural forest fires observed near Verkhoyansk in mid July 1994; The ^{222}Rn flux chamber and the static chamber for CO_2 flux measurement of Uchida and Nojiri; The scintillation cell (110 ml) for ^{222}Rn analysis, into which the soil gas is injected with a syringe; A phytotron at FFPRI, Sapporo used by Koike et al. for a growth experiment with CO_2 and temperature control; Measurement of gas exchange rates of Scotch pine raised under elevated CO_2 and temperature.

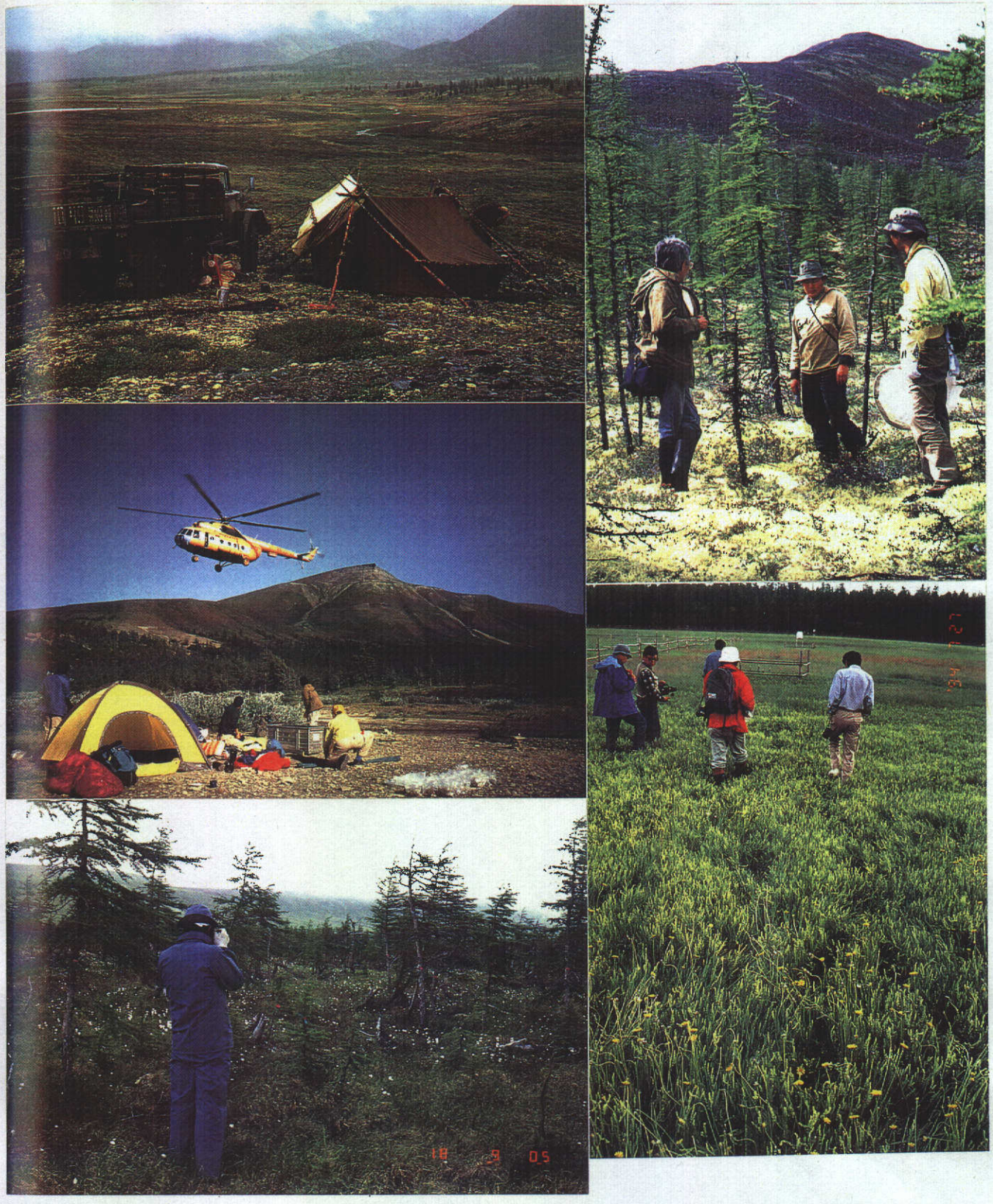

Counter clockwise from top left corner; Campsite of Toda, Vinokurov and others at 1,280 m a.s.l. in the alpine tundra of Verkhoyanskiy Mountains; Landing site at the latitudinal tree line at 72°N, 125°E near Tiksi where soils, population ecology of larch trees, and tree line dynamics were examined; Experimental plot of larch forest near the tree line (same location as the last photograph); The Model Alas Experimental Field of Yakutsk Institute of Biology, 60 km west of Yakutsk; Vegetation at a transition zone from taiga to alpine tundra in Verkhoyanskiy Mountains north of Oimyakon.

Proceedings of the Third Symposium on the Joint Siberian Permafrost Studies between Japan and Russia in 1994

KUNIHIDE TAKAHASHI
AKIRA OSAWA
YOICHI KANAZAWA
editors

held at Tsukuba, Japan
30–31 January 1995

Forestry and Forest Products Research Institute

National Institute for Environmental Studies
Center for Global Environmental Research
Global Environment Division

Hokkaido University
Institute of Low Temperature Science
and Faculty of Engineering

Editors:
Kunihide Takahashi
Akira Osawa
Yoichi Kanazawa

Printed:
i WORD
N3E5, Sapporo, 060 Japan

Published in March 1995
Sapporo, Japan

Preface

The third symposium on the joint Siberian permafrost studies between Japan and Russia was held at Forestry and Forest Products Research Institute in Tsukuba for two days, 30–31 January 1995. There were over sixty participants from fourteen universities and three National Institutes of Japan. The organizations of the Russian co-authors covered one university and four institutes.

The potential role of the Siberian permafrost area on global warming, especially on carbon dioxide budget and release of methane, is presently one of the most urging problems of the world. However, there had been few investigations on these questions in Russia until very recently. In this regard, our cooperation between Japan and Russia that started in 1992 belongs to a work of pioneers.

Research activities of the Japanese investigators have been conducted smoothly through support and advice of Russian scientists. Last year, the joint effort has been organized with several different budget programs and without any specific leadership, as in the case in the previous years. It started as exchange of information and discussion of field schedule and instruments. Mutual arrangement of field transportation followed.

Organization of the scientific groups is as follows: 1) atmospheric team, 2) forest team, 3) biology team, 4) permafrost team, and 5) air pollution team, and covers atmospheric, biological, and geological sciences. The participating scientists belong to National Institute for Environmental Studies, Forestry and Forest Products Research Institute, Institute of Low Temperature Science, Hokkaido University, Tohoku University, The University of Tokyo, Global Environmental Forum, and Tokyo Gas Co. in Japan. The Russian organizations include Permafrost Institute, Yakutian Institute of Biology, Institute of Microbiology, Institute of Chemical Physics, Moscow State University, Central Serological Observatory, Center of Nickel Experimantal at Noril'sk, and Sukachev Institute of Forest. Scientists of other organizations are also joining the program as one will find in the following pages.

Results of our research programs have been reported at the present symposium; most of them are still under investigation, and their results being preliminary. Purpose of this volume is information exchange, not reporting of the final results. Therefore, I hope that the readers contact the authors prior to citing any part of the results contained in this publication. Telephone and fax numbers and addresses are provided for all papers.

March 1995

Kunihide Takahashi
Forestry and Forest Products
Research Institute

Table of Contents

1

Ice Complex/ Hydrology

Geomorphic change in relation to thawing of "Edoma" on the southern coast of the Bolshoi Lyakhovsky Island, east Siberia

KIYOSHI SAIJO[1], DAISUKE NAGAOKA[2], and MASAMI FUKUDA[3]

[1]*Department of Geoenvironmental Science, Tohoku University, Sendai 980-77 Japan*
Tel: +81-22-222-1800; Fax: +81-22-262-6609
[2]*Graduate School of Environmental Earth Sciences, Hokkaido University, N10W5, Sapporo 060 Japan*
[3]*Institute of Low Temperature Science, Hokkaido University, N19W8, Sapporo 060 Japan*

Introduction

Massive ground ice with frozen soil pillars, called "edoma" which means "diminishing land" in local language, is widely distributed in lowlands of the East Siberia. It has been pointed out that edoma was mainly formed in the last glacial stage as the result of growth of syngenetic ice-wedge (Popov 1969, Kaplina and Lozhkin 1984, Sone 1993). As estimated from its name, edoma suffers noticeable erosion due mainly to thawing. In particular, edoma exposed along coast and river is subject to drastic geomorphic change. This report presents the characteristics of geomorphic change in relation to thawing of edoma on the coast of the Bolshoi Lyakhovsky Island on the basis of the observation during the field work in the summers of 1993 and 1994.

Study area

The study site is situated on the southern coast of the Bolshoi Lyakhovsky Island (Fig. 1). The surrounding area including the study site belongs to continuous permafrost zone. According to the measurement from August of 1992 to July of 1994 at Kalakhari Island near the Lena Delta, ground temperature at 20 cm depth, as well as air temperature, exceed 0 °C from middle of June to Middle of September (Nakayama 1995). It is estimated, therefore, that thawing of edoma takes place during a summer season, especially in July and August.

Geomorphic change

The field work was carried out from August 5th to 19th in 1993 and August 20th to 25th in 1994. Thawing of the edoma and consequent geomorphic changes occurred quite visibly in the course of the field work. The major geomorphic changes, landforms, and the outline of geology along a profile across the coast are schematically illustrated in Fig. 2.

Many dome-like mounds called "baidzharakhi", most of which have a diameter about 3 to 4 meters, are scattered on the ground surface underlain by top of edoma. They are composed of frozen soil pillars. It is estimated that the baidzharakhis have appeared as the result of sinking of surrounding ground surface due to thawing of the ground ice.

Melting of the ice occurs very rapidly on the steep wall where the edoma itself is exposed. The melt water flowing down on surface of the wall can be observed almost always in daytime. As a result of melting of the ice, the active layer above it overhangs, falls down frequently, and the marginal line of the wall retreats. The hole, which was digged for a work on a point located about five meters landward from the edge of a wall on August 8th of 1993, almost disappeared at the time of the field work in 1994. This means that the retreating rate of the wall amounts to about five meters per year, though retreat of the wall mostly takes

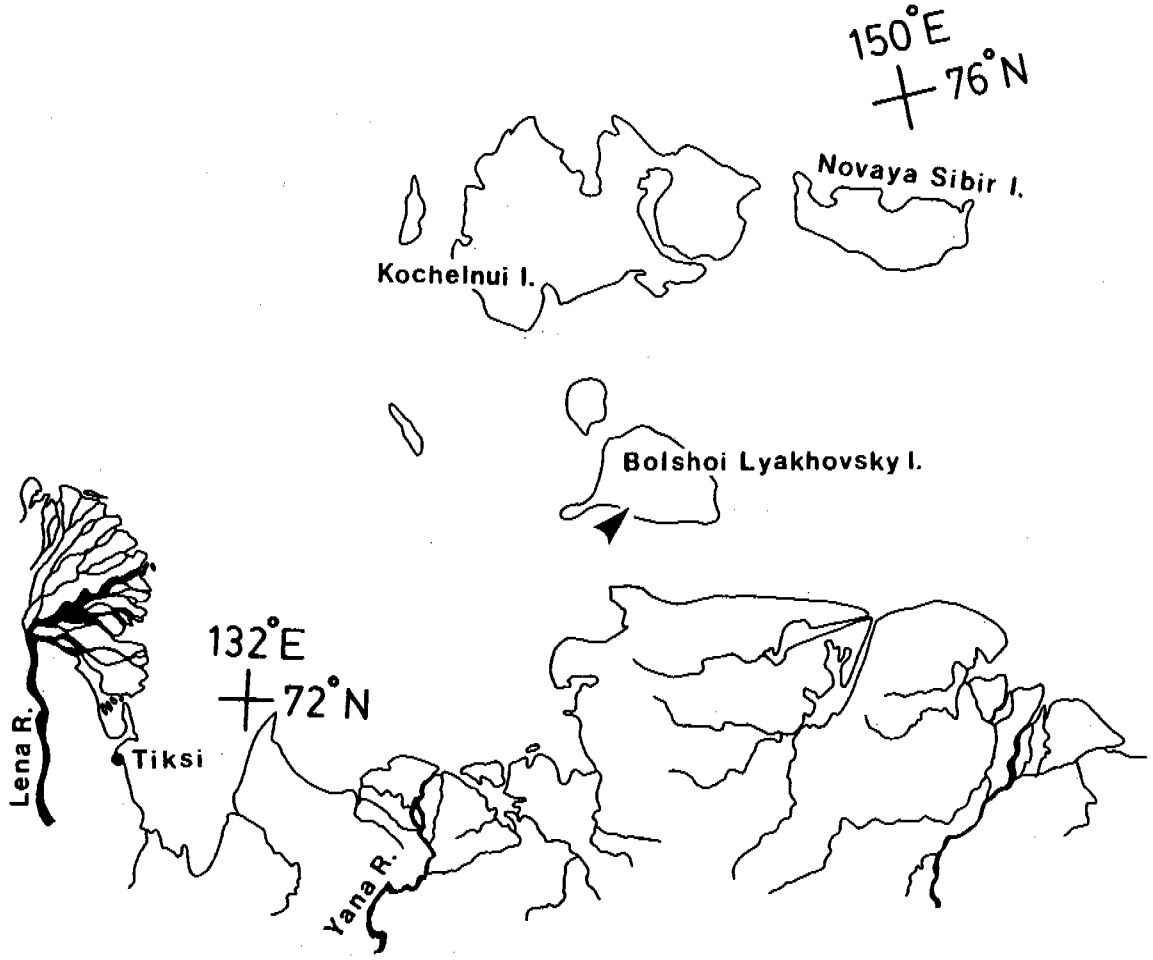

FIG. 1. Study area.

place not constantly over a year but is concentrated from June to September.

Terrace-like gentle slope is commonly recognized in front of the wall that comprise the edoma. The level of this gentle slope seems to be basically determined by top of the ice-poor lacustrine underlying the edoma. Remained ice and conical baidzharakhis are distributed on the slope surface, where the ground is widely muddy due to the existence of fine material saturated with the melt water from the upperslope. Small streams originated from the melt water flow in places.

Terrace-like gentle slope usually faces the sea with bluff of more than several meters high. Notch is formed at the base of the bluff as the result of thermal erosion by the waves. In cases when the notch erodes the bluff very deeply, the overhanged part by the notch collapses finally. Small fans developed at the outlets of the streams in consequence of deposition of the fine material transported by the melt water.

These are the characteristics of the geomorphic change occurring in summer seasons, and the landforms on a profile from top of edoma to shoreline. It is estimated that this geomorphological pattern is being preserved although both of the wall composed of edoma and the bluff facing sea seem to retreat at a rate of several meters per year.

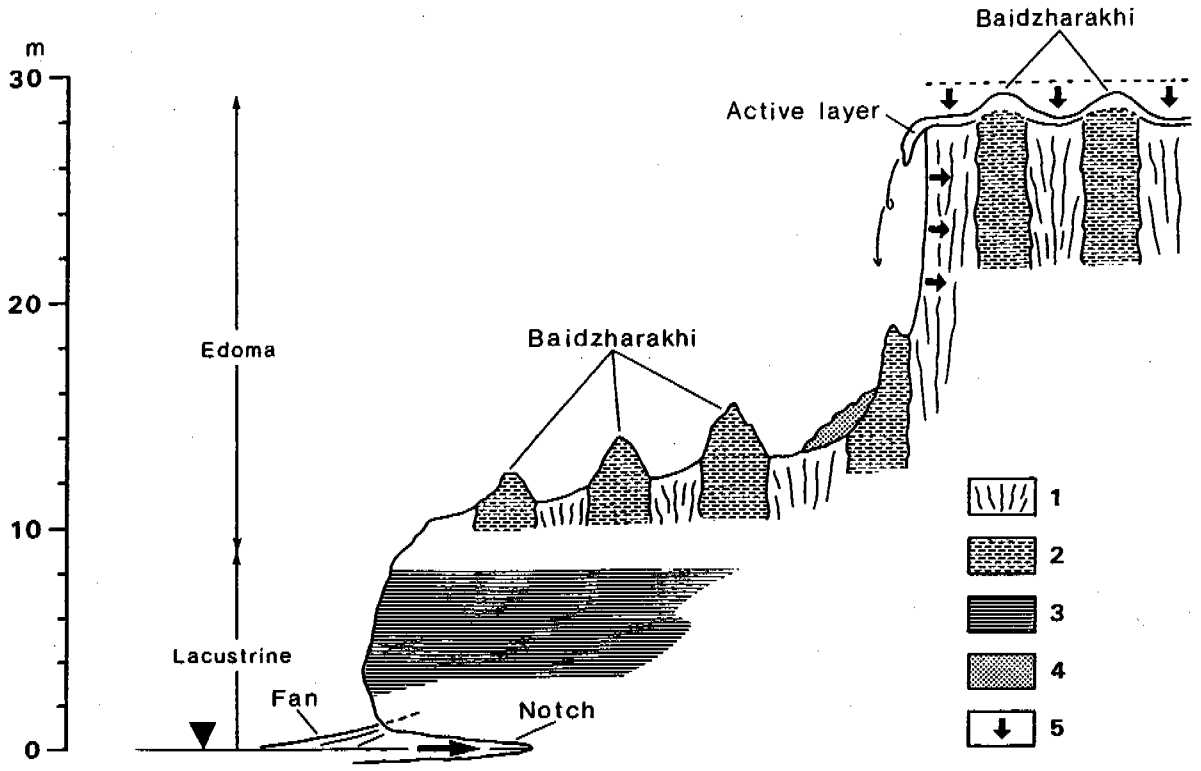

FIG. 2. Schematic geomorphological profile across the coast. 1, Ground ice(edoma); 2, Frozen soil pillar (edoma); 3, Lacustrine (ice-poor); 4, Collapsed material; 5, Thermokarst.

References

Kaplina, T.N., and A.V. Lozhkin. 1984. Age and history of accumulation of the "Ice Complex" of the maritime lowlands of Yakutiya. Velichiko A.A. (ed.) Late Quaternary Environments of the Soviet Union:147–151, University of Minnesota Press, Minneapolis

Nakayama, T. 1995. Estimation of methane emission from natural wetlands in Siberian permafrost area. Doctoral Dissertation, Hokkaido University, pp.123.

Popov, A.I. 1969. Underground ice in the Quaternary deposits of the Yana–Indigirka lowland as a genetic and stratigraphic indicator. Péwé,T.L.(ed.) The Periglacial Environment:55–64, McGill–Queen's University Press, Montreal

Sone, T. 1993. Origin of the ice–complex in the Bykovsky Peninsula, East Siberia. Inoue,G.(ed.) Proceedings of the Second Symposium on the Joint Siberian Permafrost Studies between Japan and Russia in 1993:19–21.

Sedimental environment of the Edoma in high Arctic eastern Siberia

DAISUKE NAGAOKA[1], KIYOSHI SAITO[2], and MASAMI FUKUDA[3]

[1]Graduate School of Environmental Earth Science, Hokkaido University, N10W5, Sapporo 060 Japan
Tel: +81-11-716-2111; Fax: +81-11-706-7142
[2]Department of Geoenvironmental Science, Tohoku University, Sendai 980-77 Japan
[3]Institute of Low Temperature Science, Hokkaido University, N19W8, Sapporo 060 Japan

Introduction

Large plain of several decameters a.s.l. extends along the coast of the Arctic Sea in the eastern Siberia. In this plain, there are many big and small lakes and rivers. Main rivers are the Lena river that is situated in the western side of the plain, the Yana river and the Indigirka river. The region facing the Arctic Sea is a continuous permafrost zone. Permafrost in the region mainly consists of massive ground ice. The lakes in the plain are thermokarst lakes (alas) that result from melting of the permafrost. The permafrost accompanied by the massive ice is exposed on the cliffs along some parts of the Arctic coast, the riverside and the lakeside. The permafrost is called the Edoma or the Ice-complex. The Edoma is composed of pillar-shaped frozen soil (sediments) besides the massive ice. The soil pillars are distributed at regular intervals of several meters in the massive ice, and contain a lot of ice lenses and organic materials. The massive ice in the Edoma is considered as ice wedge growing concurrently with sedimentation, "syngenetic ice wedge".

We investigated the Edoma of this region in the summers of 1992-1994. This report aims to consider the sedimental environment of the Edoma based on ^{14}C dates and grain size analysis.

Facies of the Edoma

Study sites are at the northeast coast of the Bykovsky Peninsula at the end of the Lena Delta (Loc. 1), the south coast of Bolshoi Lyahovsky Island at southern part of the New Siberian Islands (Loc. 2), and Oiyagosky Yar in north coast of the large plain (Loc. 3) (Fig. 1). Facies of the Edoma in each sites are described as follows:

1) Bykovsky Peninsula. In this site, the Edoma is exposed on the whole cliff about 40m in height. Frozen soils (sediments) in the Edoma are formed five to eight m diameter of pillars, and consisted of dark gray silt, silty fine sand and sandy silt which include organic materials (Fig. 2). The upper part of the sediments is coarser than the lower part according to the grain size analysis. This result suggests that the sediments are transported by the Lena river (Nagaoka, 1993). In the sediments, several peat layers are found (Fig. 2). Using six samples taken from these peat layers, ^{14}C dating carried out with accelerator mass spectrometer (AMS) at Nagoya University. Results of the measurements are shown in Table 1.

2) Bolshoi Lyahovsky Island. In this site, the Edoma exposed in a part of the cliff about 30 m in height and its lower boundary is found at a height of six m a.s.l. Diameter of frozen soil pillars is four to five m, which is a little shorter than that in the Bykovsky Peninsula. The sediments are brown and mainly consisted of silt containing organic materials (Fig. 3). In the sediments, four peat layers are found. Six samples from these peat layers were measured for ^{14}C dating (Table 1).

3) Oiyagosky Yar. In this site, the Edoma is exposed in a part of the cliff about 35 m in

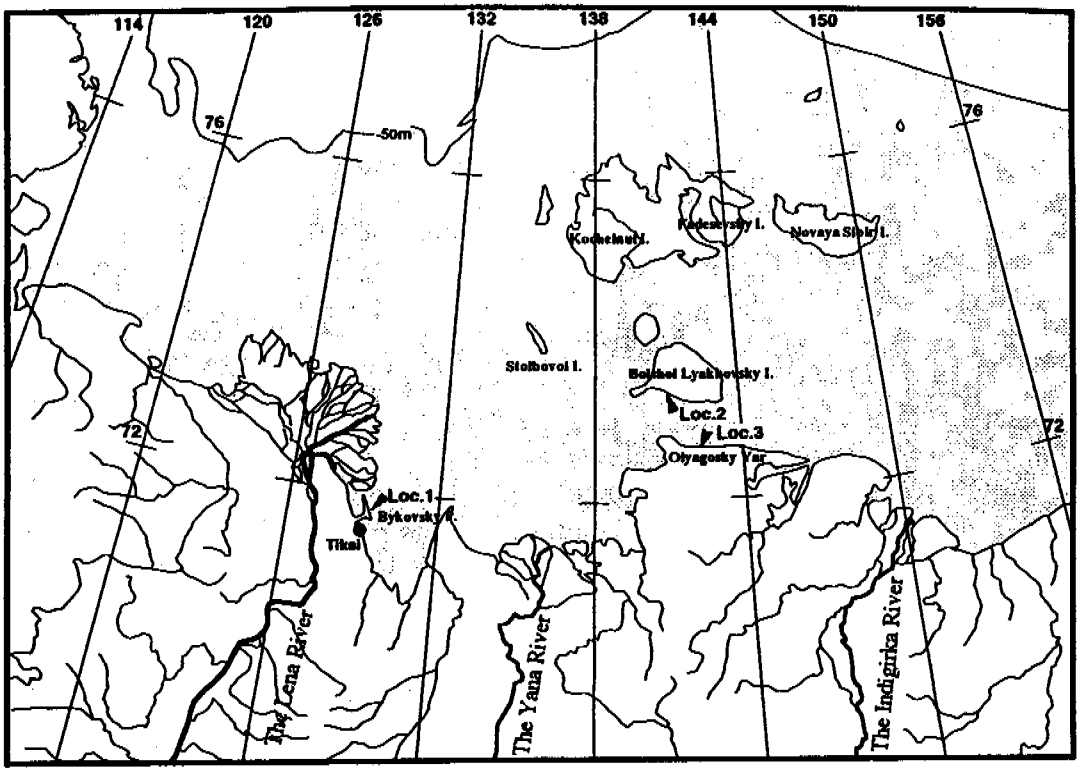

FIG. 1. Location of the study sites.

TABLE 1. Results of ^{14}C dating.

Sample No.	Location	Material	Age	Code No.
IC1	Loc. 1	Peat	11,090 ± 270	NUTA-2231
IC2	Loc. 1	Peat	25,740 ± 1100	NUTA-2234
IC3	Loc. 1	Peat	32,850 ± 1030	NUTA-2237
IC4	Loc. 1	Peat	28,300 ± 370	NUTA-2839
IC5	Loc. 1	Peat	24,880 ± 400	NUTA-2795
IC6	Loc. 1	Peat	21,430 ± 160	NUTA-2796
IC7	Loc. 2	Peat	7,370 ± 820	NUTA-2840
IC8	Loc. 2	Peat	28,710 ± 400	NUTA-3532
IC9	Loc. 2	Peat	30,980 ± 350	NUTA-2841
IC10	Loc. 2	Peat	34,210 ± 1850	NUTA-2797
IC11	Loc. 2	Peat	>39,650	NUTA-2842
IC12	Loc. 2	Peat	>42,240	NUTA-2798
IC13	Loc. 3	Peat	22,940 ± 390	NUTA-3521
IC14	Loc. 3	Peat	>41,770	NUTA-3522
IC15	Loc. 3	Peat	>40,200	NUTA-3542

height and its lower boundary is found at a height of eight m a.s.l. Sediments mainly consisted of silt containing organic materials, which are similar to that in Bolshoi Lyahovsky Island (Fig.4). Five peat layers are found and three samples from these peat layers were measured for ^{14}C dating (Table 1). Besides, the pollen analysis were carried out using other samples taken from the sediments. According to the result, a lot of spores of a green algae, "*Botryococcus*" are found in the samples. This suggests that the sediments were accumulated

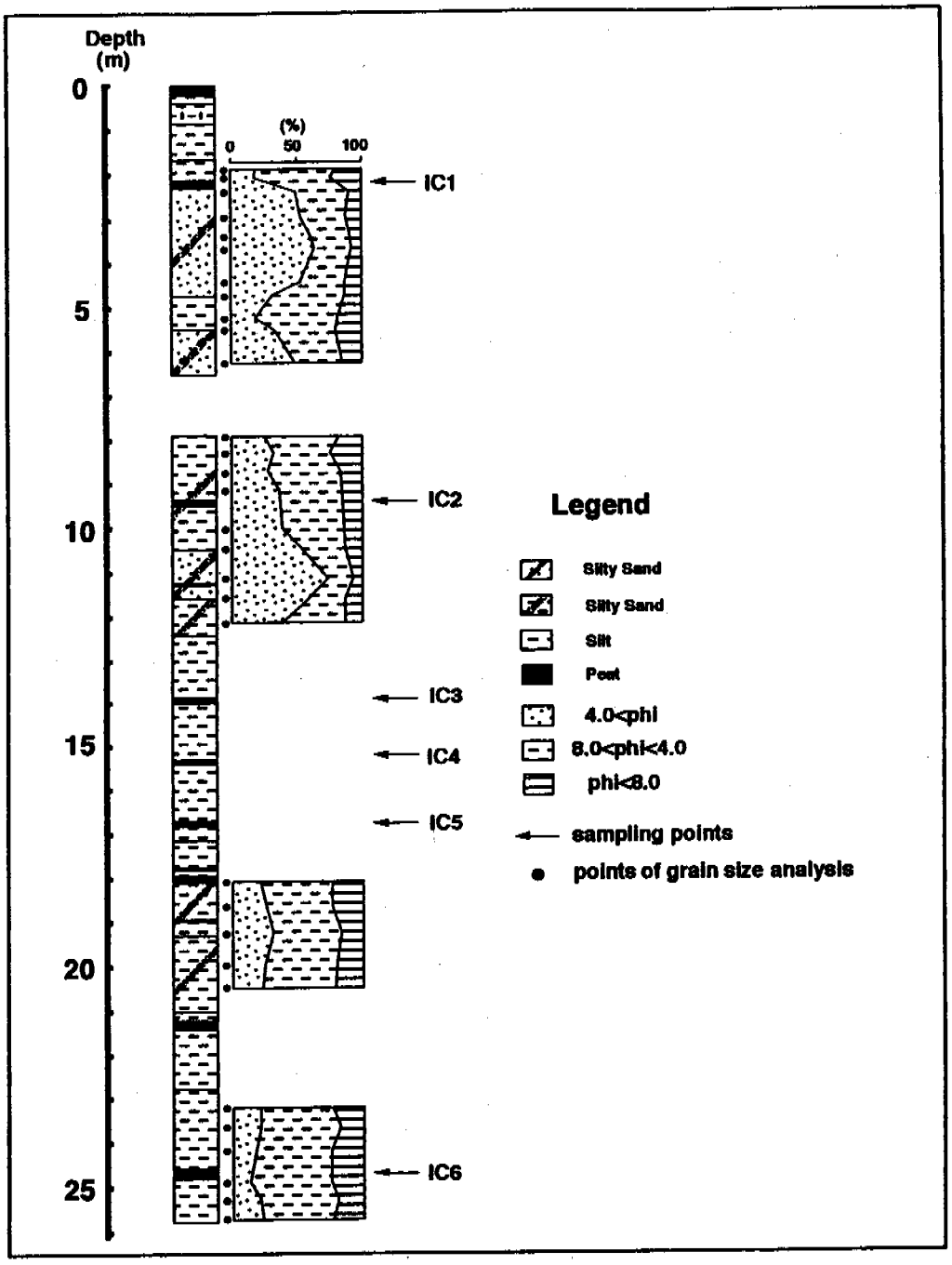

FIG. 2. Collumnar section and compositional ratio of the Edoma at Loc. 1.

in deep swamps.

Discussion

Results of ^{14}C dating indicate that the period of formation of the Edoma in eastern Siberia was before 40,000 y.BP to about 23,000 y.BP. This period is called "Karginkiy Interstadial" in Siberia, and considered that the climate has been cooler and the sea level was lower than

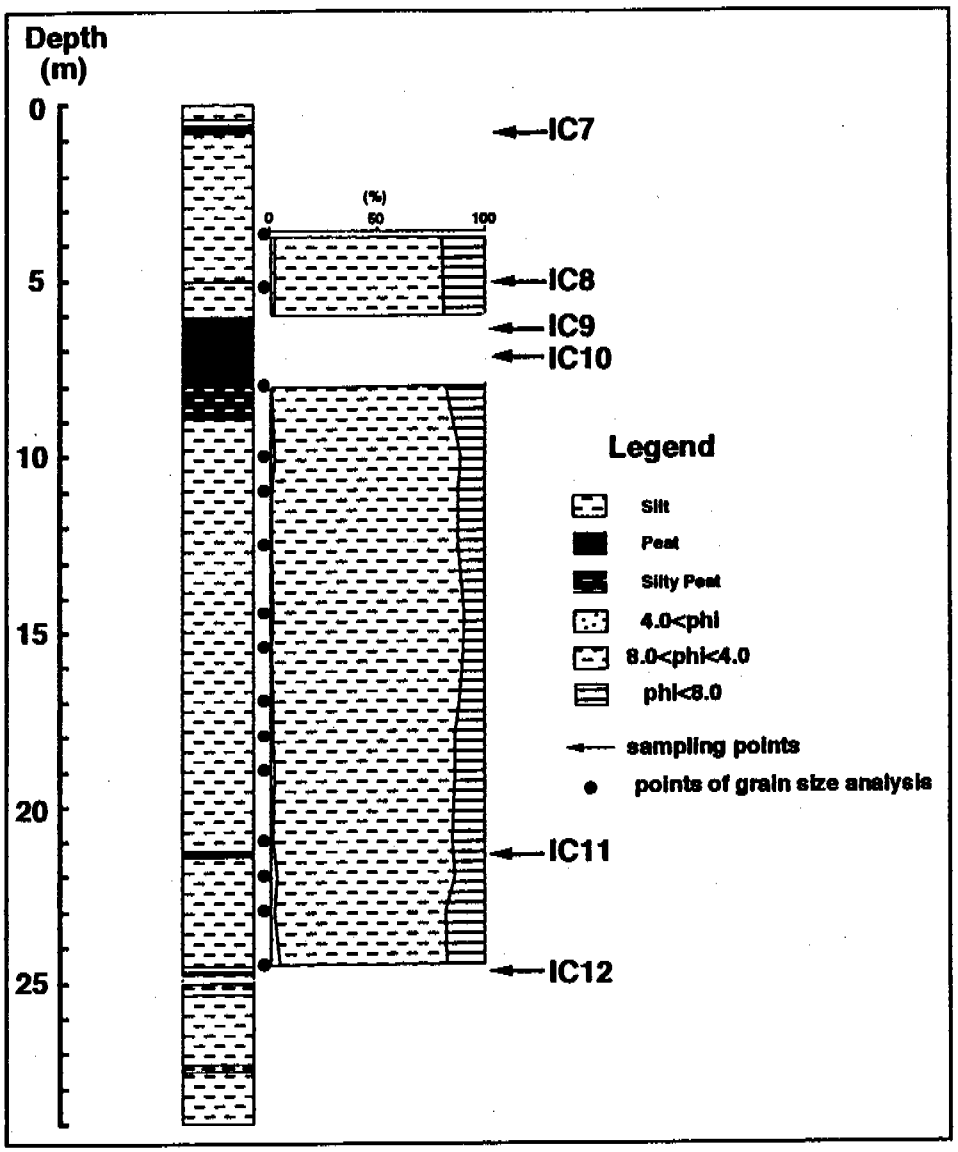

FIG. 3. Collumnar section and compositional ratio of the Edoma at Loc. 2.

present in the world. After that, the glacial stadial called "Sartan Glaciation" came. Therefore, it is concluded that formation of the Edoma in eastern Siberia was terminated until Sartan Glaciation that was the coldest period during the last glaciation.

The results of ^{14}C dating also indicate that formation of the Edoma in the Bykovsky Peninsula stopped probably after the termination at Bolshoi Lyahovsky Island and Oiyagosky Yar. In the Bykovsky Peninsula, the termination of the Edoma formation is considered at about 20,000 y.BP, while the beginning of the Edoma formation is unknown, because lower boundary of the Edoma exists under the sea. On the other hand, the Edoma formation is considered to have started before 40,000 y.BP and terminated about 30,000 y.BP. This may result from a difference between two sedimental environments; one (the Bykovsky Peninsula region) is situated near the Lena river, so that in this region, the Lena river supplied sediments steadily. The others (Bolshoi Lyahovsky Island and Oiyagosky Yar region) are located far from big rivers, so that there was a calm environment like a swamp in this region. In the Bykovsky Peninsula region, therefore, the Edoma grew until later because of accumulation by the Lena river. In the Bolshoi Lyahovsky Island and the Oiyagosky Yar

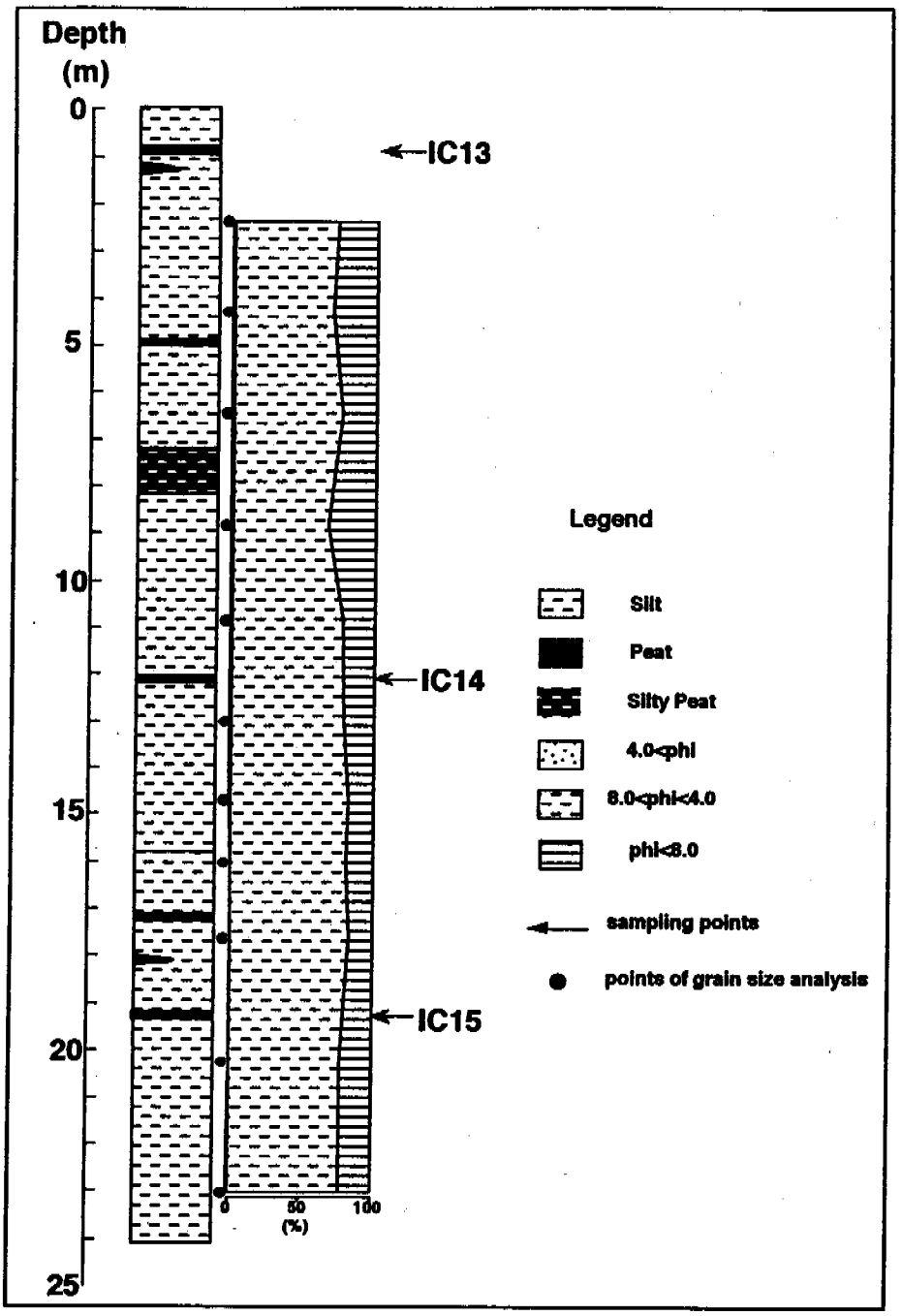

FIG. 4. Collumnar section and compositional ratio of the Edoma at Loc. 3.

region, formation of the Edoma was easily disturbed by a little change of the environment (ex. cooling etc.) because of less supply of the sediments.

In our study on the Edoma, we face a question of why the Edoma is exposed on the cliffs of about 30 to 40 m in height. During the period of formation of the Edoma, the sea level was, as mentioned above, lower than the present in the world. On Bolshoi Lyahovsky Island and Oiyagosky Yar, the lower boundary of the Edoma is six to eight m a.s.l. This fact gives us a clue for reconstruction of the paleoenvironment in eastern Siberia.

In order to answer the question, we propose existence of small ice sheets on the exposed continental shelf during the last glaciation and isostatic rebound during the postglacial age. The reason is as follows. Since the continental shelf 50 m below the sea level extend over the Arctic Sea, if the sea level decreases, it would be exposed. When the sea level was low, the sea ice in the Arctic Sea would have expanded toward the continental shelf. Ice from

major rivers also would have accumulated close to the sea ice on the continental shelf. If this process was maintained, ice sheet would have grown on the continental shelf. Moreover, in summer seasons, the ice sheet would have cut off streams to the sea, which would have resulted in formation of large swamps in front of the ice sheet. In other words the Edoma formed a swamp-like environment in front of the ice sheet. After the glacial age, climate grew warm in the world, and the ice sheet melted. as the result, upheaving due to isostatic rebound formed the cliffs exposing the Edoma.

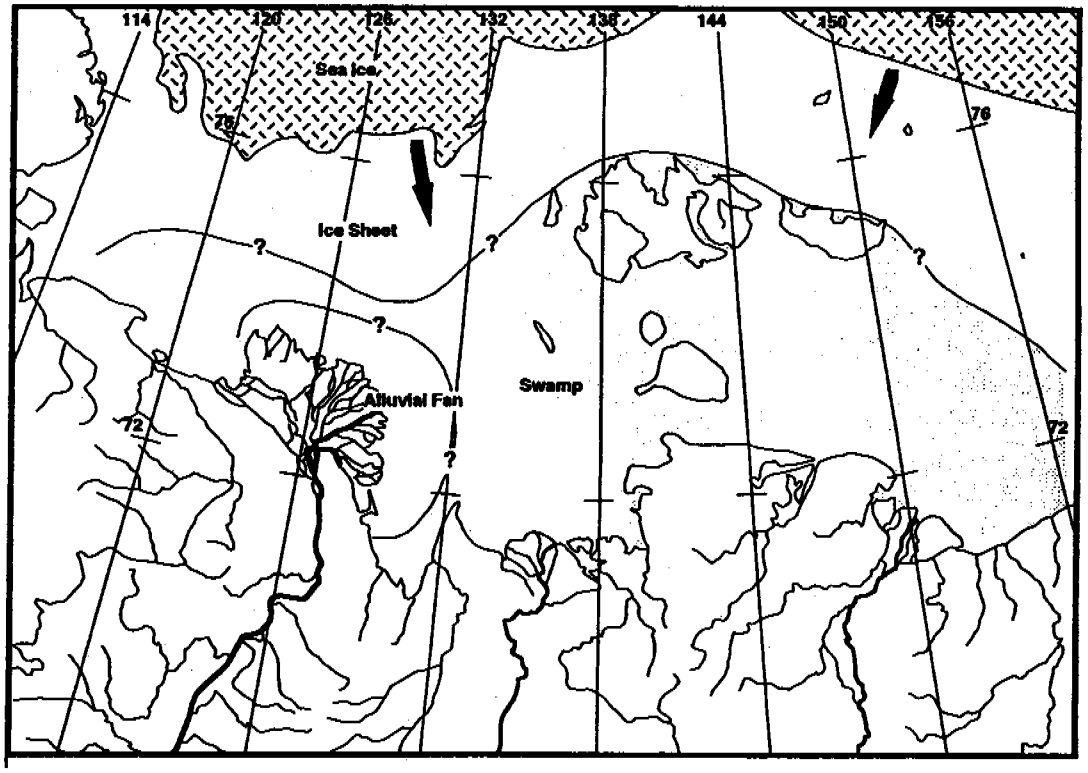

FIG. 5. Schematic sedimantal environment of the Edoma.

Radiocarbon dating of methane obtained from air in the ice complex (Edoma), in Arctic coast area of east Siberia

JUN MORIIZUMI[1], TAKAO IIDA[1], and MASAMI FUKUDA[2]

[1]*Department of Nuclear Engineering, School of Engineering, Nagoya University, Furo-cho, Chikusa-ku, Nagoya 464-01 Japan*
Tel: +81-52-789-4676; Fax: +81-52-789-3791
[2]*Institute of Low Temperature Science, Hokkaido University, Kita-19, Nishi-8, Kita-ku, Sapporo 060 Japan*

Introduction

In lowland areas of eastern Siberia along Arctic coast and delta regions of major rivers, ground ice exists in the permafrost in large scale. The ground ice exhibits unique features, and is specially termed as Ice Complex or Edoma by Russian researchers. Genesis of the Ice Complex has been controversial for a long time. Popov (1969) indicated that the Ice Complex developed by the alternation of growth of the ice-wedge and sedimentation over the ground surface. This process of ice-wedge growth is termed as syngenetic ice-wedge. Kaplina and Lozhkin (1984) compared the results of ^{14}C dating obtained from peat layers in the Ice Complex at various locations in the lowland areas along the Arctic coast. They pointed out that the main part of the Ice Complex formed during Interstadial in last Glacial Period between 40,000 yBP and 25,000 yBP. Fukuda (1993, 1994) suggested that the Ice Complex developed during the last Interstadial locally called as Karginsky Interstadial. He also showed that highly concentrated methane was contained in air bubbles in the Ice Complex. Oxygen Isotropic concentration profiles obtained from the ice samples also implied a paleo-temperature condition during the Karginsky Interstadial. Based on results of these analyses, he concluded that the Ice Complex developed under a unique climatic condition during the last Interstadial. There still remains vagueness on the genesis and age of the Ice Complex formation. Especially ^{14}C datings were made using indirect samples of the Ice Complex. As the Ice Complex consisted of ice and sediment parts, all previous ^{14}C datings were carried out using organic materials in the sediments. However, sedimental structure of the frozen materials was secondarily disturbed. Sometimes, results of the dating disagree with sediment stratigraphy: young ages were yielded from sediments at lower layers. Thus, it is desirable to use the organic materials from the ice as to obtain a direct dating information of the Edoma. As Fukuda indicated in the last report, the highly concentrated methane in the air bubbles of the Ice Complex was traced both in upper and lower levels at the Edoma exposures. If methane is extracted in certain amounts, one can adopt the AMS technique to determine the concentration of ^{14}C. Wahlen et al. (1989) applied this method and determined the atmospheric concentration of ^{14}C. Present authors also attempted the AMS method to determine ^{14}C dating of air in the Ice Complex, which might be a direct information of the age of the Ice Complex.

Sites and sampling of air from ice complex

The surveyed sites of this study were located at the southern coast of Big Lhyavosky Island and the coast of Oiyagoskii Yar in main land of Siberia, shown in Fig.1. Along the both coasts of Big Lhyavosky Island and Oiyagoskii Yar, the Ice Complex is widely exposed

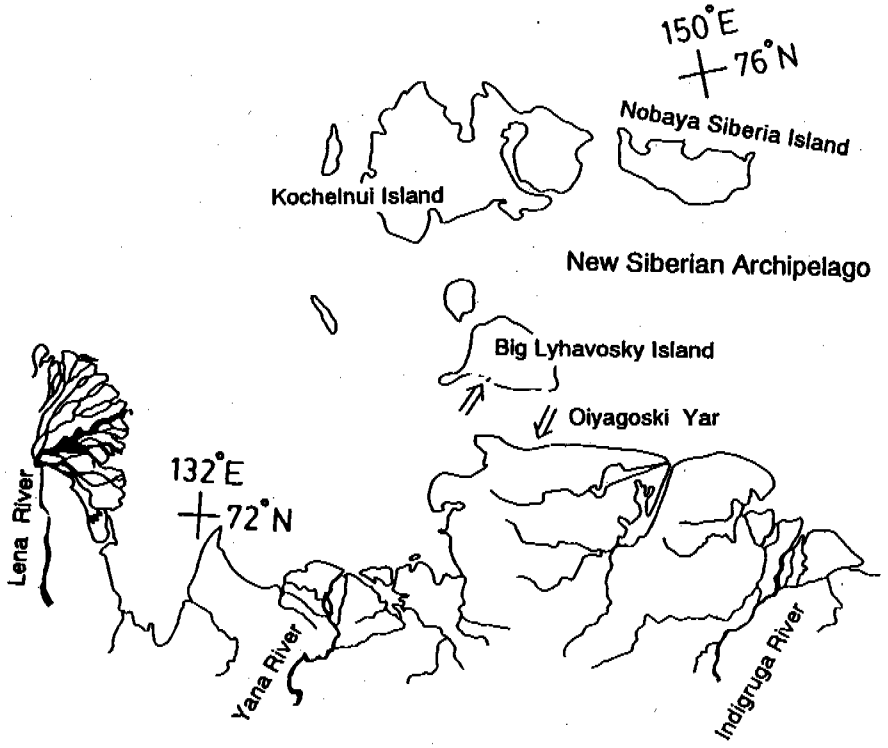

FIG. 1. Location map of surveyed area.

with the height of 30 m or higher. In 1993 and 1994, on-the-spot survey and sampling of ice from the exposures were made. At Oiyagoskii Yar, ice blocks were quarried out at each one m intervals by a chain saw. On the top of the Edoma, new ice-wedge penetrated into a previously formed Edoma. The relationship of two ice mass was clearly shown in Photo. 1. Previous data of sediments overlaying Edoma indicated penetration of a new ice-wedge that occurred in Holocence. Regarding the determination range of AMS, the ice was sampled from this new ice-wedge. Ice blocks were soaked into hot water containing over-saturated salt. During the process of thawing, the trapped air in the ice was released to the water. These air bubbles were collected with a submerged funnel, and accumulated into a glass holder connected at the top of the funnel. As the water was saturated with salt, additonal air did not disslove into the water, avoiding contamination from the present atmospheric gases.

Concentrations of methane in the air samples were determined by means of the portable Gas Chromatography on-the-spot. Once the air samples were collected into the glass holder, each sample was subjected to gas composition analysis just in front of the exposure. The resolution of the measurements of portable Gas Chromatography is about ±10 ppm in case of methane and carbon dioxide determinations. The required minimum amount of carbon for ^{14}C dating using the AMS system (at Dating and Materials Research Center, Nagoya Univ.) is one mg as pure carbon (Nakamura and Nakai 1988). This amount of carbon is obtained from pure methane of 1.9 m litter in volume under atmospheric pressure. And one litter of air with 0.2 % of methane concentration contains about one mg of carbon. The results of gas composition analyses for two samples at Oiyagoski Yar and Big Lhyavosky Island were shown in Figs. 2a and 2b. Sample OG34 contains rather critical carbon amount than LZ-1.

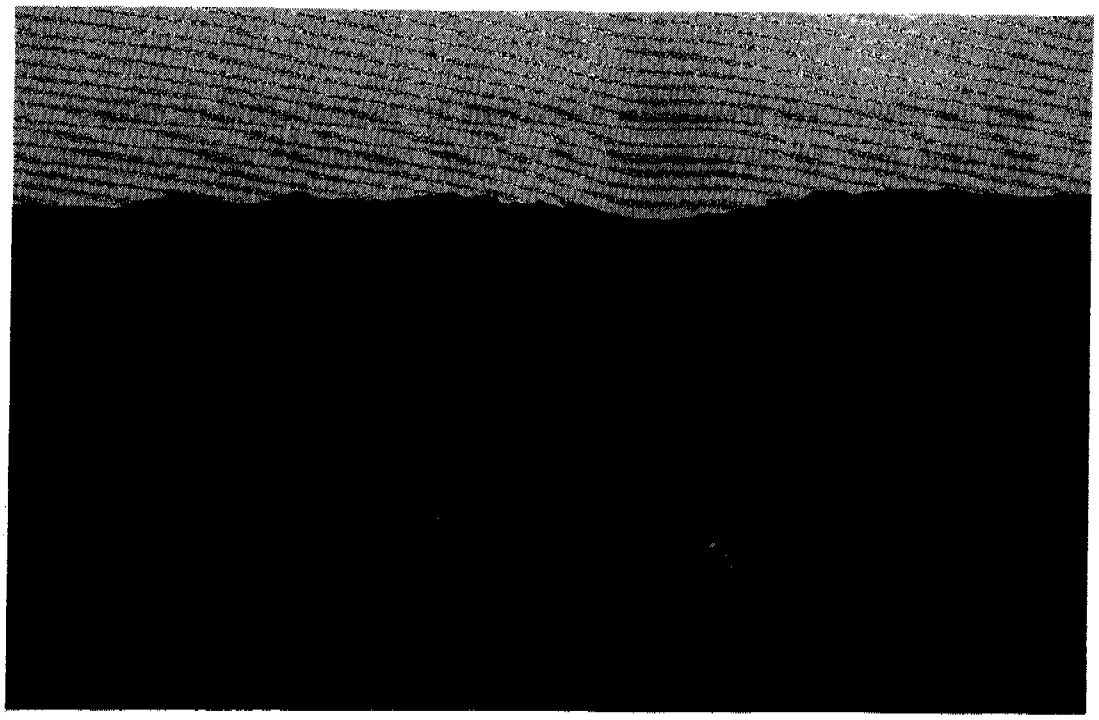

PHOTO. 1. Ice–wedge and Edoma at Oiyagoskii Yar.

Experimental procedures

The separation of methane from the sampled air was made by the adsorption process to an activated charcoal in the line of Gas Chromatography Measurement System (Wahlen et al. 1989, Moriizumi 1993). The procedure of separation in the line of GC is shown in Fig. 3. At first, air sample is cooled by the liquid nitrogen as to trap vapor and carbon dioxide. At the second trap, which is filled with activated charcol of 76 g, air sample is cooled again by liquid nitrogen and one litter of air is absorbed within one minute. Then the second trap is cooled by a mixture of dry-ice and ethanol at the temperature of −80 °C. The released nitrogen and oxygen at that temperature are exhausted by a vacuum pump. Remaining

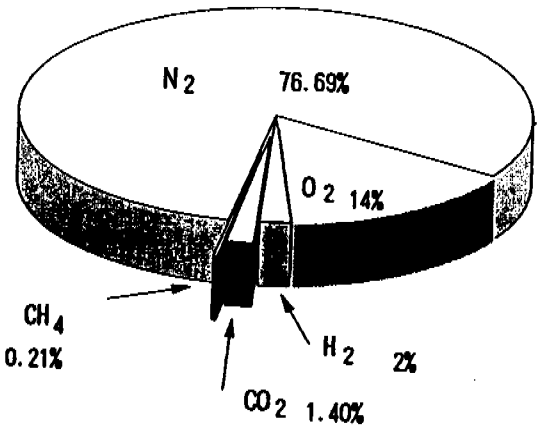

FIG. 2a. Gas composition of sampled air (OG34) at Oiyagoskii Yar (in volume).

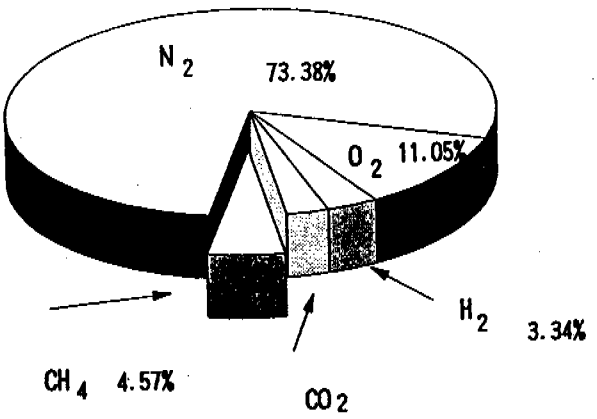

FIG. 2b. Gas composition of sampled air (LZ–1) at Big Lhyavosky Island (in volume).

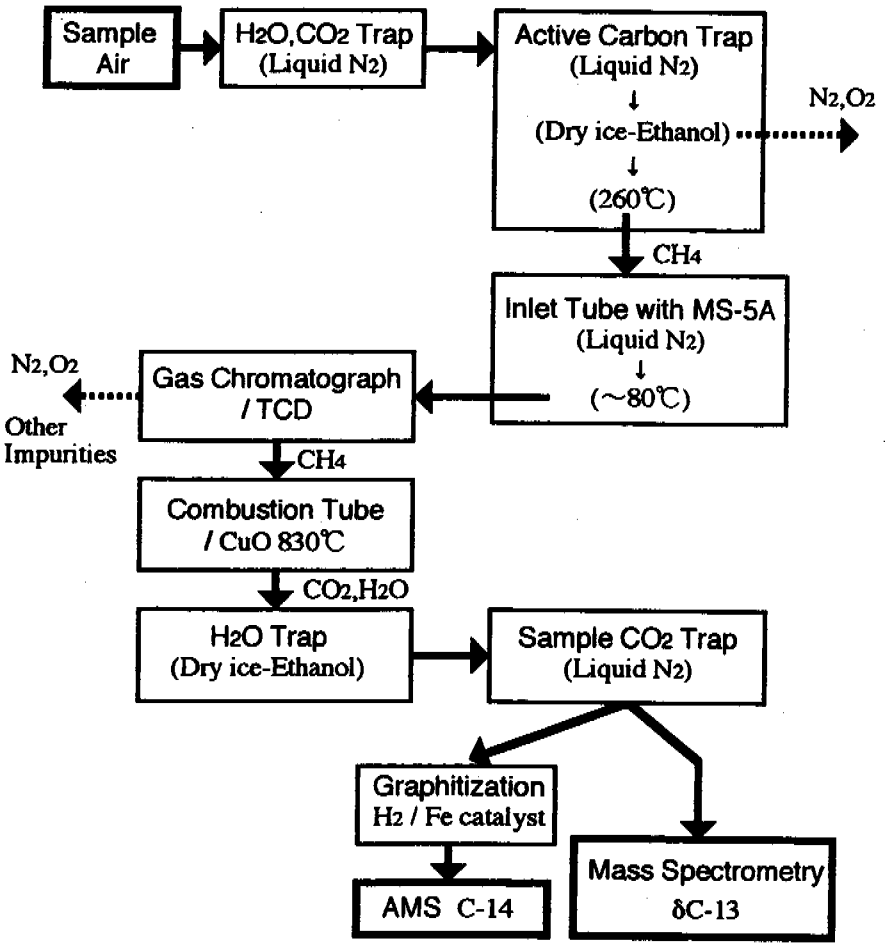

FIG. 3. Schematic diagram of procedure for separation and refinement of methane in the air sample and measurements of its carbon isotopic composition.

methane adsorbed on the charcol is released in the process of heating up to +260 °C and introduced into the third trap, in which a small amounts of molecular sieve (MS–5A) is placed at the bottom. Again, that trap is cooled by liquid nitrogen as to adsorb methane to the third trap. Finnaly, the trap is heated up to the room temperature. Released methane is tranfered by He carrier gas into the line of Gas Chromatography. Separated methane with carrier gas is oxidized by heating up to +830 °C with CuO catalyst. Final product of CO_2 is cooled by the liquid nitrogen again. Some parts of the obtained CO_2 is subjected to the measurement of $\delta^{13}C$ by means of Mass Spectrometry (Finnigan MAT252). The other parts of CO_2, that is deoxidaized by H_2 with Fe catalyst and is turned to graphite, is subjected to determination of the concentration of ^{14}C by means of the AMS system.

The collection efficiency of methane from the air sample was evaluated using a prepared air sample of one litter containing 1.99 ml of methane. Ninety–six point four percent of methane was collected as the final product. Precautionary treatment was made as to avoid the contamination by the present air, and to eavulate the effect of isotopic fractionation of carbon in the process of separation. If the isotopic fractionation occurrs during the process of separetaion, the concentration of ^{13}C may change after the treatment. In addition to the effect of isotopic fractionation, foreign carbon contains diffrent concentration of ^{13}C. If one compares two values of $\delta^{13}C$ obtained from the original methane and the processed methane, it is possible to evaluate the level of the effect and degree of isotopic fractionation and contamination. The result of evaluation is shown in Fig.4. It is clear that there are no diffrences in the $\delta^{13}C$ values, implying a proper treatment for the separation of methane.

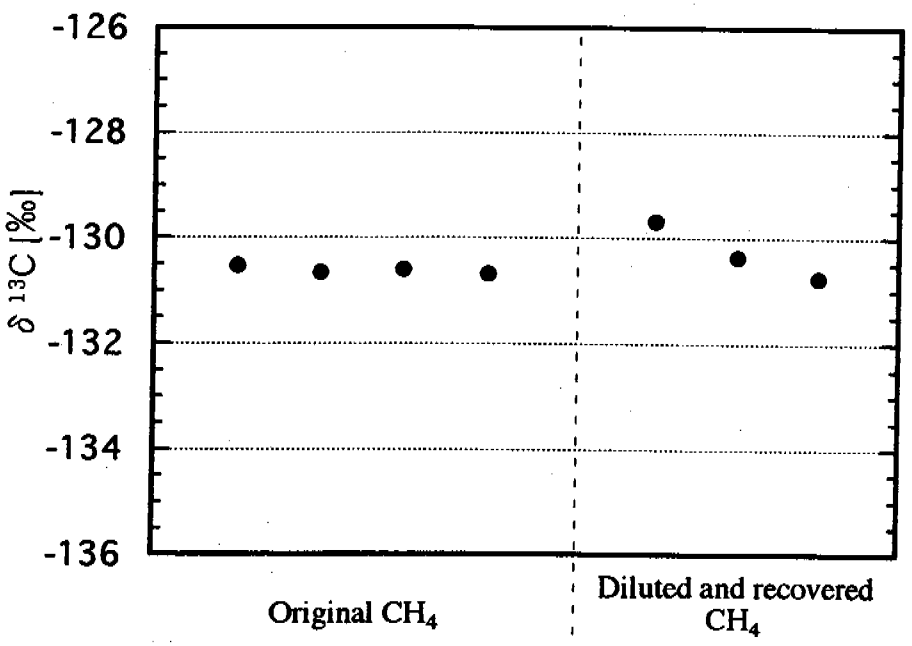

FIG. 4. Comparison of $\delta^{13}C$ values between the original methane and recovered methane.

Results and conclusion

The results of measurements are summarized in Table 1. The normalization for ^{14}C concentration is made as to ajust the $\delta^{13}C$ value to −25‰. (Stuiver and Polach 1977, Stuiver 1983). For the conversion of ^{14}C concentration to dating, 5,568 years is adopted as the half-life of ^{14}C. According to Stevens and Engelkemeir (1988), the obtained $\delta^{13}C$ values indicate that the source of the methane is boigenic, which occurs in the decay process of peaty materials under anaerobic environments on the ground surface. No contamination of the present air or antropogenic source of methane was traced. Obtained ages indicated that the ice-wedges penetrated into the old Edoma in the Holocence. Additional dating results using organic materials were obtained by the AMS. In the Edoma, there exit highly organic layers adjacent to the ice. In case of Oiyagoskii Yar, ^{14}C dates obtained from the organic sediments are shown in Fig. 5. As previously mentioned, main part of the Edoma developted during Karginsky Interstadial. Uppermost dating of 22,940 yBP implies that the Edoma formation terminated at the end of Karginsky Interstadial. The penetrated new ice-wedge was dated as 3839 yBP. Similar results at the Big Lhyavosky Island are shown in Fig. 6. Dating result of 7,370 yBP from the sediment near the surface of the Edoma implies that the Edoma tended to be eroded after the Holocence. The obtained date for LZ-1 from the penetrated ice-wedge coincided with the value for the sediment. Both dating results of methane from the ice suggest that the new ice-wedge tended to penetrate into the Edoma during the Holocence. The profiles of methane concentrations at both sites indicate that dating for upper part Edoma is plausible.

Present authors attempted to deterime ^{14}C dating of methane obtained from ground ice in Siberian permafrost. By appropriate treatments for separation of methane from air samples and process of measurements, ^{14}C dating for fossil air was sucessfully done. Results of dating suggest that the ice-wedge penetrated into the old Edoma after Holocence. Further attempts will be made as to deterime the direct ^{14}C dating of air samples from ground ice in the permafrost.

References

Fukuda, M. 1993. Genesis and Occurrence of Ice Complex (Edoma) in Lowland area along Arctic coast of eastern Siberia near Tiksi. In Proceedings of First Sympoium on Joint Siberian Permafrost Study between Japan and Russia in 1992:101-103.

Fukuda, M. 1994. Occurrence of Ice-Complex (Edoma) in Lena River Delta Region and Big Lhyavosky Island, High Arctic Eastern Siberia. In Proceedings of the Second

TABLE 1. Results of measurements.

Sample	CH_4 Concentration(%)	$\delta^{13}C$(‰)	^{14}C Dating(yBP)
OG34	0.21	−71.3	3,539 ± 87
LZ-1	4.57	−72.1	4,782 ± 113

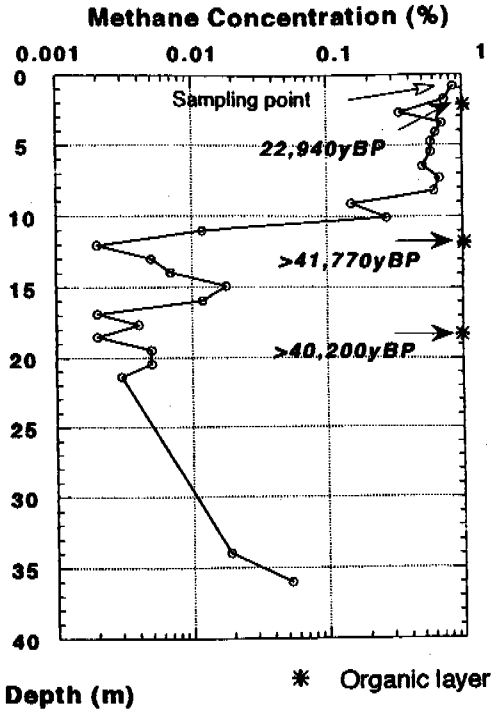

FIG. 5. Methane concentration profile with ^{14}C dating results at Oiyagoskii Yar.

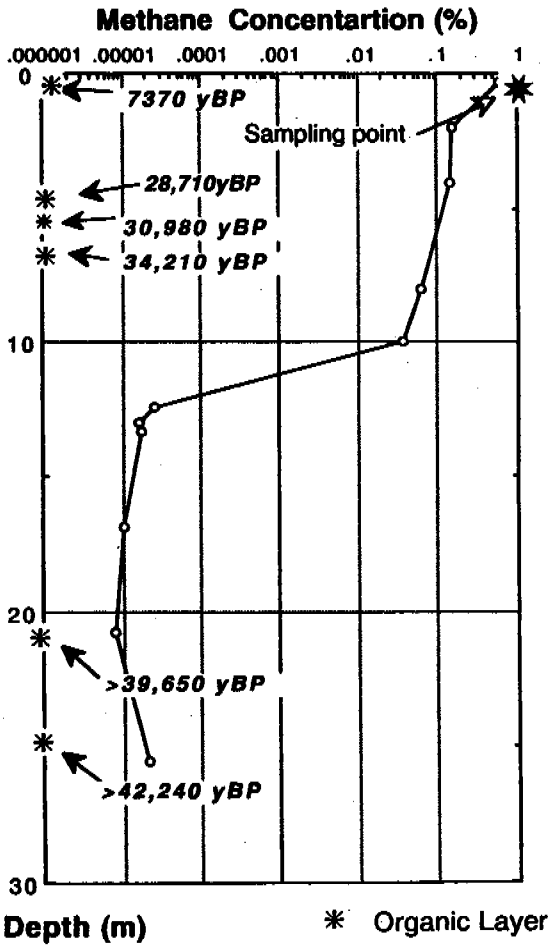

FIG. 6. Methane concentration profile with ^{14}C dating results at Big Lyhavosky Island.

Sympoium on Joint Siberian Permafrost Study between Japan and Russia in 1993:5–13.
Kaplina, T.N., and A.V. Lozhkin. 1984. Age and History of Accumulation of the "Ice Complex" of the Marinetime Lowlands of Yakutia. in Late Quaternary Environments of the Soviet Union, edited by A.A. Velichiko, Univ. of Minnesota Press,147–151.
Moriizumi, J. 1993. Master Thesis, Department of Nuclear Engineering, Nagoya Univ. (*In Japanese*)
Nakamura, T., and N. Nakai. 1988. Fundamentals of radiocarbon dating — with accelerator mass spectrometry — , Mem. Geo. Soc. Japan., No.29:83–106. (*In Japanese*)
Popov, A.I. 1969. Underground ice in the Quaternary deposits of the Yana–Indigirka lowland as a genetic and stratigraphic indicator. In The Periglacial Environments, ed. by T. Pewe, 55–64.
Stevens, C.M., and A. Engelkemeir. 1988. Stable carbon isotopic composition of methane from some natural and anthropogenic sources. J. Geophys. Res., 93:725–733.
Stuiver, M., and H.A. Polach. 1977. Discussion Reporting of ^{14}C Data, Radiocarbon, 19, No.3:355–363.
Stuiver, M. 1983. International agreements and the use of the new oxalic acid standard, Radiocarbon, 25, No.2:793–795.
Wahlen, M. et al. 1989. Carbon–14 in Methane Sources and in Atmosheric Methane: The Contribution from Fossil Carbon. Science, 245:286–290.

Study plan on the water and energy cycle and land surface processes in Siberia

TETSUO OHATA[1], YOSHIHIRO FUKUSHIMA[1], TAKESHI OHTA[2], and TETSUZO YASUNARI[3]

[1]Institute for Hydrospheric-Atmospheric Sciences, Nagoya University, Furo-cho, Chikusa-ku, Nagoya 464-01 Japan; Tel: +81-52-789-3478; Fax: +81-52-789-3436
[2]Faculty of Agriculture, Iwate University, 3-18 Ueda, Morioka 020 Japan
[3]Institute of Geoscience, University of Tsukuba, Tenoudai, Tsukuba 305 Japan

Introduction

A project called GAME (GEWEX Asian Monsoon Experiment) within the framework of WCRP/GEWEX (Global Energy and Water Experiment) has been discussed at Japan National Committee for WCRP since 1991. GAME was approved as a international project in January 1994 by GEWEX SSG. The main objectives of the Project are;
1) to understand the role of Asian monsoon in the global energy and water cycle;
2) to improve the simulation and seasonal prediction of Asian monsoon by the global climate models and numerical forecasting models;
3) to understand multi-scale interactions in the energy and hydrological cycles in the Asian monsoon regions; and
4) to access the impact of monsoon variability on the regional hydrology cycle.

The strategy for implementing the above objectives are;
1) intensive regional observations;
2) satellite-based observations;
3) long-term monitoring of the surface radiation and energy budgets;
4) four-dimensional data assimilation;
5) modeling studies; and
6) data archives.

The area of the regional studies related to above 1, are planned in the regions of tropical monsoon regions, sub-tropical and temperate monsoon regions, Tibetan Plateau and Siberian Permafrost regions. The first phase of the study is from 1996 to 2000, and second phase is from 2001 to 2005. The following is the tentative plan proposed by the university groups in the above committee as for Siberia region. Science plan of GAME is published as Japan National Committee for WCRP (1995). A Japanese version of this plan of Siberian Region is reported in Ohata and Ohta (1995). Some parts of this report are already described in Yasunari (1994) presented at the same symposium held in January 1994.

Description of regional study in Siberia

Background and aim of study.—The importance of land surface processes in the regional and global water cycle has been recognized in recent years. Many large projects investigating the relation of interactions on low to highly vegetated land surface and atmosphere system have been done and are also planned in various regions. However, such works have been limited in the permafrost area which dominates large area on continents. Among such area, Siberia being located at the northern half of the Eurasian continent, holds the widest permafrost area, but have not been an object of investigation in the past.

The land surface in Siberia is characterized by tundra and taiga which mainly consists of coniferous tree belts. The surface layer of the permafrost, snow cover and vegetation

contributes much to the water/energy fluxes and strongly regulates the various components of the water cycle such as the evapotranspiration and runoff. The seasonal cycle and variation of water cycle in this region is characterized by the interaction between the cryosphere, biosphere and atmosphere. Furthermore, the large rivers which drain northward from this region contribute fresh water supply to the Arctic Sea which in turn modify the hydrological and thermal conditions of the Arctic Sea. The variation of runoff of these large rivers is determined through the water cycle processes on land surface, and will have influence on the climatic conditions in the Arctic. However, these processes have not yet been studied in depth nor fully clarified.

The present global warming been predicted to be occurring most intensely in the northern part of the Eurasian continent radically over Siberia where permafrost zone is dominating. Spatial and temporal distribution patterns of snow and ice will also change by interacting with the permafrost conditions. They will affect the water cycle through change in ground surface conditions, soil moisture, hydrology and evaporation. In order to understand the possible changes, processes needs to be modeled, but the land surface processes in taiga and tundra regions have not been clarified yet.

Based upon these scientific backgrounds, the present study focuses on the investigation of the characteristics of water and energy cycles in the Siberian region under various spatial and temporal scales to clarify 1) the physical processes related to water/energy fluxes and storage of water and heat on land surface, 2) the role of land surface processes including snow cover, permafrost and vegetation in regional water cycle, and 3) their variabilities. This study will primarily be based on field observational study, and analysis of conventional data sets and model these processes for variability study and climate models. This study is proposed as one of the core projects for the GAME which contributes to the main aim of GEWEX, that is the global water–energy cycle, through the regional study of area where it is characterized by seasonal snow cover and permafrost.

Two main study themes.—The main study themes are as follows:

1) seasonal and interannual variation of the surface water/energy fluxes and surface conditions, and land surface–atmosphere interactions on representative surfaces in the tundra and taiga region.
2) seasonal variation of hydrological processes in a small drainage area in tundra and taiga region.
3) long–term variation of regional climate, land surface conditions, and surface water/heat fluxes by use of existing data sets and automatic station network.
4) large–scale water/energy circulation in the large drainage area, and their relation to the thermal and thermodynamic conditions in the Arctic ocean and influence to climatic variation.

Study regions and sites.—The following drainage areas and sites will be taken as study areas.

1) Drainage area: Lena, Yenisei, and Ob will be taken as the large drainage areas.
   Yenisei, Ob: drainage area analysis will be made by permanent station data.
   Lena: intensive land surface study and drainage area study will be made.
2) Study sites within Lena River basin:
   a) Tiksi (72°N, 129°E): tundra, small drainage area will be taken.
   b) Yakutsk (62°N, 129°E): taiga, small drainage area will be taken.
   c) Nogorny (56°N, 125°E) or Aldan (58°N, 125°E): mountain taiga.
   d) Tynda (55°N, 125°E): mountain taiga. Facility of State Hydrological Institute.

a), b) and c) or d) will be considered as intensive observation areas. The height of trees in

taiga region is approximately 15m.

Plan of investigation.—Following will be the tentative study plan.

1) Measurement of land surface fluxes of water and energy on different land surfaces (spatial scale: less than 10 km^2) (corresponds to study theme 1). Long-term data of atmosphere-land surface condition and one dimensional surface fluxes will be obtained by use of tower measurements. All the water/energy fluxes and storage components will be measured and they will be modeled. Relationships between permafrost ground layer, forest and evapotranspiration will be investigated intensely. Duration of this measurement will be five years or more in order to clarify interannual variations.

2) Observation of hydrological cycle in small drainage area (spatial scale: 100 km^2 to 10,000 km^2) (corresponds to study theme 2). This is the main scale of the field observation. Method of study consists of establishment of measurement network within the drainage area. Analysis of data from permanent stations, surface and ground measurements, air-borne measurements and analysis of satellite data will be made. This scale will contribute to the establishment of the macro-hydrological model. Duration of this measurement will be 1 to 2 summer seasons.

3) Observation of atmosphere-land surface interaction (corresponds to theme 1). Influence of land surface variation to the atmospheric conditions by radiosonde observations will be investigated. Hydrological effect due to snow cover melting, characteristics of the atmospheric boundary layer and others will be clarified. Observations will be made in some periods during one annual cycle including winter.

4) Data collection and analysis of water cycle components in the large drainage areas (corresponds to study themes 3 and 4). Study drainage areas will be Lena, Yenisei, and Ob. Analysis will be done for areal precipitation, snow cover and river runoff and snow cover, and mapping the surface conditions from satellite data. Data collection of surface meteorological data, aerological data, land surface data and hydrological data.

5) Observation concerning interpretation of existing data and acquisition of surface meteorological data for areal water/energy balance study (corresponds to study theme 3 and others). Establish automated observation network as part of (AAN; Asian AMeDas Network) needed for the regonal water/energy balance evaluation and interpretation of the long-term data set. Data evaluation will be done.

Concluding remarks

Siberian Regional Study is just at the start line. Proposed time schedule of the study period is: preparation period (1994-95), phase 1 (1996-2000), and phase 2 (2001-2005).

Presently, researchers from seven universities are active in promoting this project. In the future, GAME itself will begin to take international structure and finalize the study and implementation plans. This may force to change slightly the descriptions of the project.

As GAME holds international study fields, it needs to collaborate and negotiate with the other international projects in the similar area, such as WCRP/ACSYS, IGBP/BAHC and BIG and others. Also, there is a need to cooperate with the existing national projects in Japan.

References

Japan National Committee for WCRP. 1994. GEWEX Asian Monsoon Experiment (GAME) Science Plan. Japan National Committee for WCRP. p. 88.

Ohata, T., and T. Ohta. 1995. GAME Observational Project çW, Siberia. J. Japan Soc. Hydrol and Water Resour., 8, No. 2.

Yasunari, T. 1994. Energy and Water Cycle in Siberia. in Proceedings of the Second Symposium on the Joint Siberian Permafrost Studies between Japan and Russia in 1993 (Ed. G. Inoue). NIES/FFPRI/HU, p.231.

2

Methane/ Atmospheric Chemistry

Estimation of methane emission from Siberian tundra wetlands

TOMOKO NAKAYAMA

Institute of Low Temperature Science, Hokkaido University, N19W8, Sapporo 060 Japan
Tel: +81-11-716-2111 Ext. 5491; Fax: +81-11-706-7142

Introduction

Tundra wetland in the arctic region has been identified as a major source for the atmospheric methane. In the tundra wetland, methane is produced by decay of organic soil during summer in an active layer, which denotes the uppermost seasonal thaw layer of the permafrost. It has been observed that methane flux is positively correlated with ground temperature (e.g., Crill et al. 1988, Bartlett et al. 1992) and with thaw depth (Whalen and Reeburgh 1992), thus suggesting a positive feedback between the methane emission and climatic change. It is therefore important to estimate both the present methane emission from the tundra wetland and its future change.

In previous studies, the annual methane emissions from the tundra wetlands have been estimated using area of wetland, daily methane flux measured in the field, and length of the methane production season. In general, the methane flux has been averaged for summer measurements in several limited regions, mainly North America. However, this estimation is not accurate due to the lack of consideration in seasonal and spatial variabilities of the methane flux.

The objective of this study is to provide a more accurate estimate of the methane emission from the tundra wetlands in Siberian permafrost area. On the basis of the data obtained from the field observations in the methane flux and other environmental factors in a Siberian tundra area in 1993, the daily methane flux is expressed as a function of environmental factors. Using this function, the annual methane flux and emission from Siberian tundra wetlands are estimated with explicit seasonal and spatial consideration.

Relationship between methane flux and environmental factors

Time-series variations of the methane flux, water table depth, thaw depth and ground temperatures were observed on Mustakh Island (71.5°N) located off the coast of Tiksi, Sakha republic, Russia, in July and August, 1993 (Nakayama and Akiyama 1994). The methane fluxes were measured at two fixed sites; One was a waterlogged site covered with sedge (site MW) and the other was a dry site covered with moss (site MD). The results of the measurements are shown in Fig. 1. The values of methane flux of the sites MW and MD were different from each other due to their different conditions of soil moisture. The range of methane fluxes at the site MW was from 15.9 to 76.3 [mg CH_4 m^{-2} day^{-1}], while at the site MD, the methane fluxes were nearly zero. The daily mean temperature averaged in thawed layer (MDGT: mean daily ground temperature) fluctuated between 0.5 and 5.3 °C during the observational period. The temporal variation of daily methane flux at MW was similar to that of the MDGT.

It is known that the methane production by methanogens (methanogenic bacteria) in anaerobic wetland soil is affected by the soil moisture and the ground temperature. The thaw depth is also an important factor because the methanogens start to produce methane when the ground temperature rises above 0°C. In this study, a parameter "centimeter-degrees" is introduced as the factor controlling the methane flux from the tundra wetland. This parameter

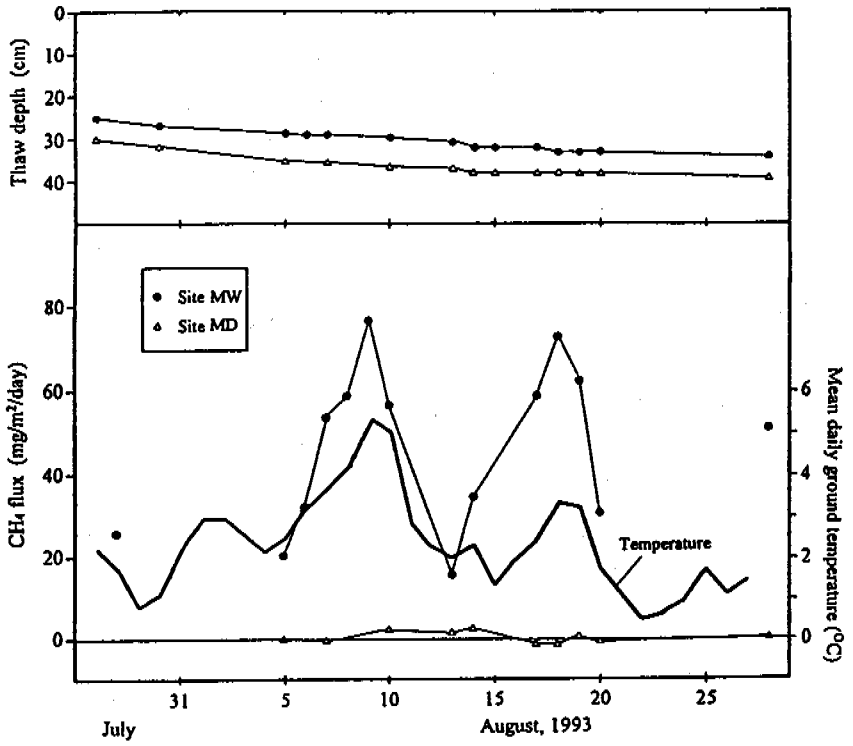

FIG. 1. Temporal variations of methane flux, thaw depth, and mean daily ground temperature at the sites of MW and MD in Mustakh Island, in July and August 1993.

is defined as a product of the thaw depth and the MDGT. Similar parameter was also proposed by Whalen and Reeburgh (1992). It is a significantly reasonable index of methane emission from the tundra wetland, since it accounts for the integration of net microbial activity over a thaw layer.

The results of the time-series observation on Mustakh Island indicate that the daily methane flux from the MW site was significantly correlated with the centimeter-degrees and expressed as a linear function of it. The annual methane fluxes from the Siberian tundra wetlands are estimated using this linear relationship, assuming that Mustakh Island is a representative site of these areas.

Calculation of ground temperature profile and thaw depth

Ground temperature profile and thaw depth can be calculated using a heat conduction model with phase change (Nakayama et al. 1993). The centimeter-degrees is obtained from these values. In this model, one-dimensional heat conduction equation is numerically solved using an implicit finite difference technique. Time step and grid spacing are 1 day and 10 cm, respectively. The following parameter are required for the numerical simulation. The first groups are properties of sediments, such as thermal conductivity, volumetric heat capacity and volumetric water content. These parameters were calculated from densities of the sediments, fluctuations of the ground temperatures, and water contents, which were measured on Mustakh Island and other sites in Siberian tundra wetlands. The second required parameters are the upper and lower thermal boundary conditions. The condition of the upper

boundary is given as annual fluctuation of mean daily ground surface temperature. The lower boundary is at a depth of 10 m below the surface and its condition is assumed to be a constant temperature which is equal to mean annual ground surface temperature. In order to apply this model to the place where the ground temperature is not measured, the annual variation of ground surface temperature is given in the sinusoidal form using its annual mean and annual range values.

Using this model, the MDGT and the thaw depth were calculated for Kalakhari Island in 1993. The island is located at the mouth of the Lena river (72.0 °N). The annual mean and annual range of ground surface temperatures in 1993 were −11.3 °C and 36.0 °C, respectively. The centimeter–degrees were obtained from the calculated MDGT and thaw depth, and thus the daily methane fluxes were estimated. The results are shown in Fig. 2. This figure implies that methane is released from early June to the middle of September and the annual methane flux is 4.0 [g CH_4 m^{-2} yr^{-1}].

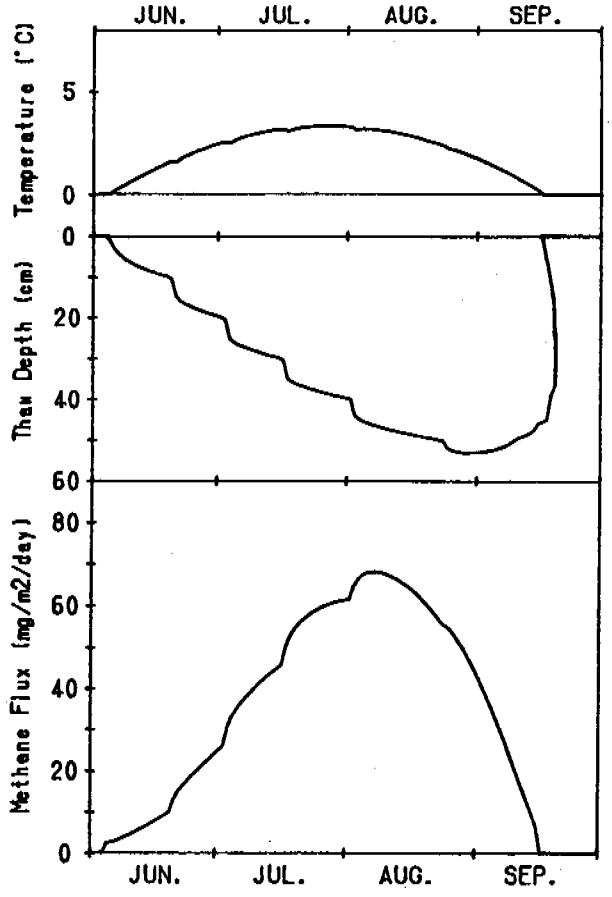

FIG. 2. Simulation of MDGT (upper), thaw depth (middle) and methane emission (lower) on Kalahari Island.

Estimation of methane emission

Aselmann and Crutzen (1989) reported the distribution and percentages of global natural wetlands on a 2.5° latitude by 5.0° longitude grid system. Using this information and a vegetation map of the Siberian region, the area of Siberian tundra wetland is estimated as 202.3 x 10^9 m^2. In this study, the annual methane emission is estimated for the 2.5° x 5.0° grid system from 67.5 °N to 75.0 °N and from 50.0 °E to 180.0 °E, including the Siberian tundra area. The annual mean and annual range of air temperature are roughly given from contoured maps by Gavrilova (1981) and Fukui et al. (1985). The percentages of area covered by wetlands, annual mean and annual range of air temperature for each grid are shown in Table 1. These data are used in the numerical solution.

The results of computations are summarized in Table 2. The annual methane flux [g CH_4 m^{-2} yr^{-1}] and emission [Gg CH_4 yr^{-1}] (1 Gg = 10^9 g) are calculated at each grid. The maximum flux is 14.3 [g CH_4 m^{-2} yr^{-1}] at a grid centered at 68.75 °N and 52.5 °E. The minimum is 0.9 [g CH_4 m^{-2} yr^{-1}] at a grid centered at 73.75 °N and 77.5 °E. The maximum value is about 16 times larger than the minimum because of the difference of the air temperatures. Table 3 indicates zonally summed methane emission. The total methane emission from the Siberian tundra wetlands is estimated as 1.0 [Tg CH_4 yr^{-1}]. This occupies about 1 % of the methane emission from the global natural wetlands (115 Tg).

Summary

In this study, the "centimeter–degrees", which is defined as the product of thaw depth and mean daily ground temperature, is adopted as the parameter determining the daily methane flux. Using the linear relationship between the methane flux and the centimeter–degrees, the methane emission is able to estimate taking the seasonal and spatial valiabilities of the methane flux into consideration. The total annual methane emission from the Siberian tundra wetlands was estimated as 1.0 [Tg CH_4 yr^{-1}] by calculating the centimeter–degrees from the air temperature data at each of the 2.5° latitude by 5.0° longitude grids.

References

Aselmann, I., and P.J. Crutzen. 1989. J. Atmos. Chem. 8:307–358.

Bartlett, K.B. et al. 1992. J. Geophys. Res. 97:16,645–16,660.

Crill, P.M. et al. 1988. Global Biogeochem. Cycles 3:371–384.

Fukui, E. et al. 1985. Climate of Japan and the world. Tokyodo Syuppan, Tokyo, pp. 163. (*in Japanese*).

Gavrilova, M.K. 1981. Present climate and permafrost on the continent. Academy of Science, USSR, Novosibirsk, pp. 112. (*in Russian*).

Nakayama, T. et al. 1993. Proc. Sixth Int. Conf. on Permafrost, Beijing, China, 488–493.

Nakayama, T., and A. Akiyama. 1994. Proc. Second Symp. on the Joint Siberian Permafrost Studies between Japan and Russia in 1993, Tsukuba, Japan, 37–39.

Whalen, S.C., and W.S. Reeburgh. 1992. Global Biogeochem. Cycles 5:261–273.

TABLE 1. Distribution of tundra wetland, annual mean and annual range of air temperature for the 2.5° lat. and 5.0° long. grids, including Siberian tundra wetlands.

Percentage of area covered by wetland
Mean annual air temperature (°C)
Annual range of air temperature (°C)

Longitude

Latitude	50.0 ↕ 55.0	55.0 ↕ 60.0	60.0 ↕ 65.0	65.0 ↕ 70.0	70.0 ↕ 75.0	75.0 ↕ 80.0	80.0 ↕ 85.0	85.0 ↕ 90.0	90.0 ↕ 95.0	95.0 ↕ 100.0	100.0 ↕ 105.0	105.0 ↕ 110.0	110.0 ↕ 115.0	115.0 ↕ 120.0	120.0 ↕ 125.0	125.0 ↕ 130.0	130.0 ↕ 135.0	135.0 ↕ 140.0	140.0 ↕ 145.0	145.0 ↕ 150.0	150.0 ↕ 155.0	155.0 ↕ 160.0	160.0 ↕ 165.0	165.0 ↕ 170.0	170.0 ↕ 175.0	175.0 ↕ 180.0
75.0 ↕ 72.5	-	-	-	2.3 -10.0 28.0	-	2.3 -12.0 30.0	-	2.3 -13.0 36.0	2.3 -13.5 38.0	18.1 -14.0 38.0	2.3 -15.0 38.0	6.7 -14.5 38.0	-	6.7 -15.0 40.0	4.4 -15.0 40.0	22.5 -14.0 40.0	-	-	-	-	-	-	-	-	-	-
72.5 ↕ 70.0	-	-	-	4.4 -10.0 32.0	9.5 -11.0 34.0	11.7 -11.5 36.0	4.4 -12.0 38.0	-	11.7 -12.5 40.0	2.2 -13.0 40.0	2.2 -13.5 40.0	-	-	-	-	2.2 -13.5 40.0	-	24.8 -15.0 40.0	24.8 -14.5 40.0	27.2 -15.0 40.0	11.7 -14.5 40.0	24.8 -14.0 40.0	-	-	-	-
70.0 ↕ 67.5	6.8 -4.0 28.0	8.9 -5.5 30.0	6.8 -6.5 32.0	2.3 -7.5 34.0	2.3 -9.0 38.0	6.8 -10.0 40.0	4.5 -10.0 40.0	2.3 -10.0 42.0	-	-	-	-	-	-	-	-	-	-	-	11.3 -13.5 50.0	24.8 -13.5 50.0	38.1 -13.5 40.0	8.9 -13.0 42.0	11.3 -13.0 40.0	20.2 -12.5 36.0	8.9 -12.0 34.0

TABLE 2. Estimates of the annual methane flux, the area of wetland and the annual methane emission from Siberian tundra wetlands.

Annual flux of methane ($g/m^2/yr$)
Area of wetland ($10^6 m^2$)
Annual emission of methane (Gg/yr)

Longitude

Latitude	50.0 ↕ 55.0	55.0 ↕ 60.0	60.0 ↕ 65.0	65.0 ↕ 70.0	70.0 ↕ 75.0	75.0 ↕ 80.0	80.0 ↕ 85.0	85.0 ↕ 90.0	90.0 ↕ 95.0	95.0 ↕ 100.0	100.0 ↕ 105.0	105.0 ↕ 110.0	110.0 ↕ 115.0	115.0 ↕ 120.0	120.0 ↕ 125.0	125.0 ↕ 130.0	130.0 ↕ 135.0	135.0 ↕ 140.0	140.0 ↕ 145.0	145.0 ↕ 150.0	150.0 ↕ 155.0	155.0 ↕ 160.0	160.0 ↕ 165.0	165.0 ↕ 170.0	170.0 ↕ 175.0	175.0 ↕ 180.0
75.0 ↕ 72.5	-	-	-	1.7 1.0 1.7	-	0.9 1.0 0.9	-	2.2 1.0 2.2	2.6 1.0 2.6	2.1 7.8 16.4	1.3 1.0 1.3	1.6 2.9 4.6	-	2.0 2.9 5.8	2.0 1.9 3.8	2.9 9.7 28.1	-	-	-	-	-	-	-	-	-	-
72.5 ↕ 70.0	-	-	-	3.7 2.2 8.1	3.5 4.7 16.5	4.0 5.8 23.2	4.5 2.2 9.9	-	5.0 5.8 29.0	4.2 1.1 4.6	3.6 1.1 4.0	-	-	-	-	3.6 1.1 4.0	-	2.0 12.3 24.6	2.5 12.3 30.8	2.0 13.5 27.0	2.5 5.8 14.5	2.9 12.3 35.7	-	-	-	-
70.0 ↕ 67.5	14.3 3.8 54.3	11.7 5.0 58.5	11.1 3.8 42.2	10.3 1.3 13.4	10.6 1.3 13.8	9.9 3.8 37.6	9.9 2.5 24.8	11.9 1.3 15.5	-	-	-	-	-	-	-	-	-	-	-	11.1 6.3 69.9	11.1 13.9 154.3	3.6 21.3 76.7	5.5 5.0 27.5	4.2 6.3 26.5	2.7 11.3 30.5	2.3 5.0 11.5

TABLE 3. Summary of zonal estimates of methane emission in Siberian tundra wetlands.

Latitude (degree N)	Area of wetland ($10^9 m^2$)	Annual methane emission (Tg / yr)
75.0 - 72.5	30.2	0.1
72.5 - 70.0	80.2	0.2
70.0 - 67.5	91.9	0.7
Total	202.3	1.0

CO_2 and CH_4 emission from wetlands in west Siberia

G. INOUE[1], S. MAKSYUTOV[1], and N. PANIKOV[2]

[1]*National Institute for Environmental Studies, Onogawa, Tsukuba, Ibaraki 305 Japan*
Tel: +81-298-51-6111; Fax: +81-298-51-4732
[2]*Institute of Microbiology, RAS, 7/2 prosp. 60-let. Oktyabrya, Moscow 117811 Russia*

Abstract. CH_4 and CO_2 emissions were measured by chamber technique in a number of wetlands typical of west Siberia. CH_4 emission rates varied from -20 to 2400 mg CH_4/day/m^2 depending on the environmental factors. A positive relationship was found between the emission rate and the following variables: soil temperature, ground water level, and soil acidity, although respective correlation coefficients were mostly low. Spatial distribution of CO_2 emissions was normal, while CH_4 fluxes were distributed log-normally. The methane fluxes from W-Siberian wetlands turned out to be one order of magnitude higher than that reported for natural wetlands of Canada and Europe. Natural wetlands in west Siberia may play a significant role in the global budget of atmospheric methane.

Introduction

Northern wetlands contain about 14% of the global stored organic carbon, and are believed to be the largest natural source of atmospheric CH_4 (Matthews and Fung 1987, Cicerone and Oremland 1988). Evidence for this statement comes primarily from the data on latitudinal distribution of CH_4 and ^{13}C-CH_4 in atmosphere with maxima of total methane concentration and its light 'biogenic' isotope at high latitudes (Fung et al. 1991, Quay et al., 1988). However recent direct measurements undertaken mainly in USA and Canada (Roulet et al. 1992, Harris et al. 1993) revealed rather low intensity of CH_4 emission from boreal and sub-Arctic wetlands: extrapolation of flux studies provide the range of 10-35 Tg yr^{-1}, which is one order of magnitude lower than the previous global estimates of 100-200 Tg yr^{-1} (IPCC 1992). To resolve this contradiction we need more reliable and complete data on the sources and sinks of methane. A large gap is now evident for wetlands located in the former USSR, particularly for the biggest West Siberian Lowland, which has not been surveyed for the methane emission. The present communication summarizes the results obtained by a research team of NIES and Moscow Institute of Microbiology in collaboration with other Institutes on extensive and mechanistic studies of CH_4 and CO_2 emission to atmosphere from natural wetlands.

Study sites

The measurements of CH_4 and CO_2 fluxes were performed in the Tomsk Area, Settlement Plotnikovo, Field Station of the Institute of Soil Science and Agrochemistry, RAS. This site belongs to Vasyugan Lowland, the main part of West-Siberian Lowland, the biggest wetland of the World. Measurements were performed in July-August of 1993-1994 at 3 particular sites: i) Floodplain of Iksa river (narrow strip of wetland along the main river stream which varies in width from 2-3 to 50 m); ii) Bakchar bog, which occupies flat watershed between rivers Iksa and Bakchar, total area is about 20 km × 150 km. The bog's margin is covered by sparse pine forest, the central accessible part of the wetland is a non-forested ombrotrophic bog, plant community is represented by *Eriphorum, Carex* sp. and *Sphagnum* sp., peat thickness is typically 1.0-1.5 m, pH 3.5-5. The measuring chambers

were installed every 50–100 m along the transect from the periphery to the center of the bog at two locations: 57°01'N, 82°35'E (3–6 km northbound from motorway Tomsk–Bakchar) and 56°53'N, 82°50'E (6–8 km in southbound direction). We were not able to include the very center of the Bakchar bog for sampling, 10–20 km from the motorway, where peatland is associated with mosaic of small and medium lakes (up to 1–2 km in diameter); iii) Iksa bog, ombrotrophic and mesotrophic bogs located on flat watershed between rivers Iksa and Shegarka, total area 15 km × 180 km, physiographic conditions and plant community are similar to that of Bakchar bog. The location of the fluxes measurements was 56°58'N, 83°11'E.

Methods

Net CH_4 and dark CO_2 fluxes were determined by static chamber technique (Whalen and Reeburgh 1988). The chamber consisted of two parts: i) a permanent square stainless steel base (40 cm × 40 cm), and ii) a removable solar reflecting, insulated plastic cover. The base was inserted into the soil not later than 0.5 h before the start of measurements to bring the system to equilibrium. To avoid false gas evolution caused by peat compaction, each measuring site was provided with light bridges for accommodation of operator. Four duplicate air samples were taken from the chamber at 10–15 min intervals to plastic bags and delivered to a field laboratory within 1–4 hr. Methane concentrations were analyzed by gas chromatograph Chrom 5 (Czechoslovakia) or Zvet–110 (USSR) equipped with a flame ionization detector. Carbondioxide concentrations were measured by LiCor (USA). The minimum detectable fluxes were as low as 0.001 mg of carbon (CH_4 or CO_2) per m^2 per hr. Determination of dissolved CH_4: peat samples were taken from different depth by a borer and quickly (1–2 sec) transferred to gas–tight flask, dissolved gases were then displaced with saturated NaCl and analyzed by GC. Other determinations: the temperature of the air and peat (at the depth 2–5 cm) was measured by thermistors or mercury thermometers, pH and Eh were determined respectively with glass and platinum electrodes (portable potentiometer pH–150, USSR) at the water table level.

In 1994 a micro–meteorological technique has been applied to studying the methane flux at night time. A combination of a sonic anemometer with a microwave temperature profiler was used for studying the vertical profile of atmospheric temperature and turbulence parameters near the ground. An automated sampling system took the air samples from the 5 m tower every 2 hours for analysis with GC (CH_4) and NDIR (CO_2). Night time build–up of the concentration has been observed that will be used for flux estimations.

Results and discussion

Spatial variability of fluxes.—For several occasions we had the possibility to avoid the effects of temporal changes and examine the variations in sizes of CO_2 and CH_4 fluxes measured at one and the same time. Generally, variability of CO_2 fluxes was very low: coefficient of variation (CV) (standard deviation/mean × 100%) for the most studied wetlands remained within the limits 2–10%. Methane fluxes were characterized by one order greater variability with CV 80–240%. Carbondioxide and CH_4 fluxes were differentiated also in terms of the distribution type. For instance, in Bakchar bog we have found normal distribution of CO_2 evolution rates (Kolmogorov–Smirnov test, significance level 0.999), while methane emissions were distributed log–normally (Figs. 1 and 2). Log–normality implies that values below the mean occurring more often than the values above the mean (median is significantly less than the mean), but there are few "hot–spots" of very intensive

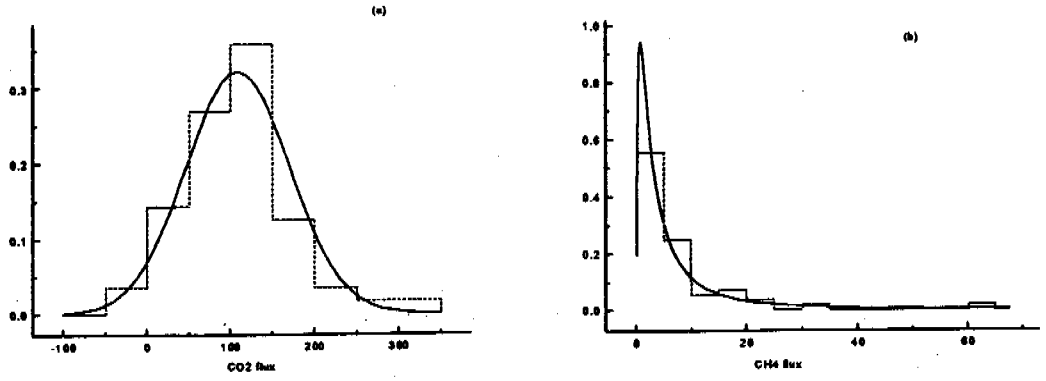

FIG. 1. Frequency distribution of CO_2 (a) and CH_4 (b) fluxes from Bakchar and Iksa bogs (n=56). Measurements were made by chamber technique along 3 transects (see site description). The data were approximated either by Gaussian function (CO_2 fluxes, mean 108.8 and standard deviation 62.7 mg C $h^{-1}m^{-2}$) or by log-normal distribution function (CH_4 fluxes, mean 1.31 and standard deviation 1.58 mg C $h^{-1}m^{-2}$).

methane emission (up to 2 g CH_4/day/m^2!) which strongly affect the overall flux. Mathematical expectation EX of any log- normally distributed random variable X is no longer equal to mean (as in the case of normal distribution) and is calculated as follows: EX = exp ($M+SD^2/2$), where M and SD are, respectively, mean and standard deviation for log X. Confidence limits for log-normally distributed fluxes may be estimated by Student's test only for n > 30 (Sharaf et al. 1986). In our case (n = 56) 0.95-confidence range for Bakchar bog was as much as 144-323 mg CH_4/day/m^2.

The relationship of emission with environmental factors.—Correlation-regression analysis was applied to the array of single-point measurements made in one and the same time of the year (second half of July, 1991-1993) for different sites (n = 177). Chosen environmental parameters were the air and soil temperatures, level of ground water table (GWT), pH, Eh, atmospheric pressure, and phytomass.

Thus, we can see that single-parameter relationships have very low predictive ability with respect to methane emission. One possible reason for this failure is that some factors (temperature, nutrient content, primary productivity etc) have almost the same strong effects on different elementary processes having opposite direction, e.g. methane generation and consumption. Therefore it seems to be very important to differentiate these two components of the CH_4 cycle.

TABLE 1. Correlation between CH_4 emission and ground water level as dependent on sampling size.

Site and time of measurements	n	Correlation coefficient
Iksa bog, 1993	16	-0.607
Bakchar and Iksa bogs, 1993	56	-0.288
West Siberia, 1992/93	79	-0.229
All sites, 1991/93	93	-0.157

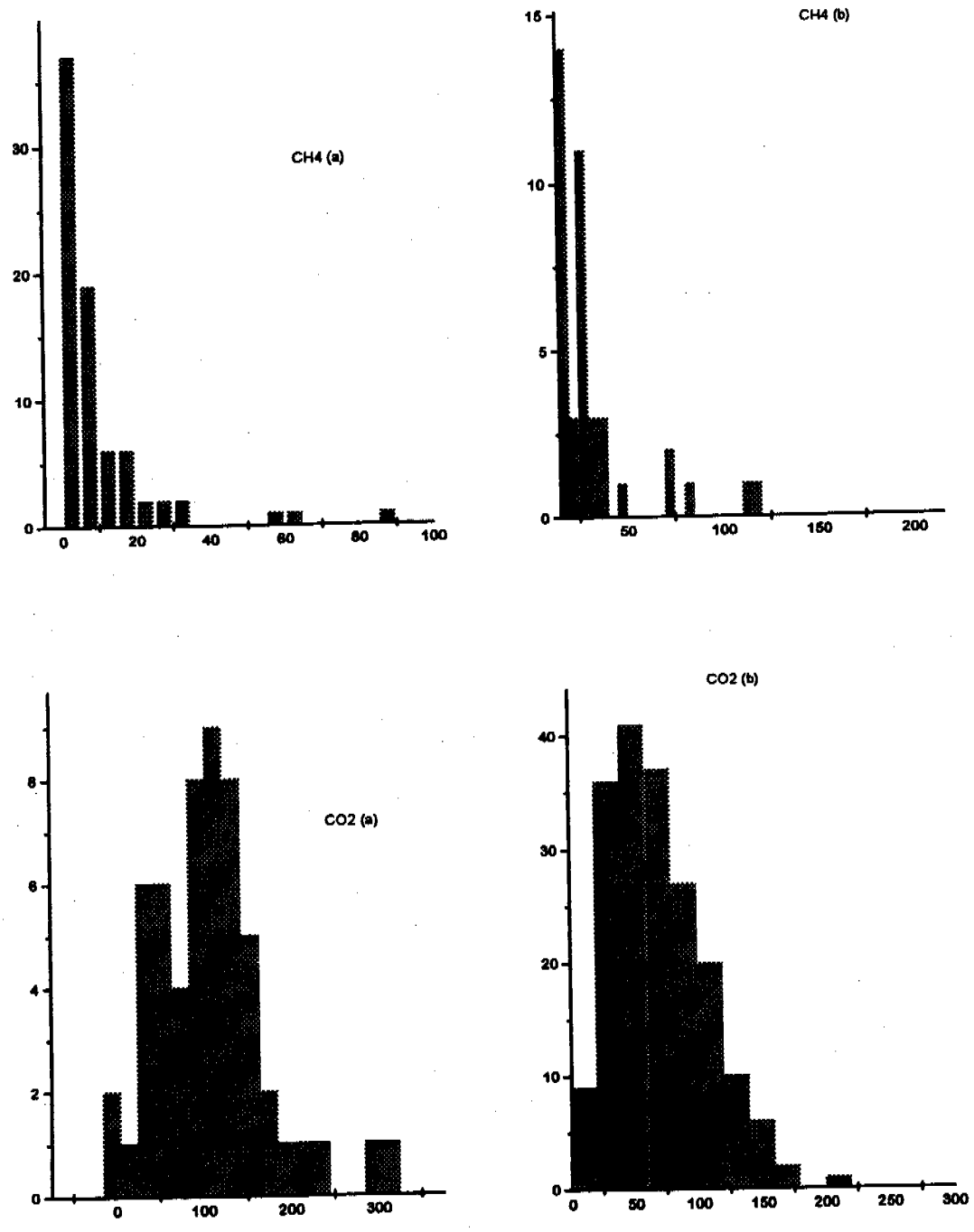

FIG. 2. Frequency distribution of CO_2 and CH_4 fluxes in 1993 and 1994. Two subsets are presented: a) Data for different sites measured at approximately the same time (July–August, about the noon from 10 a.m. till 2 p.m.); b) Data obtained for 6 permanent sites around the tower at various times.

Intersite comparison of methane fluxes.—Results of the CH_4 flux determination are summarized in the Table 2. Methane emission rates varied with a wide range from -20 to 2400 mg CH_4/day/m^2. The general feature of all sites was the large standard deviation and skewed distribution of the fluxes (median less than the mean).

Contribution of methane to total C emission was roughly estimated by the CH_4/CO_2 ratio. This ratio was usually more than 0.01 in flooded sites and depressions, where anaerobic microbial processes prevail over aerobic ones. At these sites, methanotrophic populations were not able to develop effective filter for the CH_4 consumption, because of reduced O_2 availability or some other unknown reasons. The lowest emissions were recorded in the ombrotrophic bogs of Tver Area. More intensive emissions were measured in Moscow area and polar Ural. But the highest numbers were obtained for Bakchar and Iksa bogs of Vasyugan Lowland with average CH_4 flux of 233, and 0.95 confidence range of 144–323 mg/day/m^2. Our data for Siberia are close to the emission values reported for Minnesota region with a range 93–402 mg/day/m^2, and are much higher than the fluxes measured at Hudson Bay Lowland with the average of six and 28 mg/day/m^2 for forested and non-forested bogs, respectively (Roulet et al. 1992, Harris et al. 1993). There are no explanations of this considerable divergence for one and the same type of wetlands. In any case, these results indicate how misleading may be the extrapolation of flux measurements from one region to another, even though vegetation and climate regimes may be broadly similar.

Conclusions

Spatial and temporal variations were shown to be basically different for CO_2 and CH_4 fluxes from wetlands. Dark evolution of CO_2 is normally distributed and characterized by regular diurnal, weekly and seasonal cycles closely related to plant productivity and environmental factors. Emission of methane is more variable with log-normal distribution pattern, chaotic and less predictable dynamics. The relationship of CH_4 fluxes with environmental factors may be successfully revealed by considering not only net flux but also separately the processes of methane formation and consumption. Our results indicate, that natural wetlands in west Siberia may play a significant role in the global budget of atmospheric methane. There is an urgent need for systematic measurements of CH_4 emission from these sites by combination of a chamber method with micro-meteorological and aircraft techniques.

References

Cicerone, R.J, and R.S. Oremland. 1988. Biogeochemical aspects of atmospheric methane, Global Biogeochemical Cycles, 2, 299–327.

Fung, I., J. John, J. Lerner, E. Matthews, M. Prather, L.P. Steele, and P.J. Fraser. 1991. Three-dimensional model synthesis of the global methane cycle, J. Geophys. Res., 96D: 13033–13065.

Harris, R., K. Bartlett, S. Frolking, and P. Crill. 1993. Methane emissions from northern high-latitude wetlands, In (R.S. Oremland, ed.) Biogeochemistry of global change: radiatively active trace gases, Chapman & Hall, New York, 449–486.

IPCC. 1992. Climate change 1992: The supplementary report to the IPCC Scientific Assessment (J.T. Houghton, B.A. Callander, and S.K. Varney, eds.), Cambridge University Press, Cambridge.

Matthews, E., and I. Fung. 1987. Methane emission from natural wetlands: global distribution, area, and environmental characteristics of sources, Global Biogeochemical

TABLE 2. A summary of methane flux measurements from studied Russian wetlands (flux units are mg CH_4 m^{-2} d^{-1})

Site	*Habitat,* number of measurements	*Mean*	*Stand.* Dev.	*Median*	*CH4/CO2* flux ratio
Halmer-Yu 67° 59'N 64° 42'E	Wet tussock tundra n=5	59.5	107.5	12.2	n.d.
Syktyvkar 61° 41'N 50° 45'E	Forested bogs n=9	19.2	46.1	3.5	n.d.
Kolyma 73° 46'N 161° 26'E	Polygonal bog complex n=13	27.5	21.4	25	n.d.
Sosvyatsky Moch, Tver 56° 10'N 32° 12'E	Drainage ditch n=123	68.9	74	54.7	0.0347
	Center n=205	9.5	19.3	5.1	0.0046
Moscow 54° 55'N 37° 38'E	Forested bog n=4	153.6	301	153.6	0.065
86 Kvadrat Tomsk 56° 22'N 84° 40'E	Forested bogs and fens n=23	21.1	43.8	6.7	0.006
Plotnikovo Vasyugan Lowland 56° 56'N 83° 10'E	Ombrotrophic bogs n=56	233.9	326.1	132.2	0.067
	Floodplain n=56	85.4	116.8	38.5	0.0144
Stand. Dev	standard deviation				

Cycles, 1:61–86.

Panikov, N.S., and A.Ju. Gorbenko. 1992. The dynamics of gas exchange between soil and atmosphere in relation to plant–microbe interactions: fluxes measuring and modelling. Ecological Bulletins, 42:53–61.

Panikov, N.S., A.M. Semenov, A.L. Tarasov, A.S. Belyaev, I.K. Kravchenko, M.V. Smagina,

M.V. Palejeva, V.V. Zelenev, and K.V. Skupchenko. 1993a. Methane production and uptake in soils of the European part of the USSR, J. of Ecological Chemistry, 1:7–18.

Panikov, N.S., A.A. Titlyanova, M.V. Palejeva, A.M. Semenov, N.P. Mironycheva-Tokareva, V.I. Makarov, E.V. Dubinin, and S.P. Efremov. 1993b. Methane emission from wetlands of southern part of West Siberia. Dokl. RAS, 330, 3:388–390.

Quay,P.D., S.L. King, J.M.Lansdown, and D.O. Wilbur. 1988. Isotopic composition of methane released from wetlands: Implications for the increase in atmospheric methane, Global Biogeochemical Cycles, 2:385–397.

Roulet, N.T., R. Ash, and T.R. Moore. 1992. Low boreal wetlands as a source of atmospheric methane, J. Geophys. Res., 97D:3739–3749.

Samarkin, V.A., D.G. Fedorov-Davydov, M.S. Vecherskaya, and E.M. Rivkina. 1993. CO2 and CH_4 emission on cryosols and subsoil permafrost and possible global climate changes, Adv. in Soil Science. (*in press*)

Sharaf, M.A., D.L. Illman, and B.R. Kowalski. 1986. Chemometrics. J.Wiley & Sons, New York.

Slobodkin, A.I., N.S. Panikov, and G.A. Zavarzin. 1992. Microbial formation and uptake of methane in tundra and boreal wetlands, Mikrobiologia, 61:683–691.

Whalen, S.C., and W.S. Reeburgh. 1988. A methane flux time series for tundra environments, Global Biogeochemical Cycles 2:399–409.

Continuous measrements of atmospheric methane and carbon dioxide at Yakutsk monitoring station

S. MAKSYUTOV[1], G. INOUE[1], N. FEDOSEEV[2], and D. FEDOSEEV[2]

[1]*National Institute for Environmental Studies, Onogawa, Tsukuba, Ibaraki 305 Japan*
Tel: +81-298-51-6111; Fax: +81-298-51-4732
[2]*Permafrost Institute, Yakutsk 10, 677018 Russia*

Introduction

Most of the atmospheric monitoring sites are located in remote locations, far from the large greenhouse gas source–sink areas (Boden 1991). Remote location makes observations useful for the global scale estimations, reducing ability to resolve regional scale variations. Yakutsk monitoring station is located in the forested area 18 km west of Yakutsk city. That point is downstream of a large area covered by Siberian forests and wetlands. The advantage of this place is that we can expect stronger methane and CO_2 signals from the Siberian ecosystems than in more remote locations. Continuous observations are necessary for achieving a reasonable level of an air mass classification, and for detecting concentration change caused by the synoptic scale atmospheric motions. Atmospheric composition measurements have been conducted since 1993: continuous measurements began at November 1993. This paper presents results of the preliminary data analysis.

Measurements and data correction

Sampling ports are located at a radio tower on the levels of 11, 44 and 77 m above the ground. Analysis is done by HP gas chromatograph with FID. Data are taken automatically, analysis cycle is repeated every two hours, providing 12 analysis a day for each sampling level and for the standard gas. The CO_2 and CH_4 concentrations are determined. Standard gas concentrations were analyzed separately and are determined to be 1.78 ppmv CH_4 and 361 ppmv CO_2. Concentration is obtained from ratio of a sample peak area to standard gas peak area. Some inconsistency with other standards is possible because of the different preparation methods. Correction was made by calculating the ratio of a component peak area in a standard gas to its concentration. Then this correction factor was interpolated in time to the moments of an air sample analysis. After that the concentration values are determined in the air samples. When concentrations at different levels are taken at different times, the concentration values are interpolated to the same time frame.

Selecting background conditions

During stable atmospheric conditions, vertical exchange is inhibited by the temperature stratification. This leads to a significant difference between surface layer and upper part of PBL. Also, a vertical concentration gradient at tower altitudes is larger during stable conditions if there is an influence of local sources. The data were filtered by rejecting the records with large concentration differences between levels. A concentration difference threshold of 0.01 ppm CH_4 and one ppm CO_2 was used for calculating monthly and weekly averages. It will be shown that this simple procedure is not effective in eliminating the cases with significant stratification so the monthly average concentration could not be regarded as

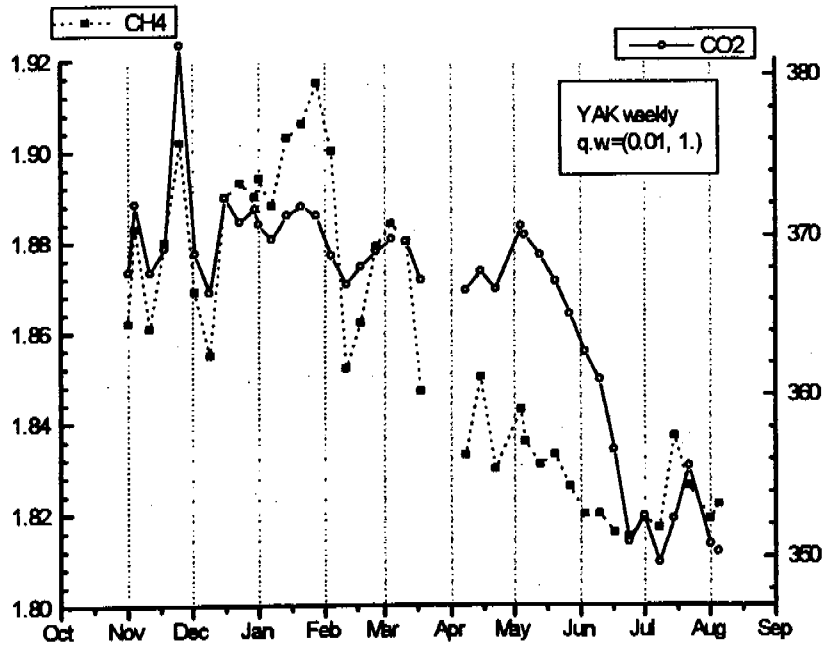

FIG. 1. Weekly average of CH_4 and CO_2 concentrations.

a value corresponding to PBL's vertically averaged value.

Results and discussion

Seasonal variation.—Seasonal variation. Weekly and monthly average values are presented in Figs. 1 and 2, respectively. Concentrations from the uppermost level are taken as reference. Dates correspond to the beginning of the period of averaging.

It is interesting to compare the concentration variations to those at Alert station. Most recent Alert station data provided by NOAA CMDL are used. Comparing the Alert station data to other high latitude stations at Mold Bay and Point Barrow, we may see that those show a similar seasonal cycle, with the same minimal and maximal values. What is important to mention is that a strong winter maxima of the methane and carbon dioxide concentrations observed at high latitudes. In Fig. 3, Alert station data are plotted together with Yakutsk station monthly averages. Yakutsk station's methane concentration data were corrected at this plot by subtracting an offset of 45 ppb. This makes it easier to compare the amplitude of a seasonal variation observed at those locations.

In general the seasonal variation has the same pattern in both locations. The time lag between springtime decrease of the concentration is approximately the same. An important difference one can mention is the amplitude of seasonal variation which is larger at Yakutsk. Without additional inter–calibration, it is difficult to say how much the summer values differ; however, winter values of Yakutsk are significantly larger. One possible explanation is that very strong stability is developed over Yakutia in the winter season, because of the radiative cooling. This leads to a buildup of concentrations near the ground. Although the station is downstream of the rural area, this could be an important factor. Relationship between methane and carbon dioxide in summer and winter is shown in Fig. 4, where one can see that in winter there is a positive correlation between carbon dioxide and methane concentrations, while it is not so clear in the summer. The correlation was also observed at Alert (Hopper

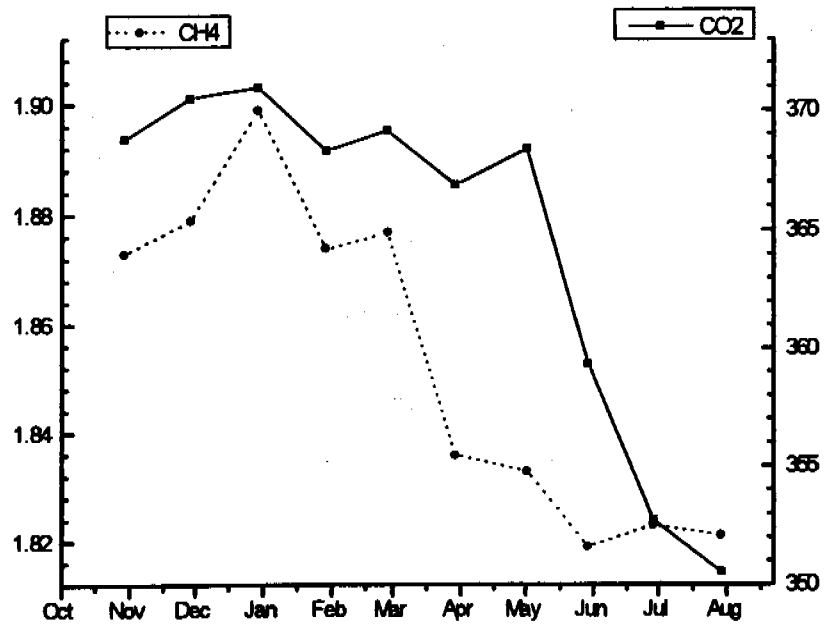

FIG. 2. Monthly average of CH_4 and CO_2 concentrations.

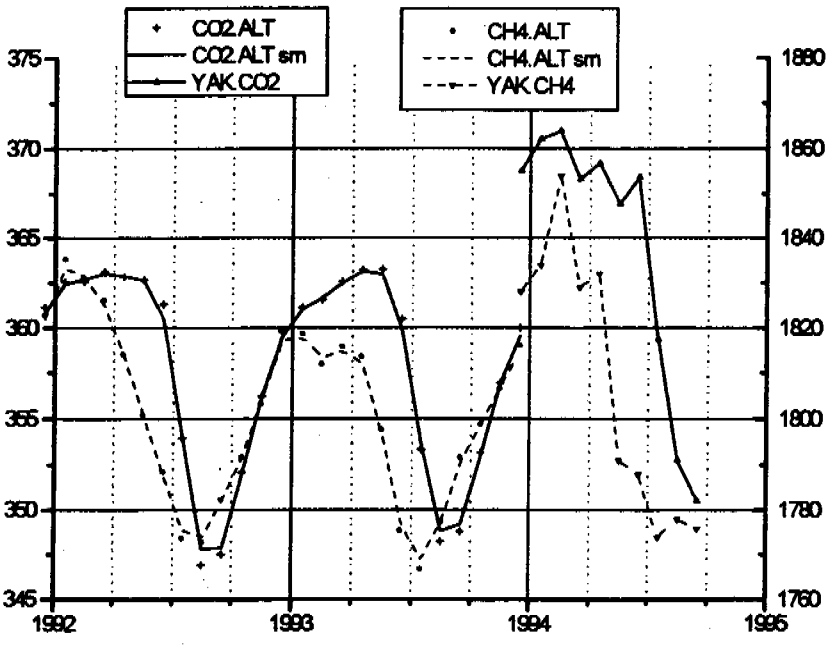

FIG. 3. Monthly means of CH_4 and CO_2 concentrations at Alert and Yakutsk.

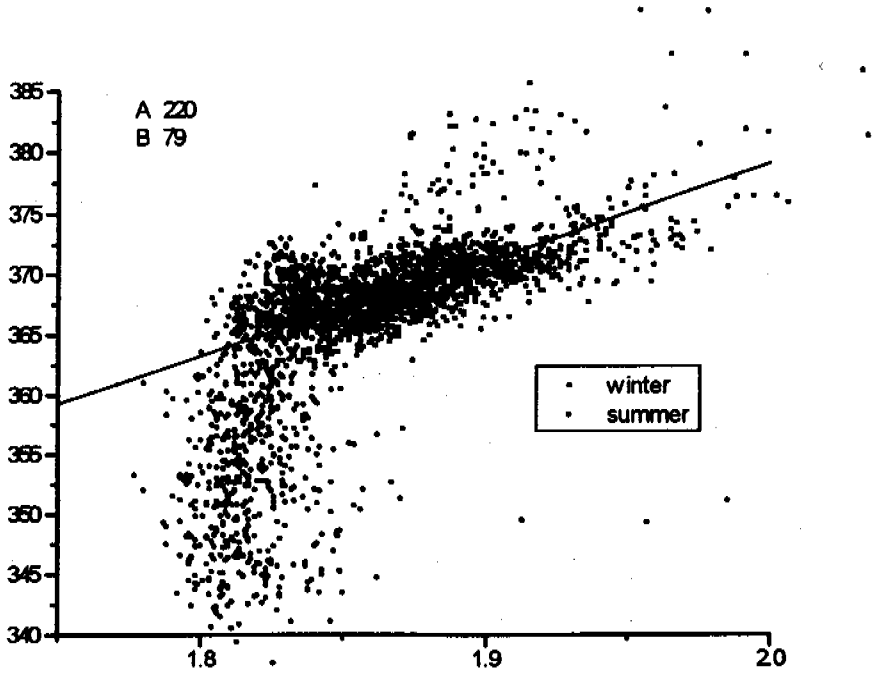

FIG. 4. Winter and summer relationships of CO_2 *versus* CH_4 concentrations.

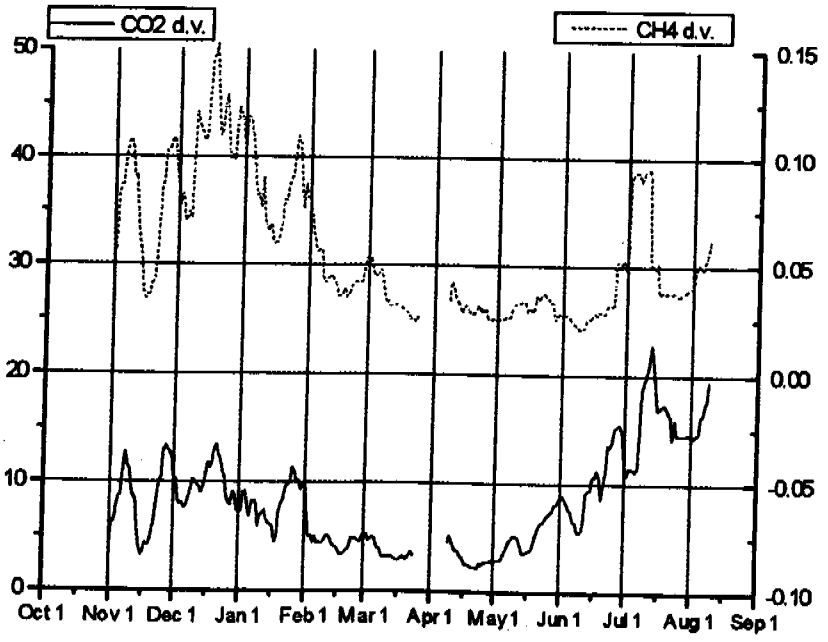

FIG. 5. Weekly averaged amplitude of a diurnal variation in CH_4 and CO_2.

1994). Winter time relationship can be expressed by the following regression formula:

$$CO_2 = 220 + 79 \cdot CH_4,$$

where concentrations are given in parts per million. The value of a regression slope agrees well with the results of airborne observations in March 1989 (Conway 1993). In summer, positive correlation exists between methane and carbon dioxide concentrations at nighttime locally, but the base value of CO_2 is changing during the season so it is hidden in the Fig. 4.

Diurnal variation.—Both in the summer and winter we could observe a correlation between carbon dioxide and methane. During the winter, the concentration variation does not show significant diurnal cycle, while in the summer, both methane and carbon dioxide exhibit apparent diurnal cycles with maximum after midnight and minimum in late afternoon. Diurnal variation of the concentration has been observed in the summer at all levels. Fig. 5 shows the weekly averaged amplitudes of daily variation (difference between daily maximum and minimum) for both methane and carbon dioxide.

The amplitude is high in winter as a result of slow mixing and accumulation of the emitted gases near the ground. The amplitude goes down in the spring as a result of better mixing in the boundary layer. In summer, the amplitude increases again as a result of biogenic emissions and night–time inversions in the surface layer. After the winter maximum, the CO_2 amplitude decreases in February and starts growing at the beginning of May. Amplitude growth continues from May up to the middle of July, which account for the intensification of the respiratory activity with the increase of the surface temperature and growth of the plants. In the case of methane, there is no such pronounced increase in the amplitude in the summer.

Flux estimation.—Assuming that the inversion develops up to 300 m altitude at nighttime in the summer, it would be possible to estimate nighttime emission rates of methane and carbon dioxide. Table 1 summarizes the emission rate estimates for typical amplitude ranges and approximate values of nighttime inversion height and duration. Fluxes were calculated using a formula:

TABLE 1. Nocturnal emission rate estimates.

Accum. time (h) t =	8	H =	300 m		
			Fluxes		
Gas	ΔC ppm	g/m^2/h	gC/m^2/h	g/m^2/d	
CH4	0.02	0.00050	0.00037	0.012	
CO2	20	1.37	0.37		

$$Flux = \frac{\Delta C \cdot H}{t}$$

Here ΔC = amplitude of diurnal variation, H = inversion layer thickness, t = accumulation time.

The estimated value of a methane emission rate corresponds to local sources from a natural ecosystem consisting of a forest with few alas observation spots. The methane emission rate is an order of magnitude lower than that at the alas spot. This is reasonable because the area fraction of alas is few percent of the total area, and there are few other sources of the methane.

Summary

1. Seasonal variation of CO_2 and CH_4 concentrations at Yakutsk is similar to that observed by background monitoring stations at high latitudes, with larger amplitude because of higher average concentrations in winter months.

2. Strong stability in winter leads to frequent observations of polluted plumes of anthropogenic origin, without a significant diurnal cycle. This effect is stronger at Yakutsk compared to other monitoring stations because of the dry continental climate.

3. Diurnal cycle of concentration variation is observed in the summer. The amplitude of the nighttime increase of the concentration gives a way to estimate local fluxes of CO_2 and CH_4.

References

Boden, T.A., R.J. Sepanski, and F.W. Stoss (eds.) 1991. Trends 91', Compendium of data on global change. ORNL/CDIAC–46, Oak Ridge, TN, 700 pp.

Conway, T.J., L.P. Steele, and P.C. Novelli. 1993. Correlations Among Atmospheric CO2, CH4 and CO in the Arctic, March 1989. Atmospheric Environment, 27A(17–18): 2881–2894.

Hopper, J.F., D.E.J. Worthy, L.A. Barrie, and N.B.A. Trivett. 1994. Atmospheric observations of aerosol black carbon, carbon dioxide, and methane in the high arctic. Atmospheric Environment. v. 28, n. 18, pp. 3047–3054.

Airborne measurement of atmospheric CH_4 over the West Siberian Lowland during the 1994 Siberian Terrestrial Ecosystem–Atmosphere–Cryosphere Experiment (STEACE)

Y. TOHJIMA, S. MAKSYUTOV, T. MACHIDA, and G. INOUE

National Institute for Environmental Studies, 16–2 Onogawa, Tsukuba 305 Japan
Tel: +81–298–51–6111; Fax: +81–298–51–4732

Introduction

Atmospheric methane (CH_4) concentration has increased rapidly during the past few hundred years. Since CH_4 absorbs infrared radiation at 7.66 μm, its increase in the atmosphere will contribute to global warming. In addition to this, CH_4 also plays an important role in the photochemical reactions initiated by reaction with hydroxyl radical (HO). Therefore it is considered that the increase will also affect the balances of the other reactive constituents.

CH_4 is produced mainly by bacterial methanogenesis under anaerobic conditions which occurs in wetlands, paddy fields, ruminant digestive systems and so on. Besides the bacterial CH_4, it is considered that about 20% of the atmospheric CH_4 originated from natural gas which is associated with oil/gas systems and coal mining.

The West Siberian Lowland (WSL), in which there are vast wetlands and a lot of gas and oil fields, is believed to play an important role as a source of atmospheric CH_4. To investigate the distribution of greenhouse gases including CH_4 and CO_2 over Siberia, the National Institute for Environmental Studies and the Central Aerological Observatory have collaborated on a flight experiment as a part of the Siberian Terrestrial Ecosystem–Atmosphere–Cryosphere Experiment (STEACE) since 1992. Here, we present results of the flight measurements over the WSL, especially over wetland and oil/gas field, during the STEACE in 1994.

Experimental

CH_4 measurement system used during the flight experiment in 1994 was the same as that in 1993. Continuous detection of the atmospheric CH_4 concentration was carried out by a C/FID (Combustion/Flame Ionization Detector) system developed by Tohjima and Wakita (1994). Sample air is passed through a heated column filled with Pt catalyst, on which non–methane hydrocarbons (NMHC) are reduced by combustion. Then the sample air is directly introduced to the FID. The C/FID system was calibrated by two standard air containing known amount of CH_4 (1.855 and 2.368 ppmv). The CH_4 concentrations were also measured by a gas chromatograph (GC) every 5 minutes.

Although the CH_4 concentration measured by the GC and the C/FID showed a good correlation, the concentration by the C/FID is slightly higher than that by the GC, and the discrepancy increased with the concentration. This discrepancy may be explained by the incompleteness of NMHC combustion. Using a linear regression line, the estimate of the CH_4 concentration by the C/FID was corrected so that it agrees with that by the GC. The accuracy of the C/FID system is 0.02 ppmv. The detail about the measurement system was given by Tohjima et al. (1994).

We loaded meteorological and chemical equipment including the C/FID system on an aircraft, Ilyushin–18, and carried out in–situ measurements, which were described in detail

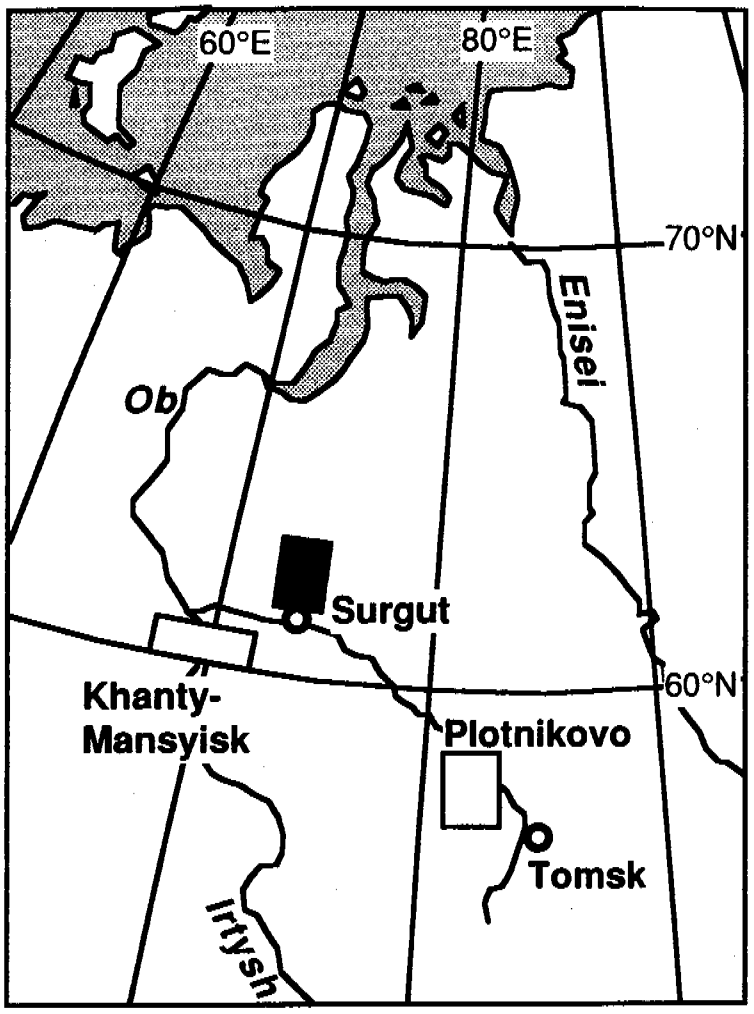

FIG. 1. Map showing the West Siberian Lowland. Study areas for flight observation are indicated by white rectangles (wetlands) and black rectangle (oil field).

by Inoue et al. (1994).

Results and discussion

Wetland.—We carried out airborne measurement over wetlands at Khanty–Mansiysk (61.05°N, 69.00°E) on July 31 and at Plotnikovo (57.85°N, 83.08°E) on August 3, 5 and 6, 1994. The flight pattern was designed to traverse the source area at several different altitudes sequentially, from lower to higher. For example, the results observed at Plotnikovo on

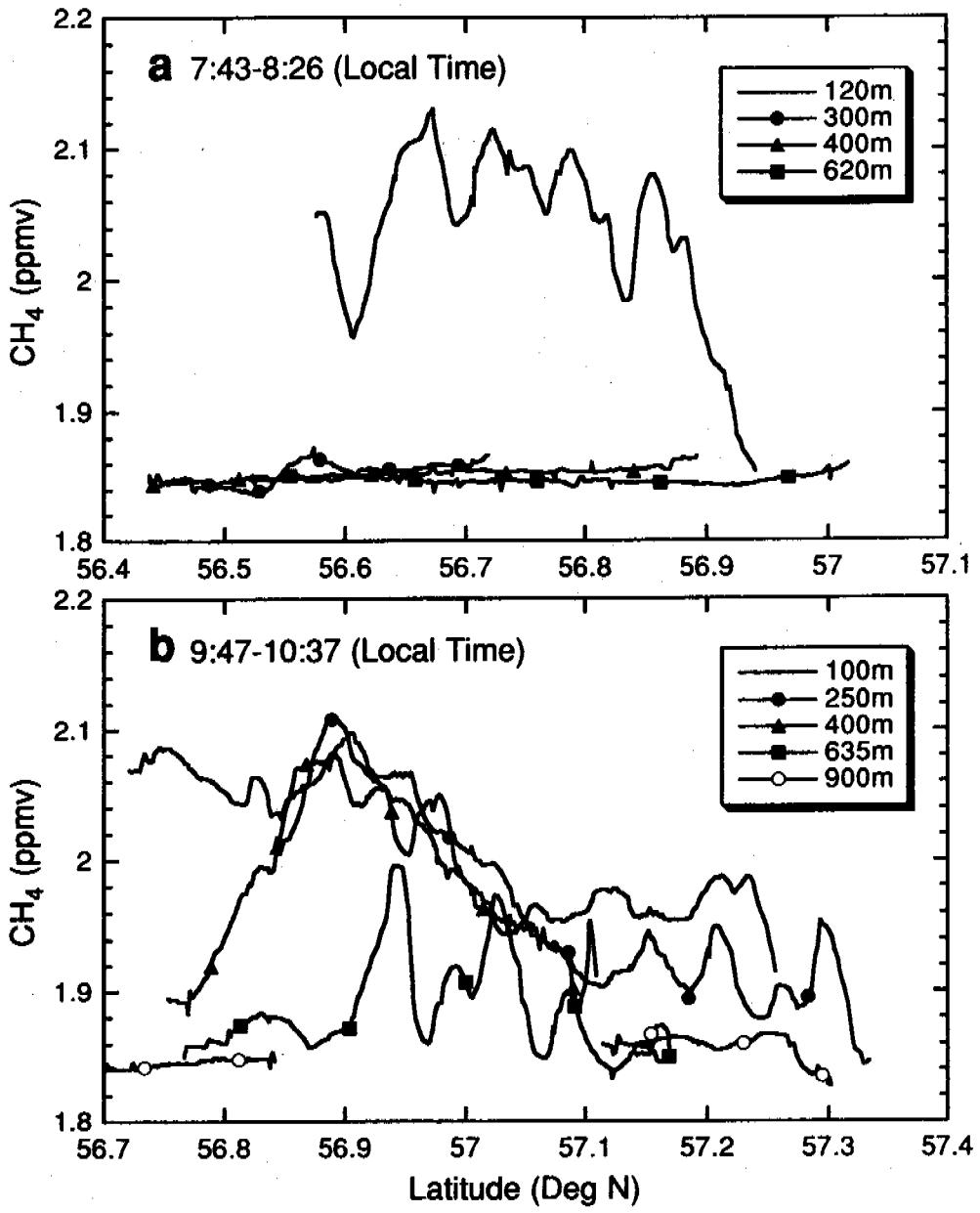

FIG. 2. Horizontal distribution of CH_4 concentration observed in Plotnikovo on August 3, 1994: (a) 7:43–8:26 local time and (b) 9:47–10:37 local time.

August 3 is shown in Fig. 2, where the horizontal CH_4 distributions covering more than 50 km are plotted along latitude. The distribution was observed from 07:47 to 08:29 local time (Fig. 2a) and from 09:42 to 10:37 local time (Fig. 2b)

In Fig. 2a the CH_4 concentration at an altitude of 120 m was significantly high and had a large variation, while the concentrations at higher altitudes were lower and had little variation. The distribution in Fig. 2b is different from that in Fig. 2a. Distribution at the higher altitude showed rather high concentration and, even at 600 m, the distribution showed a rapid change. The average CH_4 concentrations both from 7:44 to 8:29 (open circles) and from 9:42 to 10:37 (closed circles) are plotted against altitude in Fig. 3. These vertical profiles also depict a temporal change in distribution.

The observed changes in the CH_4 distribution may be explained as follows; during daytime, CH_4 that was emitted from the wetland is rapidly transported to the overlying atmosphere by vertical convection. At nighttime, strong temperature inversion is formed near the ground surface, where CH_4 from the wetland is accumulated. When insolation heats up the ground surface in the morning, the inversion layer is destroyed and the mixed layer grows. The change in the horizontally averaged CH_4 profiles clearly reflects the CH_4 transport process with growth of the mixed layer.

The CH_4 emission rate averaged over the observation area can be estimated from the amount of CH_4 in the mixed layer and the accumulation time. To evaluate the amount of CH_4 in the mixed layer, we must know the initial profile over the wetland before accumulation within the inversion layer. Moreover, the time of inversion-layer formation is also required for the calculation.

At the ground station in the wetland of Plotnikovo, the vertical temperature profile from the ground to the altitude of 600 m was measured by millimeter-wave scanning radiometer (Troitsky et al., 1993). The result indicated that the temperature inversion began to form at about 21:00 local time during the period of the flight experiment. At the same ground station the CH_4 concentration in the surface air was also measured every 2 hours. The local minimum value of the concentration in the afternoon on August 2 was observed at 21:20 local time, which agreed well with the result of the temperature profile. The minimum at the ground surface, indicated by an arrow in Fig. 3, was almost the same as the concentration over the mixed layer (Fig. 3). It suggests that the air mass in the mixed layer was well mixed and that, just before the formation of the inversion layer, the vertical CH_4 profile is rather straight up to several hundred meters. The shaded area in Fig. 3 is, therefore, the first approximation of the amount of CH_4 accumulated from the formation of the inversion layer to the time of the observation. In the actual calculation, we used vertical profiles that observed when the mixed layer developed up to several hundred meters for a practical reason.

Table 1 summarizes the amount of the accumulated CH_4, the accumulation period and the average emission rate at Plotnikovo. There are large variation in the estimation of the CH_4 emission rate, ranging from 40 to 146 $mg/m^2/day$. In Khanty-Mansiysk the aircraft flew over the area dominated by wetland and the area dominated by forested wetland on July 31, 1994. Assuming that the accumulation period in Khanty-Mansiysk is the same as that at Plotnikovo, we calculated the emission rates, which are also listed in Table 1. The emission rates were not so different between the wetland and the forested wetland.

The CH_4 emission rate presented here is based on many assumptions. For example, we assumed that there is no horizontal movement but only vertical mixing of the air. We also assumed that the CH_4 concentration at the ground surface is the same as that at the lowest altitude, usually about 100 m. Furthermore, the decision of the initial concentration value is rather arbitrary. Our estimation of the CH_4 emission rate, therefore, have large uncertainty. However, we think that it is important to estimate the CH_4 emission rate averaged over a

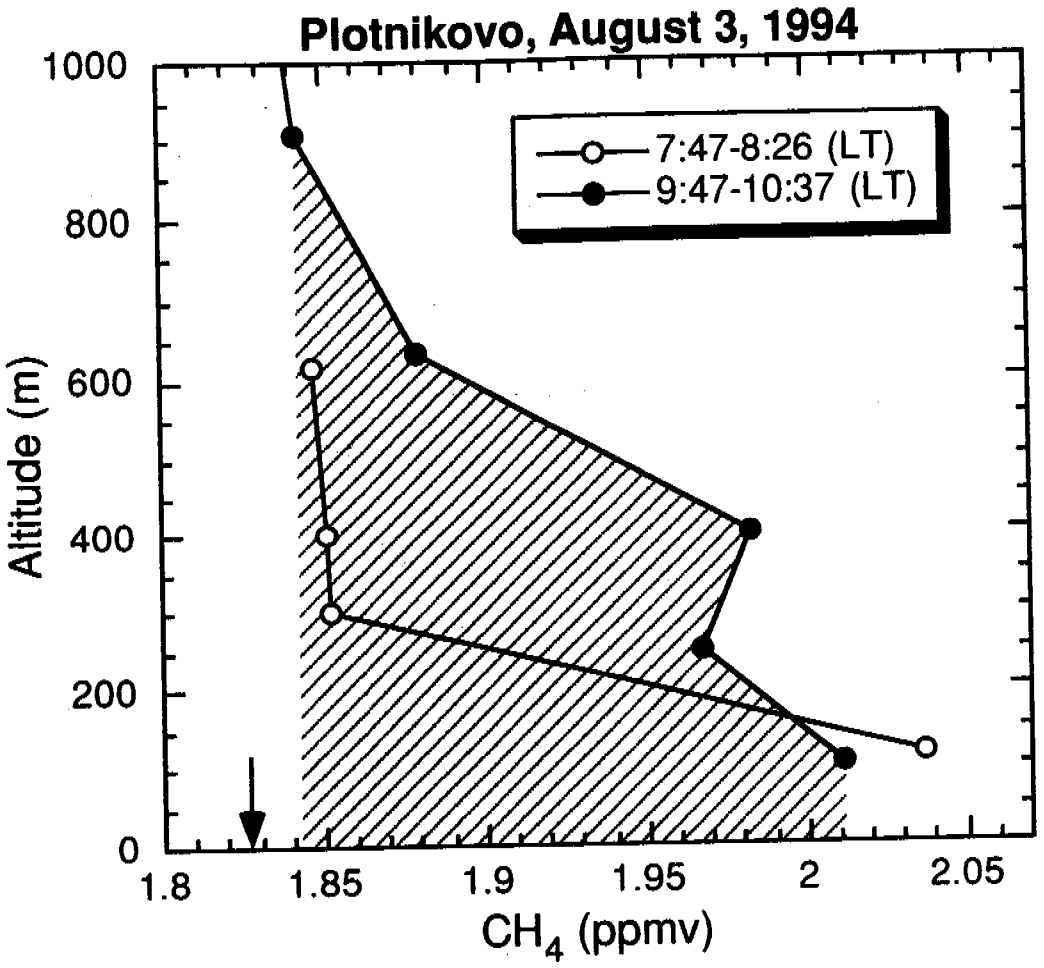

FIG. 3. Vertical profiles of the average CH_4 concentrations observed in Plotnikovo on August 3, 1994.

TABLE 1. CH_4 emission rate estimated from the CH_4 vertical profiles and the accumulation periods.

Table 1. CH4 emission rate estimated from the CH_4 vertical profiles and the accumulation periods.

Study Area	Date	Accumulated CH_4 (mg/m^2)	Accumulation Period (hour)	CH_4 emission rate ($mg/m^2/day$)
Plotnikovo	Aug. 3	55	13	102
Plotnikovo	Aug. 5	20	12	40
Plotnikovo	Aug. 6	79	13	146
Khanty-Mansiysk	Jul. 31			
Wetland		38	12.5	74
Forested Wetland		26	11.5	55

large area, because it is difficult to do so with the usual techniques including the chamber method.

Oil field.—Fig. 4 is a map showing the oil field located to the south of Surgut. In the figure the shaded area indicates the area of oil deposits. Solid triangles indicate the oil production sites. There are also underground oil pipeline (dashed lines). This area in Fig. 4 is predominately covered with wetlands and lakes; the CH_4 emission from the wetland was also expected. The aircraft flew along the thick and thin lines at the altitude about 150 m above the ground surface in the morning of August 1, 1994.

During the flight over the oil field, we observed prominent CH_4 peaks of which concentration are significantly high. Fig. 5 shows the largest CH_4 peak along the flight track in Fig. 4 (thick line). In the figures, the CH_4 concentrations measured by the C/FID (solid line) and GC (solid squares) are plotted along the longitude. The half width of the peak was about 30 seconds, corresponding to distance of about 3 km; the peak height was 0.8 ppmv. On the other hand, we were not able to find any CH_4 peaks over the oil deposit area with no oil production sites.

Such sharp and large peaks of CH_4 concentration have never been observed over wetlands without any oil/gas fields. The positions of the CH_4 peaks along flight track are also shown as open circles in Fig. 4. There are oil production sites or the underground oil pipeline or

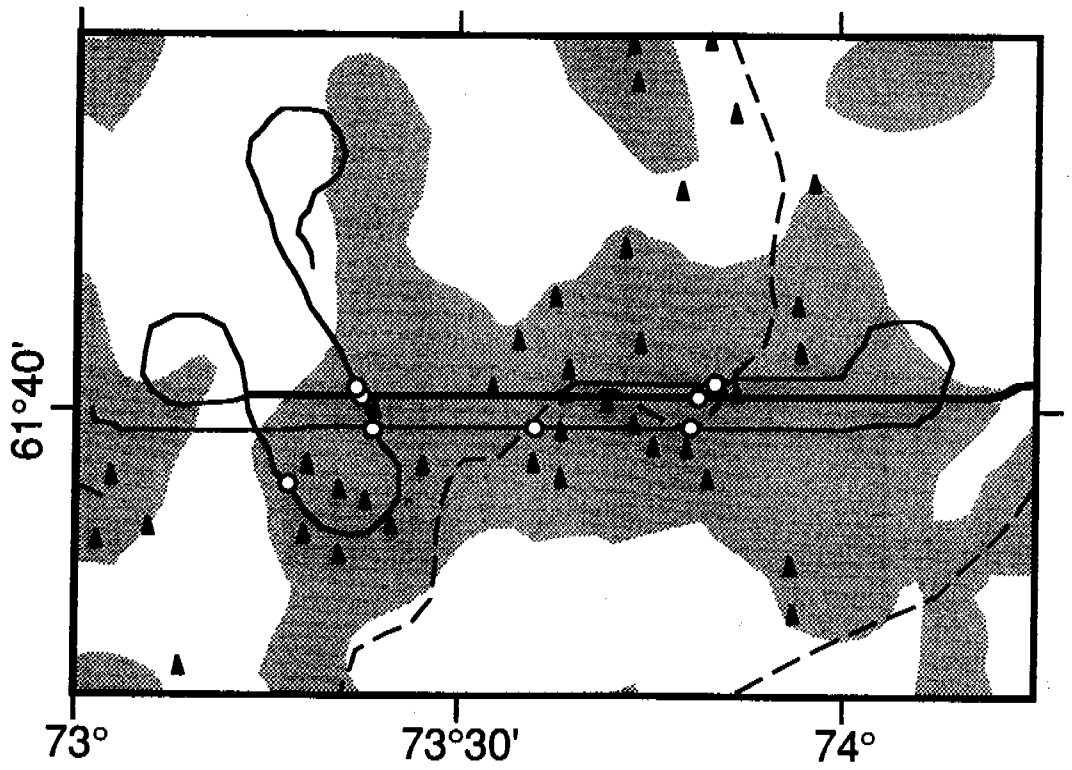

FIG. 4. Map showing survey area to the north of Surgut. Thick and thin lines indicate the flight track at an altitude of 150 m. Dashed lines are underground oil pipelines. The shaded areas indicate areas of oil deposits. Triangles indicate the oil production sites. Most of the area shown in this figure are dominantly covered with wetlands and lakes.

both near the peak positions. Therefore the CH_4 peaks may be produced by the natural gas leakage associated with the oil production or transportation or both.

Conclusions

We carried out airborne measurements of atmospheric CH_4 concentration over a CH_4 source region, wetland and oil field, in the West Siberian Lowland. In the wetland, we observed change in the CH_4 distribution associated with the growth of the mixed layer. From the amount of the accumulated CH_4 in the mixed layer, we roughly estimate that the CH_4 emission rates ranging from 40 to 150 mg/m^2/day. Over the oil field, we observed significantly sharp CH_4 peaks. Probably we detected leakage of natural gas from the oil production or transportation sites.

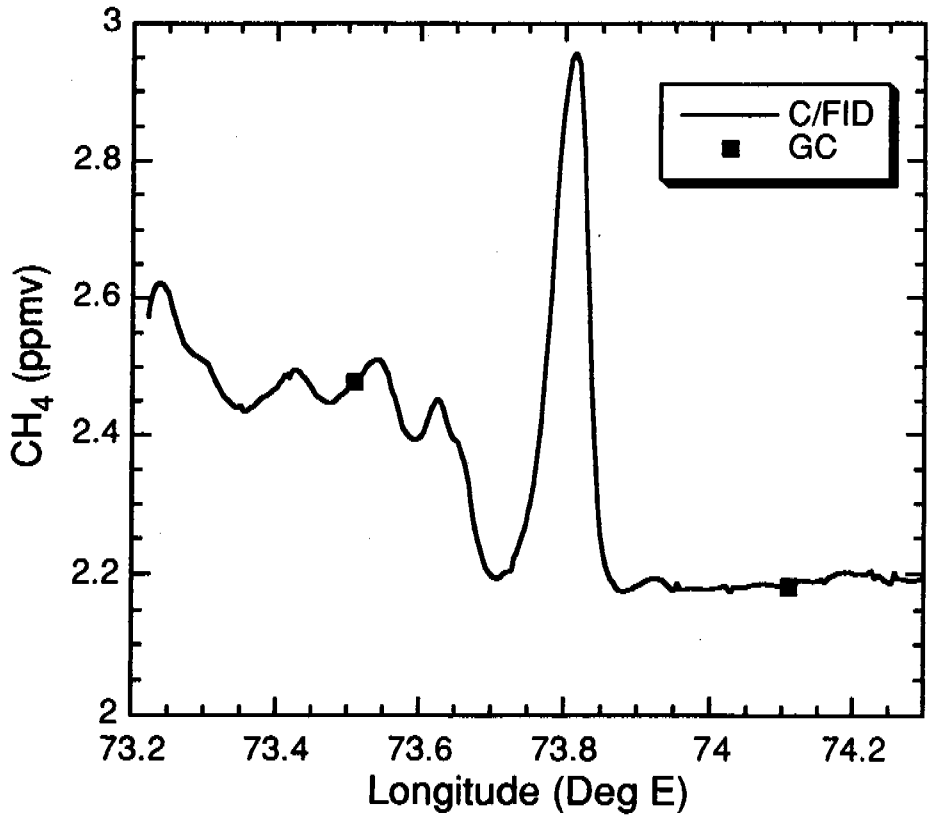

FIG. 5. CH_4 concentration measured by C/FID (solid line) and GC (closed squares) at an altitude of 150 m above ground surface along the thick line in Fig. 4.

References

Inoue, G., et al. 1994. Stratospheric ozone folding phenomena observed between Yakutsk and Tiksi, Airborne measurement of greenhouse gases over Siberia I. *In* Proceedings of the international symposium on global cycles of atmospheric greenhouse gases, Tohoku Univ., Sendai, Japan, pp.1–4.

Tohjima, Y., and H. Wakita. 1994. Development of a continuous measurement system and areal distribution of methane in some source areas, Appl. Geochem., 9:141–146.

Tohjima, Y., et al. 1994. Distribution and emission of CH_4 over the Central West Siberian Lowland "airborne measurements of greenhouse gases over Siberia III", *In* Proceedings of the Second Symposium on the Joint Siberian Permafrost Studies between Japan and Russia in 1993 (ed. G. Inoue), pp.61–76.

Toritsky, A. V., K.P. Gajkovich, V.D. Gromov, E.N. Kadygrov, A.S. Kosov. 1993. Thermal sounding of the atmospheric boundary layer in the oxygen absorption band center at 60 GHz. IEEE Trans. on Geoscience and Remote Sensing, vol. 31, N 1, January 1993:116–119.

Airborne measurement of atmospheric CO_2 concentration over the Siberia during the 1994 Siberian terrestrial ecosystem–atmpsphere–cryosphere experiment (STEACE)

T. MACHIDA, G. INOUE, and S. MAKSYUTOV

National Institute for Environmental Studies, 16–2 Onogawa, Tsukuba 305 Japan
Tel: +81–298–51–6111; Fax: +81–298–51–4732

Introduction

Atmospheric carbon dioxide (CO_2) plays an important role of maintaining global climate. Since the late 18th century, atmospheric CO_2 concentration has increased by the combustion of fossil fuels and deforestation (Siegenthaler and Oeschger, 1987). But we have only limited knowledge on understanding of the global carbon cycle quantitatively. To elucidate this problem, systematic measurements of the atmospheric CO_2 concentration have been conducted all around the world (e.g. Tanaka et al. 1987, Keeling et al. 1989, Conway et al. 1994). Since most of these observations were done either near a coast, on a small island, or on a ship, knowledge of CO_2 behavior over inland areas have been scarce.

To observe variations of the atmospheric CO_2, which is affected by the terrestrial biomass, continuous measurements of atmospheric CO_2 concentrations were carried out by using an airplane (IL–18, Central Aerological Observatory) over Siberia from July 29 to August 10, 1994.

Observation

A schematic diagram of our measurement system is shown in Fig. 1. The sampled air

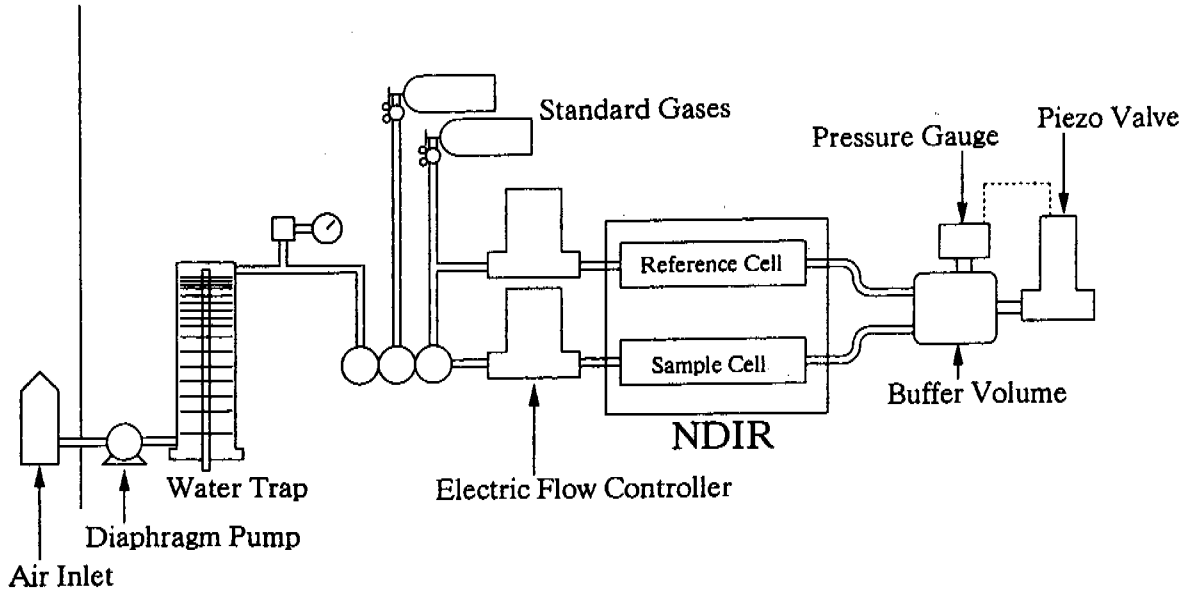

FIG. 1. Schematic diagram of the CO_2 measurement system on the airplane of IL–18.

was compressed by diaphragm pump and dried by the water trap that was cooled to −40°C by electric freezer. The CO_2 concentrations were determined against the standard gases of 331.94 and 378.69 ppmv by using a NDIR (LI-COR, type LI-6262). The flow rate of the sample and reference gases were kept constant by electric flow controllers. If one end of the reference or sample cell had been opened to the cabin atmosphere, the output of NDIR would vary in accordance with the cabin pressure change. Therefore, each end of the cell was connected to the buffer volume, and inner pressure of this volume was kept constant by a pressure gauge and a piezo valve. Fig. 2 shows the variations of CO_2 concentrations of the standard gases measured by this system during ascent of the airplane from the ground level to the altitude of 7000 m. The CO_2 concentrations in the standard gas varied only within 0.5 ppmv. This value was small enough to detect large variations of the atmospheric CO_2 concentrations over Siberia in the summer.

Results and discussion

Fig. 3 shows the spatial variations of CO_2 concentration at the altitudes of 150, 260, 380, 600 and 3000 m over a wetland near Khanty-Mansiysk (61.05°N, 69.00°E) on July 31. Between 8:15 and 9:03 local time (Fig. 3a), the CO_2 concentration at the altitude of 150 m

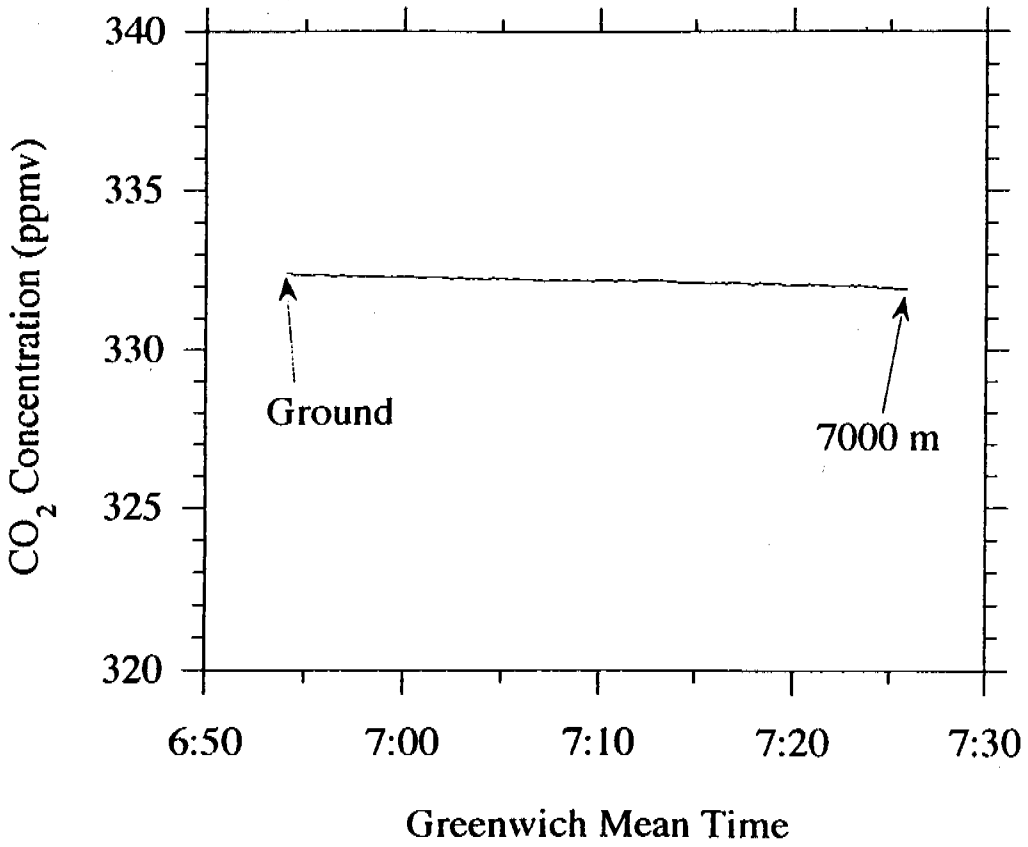

FIG. 2. Variations of the CO_2 concentration in the standard gas measured during ascent of the airplane from the ground level to the altitude of 7000 m.

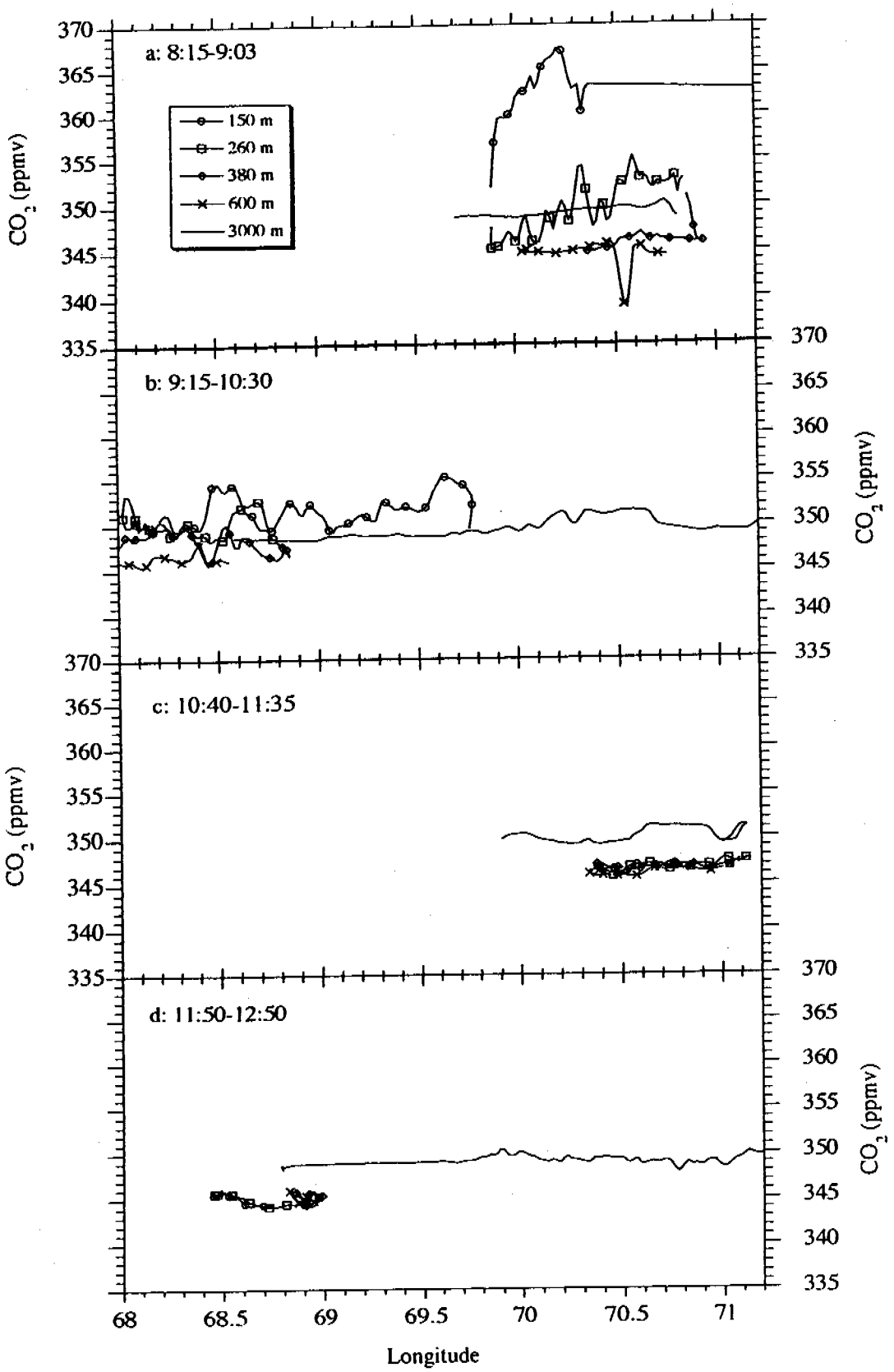

FIG. 3. Spatial variations of CO_2 concentration observed near Khanty-Mansiysk on July 31: (a) 8:15–9:03 local time, (b) 9:15–10:30 local time, (c) 10:40–11:35 local time and (d) 11:15–12:50 local time.

show a large spatial fluctuation and high values of 352–367 ppmv. The CO_2 concentration became lower with the altitude, the values being 339–346 ppmv at 600 m. But at the altitude of 3000 m, the concentrations were about 349 ppmv; larger than those at 600 m. From 9:15 to 10:30 (Fig. 3b), the CO_2 concentrations at 150 m show smaller values of 349–356 ppmv than those during 8:15–9:03 at the same altitude. On the other hand, the CO_2 concentrations at 260–600 m were higher than before. After 10:40, CO_2 concentration below 600 m took almost the same values.

The vertical profiles of CO_2 concentration on July 31 are shown in Fig. 4. Each point represents an average over horizontal distribution in Figs. 3a–d. It is clearly seen that the vertical gradient of the CO_2 concentration was extremely large at 8:15–9:03; the difference between 150 m and 600 m being about 18 ppmv. The high concentration in lower altitudes probably indicate that respirated CO_2 from land vegetation and release from oxidization of soil organic matter accumulated under the inversion layer during the nighttime. The lowest concentration at 600 m expresses the effect of biospheric CO_2 uptake during the previous daytime that remained until the morning. The upper air with low CO_2 concentration was transported downward by the growth of the mixed layer. Photosynthesis of land biomass also became strong during the daytime. Therefore, CO_2 concentration at 150 m largely decreased from 8:15–9:13 to 10:40–11:35. On the other hand, CO_2 concentration at 600 m increased during the times between 8:15–9:13 and 10:40–11:35, because high CO_2 concentration at lower altitude was transported upward. Therefore, the vertical gradient decreased with time, and disappeared by 10:40–11:35. At 11:50–12:50, vertical convection was intense, and further biospheric CO_2 uptake was observed. The diurnal variations of CO_2 concentration could not be seen at the altitude of 3000 m.

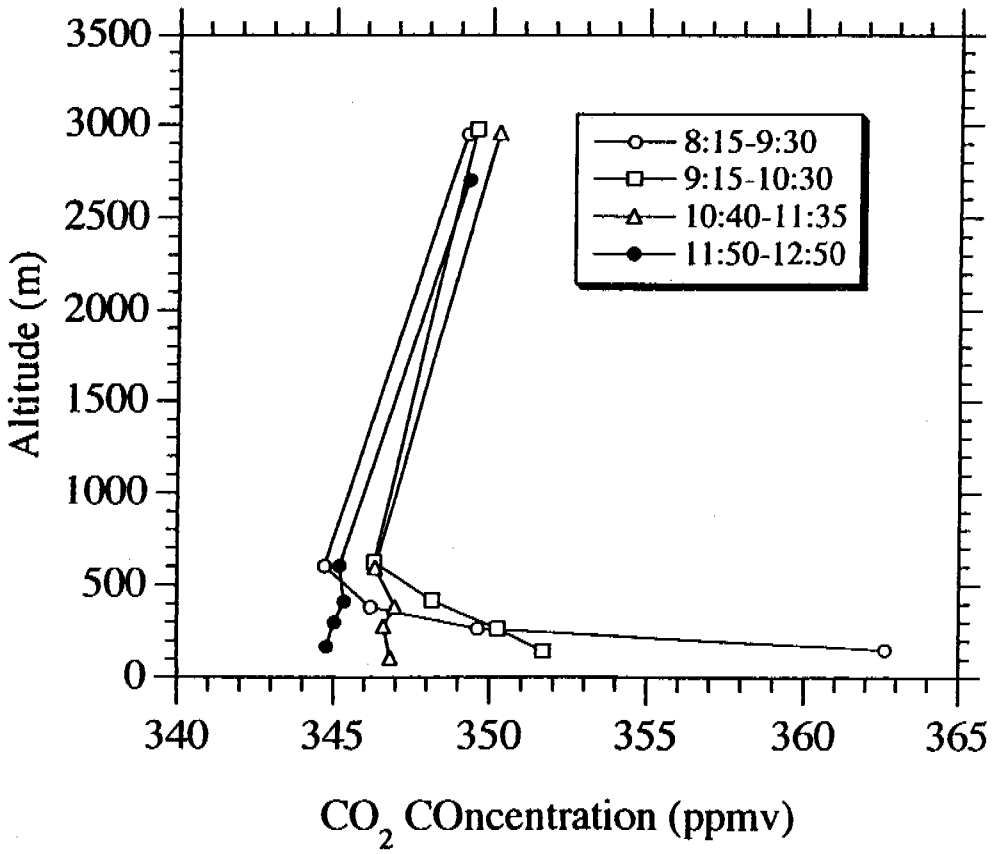

FIG. 4. Vertical profiles of CO_2 concentration near Khanty-Mansiysk on July 31.

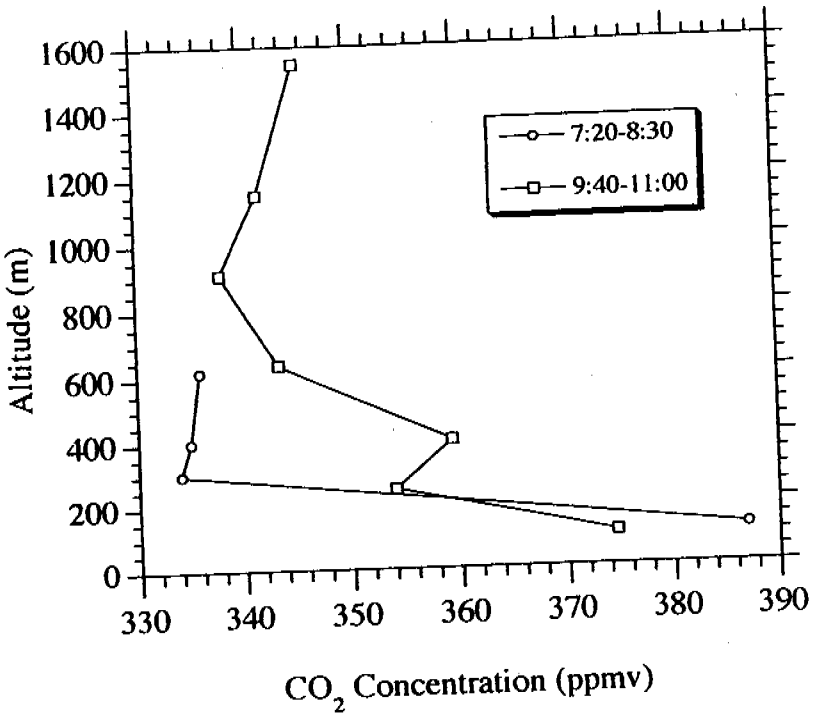

FIG. 5. Vertical profiles of CO_2 concentration near Plotnikovo on August 3.

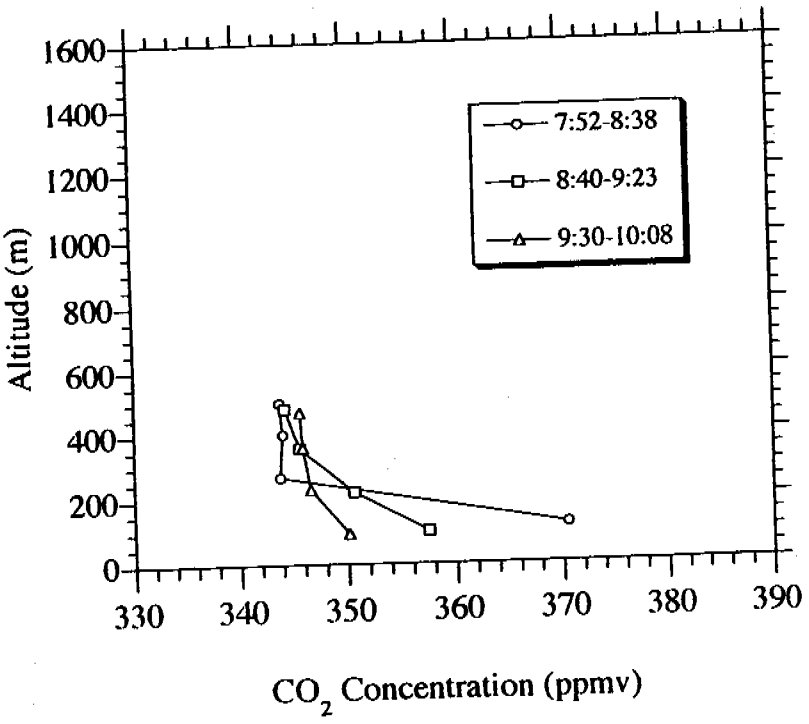

FIG. 6. Vertical profiles of CO_2 concentration near Plotnikovo on August 5.

Similar phenomena were observed near Plotnikovo (57.85°N, 83.08°E) on August 3 (Fig. 5) and August 5 (Fig. 6). But the absolute values were not consistent over the sampling dates. The CO_2 concentration at the altitude of ~100 m shows a higher value on August 3 than on August 5. Fig. 7 shows variations of surface air temperature observed near the flight

area. The surface temperature variation from 0:00 to 8:00 on August 3 shows higher values than those on August 5 by 3–5 °C. This suggests that nocturnal respiration and/or oxidization of organic matter was more active on August 3 because of the higher air temperature. On the other hand, CO_2 concentrations at higher altitudes observed in the first trial flight show lower values on August 3, being about 335 ppmv at 7:20–8:30 local time, than on August 5, being about 344 ppmv at 7:52–8:38 local time. As seen in Fig. 7, the surface air temperature between 10:00 and 17:00 on August 2 was higher by about 2 °C than that on August 4. Higher daytime temperature on August 2 probably suggests that biospheric CO_2 uptake was stronger on August 2 than on August 4, and lower CO_2 concentration remained at the higher altitudes in the morning of August 3.

Fig. 8 shows vertical profiles of CO_2 concentration over Moscow (55.45°N, 37.42°E) on July 30, Surgut (61.13°N, 73.20°E) on August 1, Kemerovo (55.25°N, 86.05°E) on August 2 and Yakutsk (62.10°N, 129.50°E) on August 9. It is clearly seen that the CO_2 concentration at lower altitude shows smaller values at all observation sites, reflecting strong CO_2 uptake by the terrestrial biomass in that season. The gradient of CO_2 concentration is relatively large over Surgut and relatively small over Yakutsk, probably accounting for the difference in activities of terrestrial biomass around these areas.

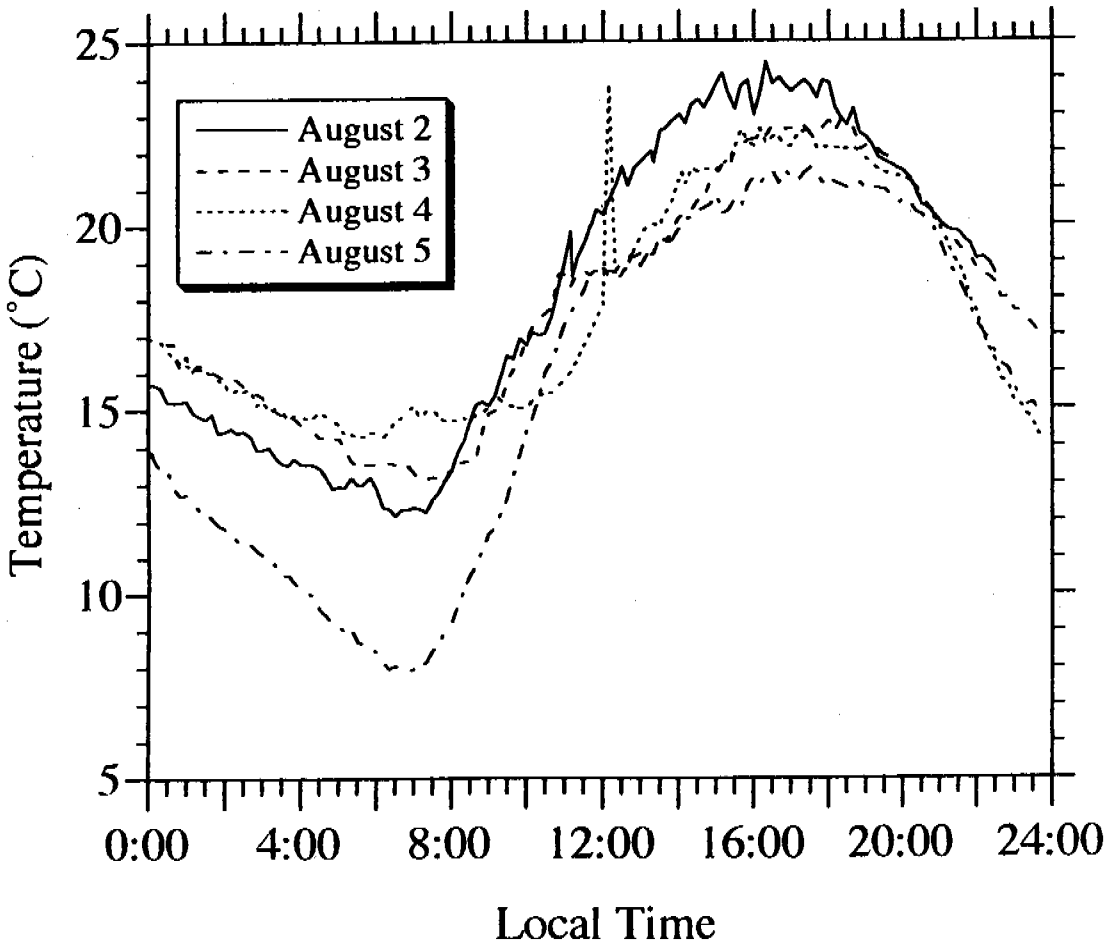

FIG. 7. Variations of surface air temperature near Plotnikovo.

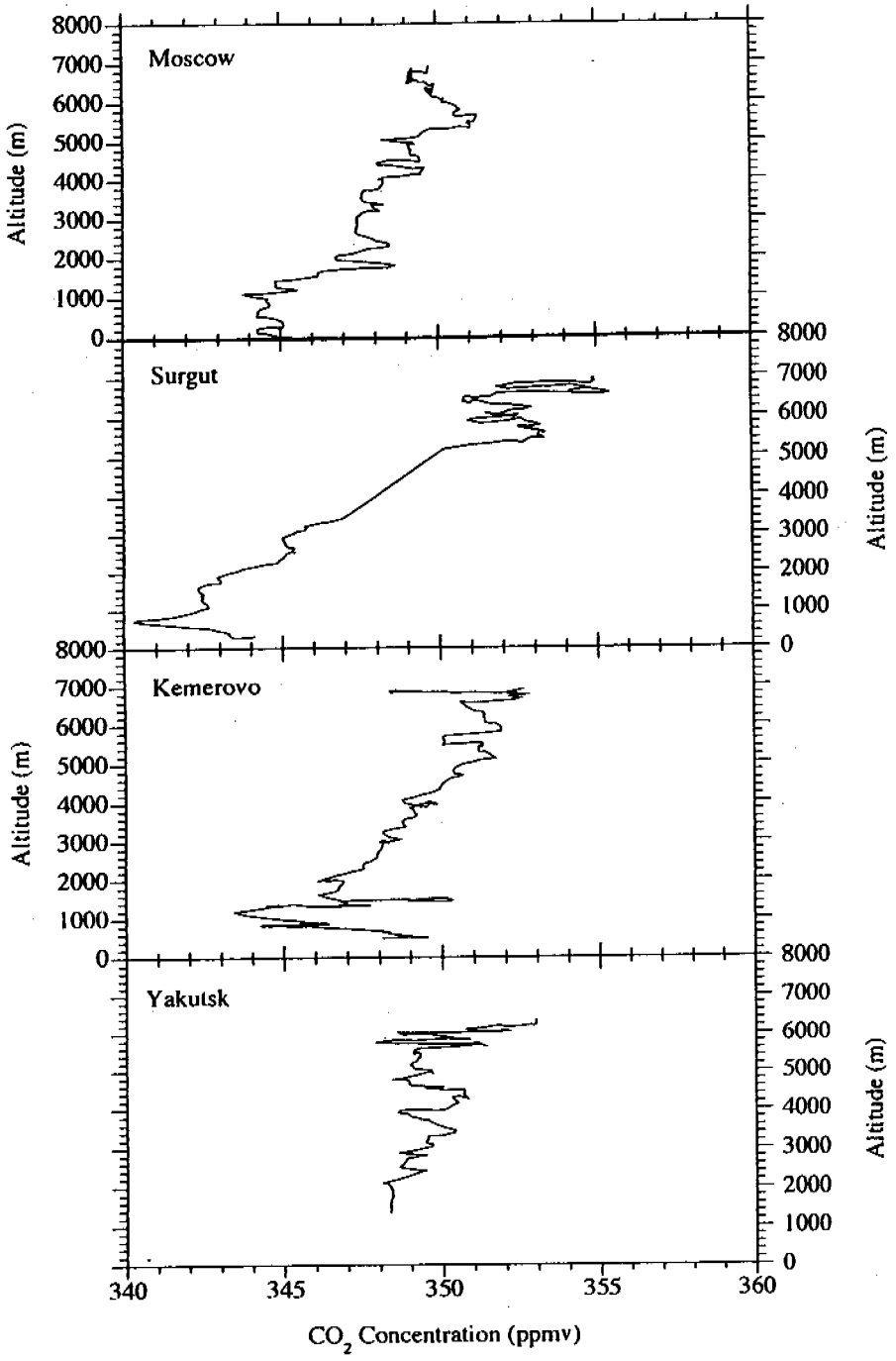

FIG. 8. Vertical profiles of CO_2 concentration over Moscow on July 30, Surgut on August 1, Kemerovo on August 2 and Yakutsk on August 9.

References

Conway, T.J., et al. 1994. J. Geophys. Res., 99:22831–22855.
Keeling, C.D., et al. 1989. Geophysical Monograph, 55:165–236.
Siegenthaler, U., and H. Oeschger. 1987. Tellus, 39B:140–154.
Tanaka, M., et al. 1987. Tellus, 39B:29–41.

Aircraft measurement of CO_2 and development of an ultrasonic anemometer

KENJI YAZAWA[1], TAKASHI TAMARU[1], MASARU NAKAMURA[1], YUUSHI TERUI[1], MASATAKA SHIRAI[1], HAJIME INOUE[2], and TOSHIAKI MACHIDA[2]

[1]*National Aerospace Laboratory, 7-44-1 Jindaiji Higashi Machi, Chofu, Tokyo 182 Japan*
Tel: +81-422-47-5911; Fax: +81-422-33-5602
[2]*National Institute for Environmental Studies, 2-16 Onogawa, Tsukuba, Ibaraki 305 Japan*

Aims of research

Following to the agreement between National Aerospace Laboratory and National Institute for Environmental Studies, a research program on global warming effect gases which are the products of fossil fuel combustion was started in 1993. The aim of the research is to investigate the fluxes of these gases in the atmosphere by measuring concentration of the gases and air velocity precisely at the same time by an airplane. Then, the vertical distributions and the fluxes of these gases can be obtained in the atmosphere.

Research procedure

Currently, the air velocity measurement techniques have not been established to get the local flux data of the global warming effect gases precisely enough. For improving this technique, development of the ultrasonic anemometer began in 1993. A series of wind tunnel tests were conducted to know the performance. Independently, the flights were made in western part of Japan to obtain the concentration data of those gases at a specific season. In the final stages of the program, the gas concentration data coupled with the precise local air data will provide the local flux data of global warming effect gases.

Research conducted this fiscal year

After the flights and measurements of global warming effect gases in last winter season, a newly designed ultrasonic anemometer was tested in the wind tunnel in July. The second series of flights were made in October to measure the global warming effect gases. The flights were made along the pacific coast from Tokyo to Ishigaki Island. The local flights are also planned in the coming February to get some data of combustion originated gases in the atmosphere at Kanto area with the preliminary test of the anemometer on board.

Measurement of global warming effect gases in fall

Previous measurement of those gases at winter time was already reported (Tamaru et al. 1994). To make a comparison of the seasonal differences, the observation flight was planned along the same fight course with the same techniques of data acquisition. The flight schedule conducted is listed in Table 1.

The airplane Dornier 228 left Chofu airfields on the scheduled date, Oct. 6. Arriving at Amami airport, it was found that the typhoon No.29 was approaching. Then the schedule was changed to fly back to Miyazaki airport so as to shelter the plane. As the consequence, three times of landing to Amami airport enabled to get three sets of data for comparison. The

TABLE 1. Atmospheric observation flight performed.

Date	Flights
1994/10/6	Chofu-Nagoya
7	Nagoya-Miyazaki-Amami-miyazaki
11	Miyazaki-Amami
12	Amami-Naha-Ishigaki
13am	Flight around Iriomote
13pm	Altitude flight test above Hateruma
14	Ishigaki-Amami-Kohchi
15	Kohchi-Chofu

relatively uniform concentration profiles obtained in vertical CO_2 distribution is attributed to the mixing effect of the atmosphere by the typhoon.

Different from the data at the winter time, comparison of measured data at the windward and at the leeward of Iriomote Island showed hardly any differences between them. It may be caused by appreciable weak velocity of air at that time.

Vertical distribution data near Hateruma Island were obtained at the altitude between 90 and 6,400 m in height. Crew and staff on board had to use oxygen supply system above 3,000m since the Do. 228 provided no pressurized cabin. Good agreements were confirmed for the data took at the time of climb and the descent. The vertical distribution of CO_2 showed a decreasing trend as the altitude increased and a little perturbation in it was observed.

Flight instrumentation system

Most of the instrumentation of the data acquisition systems were the same with the ones used in the last observation flights in winter. Only difference in the system was that the FMS (flight management system) was used to obtain flight route position and the flight data were obtained by data bus ARINC429. The data was then transformed to PCM signal and recorded by the data recorder.

Measured CO_2 data

Brief flight routes, altitude and the measured CO_2 data are shown in Fig. 1 with the course of the typhoon. The ordinate shows the deviations of CO_2 concentration from the base line of 350 ppm at the top of the altitude lines in the full span of 10 ppm which corresponds to 1000 ft span of altitude. Sudden extensions of long shoots of the lines at some locations show the span gas calibration data. The feet of the altitude lines show the geographical locations of the flights. According to this data, the CO_2 concentration between Nagoya and Miyazaki is relatively low compared to those of other locations.

Vertical CO_2 concentration variation at Amami Island is shown in Fig. 2 compared with the previous data in the last winter. In the latter data, it was supposed that there were temperature divergence region at 3,000 m in the altitude. There were many clouds observed

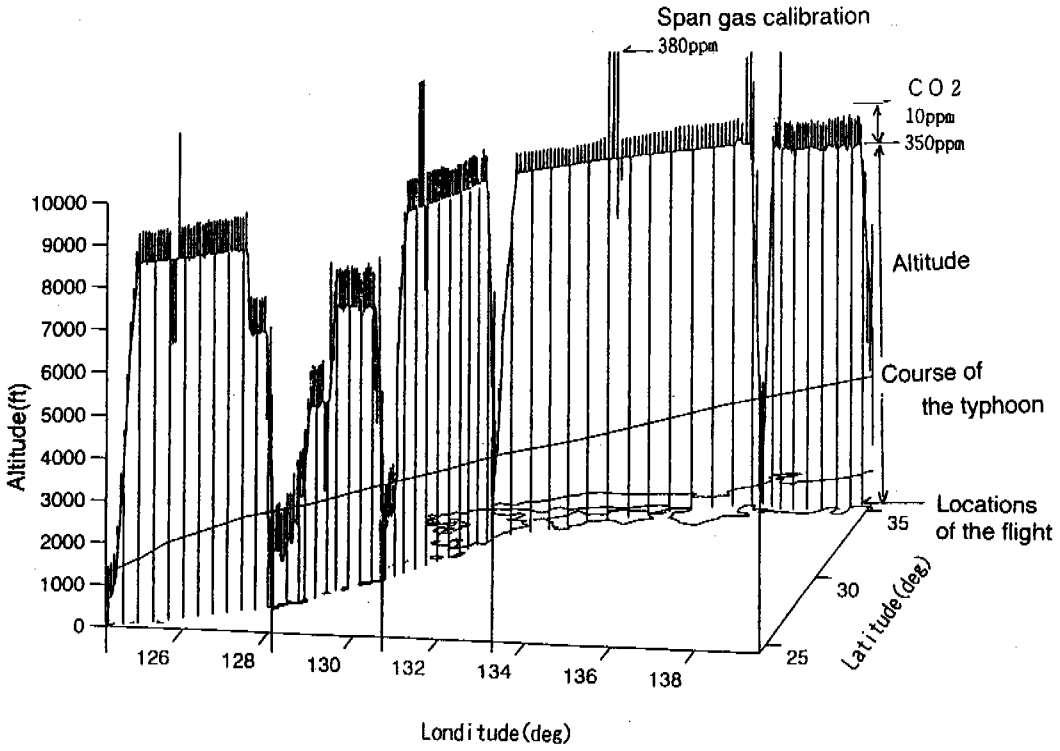

FIG. 1. Flight routes, altitude and the measured CO_2.

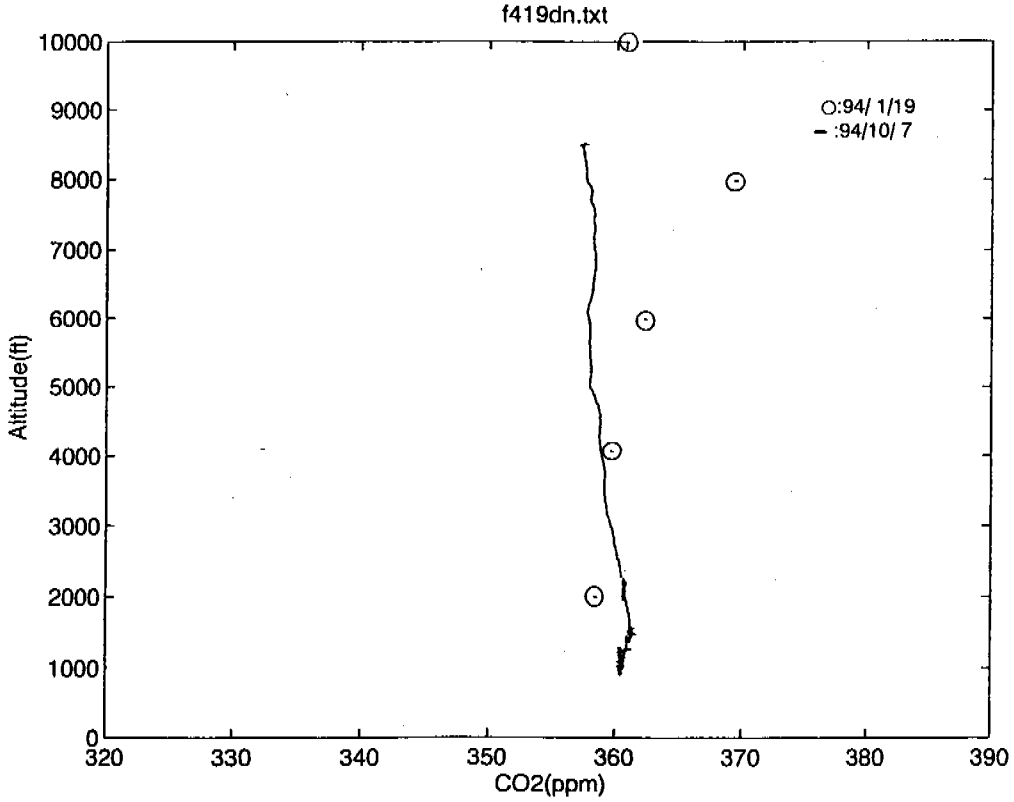

FIG. 2. Vertical CO_2 concentration compared in winter and fall at Amami Island.

at this altitude. The fall data were obtained just before the arrival of a typhoon and the weather was fine. After passing the typhoon, the concentration profile measured on 11th of October showed hardly any gradient with respect to the altitude. It comes from the mixing effect due to the typhoon winds.

Fig. 3 shows the vertical concentration profile of CO_2 at Hateruma Island. The data at the climb and the descent are shown in this figure which show good agreement between these two cases; however, there are some perturbations in each data set.

Development of ultrasonic anemometer

In order to know the pollutant gas fluxes, precise measurements of atmospheric stream velocity are required. Conventional instruments to measure air velocity, such as vane type and multi-hole Pitot tube type anemometer, cannot give us the data with enough reliability and accuracy. An ultrasonic anemometer has been used as a weather observation purpose. It has a potentially suitable characteristics also for the use of on board instrument for aircraft. The newly designed ultrasonic anemometer was developed and tested for above purposes.

Required operational conditions for the airplane is in the wind range between 50 and 100 m/s In order to extend the upper limit of the conventional measurement range, i.e.,60 m/s, doubled drive frequency, 200 kHz, was applied to the three sets of sensors which are arranged

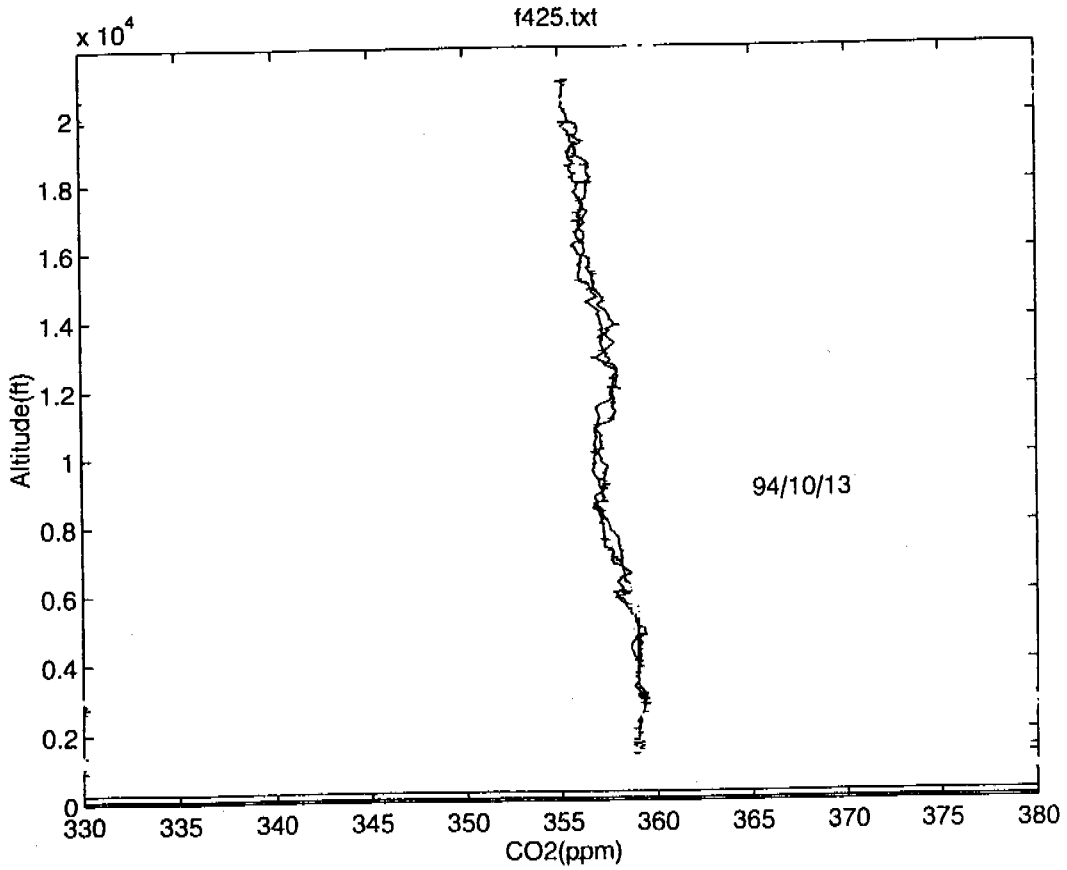

FIG. 3. Vertical concentration profile of CO_2 at Hateruma Island.

every 120 degrees apart around the support shaft. The each sensor is tilted to the windward by 10 degrees. These arrangements improved the upper limit of velocity and increased the S/N ratio.

Fig. 4 shows the probe in the wind tunnel. Fig. 5 shows the comparison between the wind velocity of the wind tunnel V and the indicated values V_{abc} obtained by the ultrasonic anemometer. Unfortunately, the wind tunnel used at this time has the limit of 55m/s in its maximum value of wind velocity. Since the anemometer has good linearity in the measured range, the tests will be performed in the other wind tunnel, e.g., transonic wind tunnel, which can provide higher velocity wind. Tests on board will be followed. Figs. 6 and 7 show the ultrasonic anemometer on the nose boom and the air sampling probes on the top of the aircraft Queenair (B-65), respectively.

Fig. 8 and 9 shows the CO_2 and flight data measurement system in the cabin. The flights to test these instrumentation are planned in the near future.

Conclusions

The instruments to measure the gas concentration and the wind velocity have been tested independently. The vertical CO_2 concentration profiles were obtained by the flights to Hateruma Island. The verification test of the developed ultrasonic anemometer was conducted in the wind tunnel and linear data were obtained up to 55 m/s in wind velocity. The instrumental equipment are ready for tests on board.

Reference

Tamaru, T., K. Yazawa, T. Machida, and G. Inoue. 1994. Measurement of Carbon-Dioxide Variation with Altitude Using Dornier 228, Proceedings of the Second Symposium on the Joint Siberian Permafrost Studies between Japan and Russia in 1993, Tsukuba, 12-13 January.

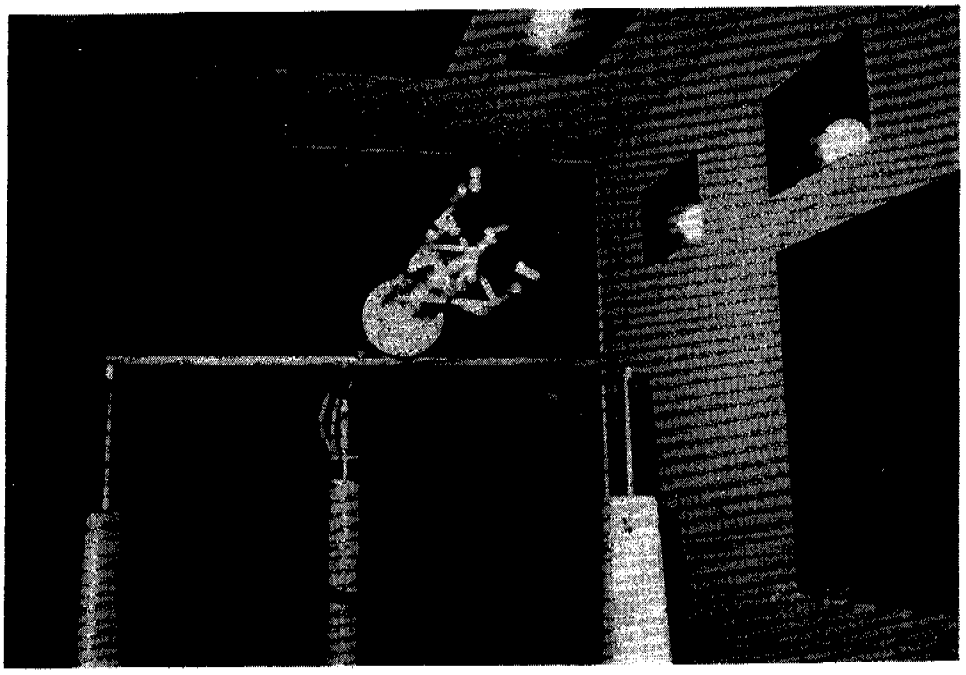

FIG. 4. Wind tunnel test of ultrasonic anemometer.

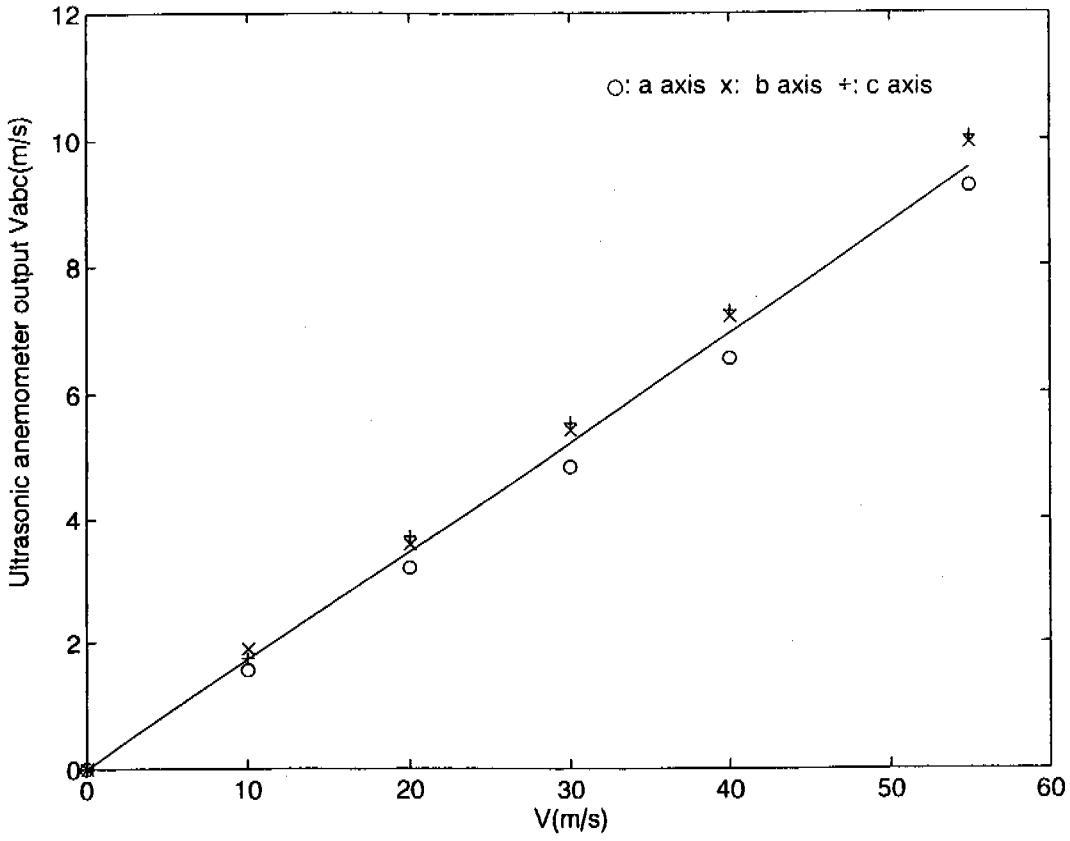

FIG. 5. Comparison between wind tunnel velocity and ultrasonic anemometer output.

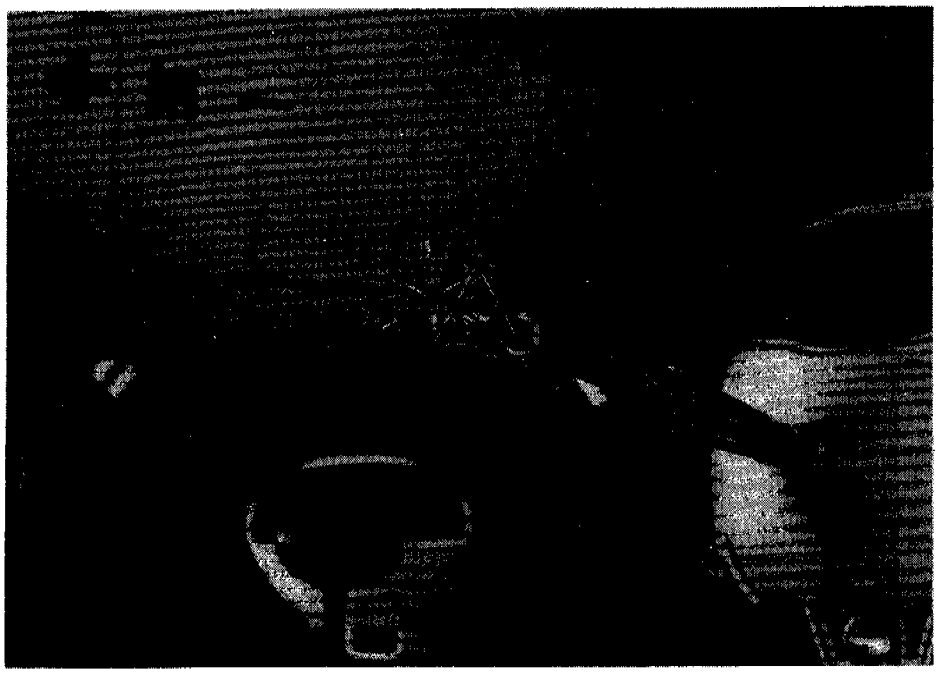

FIG. 6. Ultrasonic anemometer probe on the nose boom of B–65.

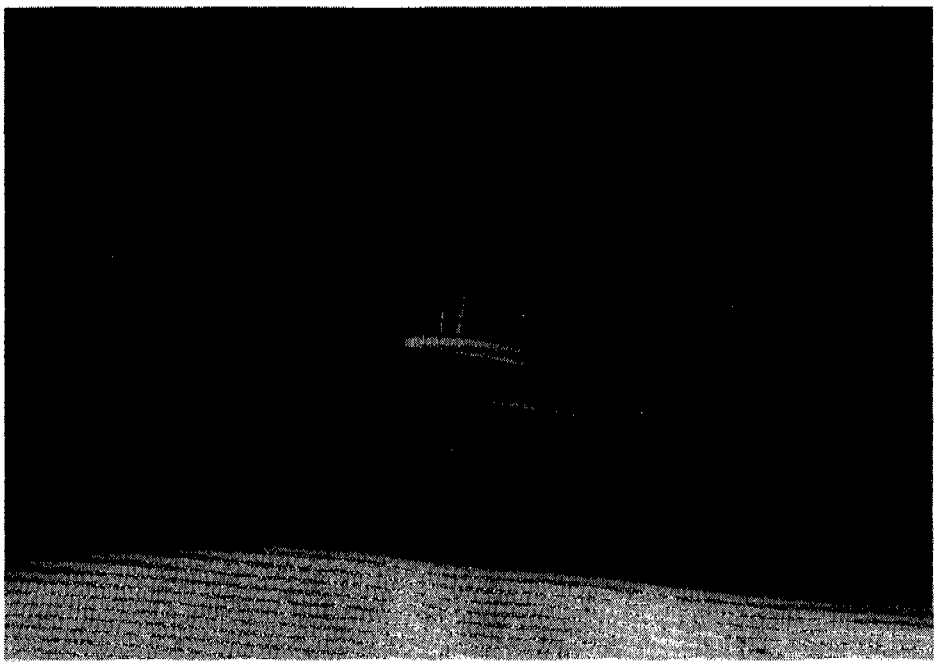

FIG. 7. Air sampling probes on the top of B-65.

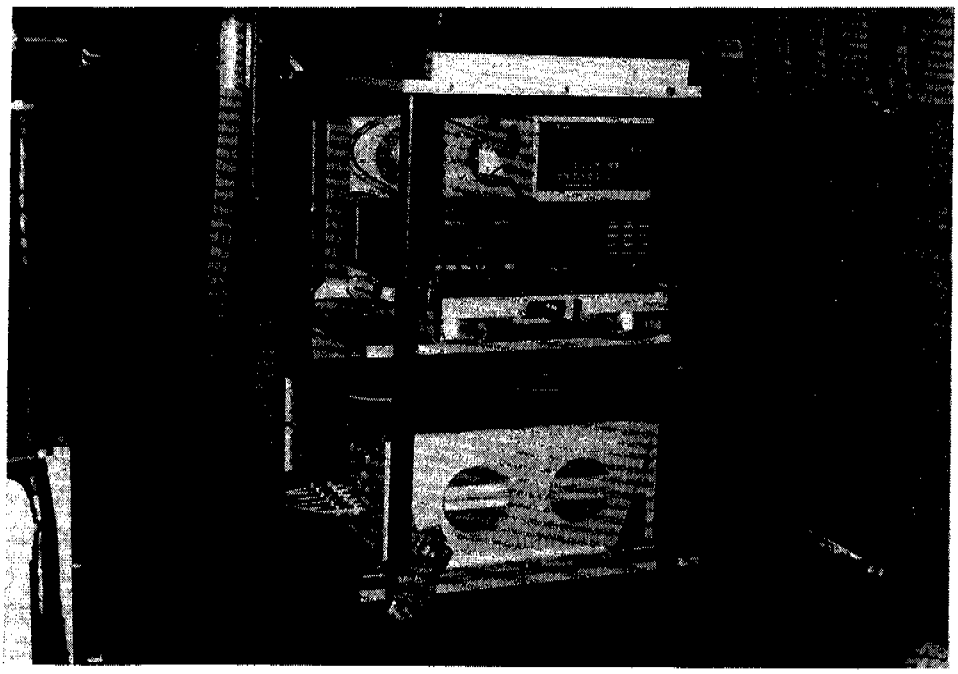

FIG. 8. Measurement system (PC,GPS, data recorder and ultrasonic anemometer).

FIG. 9. CO_2 measurement system ,INS and data processing system.

Large scale variability of atmospheric tracer concentrations over Siberia

S. MAKSYUTOV, T. MACHIDA, Y. TOHJIMA, and G. INOUE

National Institute for Environmental Studies, Onogawa, Tsukuba, Ibaraki 305 Japan
Tel: +81-298-51-6111; Fax: +81-298-51-4732

Introduction

The upper air observations play an important role in the atmospheric trace gas monitoring. Chemical composition of the free troposphere is less dependent on local fluxes than that on the surface. Providing large scale average parameters, the free tropospheric data are useful for regional-to-hemispheric scale budget estimates. Joint Japanese-Russian airborne atmospheric composition studies over Siberia (1992-1994) provide new data on the atmospheric constituents in summertime free troposphere. The important feature of the data is that most major greenhouse gases and related species are observed with a high temporal and spatial resolution equivalent to 3-5 km horizontal scale. This gives us a chance to derive correlations, and to study the relationships between individual tracers using a statistical approach.

Observations

In 1994 the free tropospheric data were obtained during transit flights on the following routes: Moscow-Surgut (Jul. 30), Kemerovo-Yakutsk (Aug. 8), Yakutsk-Surgut (Aug. 9), Surgut-Moscow (Aug. 10). The species observed in 1994 are listed here together with analysis technique and horizontal resolution: CO_2 (NDIR, 4 km), CH_4 (FID, 6 km), O_3 (UV, 4 km), NOx (12 km), CO and H_2 (GC, 4 km every 12 km), and water vapor (Lyman-a, 0.01 km).

Fig. 1 displays the horizontal variation of the concentrations observed at the altitude 7.5 km along the route Surgut-Moscow on 08/10/94. The stratospheric air intrusion event is evident with 3 peaks of the ozone concentration. Stratospheric air is indicated by the low humidity. Flat areas of low humidity correspond to very low humidity below the detection limit of the sensor. In parts of the plot, it is possible to see a negative correlation between CO_2 and CH_4, and O_3 and CH_4. High ozone of stratospheric origin is observed frequently in the upper troposphere (Browell et al. 1992, Inoue et al. 1994).

Fig. 2 shows the same species as Fig. 1 over the same area on 07/30/94. There is no evidence of a stratospheric ozone influence, but correlation between ozone, carbon dioxide and methane is clearly illustrated by this figure. This kind of correlation could be produced by an addition of a lower tropospheric (PBL) air. In summer, the PBL's ozone and carbon dioxide concentrations are lower over the rural areas because of a net sink, while methane is higher in PBL all over the year.

The correlation could be attributed to a mixing between different atmospheric pools with significantly different composition. A classification of the important pools should include dynamically separated air masses each carrying own composition (or signature). A simplified scheme may be proposed by dividing the mid-latitude atmosphere vertically into 3 classes: boundary layer, free troposphere and stratosphere. Free troposphere itself may be subdivided into lower part that is mixed with PBL by means of convective clouds and the upper part

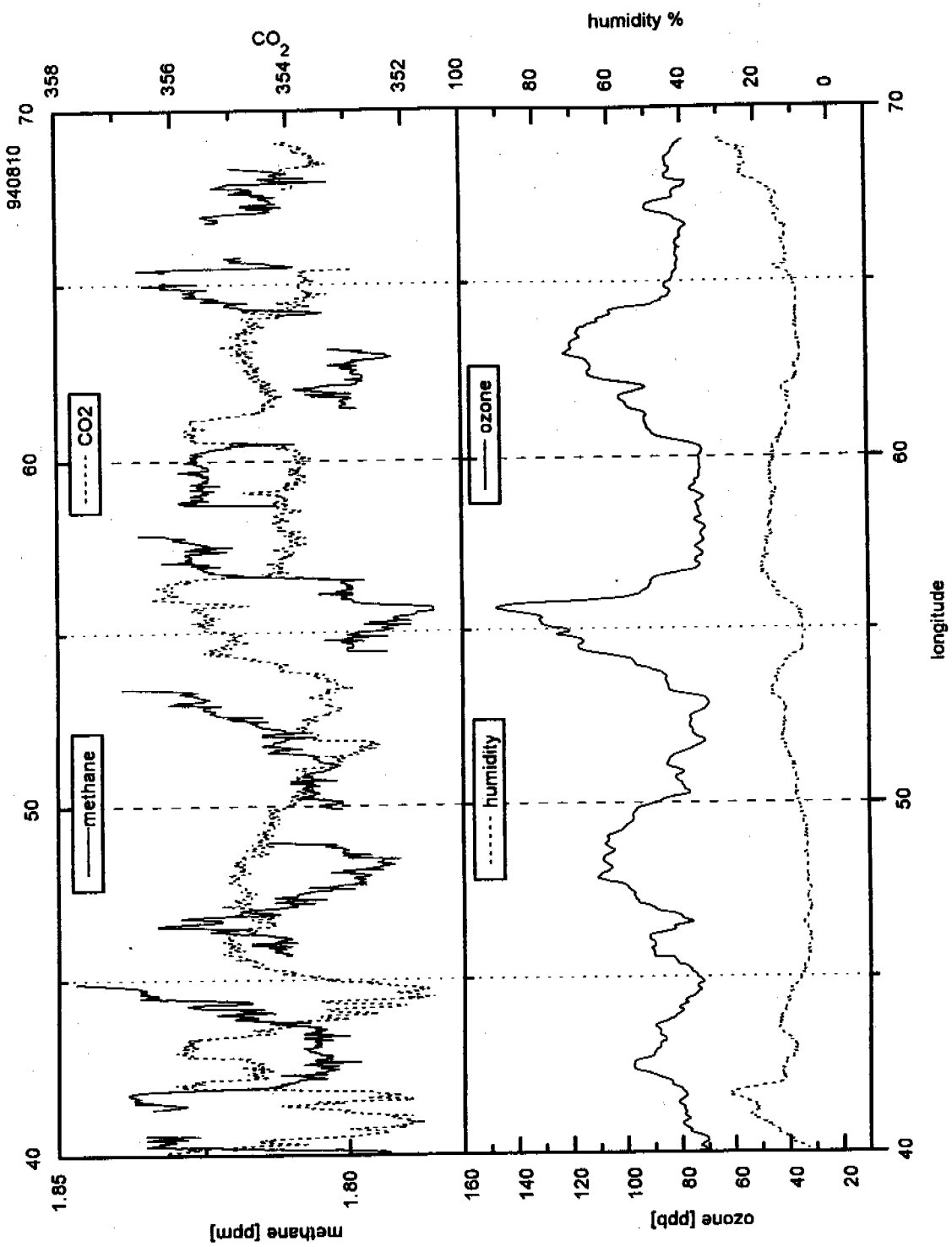

FIG. 1. CH_4, CO_2, O_3, and humidity observed 08/10/94.

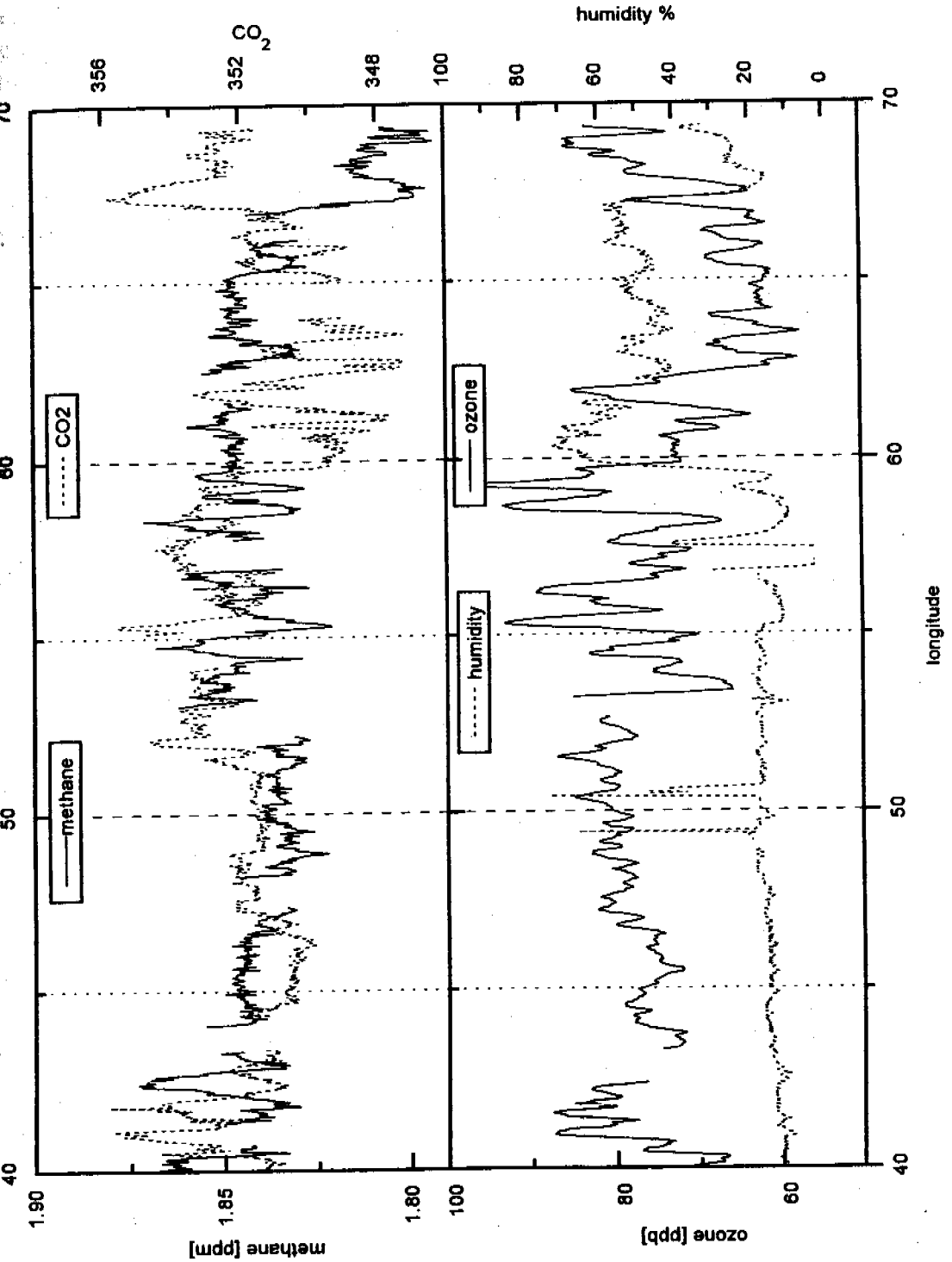

FIG. 2. CH_4, CO_2, O_3, and humidity observed 07/30/94.

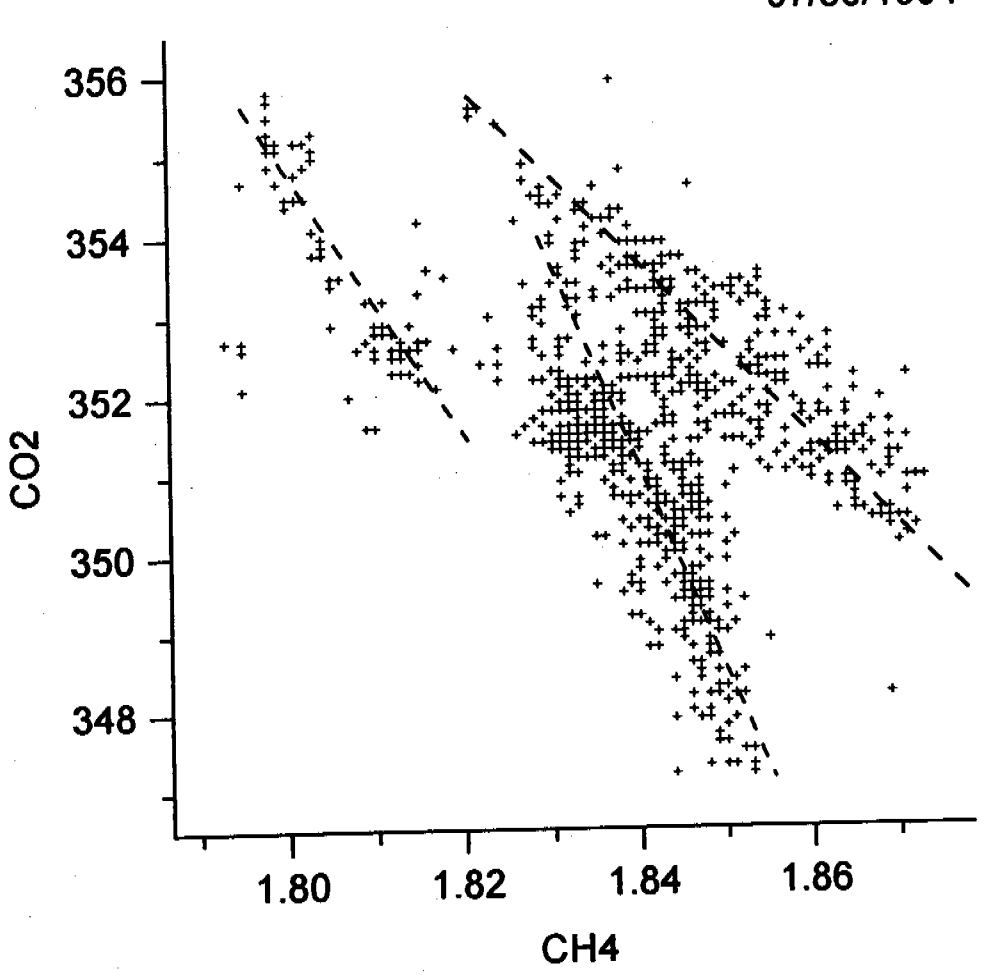

FIG. 3. CO_2 *versus* CH_4 for 07/30/94. Lines mark different clusters.

which can be reached from the PBL only by deep convection and is also influenced by stratosphere–tropospheric exchange. In addition, we should not exclude the effects of horizontal exchange between lower latitudes and higher latitudes.

Fig. 3 gives an example of a CO_2–CH_4 relationship that results from the mixing between more than 2 different pools. It is possible to distinguish three clusters on the plot that can be described by a single mixing relationship. Taking into account the data obtained in 1993 and 1994, one can observe that in many cases the correlation between CO_2 and CH_4 is very good and can be described as mixing between two or three pools. The regression analysis can give a quantitative information on the relationships between the components. The meaning of the regression slope and offset can be understood from a simple theory of the tracer transport.

Relationships between correlation and flux

Transport and diffusion of the minor tracer in the absence of the fast chemical reactions is a linear process. It keeps linear relationship between concentration at a given moment of time on one hand and initial concentration plus source on the other. In the atmosphere there are also time scales for mixing within each pool of air mass. The concentration distributions and emissions that are older than the mixing time for the pool does not affect the correlations; because the corresponding variation disappears within the mixing period. Thus, only fresh variations affect the pattern of correlation.

Let us consider two–box model that describes mixing between PBL and free troposphere.

As long as the volume of PBL is about 10 times smaller than the free troposphere, it is possible to consider the mixing as a small disturbance for the free troposphere. The concentration inhomogenieties have longer lifetime in free troposphere because of stable stratification. The concentration (mole fraction) in the PBL can be presented by an equation:

$$\frac{dC_{BL}}{dt} = F_s + K \cdot (C_{FT} - C_{BL}) \qquad (1)$$

Here F_S is a surface flux, K = exchange rate between PBL and free troposphere, C_{FT} = free tropospheric concentration. When all parameters except C_{BL} are kept constant, a steady state solution for Eq. 1 is:

$$C_{BL} - C_{FT} = \frac{F_s}{K} \qquad (2)$$

according to Eq. 2, the concentration difference is proportional to the flux ratio between the pools. In fact, we can consider the value to be the same for all long living tracers. Also the variations in free tropospheric concentrations are much smaller than those in the boundary layer. It is convenient to introduce a degree of mixing that determine a concentration in the disturbed part of the free troposphere:

$$C_M = C_{BL} \cdot (1-\alpha) + C_{FT} \cdot \alpha \qquad (3)$$

In the case of two different tracers we can get a linear relationship between concentrations combining Eqs. 2 and 3:

$$C_M - C_{BL} = F_s / F_{s1} \cdot (C_{M1} - C_{BL1}) \qquad (4)$$

Plot of Eq. 4 would look like a strait line in Fig. 3 (CO_2 *vs.* CH_4). In Fig. 3, data are grouped along three strait lines in a compact way. This is surprising, given the broad variability of CO_2 and CH_4 surface fluxes and their ratios. A significant horizontal mixing in the PBL can explain such a relationship. Particularly, the rate of horizontal and vertical mixing in the PBL should be higher than the rate of transport to the free troposphere. In that case, the fluxes from different natural and anthropogenic sources are averaged to give a smoothed horizontal distribution in the upper part of the PBL.

Major result of this two-box model is that applying regression analysis to a pair of tracers one can get an estimate of corresponding flux ratio. More sophisticated analysis is necessary to obtain the error estimation for the flux ratio and its area of influence. Applying similar considerations to an exchange between stratosphere and free troposphere, one can derive the flux ratios from the regression slope in just the same way.

Summary of the results

A regression analysis was applied to the data of each flight in order to check for variations in the correlations and regression slope. As it is shown by the simple box model analysis, the regression slope is the parameter that carries the information about the flux ratio. In Table 1, the regression slopes are presented for several flights. Data for ozone, methane, carbon dioxide and carbon monoxide are selected for this table to illustrate a rule that the range of the regression slope does not change significantly from year to year. Carbon dioxide

TABLE 1. Regression slope calculated for a pair of concentration values.

period	comment	regression slope ppb/ppb		
		O3-CH4	CO2-CH4	CO-CH4
7/18/93	ozone intrusion	*-0.6*		
7/19/93	high CH4		*-85*	
7/28/93	mid CH4		*-85*	
7/28/93	total		*-43*	
93' expedition	range	-0.5 -2.0	-40 -110	*0.5 0.9*
7/30/94	mid O3	-0.9	-46	
7/30/94	high O3	-1.9	-96	
8/10/94		-0.9	-110	
8/10/94	high O3 part	-1.3	-49	1
8/9/94				0.5

data for 1993 were provided by Izumi et al. 1994.

The data for the early spring show different correlation as has been observed by Conway et al. (1993). They found that CH_4 *vs.* CO_2 regression slope of 13.5 ppb CH_4/ppm for six flights in March 1989. A slope for CO *vs.* CO_2 appeared to be 15.8 ppb/ppm. This gives a flux ratio of CO to CH_4 to be the same order of magnitude as our observations in summer. As long as vegetation uptake is not active in March, the sign of a CH_4 to CO_2 regression slope is positive. Winter time relationships are discussed in Maksyutov et al. (1995).

High degree of correlations between the individual tracer concentrations which were observed in this and other (Conway 1993) studies suggest that the concentration variations may result from mixing beteen well mixed pools with stable concentration ratios.

Acknowledgments

Airborne studies were funded by Japan Environmental Agency and organized by CGER NIES. Contribution by researchers and staff of the Central Aerological Observatory (Russia) was crucial for the success of this work.

References

Browell, E.V. et al. 1992. Large-scale variability of ozone and aerosols in the summertime Arctic and Sub-Arctic troposphere, J. Geophys. Res., 97:16433-16450.

Conway, T.J., L.P. Steele, and P.C. Novelli. 1993. Correlations Among Atmospheric CO_2, CH_4 and CO in the Arctic, March 1989. Atmospheric Environment, 27A(17-18):2881-2894.

Inoue, G. et al. 1994. Stratospheric ozone folding phenomena observed in East Siberia in

summer 1993 – Airborne measurements of greenhouse gases over Siberia, I. *In* International Symposium on Global Cycles of Atmospheric Greenhouse Gases, Sendai, Japan, pp 1–4.

Izumi, K. et al. 1994. Distribution and uptake of CO_2 over cenral West Siberian lowland – Airborne measurements of greenhouse gases over Siberia, I. *In* International Symposium on Global Cycles of Atmospheric Greenhouse Gases, Sendai, Japan, pp 5–8.

Maksyutov, S. et al. 1995. Continuos measurements of atmospheric methane and carbon dioxide at Yakutsk monitoring station. (this issue).

Analysis of atmospheric light halocarbons at Moskow and Siberia by automated cryogenic adsorption: capillary GC/MS

NOEL M. BAUTISTA[1], YOKO YOKOUCHI[2], and AKIRA OTSUKI[1]

[1]*Department of Marine Science and Technology, Tokyo University of Fisheries, 4-5-7, Konan, Minato-ku, Tokyo 108 Japan; Tel/Fax: +81-3-5463-0398*
[2]*Division of Environmental Chemistry, National Institute for Environmental Studies, 16-2 Onogawa, Tsukuba-shi, Ibaraki 305 Japan*

Abstract: A wide array of natural and anthropogenic highly volatile halogenated hydrocarbons such as the halomethanes (e.g. CH_3Cl, CH_3Br), chlorofluorocarbons (e.g. CFC 11, CFC 12) and its transitional substitutes (e.g. hydrofluorocarbons, hydrochlorofluorocarbons) and several other halocarbons (e.g. trichloroethane, tetrachloroethylene) over Moscow and Siberian atmosphere were analyzed by an automated preconcentration system of capillary cryogenic adsorption: capillary gas chromatography–mass spectrometry. Ambient air sample collected in glass cylinders to a pressure of ca. 2 kg/cm^2 was passed through a $Mg(ClO_4)_2$ desiccant and adsorbed on a megabore PoraPLOT Q capillary column trap (10 cm x 0.53 mm ID x 20 mm FT) which was cooled to less than −80°C by a relay controlled pressure driven flush of liquid N_2. A backflush of 10 cc volume of N_2 followed before rapid thermal desorption of adsorbates at 200°C to the GC–MS unit at Selective Ion Monitoring (SIM) mode. High resolution chromatography was achieved by a tandem of PoraPLOT Q (15 m x 0.32 mm ID x 10 μm FT) and 5% PheMe Silicone HP-ULTRA 2 (50 m x 0.32 mm ID x 0.52 μm FT) capillary columns.

Introduction

Halocarbons are ubiquitous in the environment due both to natural and anthropogenic emissions. Highly volatile halocarbons are potential sources of gaseous halogens to the atmosphere and participate in a variety of atmospheric chemical reactions and processes notably ozone depletion reactions and global warming. Around a couple of thousands of halogenated substances are discharged into the biosphere by plant and animal species through natural processes constantly occuring in nature (Gribble, 1994). The most abundant of the biogenic halocarbons is CH_3Cl produced in aquatic and terrestrial ecosystem. Others include several bromine, iodine and fluorine containing natural products. Chlorofluorocarbons (CFCs) 11, 12 and 113 comprise the bulk of anthropogenic volatile halocarbons released to the atmosphere for over three decades. With the confirmation of the Montreal Protocol, the world was set to ban the use and production of these CFCs by 1996 (C&EN, 1994). Right now, transitional substitutes are in use–hydrochlorofluorocarbons (HCFCs) and hydrofluorocarbons (HFCs).

This study presents the ambient levels of several anthropogenic and natural halocarbons over the area spanning Moscow to Siberia, Russia.

Materials and methods

Preconcentration system, ambient air samples and standard gases.—The schematic of the preconcentration set-up used for analysis is shown in Fig. 1 (Bautista 1995). The adsorbent for trapping halocarbons is a 10 cm megabore PoraPLOT Q capillary column (10 cm x 0.53 mm ID x 20 μm FT), cooled to less than −80°C by a relay controlled pressure driven flush

of liquid N_2. The relay (Omron E5CX) acts on a preset temperature. The water trap placed between PV1 & PV2 is $Mg(ClO_4)_2$ (~0.500 g, 24–28 mesh, 300–710 mm) packed in a glass column (10 cm x 50 mm ID). Both the adsorbent and water traps are employed with resistive heaters for baking and reactivation. A diaphragm pump with a resultant pumping capacity of 45 cc/min, draws both the purge N_2 (20 cc/min) and the sample (25 cc/min) flowing through the sampling line. All gas flows are controlled by thermal mass flow controllers (SEC–4400R0; SEC–300: STEC Inc.) and monitored through mass flow meters indicating digital output.

The preconcentration unit is wired to a program controller (Shimadzu C–R6A Chromatopac) and interfaced to the GC (HP–5890 Series II)/MS (HP 5971A MSD) for chromatographic and mass spectrometric analysis. The GC capillary column is a tandem of PoraPLOT Q (15 m x 0.32 mm ID x 10 μm FT) and 5% PheMe Silicone HP–ULTRA 2 (50 m x 0.32 mm ID x 0.52 μm FT) capillary columns.

Ambient air samples at different sites and altitudes were pumped directly into glass cylinders to a pressure of around 2 kg/cm^2 during the research flight on July 29–August 10, 1994 from Moscow to Siberia, Russia.

Mixtures of standard gases prepared gravimetrically in steel cylinders were obtained from Taiyô Sanso Co. Ltd., Atsugi, Japan.

Procedure.—A run time program fed to the preconcentration unit through the run program controller C–R6A Chromatopac automated the control of operations from a series of valve actuation to GC injection. The chromatographic and mass spectrometric run is automated by the GC–MS Acquisition program.

A 500 cc ambient air sample pressurized in glass cylinder was introduced via PV3 passing the thermal mass flow controller at a flow rate of 25 cc/min (Fig.1). Before reaching the capillary trap initially cooled to less than –80°C, the sample passes through the water filter. PV1 was actuated after sampling to let flow 10 cc volume of N_2 (20 cc/min) to expel traces of the sample in the blank capillary to which the PoraPLOT Q capillary trap is fixed. At this stage, the cryogen flush was stopped to prevent further cooling of the trap in preparation for thermal desorption. PV2 was then actuated to let the carrier gas He flow (1.05 cc/min) toward the opposite direction of sampling; the trap heater raised to 200°C and the GC–MS turned on for data acquisition. The initial oven temperature was held for one minute at 60°C with a ramp rate of 12°C/min. At the same time the water trap was also being reactivated at 150°C with an opposite flow of N_2 (20 cc/min) for 25 minutes maintained and a flow of N_2 (20 cc/min) succeeds for 20 minute baking. The capillary and water trap were then cooled to ambient temperature before starting another run. The detector was in the Selective Ion Monitoring (SIM) mode and quantification was done in the HP Chemstation.

To prevent premature condensation of analytes along the sampling lines, a flexible heating coil kept isothermally at 200°C was wrapped around and the valves were kept at the same temperature by a heating pad to which they are fixed. Also, the sampling lines were purged with N_2 after every run to prevent contamination.

Standard gases were run once every five air analyses.

Results and discussion

System evaluation and instrument response.—Sample recovery is 100 % and adsorption is quantitative for all the compounds of interest proven by high specific breakthrough volume (>100cc/cm) of adsorbates in the capillary trap at less than –80°C cryo–adsorption

temperature.

Sequential analysis of 12 freon standard samples in a week–long period showed that the response was excellently reproducible. The relative standard deviation of the integrated peaks of the freon compounds ranged from 0.33 to 1.83% (Fig. 2).

The linearity of response was also excellent. Virtually all points lie on a straight line indicated by very high correllation coefficients of almost unity (Fig. 3).

High resolution chromatography brought out well– resolved and sharp peaks which consequently lowered the detection limits of the light halocarbons analyzed. Detection limits are as low as 0.67 pg for HCFC 123 and 0.78 for CH_3I and the rest of the halocarbons of interest are below 5 pg level.

Instrument drift was monitored from the interval runs during sample analysis. The relative responses averaged to around 95% within a week–long analysis period (Fig. 4). Frequent tuning of the mass selective detector was not necessary.

Moskow and Siberian sample analysis.—The altitude level was divided into two: low altitude (0.5–2.1 km) and high altitude (5.0–7.5 km) levels. Fig. 5 shows significant variation of iodomethane with altitude for which it was collected. Iodomethane was more than twice that of higher altitude concentration. Other halocarbons which showed significant variation were chloroform, HCFC 123, HFC 134a, and trichloroethylene with low to high altitude concentration ratios over 1.20 (Table 1). The high deviation in concentration is related to their reactivities in the ambient atmosphere. Before reaching higher altitudes, they are scavenged by several oxidation processes, especially reaction with the hydroxyl (OH) radical in the atmosphere. For the CFCs which are relatively unreactive and stable in the lower troposphere, as well as the more volatile HCFC 22, chloromethane, and bromomethane,

Table 1. Low and high altitude concentration means (pptv) of light halocarbons at Moscow and Siberia, Russia.

Molecular Formula	Code	Altitude (km) Low(0.5 - 2.1)	Altitude (km) High(5.1 - 7.5)	Ratio Low/High
CH_3Cl	CM	517.00	527.02	0.98
CH_3Br	BM	10.15	12.55	0.81
CH_2Cl_2	DCM	50.60	50.50	1.00
CH_3I	IM	0.73	0.35	2.09
$CHCl_3$	Cf	24.04	18.84	1.28
$C_2H_3Cl_3$	TCEa	159.76	147.20	1.09
C_2HCl_3	TCEy	11.68	8.14	1.43
CH_2Br_2	DBM	2.38	2.04	1.17
C_2Cl_4	T4CEy	17.22	16.98	1.01
CCl_3F	CFC 11	260.73	258.14	1.01
CCl_2F_2	CFC 12	485.86	508.96	0.95
$C_2Cl_3F_3$	CFC 113	96.77	94.33	1.03
$CHClF_2$	HCFC 22	118.56	122.92	0.96
$C_2HCl_2F_3$	HCFC 123	0.20	0.14	1.43
$C_2H_2ClF_2$	HCFC 142b	7.86	7.54	1.04
$C_2H_2F_4$	HFC 134a	2.75	2.21	1.24

variation was not so evident: they reach higher altitudes with greater ease.

Variation with respect to latitude was observed for air samples collected at high altitude and sub-zero temperatures (-11 to -30°C). Higher concentrations were observed at lower altitudes for CFC 113 (Fig. 6), chloroform and trichloroethylene and HCFC 123. Maybe greater production and release occur at lower latitudes. Halocarbons collected at lower latitude and positive temperatures (3 to 18°C), such as CFC 11 (Fig.6), chloromethane, chloroform, trichloroethane and trichloroethylene exhibited higher levels.

Interesting variation with longitude was exhibited by the three halocarbons, HFC 134a, chloromethane and iodomethane (Fig. 7). Chloromethane concentration at high altitude and sub-zero temperatures is inversely related to longitude. On the contrary, iodomethane collected at low altitude and above zero temperatures exhibited exactly the opposite. There might be an abundance of point sources at lower longitudes for chloromethane and at higher longitudes for iodomethane. Also, chloromethane is largely terrestrial while iodo-methane is mainly oceanic in origin. HFC 134a exhibited a concentration peak at 70-90 degrees longitude.

The total ion chromatograms for Moscow and Siberian ambient air samples are shown in Fig. 8. HCFC 22, chloromethane, CFC 11 and trichloroethane concentrations exhibited marked changes between the ambient atmosphere of Moscow and Yakutsk. The latter two halocarbons were higher at Yakutsk while HCFC 22 and chloromethane showed elevated levels at Moscow. Aside from the most abundant HCFC 22, other CFC transitional substitutes such as HCFC 123, HCFC 142b and HFC 134a which haven't been detected in the ambient atmosphere were already in the pptv level in the atmosphere of Siberia (Fig. 9) as well as in Moscow. Following HCFC 22 in abundance was HCFC 142b, then HFC 134a and the least abundant was HCFC 123.

Greatest deviation in concentration of halocarbons between Moscow and Siberia was exhibited by chloroform and HFC 134a (Table 2). Trichloroethane, CFC 113, HCFC 22 and HCFC 123 exhibited higher concentrations at Siberia while HCFC 142b, iodomethane, trichloroethylene, tetrachloroethylene and dibromomethane concentrations were higher at Moscow. Chloromethane, bromomethane, dichloromethane, CFC11 and CFC 12 did not show appreciable differences in ambient concentrations.

Conclusions

It was found that the concentration of light halocarbons at high altitudes depends on reactivities. The more reactive the halocarbon is, the lesser is its chance to be transported to higher altitudes and latitudes compared to the more stable and more volatile ones. Light halocarbon concen-tration over Moscow and Siberian atmosphere are higher at low latitude levels. Along with HCFC 22, the other hydrohalocarbons such as HCFC 123, HCFC 142b and HFC 134a are at detectable levels already in the atmosphere of Russia ranging from 0.5 to 7.5 kilometer altitude. HCFC 123 is still at sub-pptv level while HCFC 142b and HFC 134a have ambient concentrations of 7-9 pptv and 1-3 pptv respectively. HCFC 22 is ca. 20 pptv higher than its 1993 mean global concentration of 100 ppt (Montzka, 1993).

Acknowledgment

Thanks are due to Drs. T. Machida, H. Mukai and G. Inoue of the National Institute for Environmental Studies (NIES), and Mr. T. Hagiwara of Global Environmental Forum for the sample collection during the research flight.

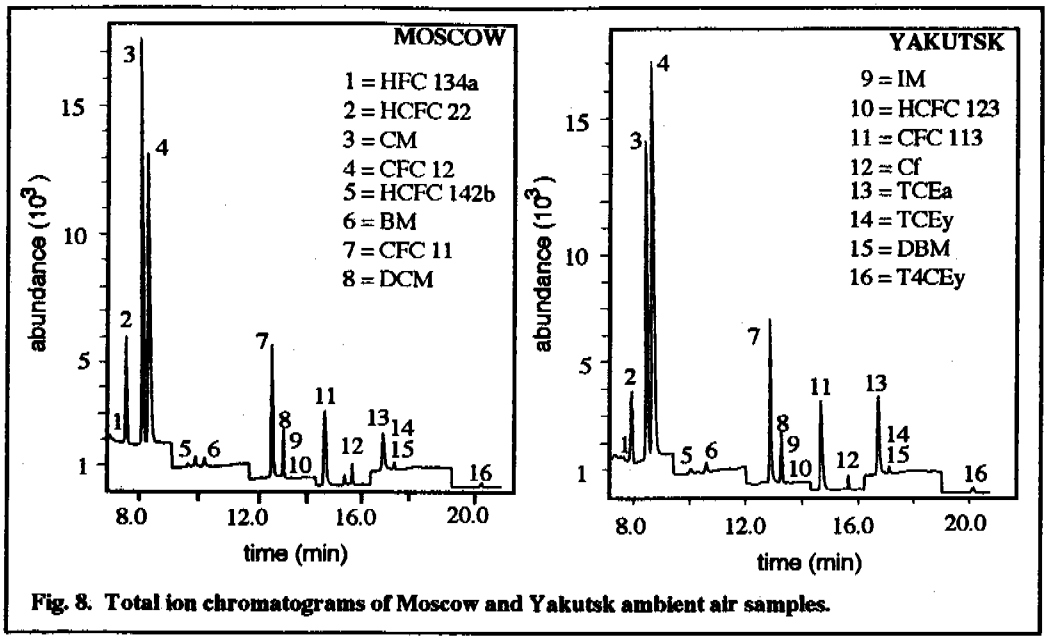

Fig. 8. Total ion chromatograms of Moscow and Yakutsk ambient air samples.

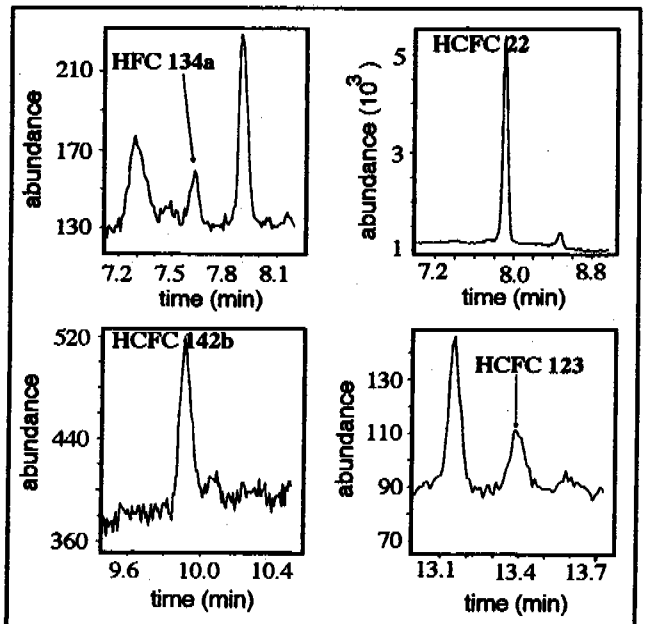

Fig. 9. Ion chromatograms of CFC transitional substitutes at Siberia, Russia.

References

Bautista, N. M. 1995. Development of a fully automated cryogenic adsorption: capillary gas chromatography–mass spectrometric system for atmospheric light halocarbons. MS Thesis. Tokyo University of Fisheries, Tokyo, Japan.

C&EN. August 15, 1994) Ozone depletion: 20 years after the alarm, pp. 8–13.

Gribble, Gordon W. 1994. The natural production of chlorinated compounds. Environ. Sci.

Technol., 28:7,310–319.
Montzka, S.A., R.C. Myers, J.H. Butler, J.W. Elkins, and S.O. Cummings. 1993. Global troposheric distribution scale of HCFC 22. Geophys. Res. Lett., 20:8,703–706.

Table 2. Mixing ratio means (pptv) of light halocarbons at Moscow and Siberia.

Molecular Formula	Code	Moscow	Siberia	Ratio
CH_3Cl	CM	544.73	522.31	1.04
CH_3Br	BM	10.07	10.06	1.00
CH_2Cl_2	DCM	54.27	52.23	1.04
CH_3I	IM	0.60	0.50	1.20
$CHCl_3$	Cf	30.07	18.54	1.62
$C_2H_3Cl_3$	TCEa	129.69	155.02	0.84
C_2HCl_3	TCEy	12.07	10.03	1.20
CH_2Br_2	DBM	2.80	2.13	1.31
C_2Cl_4	T4CEy	19.13	16.90	1.13
CCl_3F	CFC 11	268.47	258.58	1.04
CCl_2F_2	CFC 12	515.10	499.48	1.03
$C_2Cl_3F_3$	CFC 113	101.07	121.20	0.83
$CHClF_2$	HCFC 22	124.93	134.14	0.93
$C_2HCl_2F_3$	HCFC 123	0.13	0.16	0.81
$C_2H_3ClF_2$	HCFC 142b	8.27	7.60	1.09
$C_2H_2F_4$	HFC 134a	1.20	2.53	0.47

Measurements of atmospheric pollutants in Yakutsk city

SACHIO OHTA[1], TATSUYA FUKASAWA[1], NAOTO MURAO[1], SADAMU YAMAGATA[1], and VLADIMIR N. MAKAROV[2]

[1]*Department of Sanitary and Environmental Engineering, Hokkaido University, Sapporo, Japan*
Tel: +81-11-706-6832; Fax: +81-11-706-7890
[2]*Geochemical Laboratories, Permafrost Institute, Russian Academy of Sciences, Yakutsk, Russia*

Introduction

Atmospheric particulate and gaseous pollutants affect human health by causing respirately diseases such as bronchitis and asthma. They also cause photochemical smog and acid rain problems. It is, thus, important to measure their concentrations in the atmosphere. In Siberia, however, we have no data on atmospheric concentrations of these pollutants. Therefore, we started to measure the concentrations of SO_2, HNO_3 and HCl, and aerosol chemical species such as sulfate, nitrate and chloride at Yakutsk city in August 1993.

Experimental

We collected atmospheric aerosol and SO_2, HNO_3 and HCl at the fourth floor of the Permafrost Institute, Yakutsk City, every half month from August 1993. Atmospheric aerosols were collected on Teflon filter (Sumitomo Fluoropore AF07P) at a flow rate of five litter per minute. Atmospheric SO_2, HCl and HNO_3 were collected on reagent-soaked paper filters after the Teflon filter. We used the paper filters soaked with Na_2CO_3 for SO_2 and HCl sampling, and with NaCl for HNO_3 sampling.

Total particulate mass (TPM) was measured by weighing the filters with an electric balance. The collected aerosol samples on the Teflon filters were extracted ultrasonically into distilled-deionized water. The concentrations of sulfate (SO_4^{2-}), nitrate (NO_3^-) and chloride (Cl^-) in the extracted solution were determined by using an ion chromatograph (Yokogawa Electric Works Inc. IC-100). The concentrations of sodium (Na^+), calcium (Ca^{2+}) and magnesium (Mg^{2+}) were determined with an atomic absorption spectrometer (Hitachi Inc. 170-30).

The absorbed SO_2, HCl or HNO_3 on the reagent-soaked paper filters were extracted into distilled-deionized water. Sulfite in the extracted solution derived from the absorbed SO_2 was oxidized to sulfate by dropping H_2O_2. The sulfate concentrations were determined with the ion chromatograph. The chlorine concentrations derived from the absorbed HCl were also determined with the ion chromatograph. The nitrate concentrations derived from the absorbed HNO_3 were measured colorimetrically using the hydrazine reduction GR reagent method.

Results

Table 1 shows the atmospheric concentrations of total particulate mass (TPM) and aerosol chemical species at Yakutsk from second half of July 1993 through second half of July 1994. Total particulate mass at Yakutsk ranged from 7 to 39 μgm^{-3} during the period. The concentrations of the aerosol chemical species were SO_4^{2-}, 0.06-3.12; NO_3^-, 0.07-0.48; Cl^-, 0.01-0.20; Na^+, 0.03-0.18; Ca^{2+}, 0.09-0.68; Mg^{2+}, 0.01-0.09 μgm^{-3}.

The concentrations of the chemical species are also shown in Fig. 1. Yakutsk aerosol is abundant in sulfate and calcium. Sulfate increases in March through May in 1994.

TABLE 1. Atmospheric concentrations of total particulate mass (TPM) and aerosol chemical species at Yakutsk in July 1993 through July 1994 (F, first half; S, second half).

	Sampling period	TPM [μg/m3]	Cl- [μg/m3]	NO3- [μg/m3]	SO42- [μg/m3]	Ca2+ [μg/m3]	Mg2+[μg/m3]	Na+ [μg/m3]
1	1993 JUL. S	23.80	0.10	0.14	0.40	0.50	0.06	0.11
2	AUG. F	25.86	0.20	0.31	0.65	0.66	0.09	0.21
3	AUG. S	38.66	0.09	0.20	0.46	0.45	0.04	0.10
4	SEP. F	18.76	0.09	0.27	0.48	0.50	0.02	0.04
5	SEP. S	12.55	0.03	0.10	0.29	0.37	0.01	0.09
6	OCT. F	7.17	0.03	0.07	0.42	0.17	0.00	0.03
7	OCT. S	11.23	0.04	0.11	0.76	0.09	0.01	0.03
8	NOV. F	17.65	0.05	0.29	1.27	0.12	0.01	0.07
9	NOV. S	17.71	0.08	0.29	0.98	0.18	0.01	0.10
10	DEC. F	14.06	0.20	0.17	0.83	0.16	0.04	0.18
*11	DEC. S	11.09	0.04	0.12	0.43	0.14	0.01	0.04
*12	1994 JAN. F	12.48	0.04	0.12	0.70	0.11	0.01	0.06
13	JAN. S	12.59	0.03	0.09	0.46	0.13	0.01	0.04
14	FEB. F	10.76	0.05	0.18	0.88	0.09	0.01	0.04
15	FEB. S	42.05				0.27	0.03	0.12
16	MAR. F	23.77	0.05	0.48	3.12	0.31	0.03	0.15
17	MAR. S	16.66	0.06	0.25	1.37	0.30	0.02	0.12
18	APR. F	12.46	0.06	0.20	1.62	0.33	0.03	0.11
19	APR. S	7.65	0.05	0.25	1.21	0.55	0.04	0.12
20	MAY. F	13.62	0.03	0.13	0.68	0.48	0.03	0.10
21	MAY. S	17.54	0.12	0.20	1.14	0.62	0.05	0.14
22	JUN. F	2.44	0.01	0.03	0.06	0.21	0.02	0.07
23	JUN. S	12.37	0.02	0.09	0.17	0.55	0.03	0.11
24	JULY.F	13.50	0.03	0.14	0.30	0.68	0.03	0.09
25	JULY.S	8.26	0.02	0.09	0.19	0.19	0.02	0.04

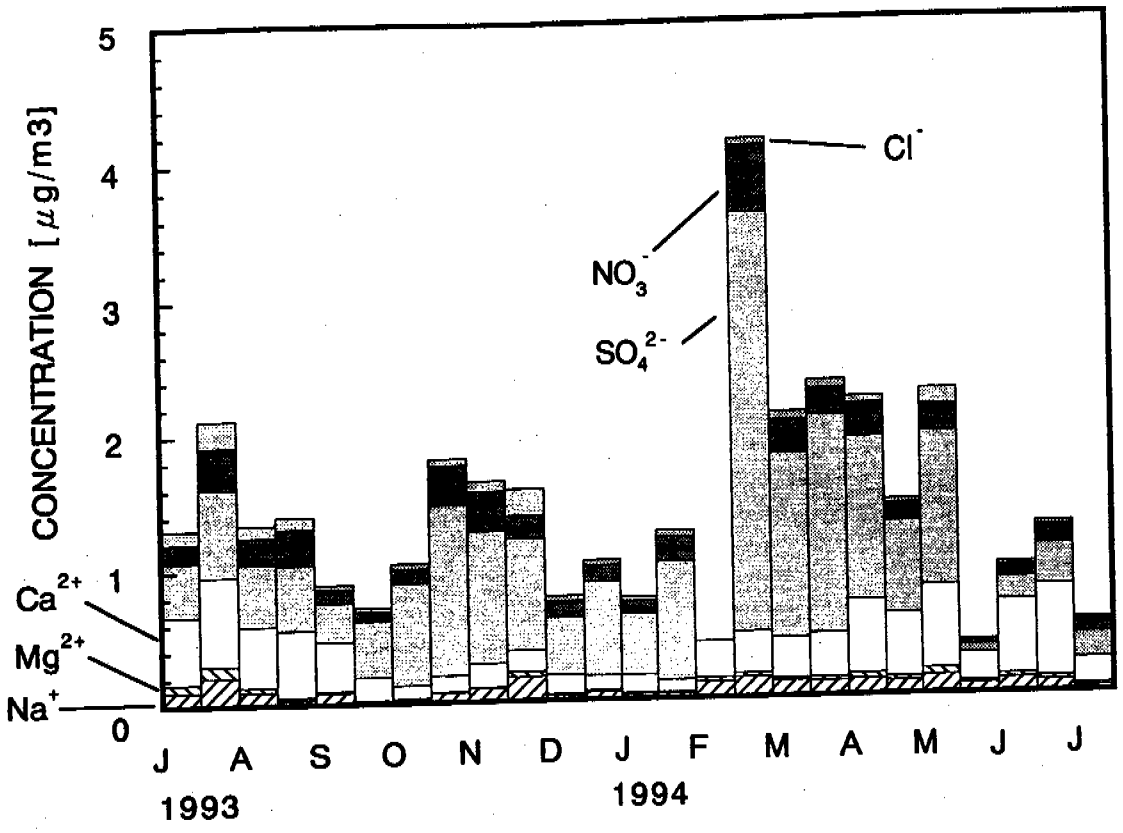

FIG. 1. Atmospheric concentrations of aerosol chemical species at Yakutsk.

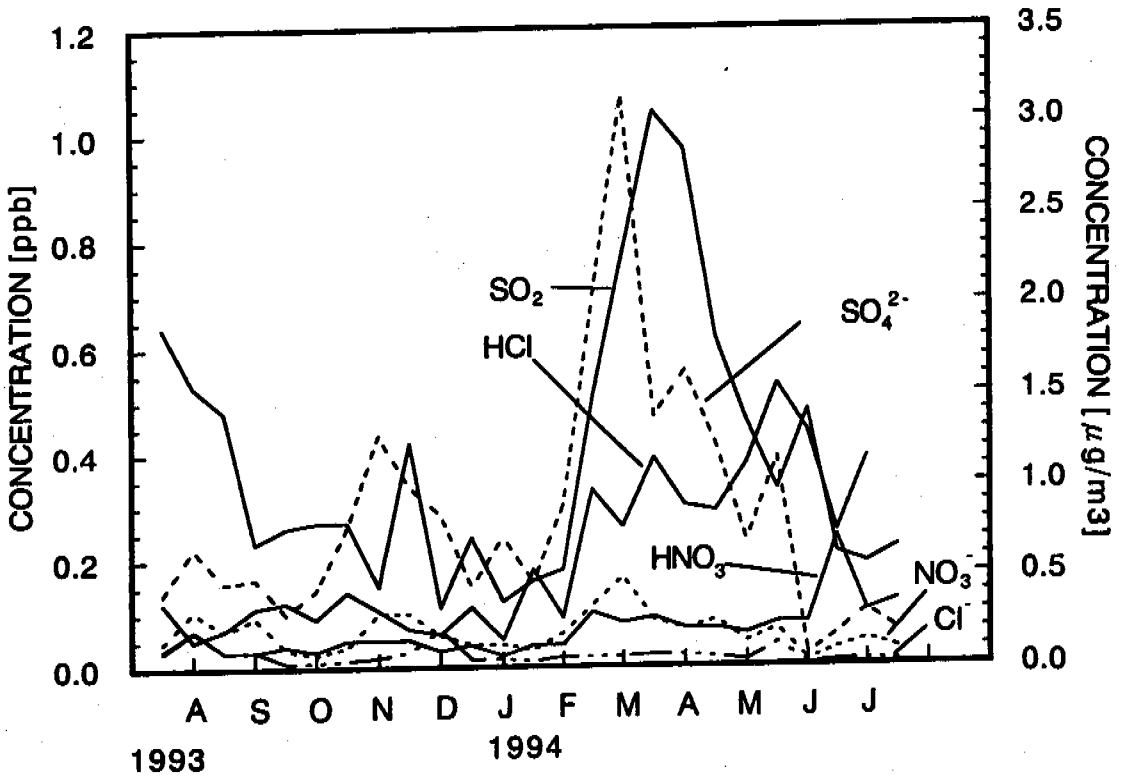

FIG. 2. Atmospheric concentrations of SO_2, HCl and HNO_3, and particulate SO_4^{2-}, NO_3^- and Cl^- at Yakutsk.

Table 2 shows the atmospheric concentrations of SO_2, HNO_3 and HCl at Yakutsk. The concentrations of SO_2, HCl and HNO_3 during the period were 0.11–1.04, 0.05–0.53 and 0.03–0.24 ppbv, respectively. Fig. 2 shows atmospheric concentrations of gaseous SO_2, HCl and HNO_3, and particulate SO_4^{2-}, NO_3^- and Cl^- at Yakutsk. The concentrations of sulfate, SO_2 and HCl remarkably increased in late winter and spring.

We compare above concentrations at Yakutsk with those at Sapporo. We measured at Sapporo of the total particulate mass and the aerosol chemical species less than 2 μm in diameter in November 1991 through October 1992 (Ohta et al., 1995).

At Sapporo TPM ranged from 10.9 to 35.0 μgm^{-3}. The concentrations of the chemical species were non–sea salt SO_4^{2-}, 1.2–5.5; NO_3^-, 0.12–1.88; Cl^-, 0.00–1.23; Na^+, 0.16–0.74; Ca^{2+}, 0.09–0.67; Mg^{2+}, 0.03–0.11 μgm^{-3}. The monthly mean concentrations of atmospheric SO_2 measured at monitoring stations in Sapporo in 1991 were 3–15 ppbv.

Total particulate mass at Yakutsk is about the same as those at Sapporo. Sulfate and nitrate concentrations at Yakutsk are less than half or one third of those at Sapporo. SO_2 concentrations at Yakutsk is less than one tenth of those at Sapporo. In Sapporo, heavy oil

TABLE 2. Atmospheric concentrations of HNO_3, HCl and SO_2 at Yakutsk in July 1993 through July 1994 (F, first half; S, second half).

	Sampling period	HNO3 [ppb]	HCl [ppb]	SO2[ppb]
1	1993 JUL. S	0.03	0.12	0.64
2	AUG. F	0.07	0.05	0.53
3	AUG. S	0.03	0.07	0.48
4	SEP. F	0.03	0.11	0.23
5	SEP. S	0.04	0.12	0.26
6	OCT. F	0.03	0.09	0.27
7	OCT. S	0.05	0.14	0.27
8	NOV. F	0.05		0.15
9	NOV. S	0.05	0.07	0.42
10	DEC. F	0.03	0.06	0.11
*11	DEC. S	0.04	0.11	0.24
*12	1994 JAN. F	0.02	0.05	0.12
13	JAN. S	0.04	0.18	0.16
14	FEB. F	0.04	0.09	0.18
15	FEB. S	0.10	0.33	0.50
16	MAR. F	0.08	0.26	
17	MAR. S	0.09	0.39	1.04
18	APR. F	0.07	0.30	0.97
19	APR. S	0.07	0.29	0.62
20	MAY. F	0.06	0.38	0.46
21	MAY. S	0.08	0.53	0.33
22	JUN. F	0.08	0.44	0.48
23	JUN. S	0.24	0.25	0.21
24	JUL.F	0.10	0.39	0.19
25	JUL.S	0.12		0.22

is combusted for domestic heating, and many diesel engine vehicles are running, which emit a large amount of particulate sulfate and gaseous sulfur dioxide. Whereas in Yakutsk, natural gas, which emitts little sulfate or SO_2, is used for domestic heating and fewer vehicles are running there than in Sapporo. Thus there are far less emission sources of sulfur oxides in Yakutsk than in Sapporo.

On the other hand, calcium concentrations at Yakutsk are about the same as those at Sapporo. Because Yakutsk is located on the riverbed of the Lena river, the ground surface is covered with fine sand rich in calsium. In spring through fall, the fine sand particles blow up and fly over the area of Yakutsk city. We continue the measurements at Yakutak for two years ahead.

3

Carbon budget of Ecosystems

Carbon and nitrogen storage of soils in a forest–tundra area of northern Sakha, Russia

YOJIRO MATSUURA[1] and DANIEL P. YEFREMOV[2]

[1]Hokkaido Research Center, Forestry and Forest Products Research Institute, 7 Hitsujigaoka, Toyohira, Sapporo 062 Japan; Tel: +81–11–851–4131; Fax: +81–11–851–4167
[2]Yakutsk Institute of Biology, Russian Academy of Sciences, 41 Lenin Ave., Yakutsk, Republic of Sakha, Russia 677891

Introduction

Major carbon and nitrogen storage in northern terrestrial ecosystems are composed of dead organic matter and soil organic matter (Swift et al. 1979). In the circumpolar region, organic soils or immature soils are prevailing in forested bog ecosystems in which large amount of C and N accumulated in dead organic matter.

Recently, the effect of global climate change on the circumpolar region is one of the critical problems in biogeochemistry. In the forest–tundra zone of eastern Siberia, however, soil types and the pool size of C and N storage are uncertain. The aim of this study is to estimate C and N storage in soils of forest–tundra ecosystems, which would be mineralized acceleratedly under the anticipated global warming in the future.

Study site and method

We selected study sites in the forest–tundra zone at a tributary of Olenok River, near the drainage divide of Lena (71°36–37'N, 125°30–32'E). Altitude of the study sites ranged from 130 m to 250 m above sea level. Soil survey was conducted in July 1994. Two toposequences were examined; one was a forest–tundra site on a flat or very gently sloping terrace, and the other was a cryoplanation terrace slope of south to south–east aspect. The vegetation type of the forest–tundra was a sparse larch forest (*Larix gmelinii*), with shrubs such as *Betula exilis*, *Ledum parstre*, and *Vaccinium vitis–idaea*. Dominant microtopography was earth hummock covered with *Eriophorum vaginatum*, and mud hummock (bare centered hummock with no vegetation) was also spatially distributed in the sparse forest. Concave surface of the forest floor was covered with *Sphagnum* moss. Sparse larch forests on the terrace are gradually replaced by tundra meadows near water channels along a soil moisture gradient. Species composition of sparse forests on the slope was almost the same as that on the flat site. The vegetation of the upper slope (upland tundra) was dominated by *Dryas* sp. and Graminoids species. Earth hummocks were remarkable on the foot slope and upper slope. There were solifluction–lobes on the lower slope and turf–banked terraces near the tree limit in the middle slope.

Site description of three soil profiles (KY–1,–2,–3) on the flat terrace was shown in Table 1A, and four (KY–4,–7,–6,–5) on the cryoplanation terrace in Table 1B, respectively. Soil descriptions of former three profiles are as follows. KY–1: (L)FH–A/Bg–2HA–2Bf (letter suffix f indicates permafrost), several pieces of buried wood were found at the boundary of Bf. KY–2: B1–Bg1–Bg2–Bf, there were many frost–induced cracks on the soil surface. KY–3: (L)FH–HA–Bg–Bf, discontinuous buried organic materials accumulated in Bg horizon. These three profiles showed gley features in mineral horizons. Four profiles on the cryoplanation terrace are as follows. KY–4 (foot slope): L–FH–AB–Bg–Bf, cracks in Bf

TABLE 1A. Site description (flat area).

Coordinate	N 71° 37', E 125° 32'		
Landform	flat area (terrace)		
Profile	KY-1	KY-2	KY-3
Altitude	150 m	150 m	150 m
Direction	N 22 W	N 22 W	N 60 W
Aspect	3°	3°	1°
Micro-topography	earth hummocks	mud hummocks	earth hummocks
Surface vegetation	Sphagnum sp.	none	Eriophorum sp.

TABLE 1B. Site description (cryoplanation terrace).

Coordinate	N 71° 36'- 37', E 125° 30'- 32'			
Landform	cryoplanation terrace			
Position	foot slope	lower slope	middle slope	upper slope
Profile	KY-4	KY-7	KY-6	KY-5
Altitude	130 m	160 m	200 m	250 m
Aspect	S 80 E	S 35 E	S 0 EW	S 15 W
Slope	8°	25°	17°	8°
Micro-topography	earth hummocks	solifluction-lobe	turf-banked terraces	earth hummocks
Vegetation	sparse forest	sparse forest	tree limit	upland tundra
Surface vegetation	Vaccinium spp. Eriophorum sp.	Vaccinium spp. Empetrum sp.	Empetrum sp. Arctous sp.	Dryas sp. Graminoids

horizon were filled with ice. KY-7 (lower slope): L(FH)-A-BC1-BC2-BC3-BCf, subsoil horizons were abundant in saprolitic gravels. KY-6 (middle slope): L-HA-A-B1-B2 -Bs-Bg-Bf, buried wood pieces occurred on the boundary of Bf and cryoturbation was found in B1 and B2. KY-5 (upper slope): L-FH-HA-A-AB-Bf, there were many boulders of platy shapes in AB and B horizons. These seven profiles were not classified as Histosols but Entisols or Inceptisols (Soil Survey Staff 1992).

Air dried samples of mineral soils were sieved through 2 mm mesh. C and N concentrations were determined by dry combustion method (SUMIGRAPH NC-800). Subsamples were dried in an oven (105°C) for determination of oven dry weight. Carbon and nitrogen storage were estimated using bulk density, element concentrations, horizon depth and fine earth and gravel ratio in each horizon.

Results

Soils of the sparse forest on the flat terrace.—Depth of the active layer in the flat terrace site was relatively shallow, but the depth varied from 20 to 60 cm of mineral soil horizon

depending on the surface condition. Organic materials accumulated in profile KY-1, covered with *Sphagnum* moss, and profile KY-3, covered with *Eriophorum*, with 10 to 20 cm depth, and active layer was found at 15 to 30 cm depth. Cryoturbation slightly occurred in the active layers. In contrast, no organic materials accumulated on the surface of profile KY-2, where was on the mud hummock without vegetation. The depth of active layer varied from 40 to 70 cm under mud hummocks, which was deeper than that of other types.

Bulk densities in A/Bg and 2Bf of the KY-1 were 1.23 and 0.69 Mg/m^3, respectively. The 2HA horizon had low bulk density (0.29 Mg/m^3). Carbon concentration in 2HA horizon was 210 mg C/g, however A/Bg contained 43 mg C/g and 95 mg C/g in 2Bf horizon. Bulk densities of KY-3 changed 0.28-0.79-0.40 Mg/m^3, along HA-Bg-Bf. Carbon concentrations of horizons in KY-3 were higher than those of every horizon in KY-1. The Bf horizon of KY-3 contained 194 mg C/g. Physico-chemical properties of KY-2 was quite different from those of KY-1 and KY-3. Upper three horizons (B1-Bg1-Bg2) had high bulk densities (1.33-1.44 Mg/m3) and low C concentrations (28-36 mg/g), while Bf had low bulk density and high C concentration. Soil pH of these three profiles were acidic, ranging from 4.6 to 5.3.

Estimated carbon and nitrogen storage in KY-1, 2, and 3 were shown in Table 2A. Although the depth of active layers were shallow in KY-1 and 3, carbon storage in mineral soil horizons exceeded 10 kg C/m^2. Organic carbon accumulated from 0 to 3 kg C/m^2 in surface organic layers. Nitrogen concentrations in KY-1, 2, and 3 were relatively low so that the C/N ratios were about 20 in every mineral soil horizon. Nitrogen storage in three soil profiles were almost directly proportional to the carbon storage. Nitrogen accumulated in organic layers of KY-1 and 3 were nearly equal to 1/10 of those in mineral soils.

Soils of the cryoplanation terrace.—As shown in Table 2B, the depth of active layers varied from site to site. The deepest active layer occurred at the steep lower slope (KY-7). The foot slope (KY-4) and the upper slope (KY-5) had only 40 cm depth of the active layer. Organic materials accumulated little on the soil surface in all sites, with loose undecomposed litter less than 7 cm thickness.

Bulk densities of mineral soil horizons in KY-4, 5, and 7 were more than 1.0. But bulk densities were relatively low in A and Bf of KY-6 (0.5-0.8 Mg/m^3). Soil pH were higher in upper slope tundra soil KY-5 (6.2-6.9), and relatively low in foot slope KY-4 (5.8-5.9) and lower slope KY-7 (5.0-6.7). Because there were no HCl reactions, carbonate did not accumulate in higher pH horizons. Carbon concentrations in KY-4, 5, and 7 gradually decreased along soil depth. Most of the mineral horizons had less than 30 mg C/g. However in KY-6, C concentration slightly increased to more than 30 mg C/g in Bg-Bf zone which was the lower part of the active layer. Woody pieces were also found in the Bf horizon of KY-6.

Estimated storage of C and N was shown in Table 2B. Carbon storage in active layers varied from 11 to 27 kg C/m^2. Tree limit zone in the middle slope accumulated the most abundant C and N storage, while tundra site in the upper slope accumulated the least C and N storage in soil. C/N ratio in mineral soil horizons of these four profiles varied from seven to 17. Carbon storage in organic layers varied 0.1-1.0 kg C/m^2. As we observed in the flat terrace site, nitrogen accumulation in soils were nearly proportional to carbon storage. N in organic layers were ranging from four to 45 g N/m^2. The proportions of N storage in organic layers to N storage in soils were smaller in the cryoplanation terrace than in the flat terrace.

TABLE 2A. Carbon and nitrogen storage in soils of a flat area (terrace).

Profile	KY-1	KY-2	KY-3
Depth of			
organic layer	10 cm	0 cm	11 cm
active layer	22 cm	48 cm	18 cm
Soil organic carbon	----- $kg \cdot m^{-2}$ -----		
organic layer	2.0	0	3.0
active layer	11.9	20.5	15.7
Soil total nitrogen	----- $g \cdot m^{-2}$ -----		
organic layer	57	0	72
active layer	520	1032	716

TABLE 2B. Carbon and nitrogen storage in soils of cryoplanation terrace.

Profile	KY-4	KY-7	KY-6	KY-5
Depth of				
organic layer	5 cm	7 cm	5 cm	4 cm
active layer	40 cm	110 cm	82 cm	41 cm
Soil organic carbon	---------- $kg \cdot m^{-2}$ ----------			
organic layer	1.0	0.3	0.1	1.0
active layer	14.3	11.6	27.4	10.9
Soil total nitrogen	---------- $g \cdot m^{-2}$ ----------			
organic layer	33	10	4	45
active layer	1014	1307	1894	738

Discussion

C and N storage pattern in soils in the flat terrace site and the cryoplanation terrace site is attributed to the differences in pedogenesis processes. Vertical movement of frost-induced cryoturbation was dominant in soils on the flat terrace so that high content of carbon and nitrogen fractions of upper horizons mingled with the subsoil. As a result of this process, the element concentration might be rather high in B horizons. Therefore, large amount of carbon and nitrogen accumulated in shallow active layers of the flat terrace.

Lateral mass movement along the slope would affect the carbon and nitrogen accumulation in soils. Tree limit formed under a steep turf-banked slope of 30-50°, and KY-6 located near the knick-point in the middle slope of the cryoplanation terrace. Because

mass accumulation induced by frost shattering occurred at the knick-point, soils near the tree limit might be associated with soil surface movement. Thus, large amount of C and N accumulated in KY-6. On the other hand, rock fragment distribution also had an important role on soil development of the cryoplanation terrace. Because of high gravel content on the lower slope, carbon and nitrogen storage in KY-7 was not so large as other profiles in spite of the deepest active layer.

Carbon and nitrogen storage in soils of our study ranged from 11 to 27 kg C/m^2 and from 0.5 to 1.9 kg N/m^2, respectively. According to a review on carbon and nitrogen pools, C and N storage in tundra ecosystems (including dry-, moist-, wet-, and rain-tundra) ranged from 3.1 to 36.6 kg C/m^3 and from 0.6 to 2.2 kg N/m^3, respectively (Post et al. 1985). The results of our study on C and N storage in soils can be converted into 11-80 kg C/m^3 and 1.2-3.7 kg N/m^3, in the unit of cubic meter respectively. These are quite large for dry- and moist-tundra ecosystems.

The amount of C and N storage in soils is related to climatic factors which restrict biotic processes such as plant production and decomposition of organic matter. Carbon accumulation in peatlands had occurred during post-glacial period in other circumpolar regions such as Scandinavia, west Siberia, North America, and northern Canada (Gorham 1991). But the climate of eastern Siberia is extreme continental, with high air temperature in the summer and extremely low in the winter (temperature fluctuations of as much as 100°C) and annual precipitation is 200-300 mm (Walter 1979, Tuhkanen 1984). Because such a severe climatic condition restricted vegetation productivity, accumulation of organic matter and formation of Histosols or peatlands might be limited in eastern Siberia. Although climatic conditions are more extreme than those of dry- and moist-tundra, the vast area of sparse larch forests exist in eastern Siberia, with relatively large C and N storage of soils in the continuous permafrost region.

Conclusion

The patterns of carbon and nitrogen storage in soils reflected different pedogenic factors, such as vertical or lateral mass movement, in each toposequence. Carbon and nitrogen storage in soils of forest-tundra zone in northern Sakha was quite large, which was almost twice as large as the storage in other tundra ecosystems where climatic conditions are milder than that of eastern Siberia.

References

Gorham, E. 1991. Northern peatlands: role in the carbon cycle and probable response to climatic warming. Ecological Applications, 1: 182-195.

Post, W.M., J. Pastor, P.J. Zinke, and A.G. Stangenberger. 1985. Global patterns of soil nitrogen storage. NATURE, 317: 613-616.

Soil Survey Staff. 1992. Keys to soil taxonomy. 5th edition, USDA SMSS Technical Monograph No. 19., Pocahontas Press, Inc., Virginia.

Swift, M.J., O.W. Heal, and J.M. Anderson. 1979. Decomposition in terrestrial ecosystems. Blackwell Scientific Publications, Oxford.

Tuhkanen, S. 1984. A circumboreal system of climatic-phytogeographical regions. Acta Botanica Fennica 127: 1-50.

Walter, H. 1979. Vegetation of the earth and ecological systems of the geo-biosphere. 2nd ed., Springer-Verlag, New York.

Growth and photosynthetic characteristics of Siberian white birch and Scotch pine seedlings raised under elevated CO_2 and temperature

TAKAYOSHI KOIKE[1,3], THOMAS T. LEI[1], TROFIM C. MAXIMOV[2], SHIGETA MORI[1], KUNIHIDE TAKAHASHI[1], and BORIS I. IVANOV[2]

[1]*Forestry and Forest Products Research Institute, Hokkaido Research Center, Sapporo 062 Japan*
[2]*Yakut Institute of Biology, The Russian Academy of Sciences, 677891 c. Yakutsk, Republic of Sakha*
[3]*Present address: Forest Science Research, Tokyo University of Agriculture and Technology, Fuchu, Tokyo 183 Japan; Tel: +81-423-67-5745; Fax: +81-423-64-7812*

Abstract. The greenhouse effects on growth and photosynthetic characteristics of Siberian white birch and Scotch pine seedlings were examined under regulated environmental conditions. The seedlings were grown at two CO_2 levels of 70 Pa and 36 Pa combined with day/night temperatures of 30/16°C and 26/12°C with a day length of 20 hours for 96 days. The height growth of seedlings was accelerated by high temperature not by CO_2. It ceased at ca. 45 days for Siberian birch and at ca. 20 days for Scotch pine under a 20-hr-day length. We observed physiological adjustments in photosynthesis CO_2 concentration. At high CO_2, chlorophyll concentration and SLA of both species decreased. Quantum yield of both species was suppressed under high CO_2. Carboxylation efficiency of pine raised at high temperature decreased. The photosynthetic rate of birch assayed at the two CO_2 levels was very similar, and there was no difference in the CO_2-photosynthesis of pine irrespective of growth conditions. Water use efficiency and stomatal limitation of both species raised at high CO_2 increased. Nitrogen use efficiency (NUE) of birch was three times larger than that of pine; however, the increase in NUE of pine raised at high CO_2 was larger than that of birch. Based on the specific responses of both species, the growth of birch may be strongly restricted by the soil nutrient condition as compared with pine.

Key words: eastern Siberia; white birch; Scotch pine; photosynthetic adjustment; nitrogen use efficiency.

Background

Recently, the gas exchange characteristics of many tree species were examined in relation to global greenhouse problems (Ceulemans and Mousseau 1994). However, there are few cases of such examinations in tree species native to eastern Asia including the eastern Siberian region (Takahashi 1994). On the terrace of the Lena river, near Yakutsk, Sakha Rep., Scotch pine (*Pinus sylvestris*) develops on hilltops of forested areas. While birch (*Betula platyphylla*) grows at disturbed areas. Forest fires frequently occur in the Siberian forest where nutrient condition becomes momentarily favorable for trees. Birch and pine are light demanding species; however, foliage habit of both species is quite different, i.e. birch is deciduous and pine is evergreen. According to the global climate change models, increase in the ambient temperature of 3 to 5 °C at higher latitudes is anticipated. Atmospheric CO_2 is also showing annual increases. Would net photosynthetic rate of Siberian white birch and Scotch pine increase when they experience a climate of elevated CO_2 and temperature? In this study, we evaluated the growth response of birch and pine native to eastern Siberia by simulating this future greenhouse environment.

Objectives in 1994

Our aim was to elucidate 1) the photosynthetic acclimation pattern of white birch and

Scotch pine to ambient CO_2 levels, and 2) the growth and photosynthetic responses of both species to elevated CO_2 and temperature. For these purposes, we raised seedlings of Siberian white birch and Scotch pine under doubled CO_2 and a 4 °C increase, and measured the photosynthetic capacity of both species acclimated to these simulated greenhouse environments.

Materials and methods

Plant materials.—Seeds of Siberian white birch (*Betula platyphylla*) and Scotch pine were collected at Spasskaya Pad Forest Experiment Station of the Yakut Institute of Biology, Sakha Rep., Russia. (63°N, 129°E). At the Forestry and Forest Products Research Institute (FFPRI) in Sapporo, the seeds were germinated on vermiculite under ambient CO_2, 25/20 °C day/night temperature, 22–hr–day length. When the seedlings were about 8 cm in height, seedlings of each species were transplanted singly into vinyl pots (diameter 15 cm, height 12 cm) filled with Kanuma pumice soil (nutrient poor). To reach this transplanting height, it took one year for birch and for two years for pine. Ten potted seedlings were transferred to the FFPRI phytotron under four CO_2/temperature treatments.

Treatments.—Ten plants of each species were raised under four treatment conditions of two CO_2 levels (36 Pa ± 3 Pa, 70 Pa ± 5 Pa) regulated with a CO_2 controller (DAIWA Air Co. LtD.), combined with two temperature regimes (day/night: 30/16°C, 26/12°C). The lower temperature regime represented the mean values of max. and min. temperature from June to August at Spasskaya Pad Forest Station. The higher temperature regime was set to a 4°C increase as predicted for the 70 Pa CO_2 environment. Day length was extended to 20 hrs with supplemental lighting (2 fluorescence lamps for plant growth, 40 W; 2 incandescent lamps, 500 W). Liquid fertilizer (Hyponex; N:P:K = 5:10:5, U.S.A.) was supplied at the rate of 140 mg $N \cdot l^{-1} \cdot wk^{-1}$. The trays containing the potted plants were always filled with water to a depth of 2.5 cm to maintain opening stomata of the seedlings. The treatments were imposed from May 6 to August 28 in 1993.

Measurements.—All gas exchange measurements were made at the artificially illuminated growth cabinet (Koito KG). The light source consisted of 16 metal halides, 6 mercury, 8 incandescent, and 16 fluorescent lamps. Light and CO_2 dependent photosynthetic rates were measured with a portable gas analyzer (Shimadzu SPB H3, ADC H3 U.K.). To generate light levels above 1200 $\mu mol \cdot m^{-2}s^{-1}$, supplemental halogen lamp (Nikon, Tokyo) was used. Gas exchange rates were measured on the third and fourth leaves from the shoot tip. The age of measured leaves and needles was always 25 to 30 days for birch and ca. 380 days for pine. For the light dependent photosynthesis measurement, neutral density cloth filters (Sekisui Petro. Chem. Co., Osaka) were placed on the top of the leaf chamber. The number of replications of each measurement was more than three times. For the CO_2 dependent photosynthetic measurements, CO_2 partial pressure was varied by mixing enriched CO_2 air and Soda–lime filtered air using a flow meter (Kojima, Tokyo) and with a cylinder of Soda lime.

Quantum yield was estimated from the initial slope of the light–photosynthesis curve determined at saturated CO_2 (> 120 Pa). Carboxylation efficiency (CE) was calculated by the initial increment of intercellular CO_2 partial pressure (C_i) and net photosynthetic rate. Maximum photosynthetic rate at saturating light and CO_2 (P_{max}) was determined to estimate the rate of RuBP regeneration. Water use efficiency (WUE; $\mu mol \cdot mmol^{-1}$) was calculated as the ratio of photosynthesis to transpiration at saturated light and a constant water vapor

pressure deficit. Relative stomatal limitation of photosynthesis (l_s: %) was estimated from the following equation; $l_s = (A_0-A)/A_0$, where A_0 is the net photosynthetic rate when stomatal resistance to CO_2 diffusion is zero, and A is the actual photosynthetic rate. After the gas exchange measurement, the projection area of birch leaves and pine needles was determined with an area meter (Hayashi AAM-5) and with an image digitizer (Planimex 25, NIRECO, Tokyo), respectively. Foliage dry weight was obtained after drying at 85°C for 48 hrs. Specific leaf area (SLA) was calculated as leaf area per dry weight ($m^2 \cdot g^{-1}$). Foliar nitrogen concentration was analyzed with a N/C corder (Yanagimoto MT 500 W and SUMIGRAPH NC-800, Sumica Chem., Osaka). Chlorophyll content of leaves was determined with Arnon's method.

Results

Height growth of seedlings and foliar characteristics. The cessation of growth of leader shoot occurred at about 45 days for Siberian birch and at about 18 days for Scotch pine after foliage unfolding (Fig. 1). Time required to reach the maximum size of both species was accelerated by high temperature not by high CO_2. The final length of leader shoot of birch was five times larger than that of pine. Individual leaf area of birch raised at high CO_2 was smaller under both temperature regimes. In contrast, there was no difference in projected needle area among treatments (Fig. 2A). In birch, SLA increased with high temperature. Both SLA (Fig. 2B) and chlorophyll (Fig. 2C) of pine were independent of treatment temperature.

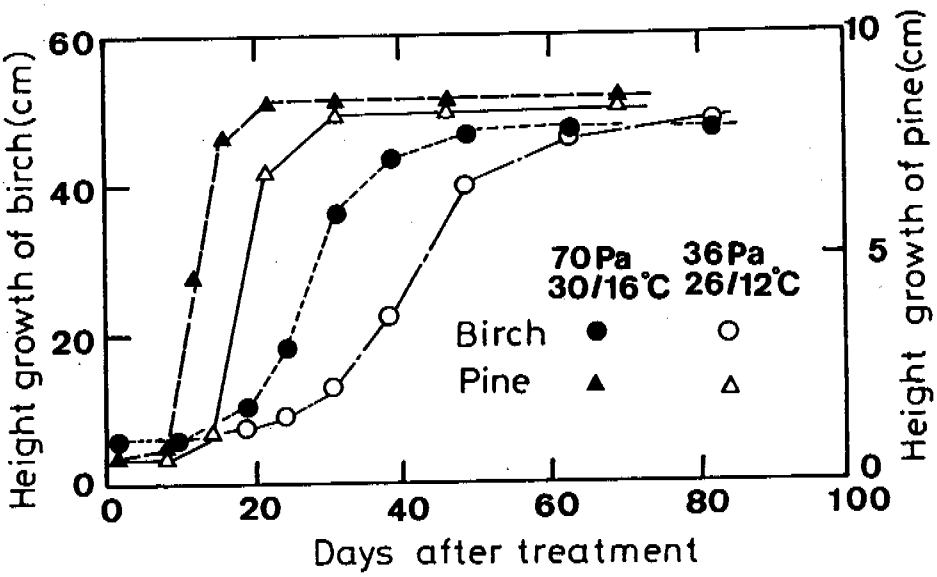

FIG. 1. Examples of the time course of height growth in white birch and Scotch pine grown under elevated CO_2 and temperature, and ambient CO_2 (control), 20 hrs day length.

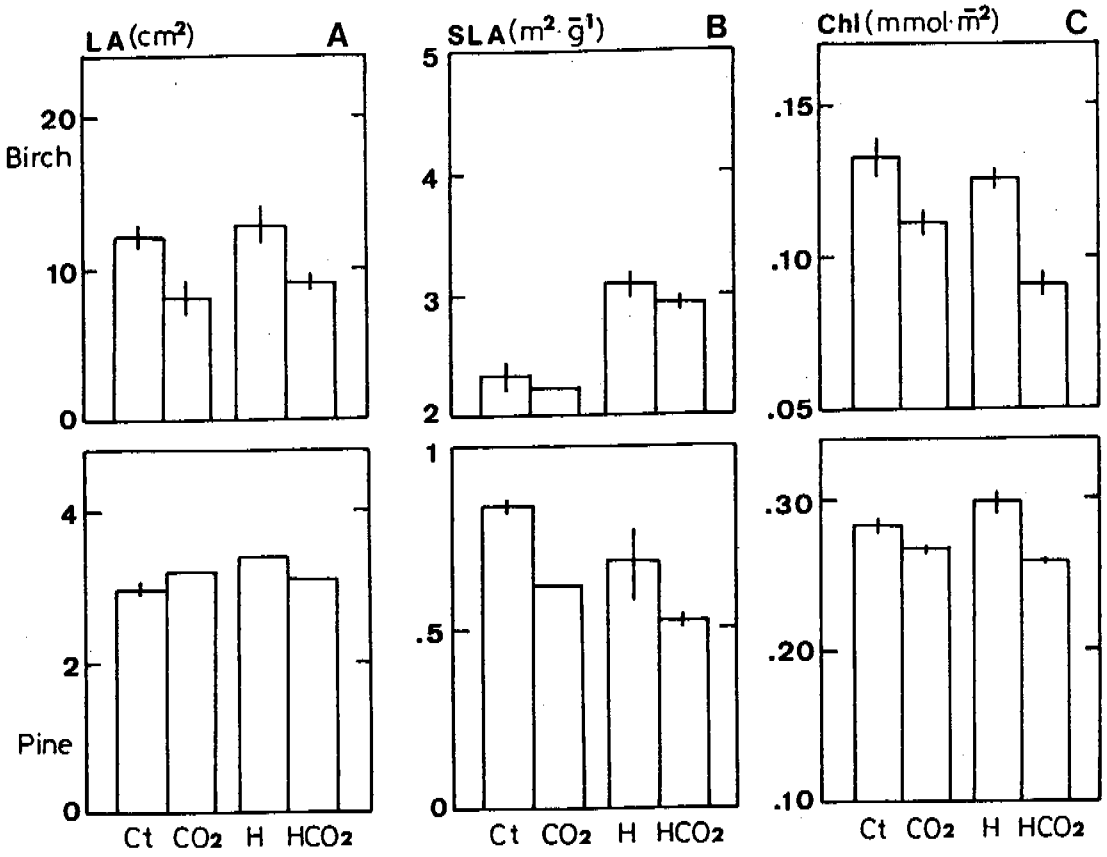

FIG. 2. Characteristics of individual leaves of Siberian white birch and Scotch pine raised under different treatments. Ct: 26/12°C, 36 Pa; CO_2: 26/12°C, 70 Pa; H: 30/16°C, 36 Pa; HCO_2: 30/16°C, 70 Pa.

Photosynthetic characteristics.—In birch, net photosynthetic rate assayed at the growth CO_2 concentration was almost the same (Fig. 3). Maximum photosynthetic rate (P_{max}) of birch raised at 70 Pa was ca. 5 $\mu mol \cdot m^{-2}s^{-1}$ lower than that of birch at 36 Pa. There was no difference in the P_{max} of pine. However, the saturating CO_2 level for net photosynthetic rates of pine differed between high and low temperature treatments at 100 Pa and 140 Pa, respectively.

Quantum yield of both species grown under high CO_2 was lower than that under ambient CO_2, especially in birch (Fig. 4A). Carboxylation efficiency (CE) of birch was slightly suppressed with high CO_2 and high temperature (Fig. 4B). While CE of pine raised at high temperature also decreased but CE at high CO_2 was higher than that at ambient CO_2. P_{max} of birch grown at 70 Pa was lower than that at 36 Pa while that of pine showed no statistical difference in all treatments (Fig. 4C). Regardless of growth temperature, WUE and l_s of birch and pine raised at 70 Pa were significantly greater than those at 36 Pa (Fig. 5). The stomatal limitation (l_s) of pine raised at 70 Pa was highest (nearly reaching to 30 %). Foliage nitrogen concentration of both species decreased with high CO_2. The nitrogen use efficiency (NUE) of birch was 3 to 5 time larger than that of pine (Fig. 6). NUE of both species raised at high CO_2 was higher that at low CO_2. In both birch and pine, increasing rate of the greatest NUE was observed in the simulated future greenhouse environment.

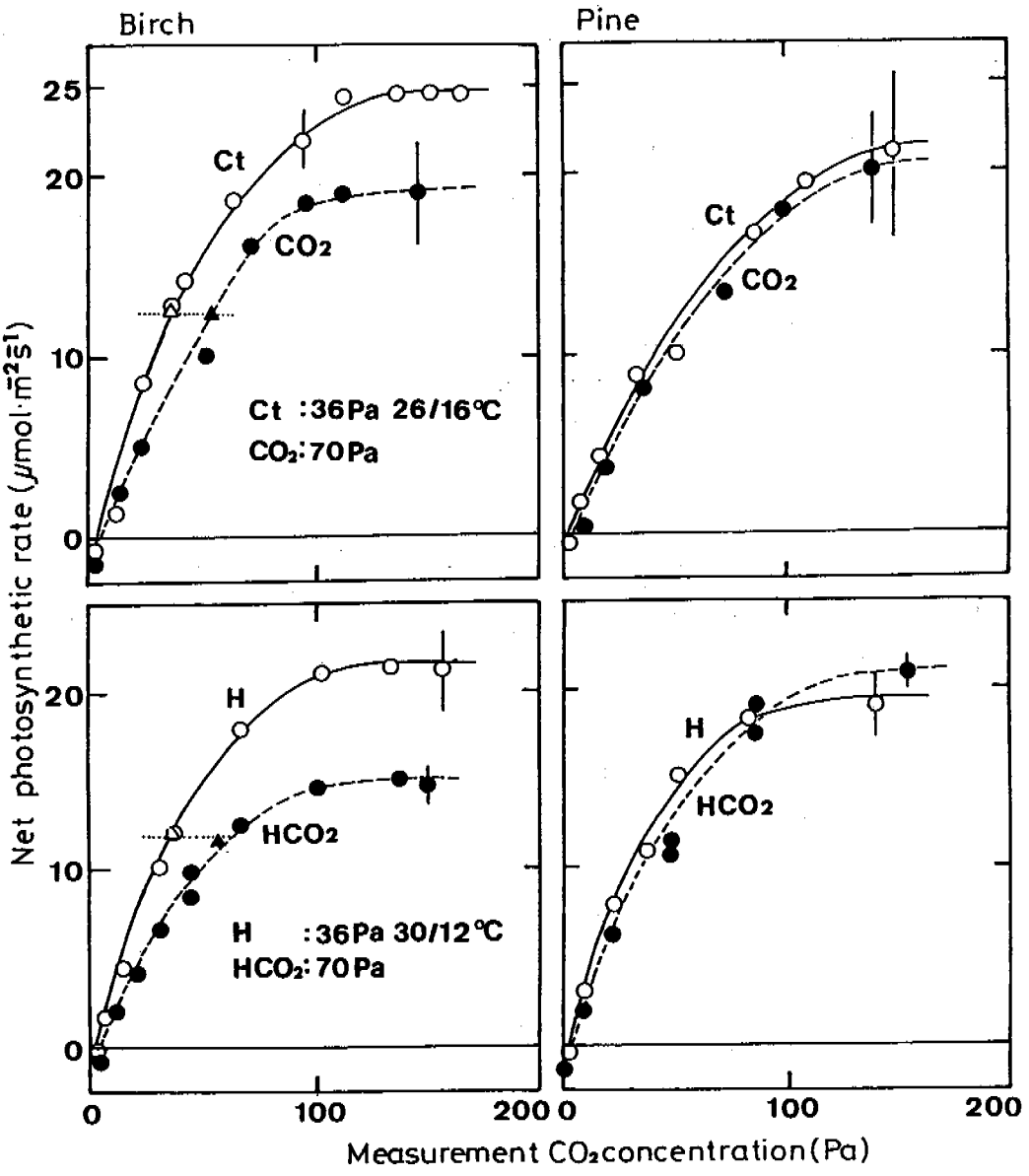

FIG. 3. CO_2–foliar net photosynthetic rate of white birch and Scotch pine seedlings raised under ambient and elevated CO_2 and temperature. Triangles in the figure indicate treated CO_2 concentration.

Reference

Ceulemans, R., and M. Mousseau. 1994. New Phytol. 127: 425–446.

Takahashi, K. 1994. Interim Report of joint research project "Carbon Storage and Carbon Dioxide Budget in Forest Ecosystem" between Japan and Russia. FFPRI, Hokkaido Res.Ctr. 105pp.

Research plan for 1995

1. To elucidate the growth response of larch under elevated CO_2 at different nutrient levels.
2. The role of soil water regime on the photosynthesis of larch under Siberian field conditions.

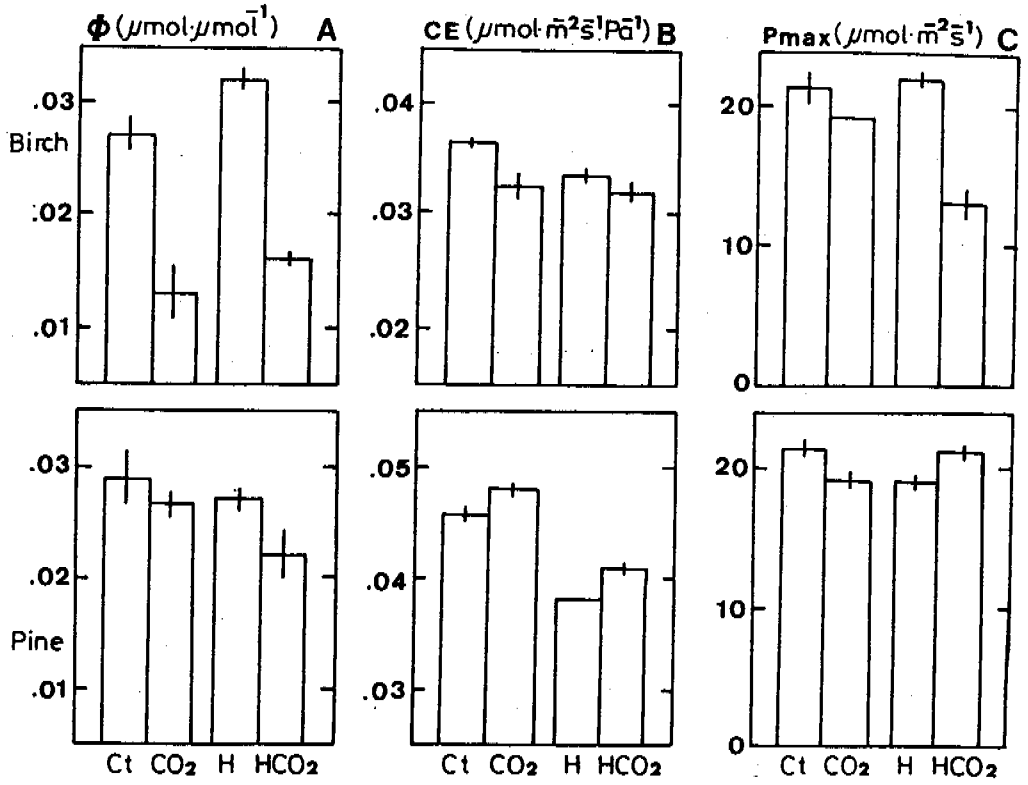

FIG. 4. Physiological parameters of the photosynthetic capacity of white birch and Scotch pine grown under four treatments.

3. To evaluate nutrient dynamics in needles of pine grown at different soil moisture condition at Spasskaya Pad Forest Station.

Acknowledgments

This research was supported in part by Japan Environment Agency (Joint Siberian Permafrost Study; Dr. G. Inoue). We thank Prof. M. Fukuda (Hokkaido Univ.) for his help in field study, and Drs. T. Sassa, S. Ohta, and Stephanov for collecting seeds. Thanks are also due to Mr. R. Ueda (DAIWA Air Co. LtD.) for designing the CO_2 controlling unit.

Publicastions

Koike, T., R.Tabuchi, and K.Takahashi. 1994. A trial of *in situ* measurement of gas exchange rates of woody plants grown at the permafrost area in eastern Siberia. Proc. First GAME/SIBERIA symposium. Inst. for Hydrospheric–Atmospheric Sci. Nagoya Univ., pp 25–30.

Koike, T., T.T. Lei, R. Tabuchi, T.C. Maximov, K. Takahashi, and B.I. Ivanov. 1995. Comparison between the photosynthetic capacity of Siberian and Japanese white birch raised under elevated CO_2 and temperature. Tree Physiol. (*in press*).

Koike, T., T.T. Lei, S. Mori, T.C. Maximov, K. Takahashi, and B.I. Ivanov. 1995. Effects of enriched CO_2 and temperature on the gas exchange characteristic of white birch and Scotch pine seedlings native to eastern Siberia. Scand. J. For. Res. (*in preparation*)

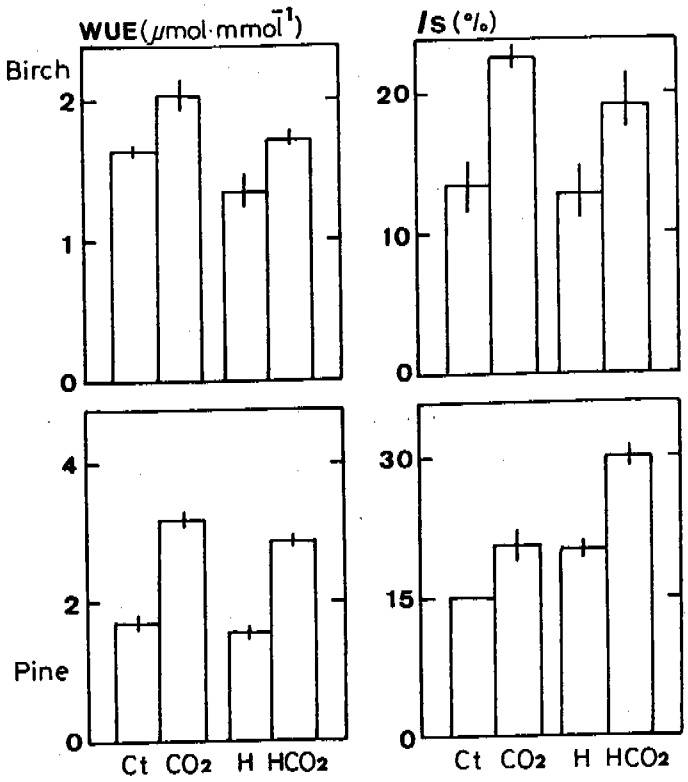

FIG. 5. Water use efficiency (WUE) and stomatal limitation (*ls*) of white birch and Scotch pine seedlings grown under four treatments.

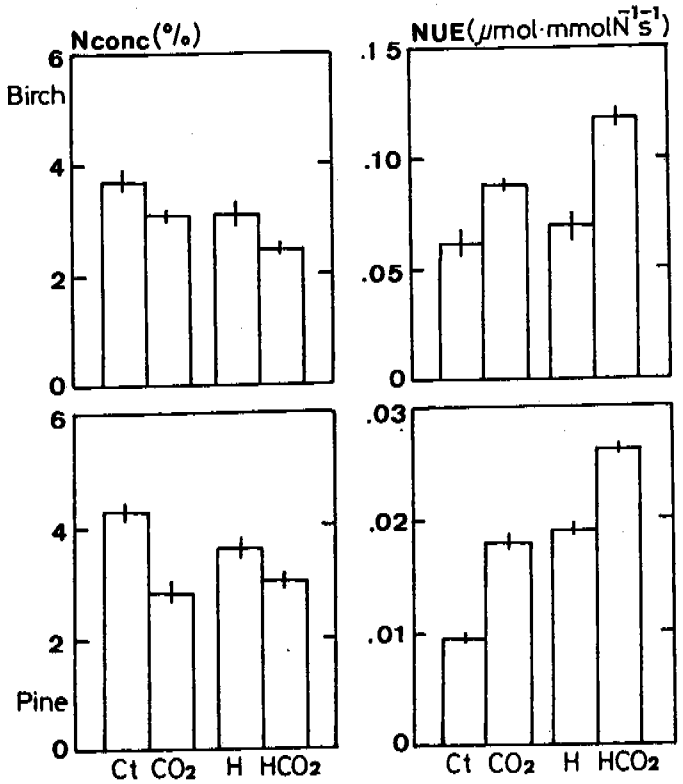

FIG. 6. Foliage nitrogen concentration and nitrogen use efficiency (NUE) of white birch and Scotch pine seedlings raised under four treatments.

A big forest fire in permafrost area of eastern Siberia

KUNIHIDE TAKAHASHI[1] and ANATOLY P. ABAIMOV[2]

[1]*Forestry and Forest Products Research Institute, Kyushu Research Center, 4-11-16 Kurokami, Kumamoto 860 Japan*
Tel: +81-96-343-3167; Fax: +81-96-344-5054; E-mail: kun23@ffprikys.affrc.go.jp
[2]*Sukachev Institute of Forest, Russian Academy of Sciences, 660036 Academgorodok, Krasnoyarsk, Russia*

Introduction

Annual extent of burning in the northern temperate and boreal forests has increased markedly in recent years (Auclair and Carter 1993). In Siberian taiga of the permafrost areas, big forest fires have occurred frequently. Dixon and Krankina (1993) reported that the annual total forest area burned by wildfires ranged from 1.41 x 10^6 to 10.0 x 10^6 ha from 1971 to 1991, and approximately 15,000–25,000 forest fires occurred annually during this period. They also estimated that mean annual direct CO_2–C emission from wildfires was approximately 0.05 Pg over this 21-year period, and total post-fire biogenic CO_2–C emmisions for 1971–1991 ranged from 2.5 to 5.9 Pg (0.12–0.28 Pg annually).

We started a cooperative project in 1994 between Sukachev Institute of Forest of Russia (SIF) and Forestry and Forest Products Research Institute of Japan (FFPRI) to estimate the effect of fires on taiga, and the release of CO_2 from forest ecosystems at Tura, Evenki Region, Eastern Siberia. We observed a big forest fire at Tura in early September of 1994.

A big forest fire at Tura in 1994

Fig.1 taken from an airplane (Antonov 2) on Setember 8 shows a big forest fire which has been burning for about a month near Tura. The burnt area which consisted of almost pure dense larch forests (Fig.2) was estimated to be approximately 700,000 ha. Ground vegetation of the damaged forests has burned completely and diminished (Fig. 3), but a part of it remained unburned (Fig. 4). Permafrost of the burnt forest has already begun to melt (Fig. 5), and some of the remained trees also began to fall to the ground (Fig. 6).

We are planning to set some test sites in this area to estimate the total biomass burned by the forest fire and the release of biogenic carbon from the soil. We also plan to investigate the difference of the damage among plant species of the ground vegetation or the micro-topographies.

Cooperative research plan between Russia and Japan

Both SIF and FFPRI have reached mutual understanding to undertake cooperative researches in the following areas: (a) Remote sensing studies for the forest site classification and pyrological zoning to estimate the carbon budget of forest ecosystems; (b) Creation of the vegatation map and the vegatation fuel map for a part of the model area; (c) Studies on consumed fuel during forest fire and emission of carbon to the atmosphere; (d) Studies on fire scar of forest ecosystem and its postfire dynamics, growth trend and budget of carbon; (e) Studies on post-fire development of edaphical conditions and after-effect of forest fires on tree species. We, both SIF and FFPRI, hope to make our research more fruitful and efficient

in the following investigation for several years.

References

Auclair, A.N.D. and Carter, T.B. 1993. Forest wildfires as a recent source of CO_2 at northern latitudees. Can. J. For. Res. 23:1528–1536

Dixon, R.K. and Krankina, O.N. 1993. Forest fires in Russia: carbon dioxide emissions to the atmosphere. Can. J. For. Res. 23:700–705

FIGURES. Numerals in the photographs indicate Figure numbers.

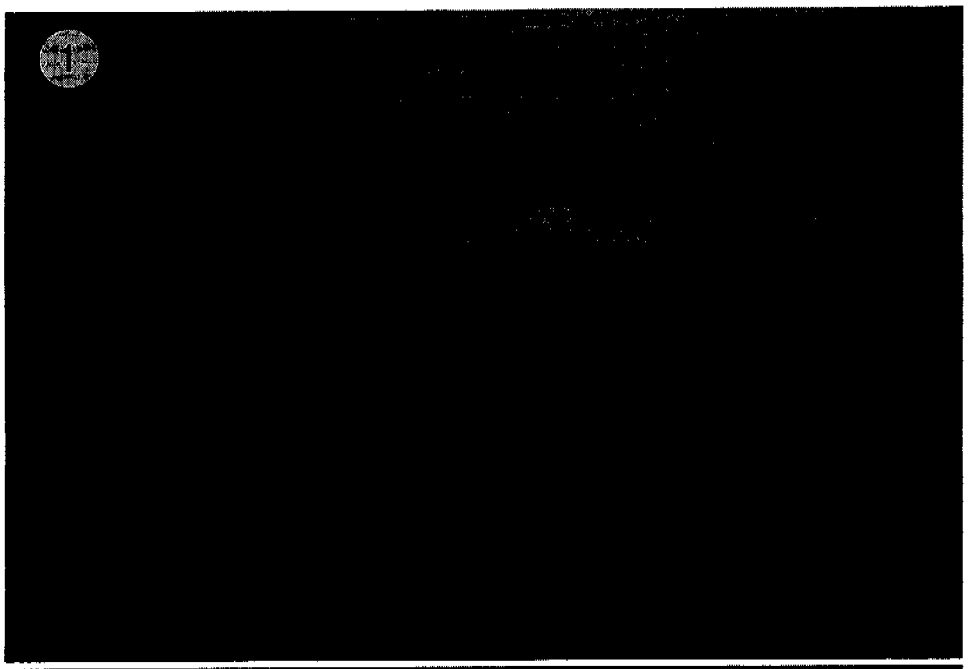

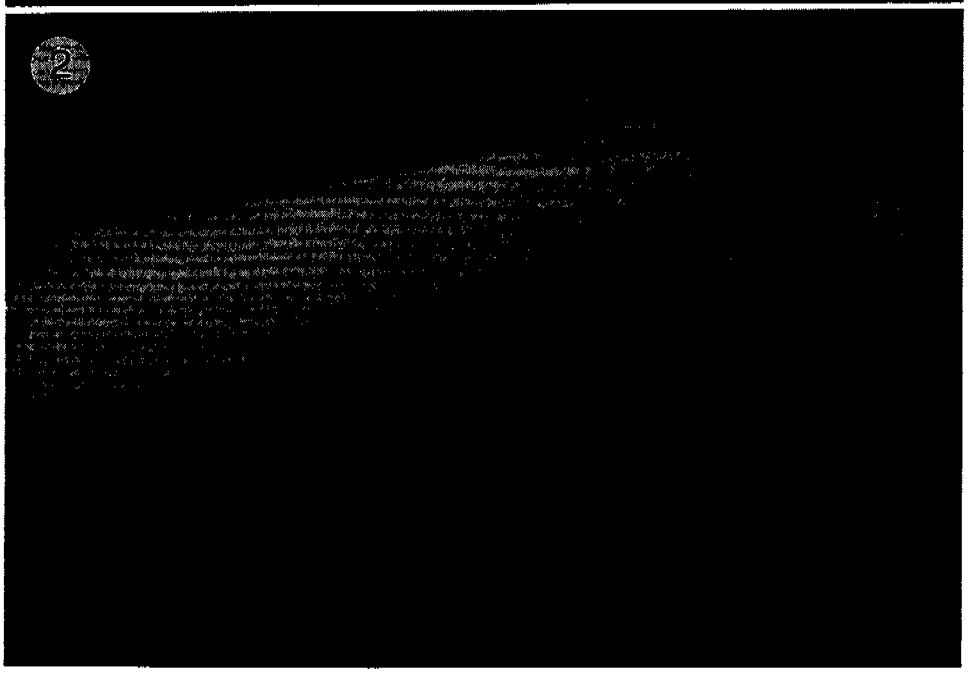


3


4

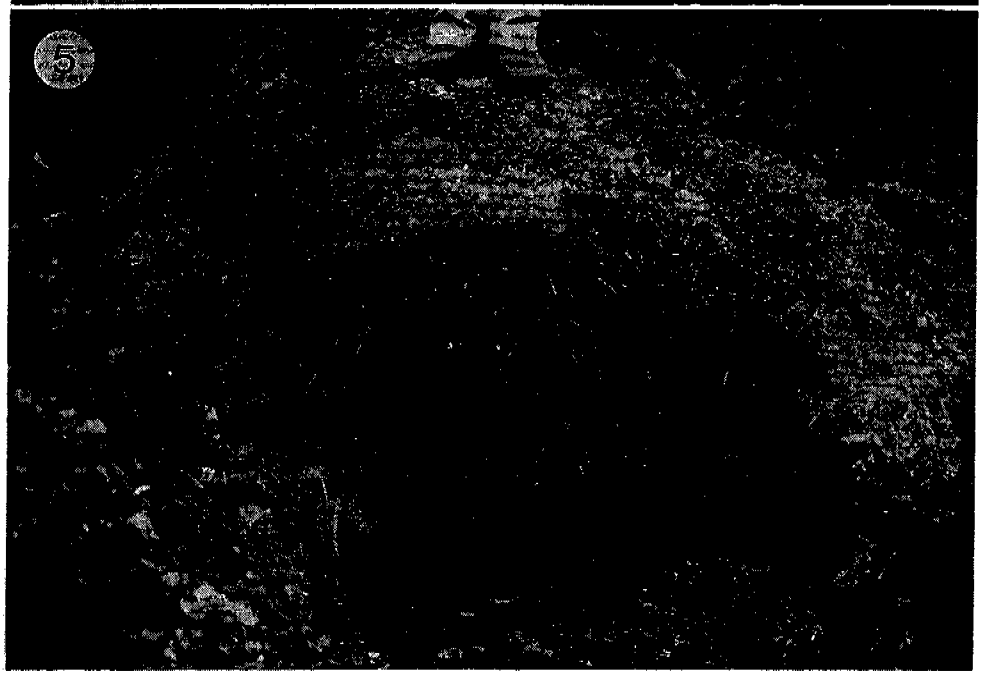
5

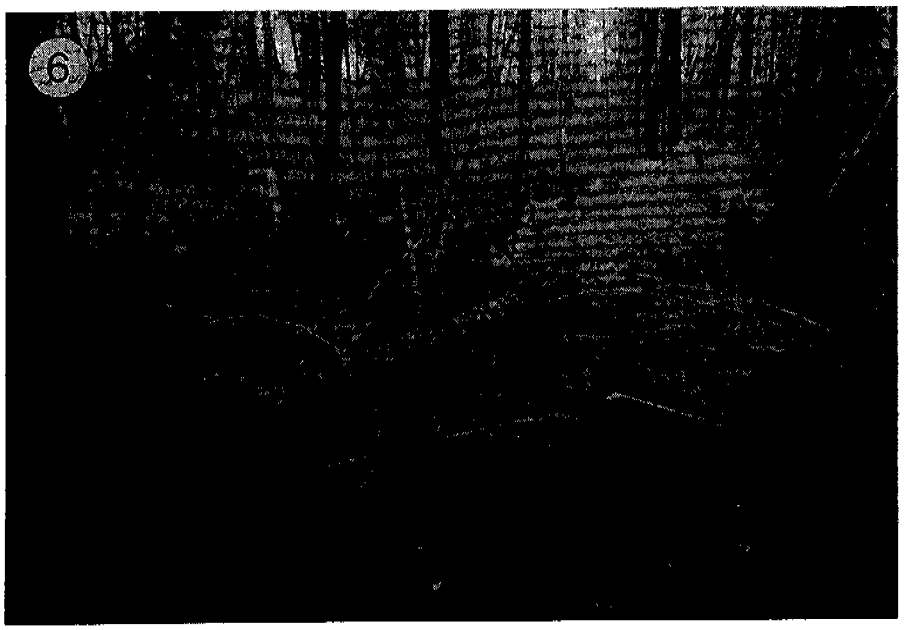
6

Measurement of CO_2 flux from forest soil using ^{222}Rn

MASAO UCHIDA[1] and YUKIHIRO NOJIRI[2]

[1]*University of Tsukuba, 1 Tennodai, Tsukuba 305 Japan*
Tel: +81-298-58-0938; Fax: +81-298-86-0387
[2]*National Institute for Environmental Studies, 16-2 Onogawa, Tsukuba 305 Japan*

Introduction

It is reported that the carbon cycling of the high latitudes, including taiga of Siberia, could be more sensitive to the global warming. The CO_2 flux, i.e., soil respiration rate, from this area has not been fully studied at the present stage, though this is an important factor for global carbon cycling. In this study, the CO_2 flux measurement by ^{222}Rn was conducted with conventional methods (static chamber method and air flow chamber method) in coniferous forests in Japan. The static chamber method was also carried out to investigate a spatial variation of CO_2 flux. The source strength of CO_2 in the soil was determined from the ^{222}Rn measurement to investigate a seasonal distribution of CO_2 production in the soil. These methods are applicable to measure CO_2 flux from the soils in Siberian taiga.

Experimental

The measurements were carried out in four forests; Tsukuba site, Mt. Tsukuba site, Nikko site and Sugadaira site from July to October, 1994. All sites are located in the central region of the main island of Japan. The dominant vegetation are *Pinus densiflora* Sieb. et Zucc except for Nikko site, where the dominat is *Larix kaempferi* Carriere.

The CO_2 flux were measured by the conventional methods and the ^{222}Rn method. The static chamber method (SC-method) determines the CO_2 flux from an increasing rate of CO_2 concentration in the chamber. The static chamber was placed over the soil surface. Gas in the chamber was sampled every five minutes by a 20 ml plastic syringe, then transferred to a 10 ml evacuated glass vial. The air flow chamber method (AF-method) was measured from the difference in concentration between the inlet and outlet of the chamber ventilated continuously by the air.

Soil gas was taken through polypropylene probes, already set into selected depths. A plastic syringe was used to draw 10 ml of air from the probes. Each sampled air was transferred to the evacuated glass vial for CO_2 analysis and the scintillation cell for ^{222}Rn analysis. The CO_2 concentration was analyzed by a gas chromatograph with TCD. ^{222}Rn activity was measured by an α-ray scintillation counter.

Determination of CO_2 flux using ^{222}Rn

The CO_2 flux by ^{222}Rn method was determined by the Fick's diffusion model (Dorr, 1990). The calculation process are described as follows,

$$j_{Rn} = D_{Rn} \times grad\ C_{Rn} \quad (1)$$

$$D_{CO2} = D_{Rn} \times D_{0CO2}/D_{0Rn} \quad (2)$$

$$j_{CO2} = D_{CO2} \times grad\ C_{CO2} \quad (3)$$

$$= (D_{0CO2}/D_{0Rn})(grad\ C_{CO2}/grad\ C_{Rn})j_{Rn} \quad (4)$$

where D_{0CO2}/D_{0Rn} = 1.3 at 15°C. From the Fick's 1st law, the diffusion coefficient of ^{222}Rn D_{Rn} was determined by the ^{222}Rn concentration gradient at the soil surface and ^{222}Rn flux from the soil. The diffusion coefficient of CO_2 D_{CO2} can be derived from the *DRn* and the ratio of the molecular diffusion coefficient, D_{0Rn}/D_{0CO2}. The CO_2 flux can thus be calculated from eq. (4). This procedure can cancel out the effect of soil moisture, total porosity and tortuosity, which have large uncertainties.

Results and discussion

The typical results of ^{222}Rn flux, ^{222}Rn profile and CO_2 profile in Nikko site are shown in Figs. 1 to 3, respectively. The results of CO_2 flux measurements by various methods are

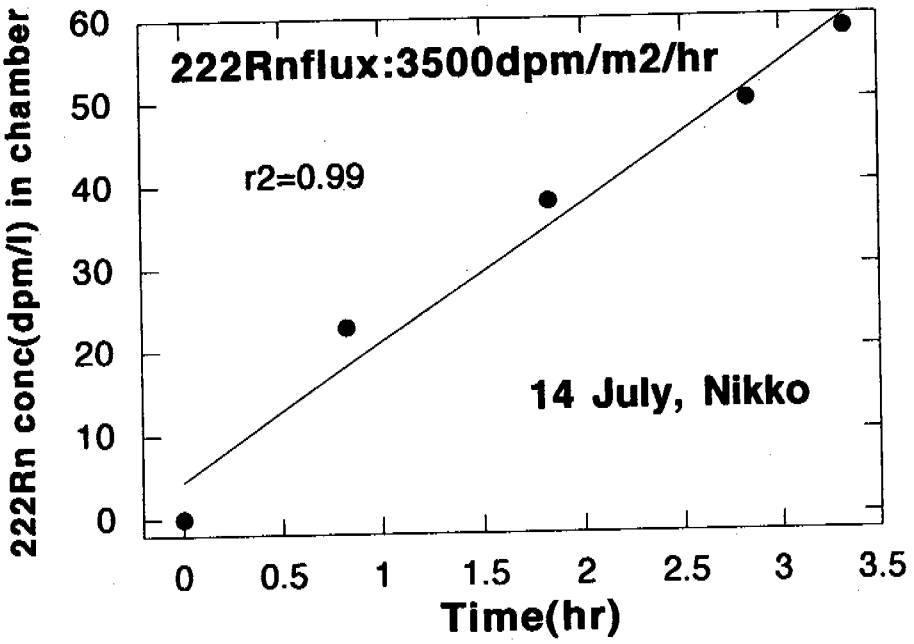

FIG. 1. ^{222}Rn concentration change with time in the chamber. ^{222}Rn flux was calculated from the concentration gradient of the regression line.

given in Table 1. The CO_2 flux by ^{222}Rn method were compared with the SC–method and the AF–method. The AF–method was carried out only in Tsukuba site. The multivariate analysis of variance was made in order to check the significance of the difference between the ^{222}Rn method and the SC–method. The difference in the two methods was not regarded as significant. Thus the validity of CO_2 flux measurement by the ^{222}Rn method was confirmed in the field experiment.

In order to investigate a spatial variation of CO_2 flux, the SC–method was applied at Tsukuba site and Nikko site. Simultaneous uses of several chambers and the relocation of them gave the spatial data. The CO_2 gas in the chamber was collected under a constant soil temperature because CO_2 flux was greatly influenced by soil temperature. The result of measurement is given in Table 2. The spatial variation was far larger than the error of the measurement. The averaged CO_2 flux of Tsukuba site by the 8 points of measurements within the distance of 5 m from the soil gas sampling proves was 329 mg $CO_2/m^2/hr$. That of Nikko site by the seven points of measurements was 242 mg $CO_2/m^2/hr$. The coefficients of variation (C.V., %), which means the spatial variation of CO_2 flux, for the four sampling

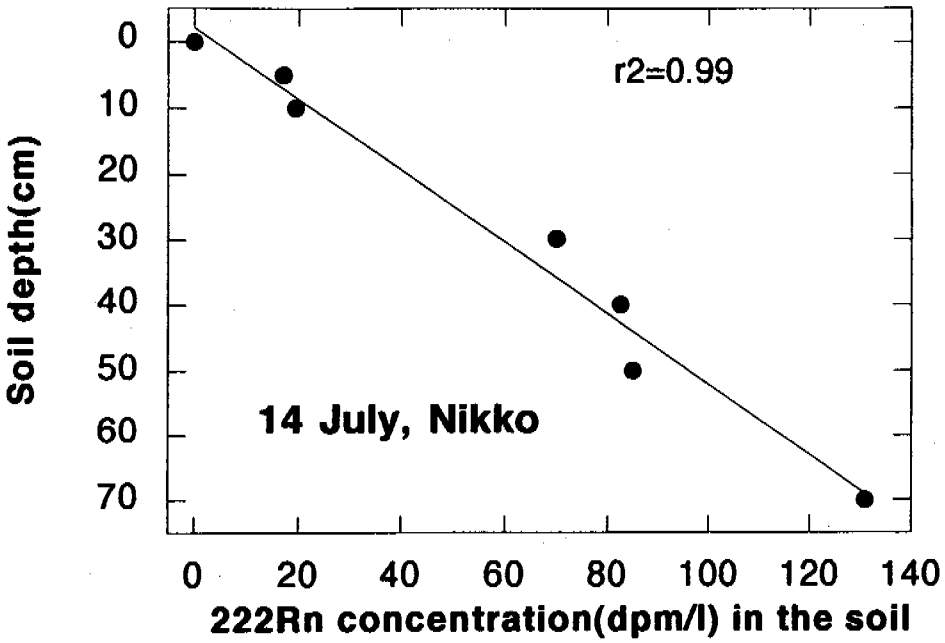

FIG. 2. ^{222}Rn concentration profiles in the soil. Soil gas was sampled in Nikko site in July 1994. ^{222}Rn activities were measured by a scintillation counter.

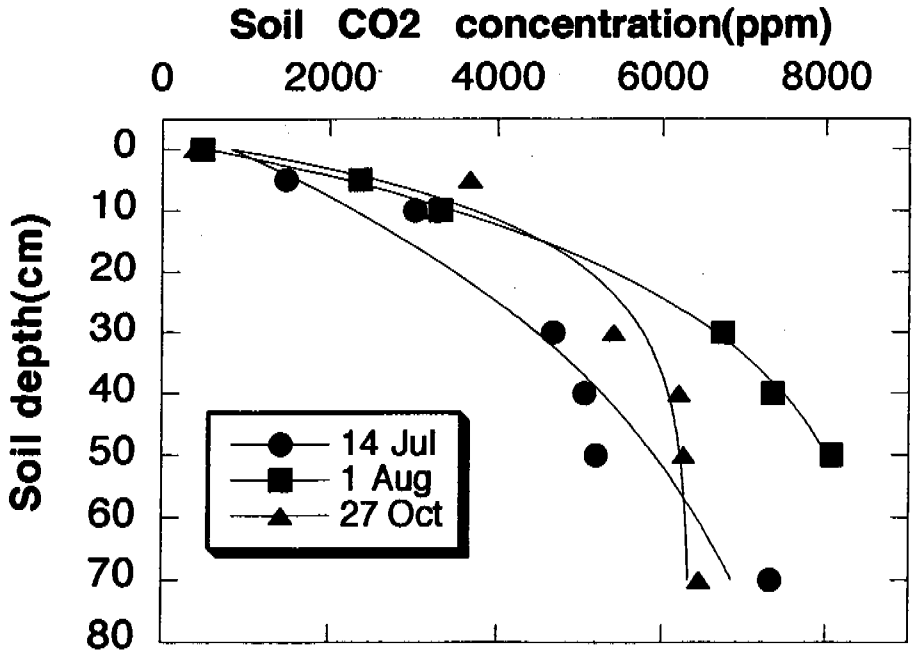

FIG. 3. CO_2 concentration in the soil air at Nikko site in 1994. Concentration gradient was calculated from an exponential fitting over the observed values.

campaigns in Tsukuba site ranged 20 and 35%. The average of the spatial variation in Tsukuba site was 27%. An intensive measurement of spatial variation of CO_2 flux was carried out in Tsukuba site on 31 October, 1994, 27 points of measurements within the

TABLE 1. Comparison of CO_2 flux by various methods.

Location&date	^{222}Rn-calibrated method	Static chamber method ($mgCO_2/m^2/hr$)	Air flow chamber method
Tsukuba, 7.11	1500	1117	928
Tsukuba, 8.9	1016	1270	
Tsukuba, 9.21	411	350	
Tsukuba, 9.26	346	380	
Tsukuba, 10.18	584	385	
Tsukuba, 10.31	514	318	
Nikko, 7.14	847	511	
Nikko, 8.1	1117	512	
Nikko, 10.27	171	130	
Mt.Tsukuba, 7.9	831	985	
Mt.Tsukuba, 8.12	594	667	
Sugadaira, 7.16	264	376	

TABLE 2. Spatial variation of CO_2 flux. CO_2 flux was measured by the static chamber method. The CO_2 concentration in the chamber was analyzed by GC/TCD.

Location & date	number of samples	average CO_2 flux ($mgCO_2/m^2/hr$)	C.V.(%)	CO_2 flux Max.	Min.
Tsukuba,9/21	8	329	20	404	218
Tsukuba,9/26	4	451	29	546	257
Tsukuba,10/18	3	286	35	385	184
Nikko,10/27	7	242	22	284	130
Tsukuba,10/31	27	310	31	596	159

CO2 flux was measured by the static chamber method. CO2 concentration in the chamber was analysed by GC/TCD.

distance of 20 m from a set of soil sampling probes was made. The averaged CO_2 flux was 310 mg $CO_2/m^2/hr$ and its C.V. value 31%. The spatial variation had no relationship with the numbers of points of measurements.

The spatial variation of CO_2 flux may be related to many factors such as soil microbial activities, water contents, soil structure, distributions of plant roots and so on. The variation of CO_2 flux should reflect the heterogeneity of the forest. A single point measurement of CO_2 flux could contain a large error due to the heterogeneity. To estimate more accurate CO_2 flux in such a heterogeneous system as a forest, the multiple measurement covering widely the target area is needed. The SC-method is thus an useful procedure to evaluate spatial variations from the ease of measurements and cost performance of instruments. Moreover by means of a combination with the AF-method, an averaged diurnal integration of CO_2 flux would be obtained. Source strength of soil CO_2 in each depth was calculated by the simultaneous measurements of CO_2 profile and diffusion coefficient of CO_2 by the ^{222}Rn method. Source strength of CO_2 Q_{CO2} was determined by the following equation.

$$Q_{CO2} = D_{CO2} \times grad\ (grad\ C_{CO2}) \qquad (5)$$

where D_{CO2} is described in eq. (2).

The source strength of soil CO_2 at Nikko site from July to October, 1994 are shown in Fig. 4. The exponential decrease is the result of curve fitting for CO_2 concentration profile and the assumption of constant diffusion coefficient in the active layer, derived from the ^{222}Rn measurement result. The source strength sharply decreased with depth in the surface layer (shallower than 50cm). In deeper layers, the source strength was very low; however, it was higher in summer than in late autumn. The change of source strength in the surface soil also corresponded with that of CO_2 flux from the soil which was measured by the ^{222}Rn calibrated method and the static chamber method.

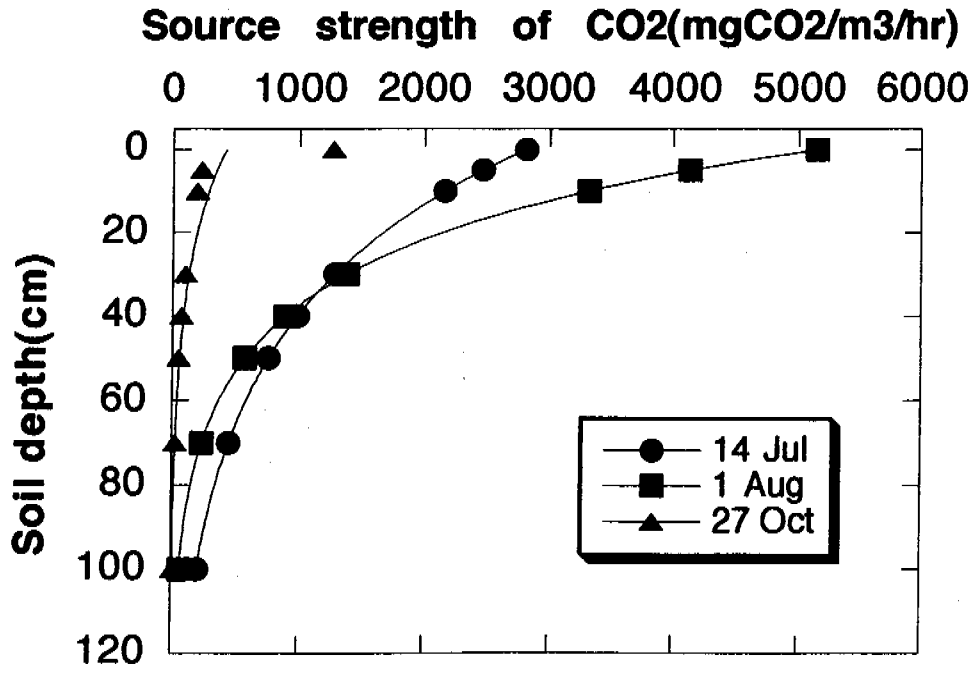

FIG. 4. Source strength of CO_2 in the soil at Nikko site in 1994. Source strength of CO_2 in the soil was calculated from the CO_2 profile and diffusion coefficient by ^{222}Rn.

Thus far it has been difficult to obtain the source strength of CO_2 in the soil quantitatively, because of the uncertainty of measurements of physical parameters in the soil such as water content, tortuosity and total porosity. The conventional methods give only the flux information, however, the ^{222}Rn method gives the CO_2 flux and the CO_2 source strength simultaneously without disrupting a soil profile. Information of CO_2 source strength is of great importance to understanding of the biological activity in forest soils.

Larch distribution and fire recovery on tundra–taiga transition zone

G. TAKAO[1], and A. KONONOV[2]

[1]*Forestry and Forest Products Research Institute, 1 Matsunosato, Kukizaki-cho, Ibaraki 305 Japan*
Tel: +81-298-73-3211; Fax: +81-298-73-3799
[2]*Yakutian Institute of Biology, Russian Academy of Sciences,*
41 Lenin Avenue, Yakutsk 677891 Russia

Summary. The post–fire recoveries of larch forests (*Larix gmelinii, L. cajanderi*) are extracted from satellite images, namely a LANDSAT MSS image in 1973 and SPOT HRV XS images in 1994, on tundra–taiga transition zone. Some areas seem to recover as larch forest, whereas others seem not to recover but to change to bare land.

Introduction

It is important to monitor the vegetation on tundra–taiga transitional zone to detect the influences of the global climate change because, on a global scale, the greatest ecological changes in response to rising levels of carbon dioxide are likely to take place in tundra, boreal forest, and polar desert zones (Tegart et al. 1990, in Maxwell 1992). However, succession of boreal vegetation is too slow and small to be observed by satellite remote sensing.

Recovery after fire is supposed to be faster and more sensitive to the climate. Wildfire have been recognized as a driving ecological factor in boreal coniferous forests and short–term climatic fluctuations could be of high biogeographical significance for long–term vegetation dynamics in the transition zone (Sirois 1992).

In this study, we use two sets of satellite images with 21–year difference to detect the changes that have taken place in the burned forest.

Study site and data

Our study site is located on the west bank of the lower part of Lena River (Fig. 1), where 'Open larch (*Larix gmelinii, L. cajanderi*) forest along tundra' covers the lowland while 'Alpine tundra' covers the mountains (National Agro–Industry Board of Yakut ASSR et al. 1989). Open larch forests are the interest of our study.

For the ground–truths–correction of satellite image analysis, observation by airplane over the site and ground surveys on three different types of larch open forests in the site had been

TABLE 1. Satellite images' type, date and coordinate.

Satellite	LANDSAT	SPOT
Sensor	MSS	HRV XS
Date	Jul 25, 1973	Jul 12, 1994
Scene coord.	140-010	254-200
		257-201

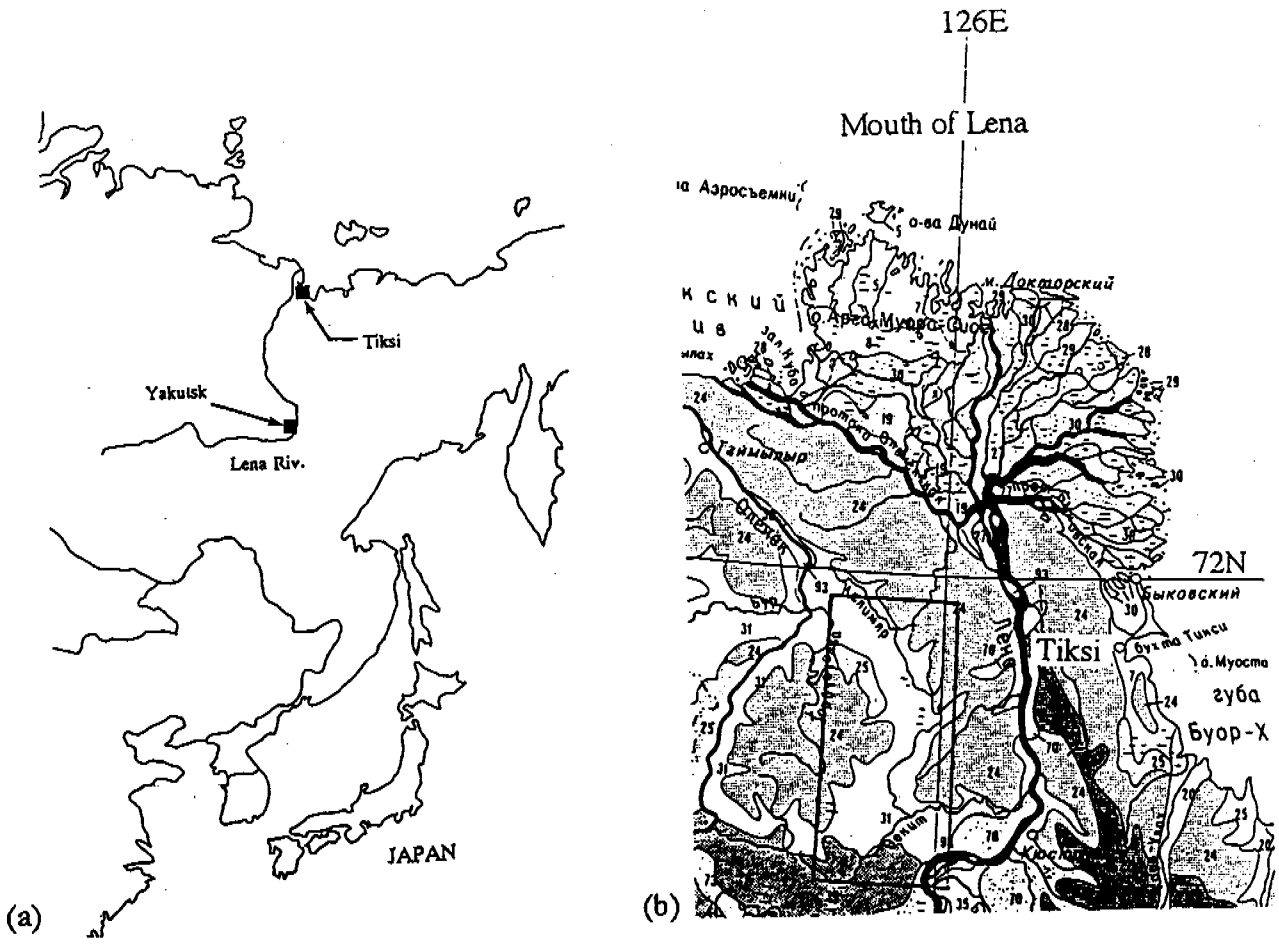

FIG. 1. Location of the study site. (a) Location of Tiksi, Yakutsk and Japan, (b) Vegetation map around the study site (National Agro-Industry Board of Yakut ASSR et al. 1989). Legend: 22, 24, 25: Alpine tundra; 31: Larch (*Larix gmelinii, L. cajanderi*) open stand along tundra; 39: Larch (*L. gmelinii, L. cajanderi*) open stand of northern taiga; 70: Alpine larch (*L. cajanderi*) open stand along taiga, etc.

TABLE 2. Sensors' characteristics (from Lillesand et al. 1994).

Sensor	MSS	HRV XS
Spatial Resolution	79 m	20 m
Wavelengths	0.5 - 0.6	0.50 - 0.59
(unit = micro meter)	0.6 - 0.7	0.61 - 0.68
	0.7 - 0.8	0.79 - 0.89
	0.9 - 1.1	

carried out in July, 1993 (see Takao 1994, Ishizuka et al. 1994). On July, 1994, further observation was carried out by an airplane on the southern part of the site. GPS was used to track the flight path and locate the surveyed forests.

To map the vegetation and its change over the site, two sets of satellite images, taken in July in 1973 and 1994, respectively, are used. The parameters of the images and their sensors' characteristics are described in Tables 1 and 2, respectively. Fig. 2 is the image of 1973. The visible bands of both sensors cover nearly identical wavelengths to each other,

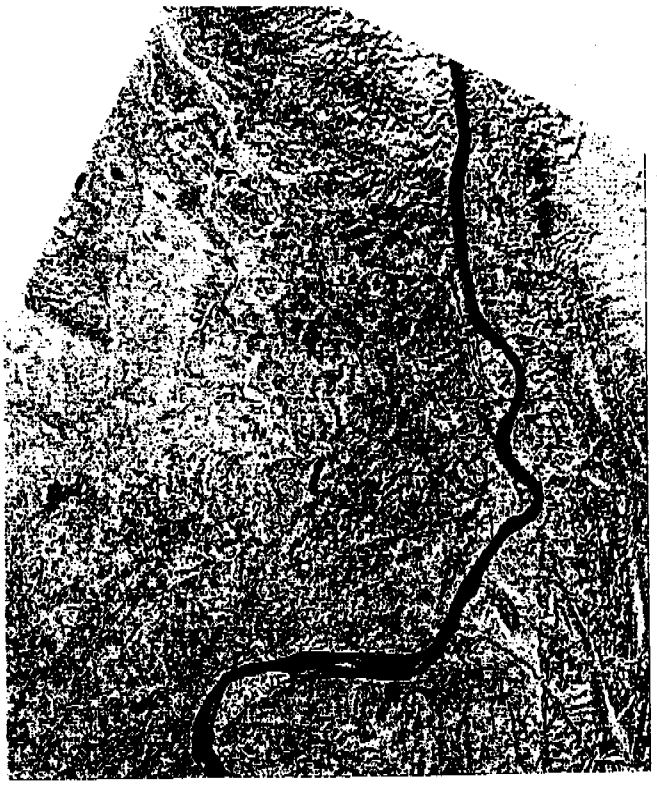

FIG. 2. LANDSAT MSS image (Band 7: near infrared, processed part of the full scene). Date = Jul. 25, 1973; Path = 140; Row = 010; Black curve is Lena River.

while the wavelengths of the infrared bands are not identical; however they still have good correlation as being described in the following section. The LANDSAT image in 1973 had been the first and only cloud-free high resolution satellite image over the site available outside of Russia until 1994, when we ordered SPOT to take new images.

Method

As the preprocessing of the images, two SPOT HRV XS images in 1994 are merged into one image (hereafter referred to simply as the 'HRV image'), overlaid onto the LANDSAT MSS image in 1973 (hereafter referred to simply as the 'MSS image'), which had been already geocoded and classified using supervised classification method (Takao 1994). Then, the common parts of the two images are extracted. In addition, pixels on the borders of the vegetation classes are removed from the images to avoid taking geocoding errors as great changes.

It is difficult to describe succession of relatively stable vegetation with the satellite images, because we have the ground information only in 1994, but not in 1973 which can be used to reconstruct the history of vegetation change. Then, by assuming that changes have not taken place on the stable vegetation, we intend to detect the changes that occurred in unstable vegetation, such as burned (fire) or sparse forest.

Among the training areas used in the MSS image classification, 16 of supposed stable vegetation types are selected to calculate the regression of the MSS image to the HRV image. However, three of the training areas, namely 'Bare soil', 'Fire' and 'Larch-G (sparse larch

forest)', are discarded (Criteria to sub-classify larch forests are described on Table 3). The regression of each band of the HRV image is calculated from the corresponding wavelength band of the MSS image using the mean value of the selected training areas, i.e. HRV XS1 from MSS 4 (r^2 = .98), HRV XS2 from MSS 5 (r^2 = .99) and HRV XS3 from MSS 7 (r^2 = .99), respectively.

TABLE 3. Criteria of larch forest sub-classification. These criteria are used to subclassify the photos taken from the airplane.

Class	Location	Criteria
Larch A	>N71, E125-126	On foot of steep slope from the mountain to the basen, sparse and low
Larch B	>N71, E125-126	On swamp or along river, sparse
Larch C	<N71, E125-126	Along river or on hill, sparse-middle
Larch D	~N70.5, E125-126	On lowland or hill along Lena river, dense
Larch G	*same as* 'Larch C'	Same as 'Larch C' in observation '94, but differ from the image '73

These criteria are used to subclassify photos taken from the airplane.

Results and discussion

Training areas of both observed by HRV in 1994 and estimated from MSS in 1973 are plotted on Fig. 3. The distance between observed and estimated points of the same training area is supposed to represent the change during these 21 years. Fig. 4 shows the Mahalanobis' generalized distance from the observed to the estimated of each training area in the HRV's three bands space. The most significant change occurs in 'Fire C', where larch could not regenerate successfully after the fire and is dry soil or rock with dead stems in 1994. Another big change occurs in 'Larch G (sparse larch forest)', which seems to move closer to the distribution of other larch classes. Among others, all grass classes are stable but some of the other classes are not. The reasons of the supposed stable classes' movement are beyond the scope of the present analysis.

We found that larches had recovered well on wet lowlands whereas rarely recovered on dry hill tops in the observations in 1993 and 1994, just as Sirois (1992) pointed out. The directions of the movements of 'Fire C' and 'Larch G' are different to each other; the former closer to 'Rock's and the latter closer to 'Larch'es or 'Grass'es. They might be the difference of recovery. The next target of the study is to map the recovery stage using satellite imagery.

Reference

Ishizuka, M., S. Uemura, T. Tsujii, and K.A. Volotovsky. 1994. Vegetation of the Boreal Forest-Tundra Transition Zone in the Basin of Lena River-I. Forest Stand Structure, *In* Proceedings of the Second Symposium on the Joint Siberian Permafrost Studies between Japan and Russia in 1993, G. Inoue, ed., pp.109-115, National Institute for Environmental Studies, Japan.

Lillesand, T.M., and R.W. Kiefer. 1994. Remote Sensing and Image Interpretation-Third Edition, John Wiley & Sons.

Maxwell, B. 1992. Arctic Climate: Potential for Change under Global Warming, *In* Arctic Ecosystems in a Changing Climate-An Ecophysiological Perspective, F.S. Chapin III, et al., eds. pp.11-34, Academic Press.

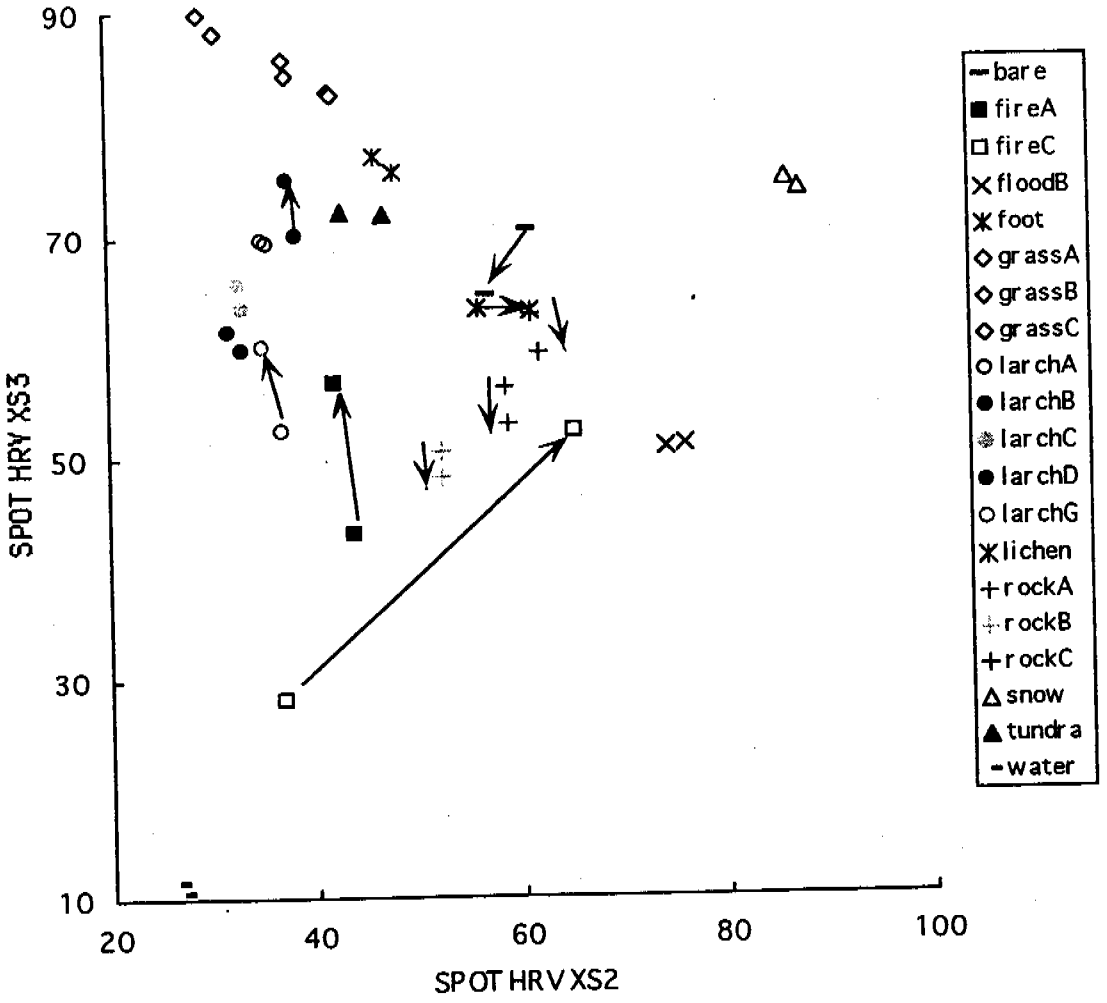

FIG. 3. Training areas' spectral changes, 1973–1994. An arrow represents the direction of change from 1973 to 1994.

National Agro-Industry Board of Yakut ASSR et al. 1989. Agronomical Atlas of the Yakut ASSR, USSR Survey and Cartography Bureau, Moscow. (*In Russian*)

Sirois, L. 1992. The transition between boreal forest and tundra, *In* A System Analysis of the Global Boreal Forest, H.H. Shugart, et al., eds. pp.196–215, Cambridge Universty Press.

Takao, G. 1994. Mapping Vegetation on Tundra–Taiga Transitional Zone Using Satellite Image, *In* Proceedings of the Second Symposium on the Joint Siberian Permafrost Studies between Japan and Russia in 1993, G. Inoue, ed. pp.91–93, National Institute for Environmental Studies, Japan.

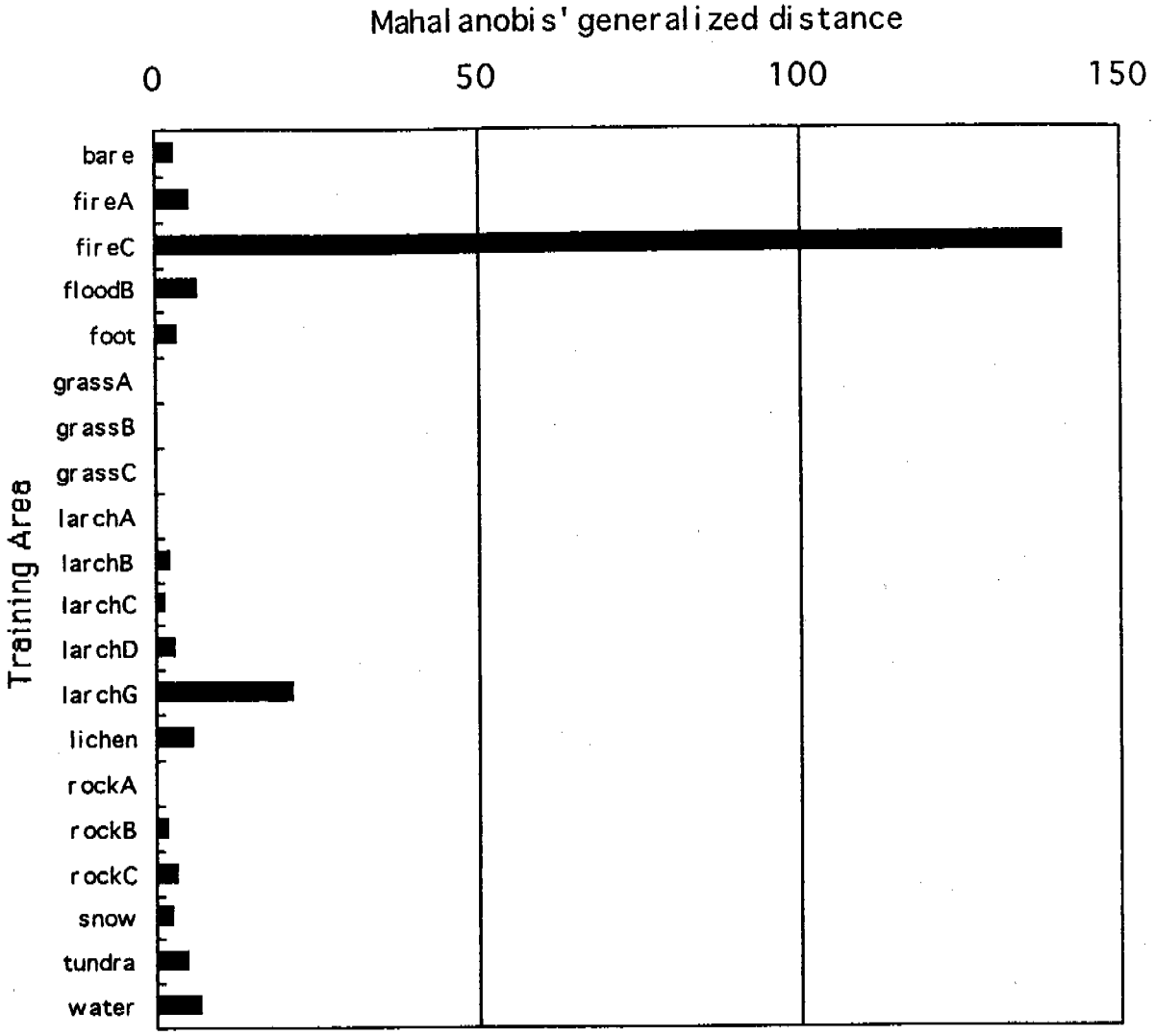

FIG. 4. Training areas' moved distance from 1973 to 1994.

Analysis of a SPOT satellite image at Plotnikovo in western Siberian wetlands

M. TAMURA, Y. TOHJIMA, and Y. YASUOKA

National Institute for Environmental Studies, 16-2 Onogawa, Tsukuba 305 Japan
Tel: +81-298-51-6111; Fax: +81-298-51-4732; E-mail: m-tamura@nies.go.jp

Introduction

Western Siberian wetlands are presumed to be large sources of atmospheric methane. Recent Japan-Russia cooperative study on airborne measurements have yielded results supporting this presumption. To evaluate the role of the western Siberian wetlands as sources of atmospheric methane, it would be necessary to classify ecosystem types in wetlands and to estimate the mean methane flux for each ecosystem type. In this study we use satellite images, such as SPOT/HRV, JERS-1/OPS & SAR and NOAA/AVHRR, for the determination of wetland areas and for the classification of wetland ecosystem types. As to the estimates of mean methane flux, there are not many data sets covering western Siberian wetlands for the moment, but it will be possible to derive estimates from the results of the ground measurements performed in the Japan-Russia Siberian project and from studies concerning northern wetlands in Canada and Alaska (Bartlett et al. 1992, Roulet et al. 1994).

In this report we present a SPOT/HRV image at Plotnikovo in western Siberian wetlands and compare the results of land cover classification with methane concentration data obtained during the 1994 flight expedition.

SOPT/HRV image at Plotnikovo

A SPOT/HRV image was obtained at Plotnikovo on 9 August 1994, three days after the intensive airborne measurements (that took place on 3, 5, and 6 August 1994) of greenhouse gases over the same area. Plotnikovo is located at longitude 85°05'E and latitude 56°51'N and in the wetland region along the Ob' river (see Fig. 1). Fig. 2 shows the area covered by the SPOT/HRV image, whose size is approximately 60 x 60 km.

The SPOT/HRV is a high resolution imaging system with a ground resolution of 20 m and has three spectral bands of green, red and near infrared wavelengths (0.50-0.59, 0.61-0.68 and 0.79-0.89). Fig. 3 shows the image taken by SPOT/HRV sensor in a black and white picture, though it has originally three color components. By using an unsupervised classification technique (Interactive self-organizing data analysis technique) we classified the image pixels into fifteen clusters in three-dimensional spectral space. We then merged them into seven categories (wetland1, wetland2, forest, water, grass, cloud and cloud shadow) using spectral feature of each cluster. Fig. 4 shows the result of land cover classification. From aerial photographs, wetland1 is identified as wetland area with high water level and wetland2 as wetland area with grasses and low shrubs.

Comparison of land cover types with methane concentration data along flight pass

During the airborne measurements of greenhouse gasses at Plotnikovo, atmospheric methane concentration showed very spiky variations when the airplane flied at very low altitude (about 250 to 300 m pressure altitude). These spiky behaviors seemed to reflect ground conditions as well as meteorological factors. We hence compared land cover types

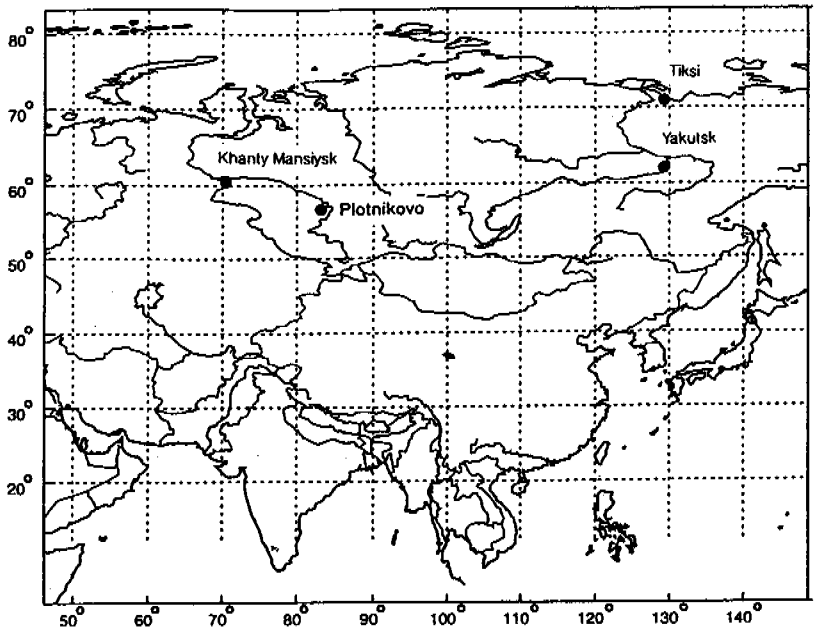

FIG. 1 Location of Plotnikovo.

FIG. 2 Area covered by the SPOT/HRV image.

obtained from a satellite image with methane concentration data along the flight pass. We indicated methane concentration with markers of different colors on the classified satellite image and a map. Fig. 5 shows the result for the data obtained from 1:00 to 2:00 a.m. GMT on 5 August 1994; white circles show methane concentration higher than 2.0 ppm and black

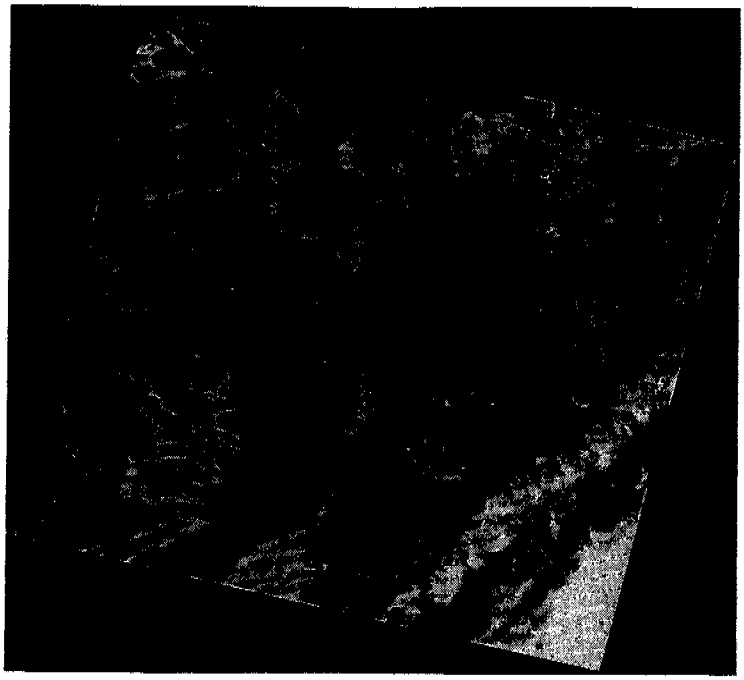

FIG. 3 SPOT/HRV image at Plotnikovo.

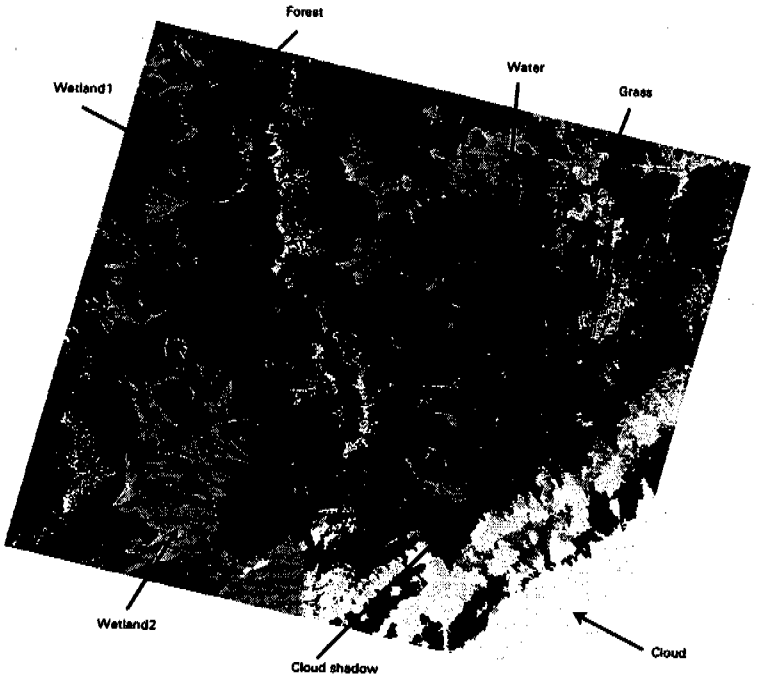

FIG. 4 Result of land cover classification.

circles show otherwise. We see that the distribution of methane concentration is not directly related to the land cover types. It seems that meteorological factors should be taken into account to interpret these results.

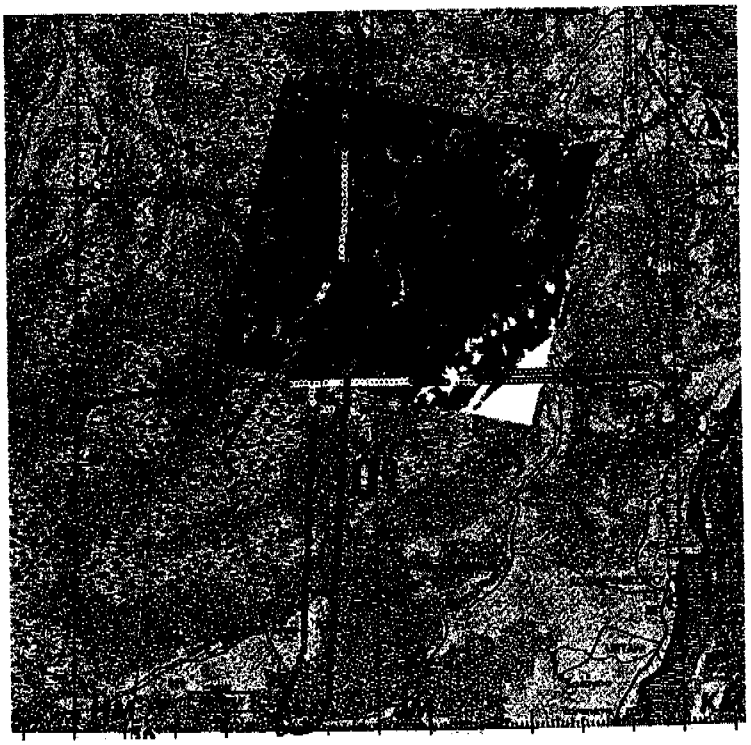

FIG. 5 Comparison of land cover types and methane concentration along the flight pass. White circles show methane concentration higher than 2.0 ppm and black circles show otherwise.

Summary

A SPOT/HRV image was obtained at Plotnikovo shortly after the flight measurements of greenhouse gases in August 1994. The image area was classified into seven categories using spectral features and aerial photographs. The result of classification was compared with methane concentration data along the flight pass. It turned out that the methane concentration was not directly related to the land cover types. It should be necessary to take meteorological factors into account as well as ground conditions to interpret the methane distribution data.

References

Bartlett, K.B. et al. 1992. Methane emission from tundra environments in the Yukon–Kuskokwim delta, Alaska, J. Geophys. Res. 97:16,645–16,660.

Roulet, N.T. et al. 1994. Role of the Hudson Bay lowland as a source of atmospheric methane, J. Geophys. Res. 99:1439–1454.

On the development of NOAA/AVHRR database

Y. IIKURA[1], H. TAOFIK[1], M. TAMURA[2], and Y. YASUOKA[2]

[1]*Faculty of Engineering, Iwate University, 4-3-5 Ueda, Morioka 020 Japan*
Tel: +81-196-29-2090; Fax: +81-196-21-1170
[2]*National Institute for Environmental Studies, 16-2, Onogawa, Tsukuba 305 Japan*

Introduction

AVHRR (Advanced Very High Resolution Radiometer) is a major sensor on the NOAA satellite that has a circular and sun synchronous orbit. As this sensor has a wide swath range (2700 km), it can cover the same area at any location on the earth twice a day. It is also known that the data of AVHRR are useful for the investigation of vegetation intensity and surface temperature.

These features of this sensor are suitable for our projects that requires the ground cover characteristics of wide Siberia region as one of the fundamental information. Therefore, we have started to collect the AVHRR data of this region and to construct the database system, which is open through Internet for users such as biologists and meteorologists.

In this paper, we first describe the procedures of NOAA/AVHRR data acquisition and show the amount of data to be stored. We point out the necessity of data compression for effective database management as well as browsing the images. Next, the analysis of the data is described with the introduction of package program named PaNDA that can perform most of the necessary procedures. We use some images around Khanty-Mansyisk for demonstrating the results of the procedures. Finally, we outline our plan of the database that is accessible through Internet.

Data aquisition

NOAA is a series of meteorological satellites launched by NASA and operated by NOAA, USA. The specification of NOAA/AVHRR is shown in Table 1. It should be noted that the spatial resolution of the sensor (IFOV) is about 1 km at the center of the scene.

After measuring the radiation from the earth, NOAA is broadcasting the measured data towards the ground constantly. So if you install an antenna and a satellite tracking system,

TABLE 1. Specifications of NOAA/AVHRR.

Orbital Element	Spectrum	IFOV	Swath Width
Sun Sync. alt.: 833km or 870km inc.:99degree	0.58~0.68 μm 0.725~1.10 μm 3.55~3.93 μm 10.30~11.30 μm 11.50~12.50 μm	1.1 km	2,700km

you can obtain the broadcasted data freely. This type of data is called HRPT (High Resolution Picture Transmission) and APT (Automatic Picture Transmission). There are many HRPT receiving facilities all over the world. In Japan, there are facilities at Tokyo (The University of Tokyo, Meteorological Agency), Sendai (Tohoku University), Nagoya (Nagoya University), and Okinawa (Environmental Agency) as far as we know.

However, there are some areas with no receiving stations. Until the Institute of Forest at Krasnoyarsk installed the facility last November, Siberia had been belonging to this category of areas. To cover these areas, NOAA has data recorders on board and transmits these data to the special receiving stations. We call this type of data LAC (Local Area Coverage). As the storage capacity of the recorder is limited, these areas are not observed constantly.

At the receiving station, the data is accumulating and they should be managed properly. For one scene, the size of data is about 100 MB, which occupies one whole CCT (Computer Compatible Tape). Although some new media, such as DAT, Optical Disk becomes available at low price, we think the problem of data storage remains very important because of the rapid accumulation of the data.

To obtain the NOAA data, you have to contact the receiving stations and need their permission to copy the data. Fortunately, there is another way to obtain the world wide NOAA data. Eros Data Center (EDC) of United States Geological Survey is gathering the HRPT and LAC data all over the world with the help of NASA. In addition, it provides us with the useful tool to check and order the data that you find useful for your study. This tool is available through Internet and called XGLIS. Try "telnet xglis.cr.usgs.gov" on your X-terminal. The data can be seen as the quicklook images.

We used XGLIS to select the NOAA data of Siberia and obtained 90 scenes from 1987 to 1993. We made quicklooks of our own for all the data we have obtained. We first sample the data every 4 pixel and line and compressed them by using standard lossy image compression algorithm called JPEG. The size of data is about 50 Kbyte and the quality of the data is good enough for you to browse and check the cloud existence. You can see these images on our WWW (World Wide Web) server. Try WWW client with URL "httpd:/ /himekami.cis.iwate-u.ac.jp/". Although we selected the scenes that were relatively cloud free, you can see some clouds in every scene. This is one of the significant problems of optical sensors.

Data processing

NOAA data is a little bit difficult for us to deal with because of the following reasons. First, each line contains the on board calibration data. Through these data make it possible to transform the CCT values into brightness temperatures, the procedure becomes complicated. Second, as it covers wide area, geometric correction should be systematically performed by using orbit information that is provided by NOAA. Third, the unit of data is 10 bits, while other image data usually consists of 1 byte (8 bit).

These tedious tasks can be done automatically by using package program named PaNDA, which has been developed by the volunteer group (The PaNDA Committee). Please contact us for more information.

For converting CCT values of Band 1 and 2 to albedo *R1* and *R2* , we use

$$R_i = (d \cdot d/z) \cdot (a + b \cdot CCT_i)$$

where d is distance between earth and sun, z is cosine of sun elevation angle, a and b are

coefficient given by NOAA. We can calculate NDVI (Normalized Vegetation Index) by

$$NDVI = (R2 - R1)/(R2 + R1)$$

to show the vegetation intensity.

Fig. 1 shows the seasonal changes of vegetation index at Khanty Mansyisk. The size of data is 512 lines by 512 pixels with 1 km spatial resolution. In May, the river was flooded and NDVI was low over the scene. In July, the flooded areas were covered by grass and NDVI became higher.

Fig. 2 shows the surface temperature estimated by

$$ST = 2.672 \cdot X4 - 1.672 \cdot X5 + 0.613$$

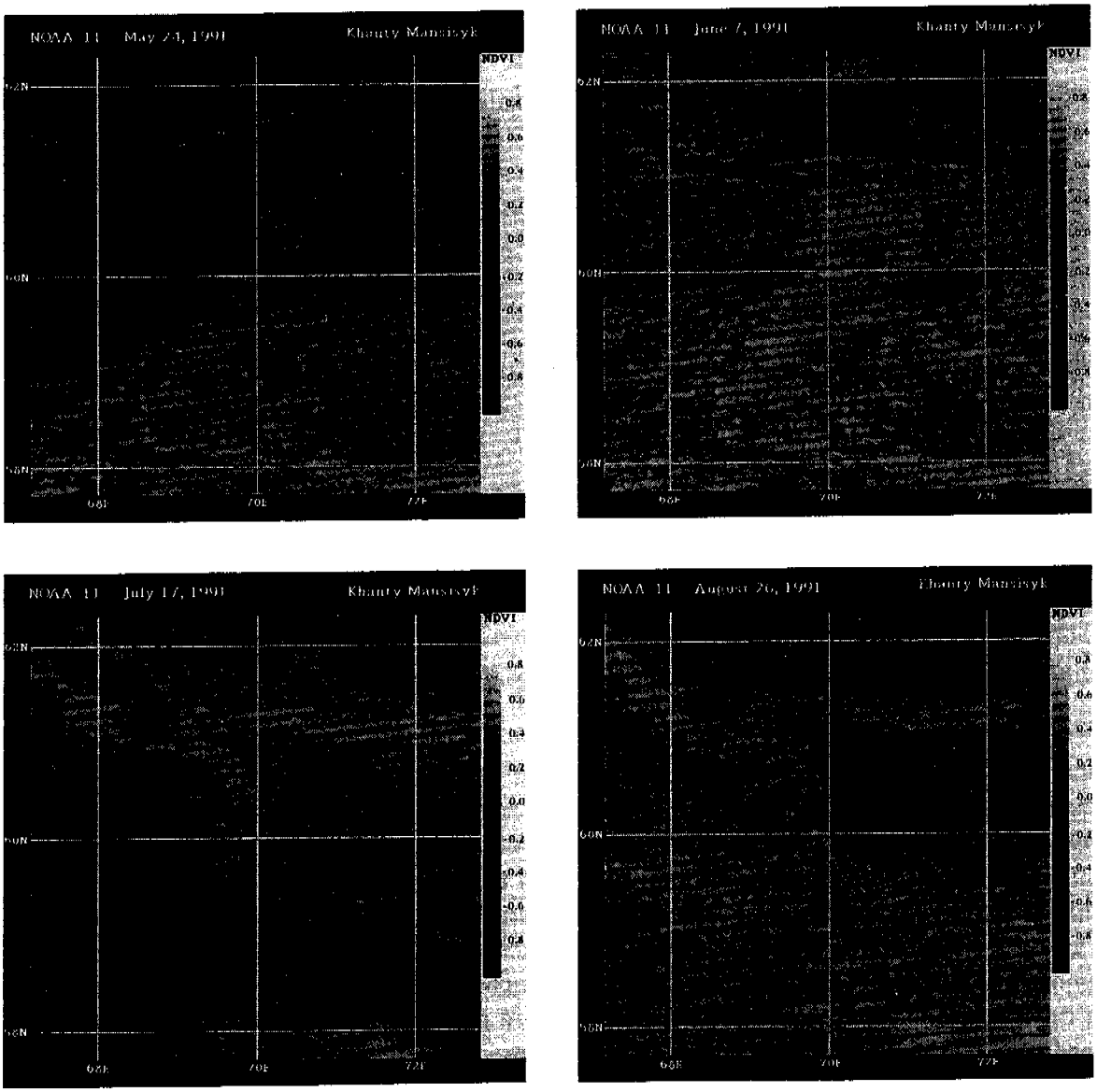

FIG. 1. Seasonal changes of vegetation index at Khanty Mansyisk.

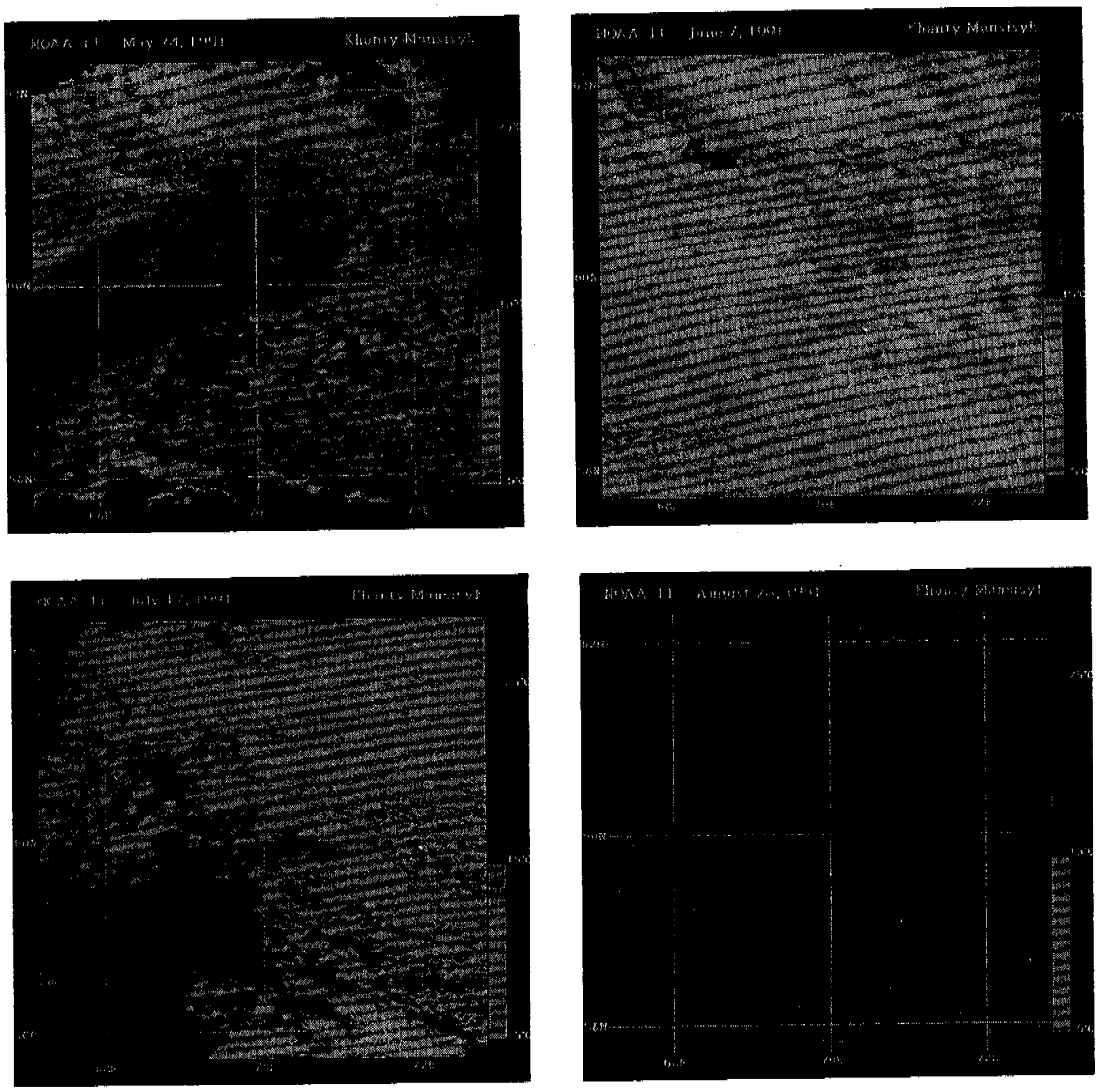

FIG. 2. Seasonal changes of surface temperature at Khanty Mansyisk.

where *X4* and *X5* are brightness temperature of Band 4 and Band 5, respectively. This equation is derived empirically to remove atmospheric effects and is called split window method. These coefficients are obtained by Tanba for Mutu Bay, Japan. The resulting images are also interesting because the estimated temperatures are higher than we expected. This is partly because the local time of observation is around noon and the surface is heated a lot by the sun shine. You should also understand that these are not the temperature in the atmosphere but on the surface . In addition, we need to know emissivity of the surface type in order to estimate the surface temperature more exactly. To obtain the surface type, we need soil map and the classification of land cover.

Database and its access

As mentioned before, we are operating WWW server on our system and open the quick

look images to the public through Internet. In addition, you can see some processed images, such as albedo and surface temperature at some areas in Siberia, such as Khanty Mansyisk, Plotonikovo and Yakutsk.

We are planning to develop this database system in terms of quality as well as quantity. You are welcome to access this database and we will appreciate any comments and suggestions on this system.

For distribution of the data, we are now developing data compression methods not only for original images but also for processed images. We have understood that there are some problems for satellite data compression. First the characteristics of satellite images are very different from natural color image. It consists of many bands and the size is very big. Second, it is used for the academic purpose, so the data is processed quantitatively. Third there are many noise factors, such as atmospheric effect and geometrical distortion.

Generally speaking, it is very difficult to compress the satellite image without loss of information. For LANDSAT/TM data, the compressed size is not less than 70% of the original size. But in the case of NOAA AVHRR, the compressed size could be reduced to about 30% by some methods based on our limited experience.

If you need more compression, you have to think about the lossy compression; it loses some part of information. So we have to evaluate the data compression not only by the compression rate but also by the distortion of the decoded image.

We are now proposing to use Mahalanobis distance as the distortion measure, which can be regarded as the extension of signal-to-noise (SNR) to multi dimensional case. As the compression method, we may use Move to Front method and Pyramid Linking method.

Conclusion

Followings are the conclusion of this paper.

1) NOAA/AVHRR image is effective to estimate the vegetation intensity and surface temperature for wide area such as Siberia. But we have to note the size and quality of the data.

2) Data compression is effective in every stage of data processing. On board data compression, we have to develop simple and robust algorithm such as Move to Front method. On the receiving station, more sophisticated method like prediction coding would be preferred.

3) You can access to our Siberia Database of NOAA/AVHRR through Internet WWW system. We will develop this database based on your advice.

4

Population & Community Ecology

Vegetation and climate during accumulating period of Edoma, inferred from pollen records

YAEKO IGARASHI[1], MASAMI FUKUDA[2], DAISUKE NAGAOKA[3], and KIYOSHI SAIJO[4]

[1]*Earthscience Co. Ltd., N39W3, Sapporo 060 Japan*
Tel: +81-11-737-6212; Fax: +81-11-737-6213
[2]*Institute of Low Temperature Science, Hokkaido University, N19W8, Sapporo 060 Japan*
[3]*Graduate School of Environmental Earth Science, Hokkaido University, N10W5, Sapporo 060 Japan*
[4]*Institute of Geography, Tohoku University, Aoba-ku, Sendai 980 Japan*

Introduction

Edoma is exposed along the Arctic coast and along rivers in the east Siberian region from 3000 to 9000 km in total length. Edoma is the ice-complex which contains numerous pillar-shape sediments. In Bykovsky Peninsula and Bolshoi Lyakhosky Island, pillar-shape sediments are exposed as walls of 26 to 28 m thickness. The sediments are mainly composed of silt, but also contain several thin layers of peat and silty peat (Fukuda, 1993; Nagaoka, 1993).

By measurement of ^{14}C dates, it was clarified that Edoma distributed in Bykovsky Peninsula and Bolshoi Lyakhosky Island formed during Karginsky Interstadial between 24 ky

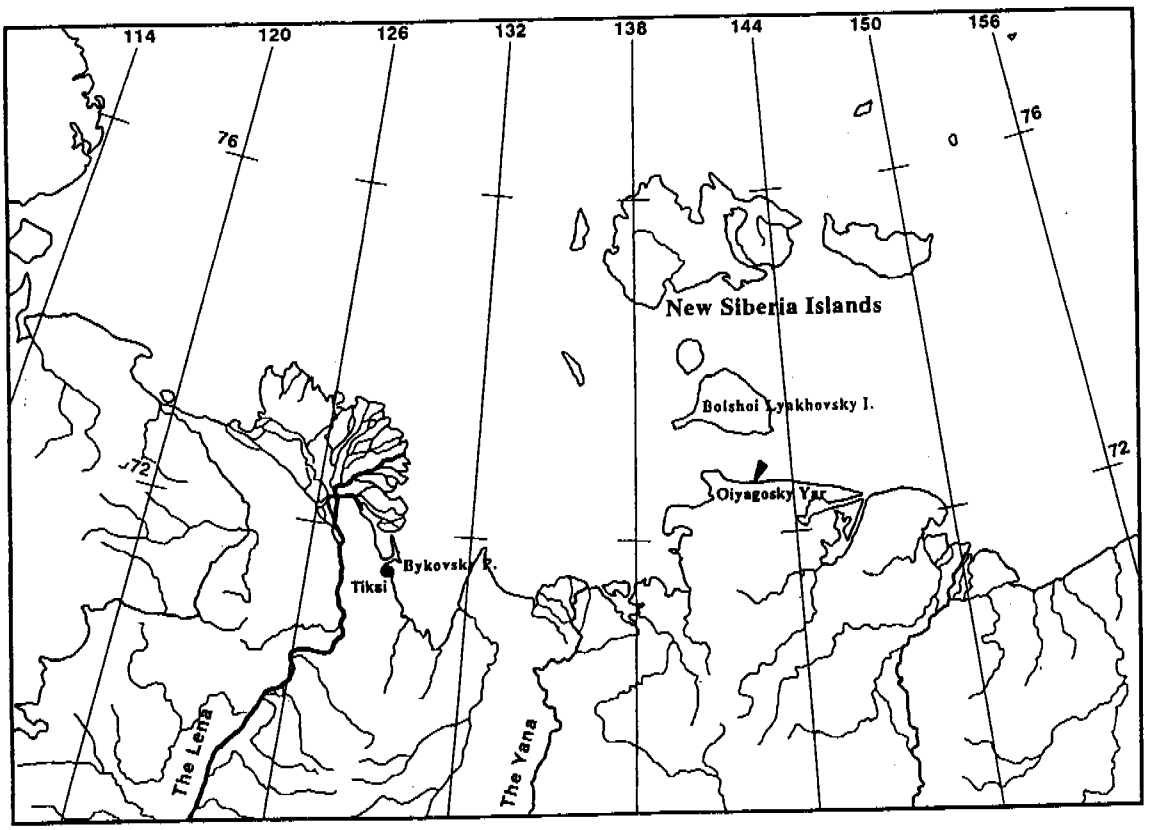

FIG. 1. Map showing studied location, Oiyagosky Yal.

and 40 ky BP. Measurement of methane concentration in ice also clarified that Edoma accumulated under very unstable climatic conditions (Fukuda, 1993). As the pillar-shape sediments contain abundant organic marerials, reconstruction of paleoenvironment by pollen analysis could be possible. However there was no palynological study about the region. In 1994's survey, samples for pollen analysis were taken from exposure of pillar-shape sediments at Oiyagosky Yal section (Fig.1). The ^{14}C ages of sediments show that Edoma around the section accumulated also during Karginsky Interstadial.

Fossil pollen assemblages of the Edoma was studied at Duvanny Yal, downstream of the Kolima River about 800 km southeast from Oiyagosky Yal. Vegetation during Karginsky Interstadial was clarified (Giterman et al., 1982). Pollen data from the same period was also clarified from Baty-sala Basin, Taimyr Peninsula, approximately 1400 km west of Oiyagosky

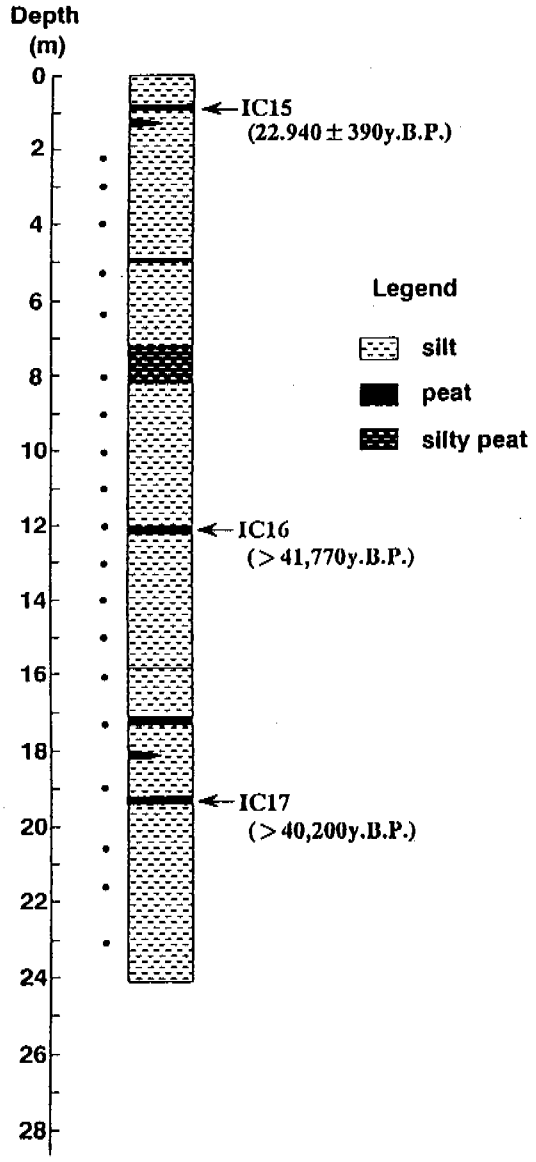

FIG. 2. Lithostratigraphy, sampling and dated horizons of Oiyagosky Yal section.

Yal (Isayeva, 1984). In this study, we tried to reconstruct paleoenvironment during Karginsky Interstadial around Oiyagosky Yal region and to correlate it with other two regions located also in the high Arctic of east Siberia.

Samples and Analytical Method

Twenty-four thick pillar-shape sediments exposed at Oiyagosky Yal section are mainly composed of silt, containing silty peat layer and seven thin peat layers (Fig.2). Age of 1 m deep peat is 22,940±390 y BP. Two ages of peat at 12 m and 19 m in depth are > 41,770 y BP and > 40,200 y BP, respectively. Nineteen samples were taken from every one-meter interval except for the uppermost part of sediments. Dried 5 g sample was treated by KOH, HF, $ZnCL_2$ and Acetolysis liquid. All pollen and spores included in each sample were counted.

Results

All samples contained pollen and spores, except for a sample taken from 20.5 m deep. Absolute pollen diagrams of trees and shrubs, of non arboreal pollen and of spores are shown in Fig. 3, Fig. 4 and Fig. 5 respectively. Highly yielded taxa are also shown in the selected pollen diagram (Fig. 6). Their percentages were calculated based on total numbers of pollen and spores. Based on characteristics of tree pollen assemblages, three pollen zones, I, II and III, in ascending order, were discriminated.

Zone I (16-23 m in depth).—Pollen numbers of both *Betula* and *Alnus* reached 40, and the number of *Salix* was 15. Those are the biggest numbers of shrub pollen in three zones. About tree pollen, *Pinus sylvestris* was less than 19 in this zone. *Picea* yielded more than 20 in the upper part of the zone. Among non arboreal pollen, Gramineae, Cyperaceae, Tubuliflorae and Caryophylaceae yielded abundantly. Also herbs such as Liguliflorae, *Artemisia*, *Valeriana*, Ranunculaceae, *Saxifraga* and *Polemonium* were contained abundantly compared with the other two zones. Although fern spores were poor, *Selaginella sibilica* began to appear in upper part of Zone I. *Botryococcus*, indicator of open water, was contained most abundantly in three zones. Nonarboreal pollen reached 90% in total. Pollen numbers from Zone I were numerous. Especially, more than 2500 pollen and spores yielded from sample 21.5 m deep (Fig.7).

Zone II (9-15 m in depth).—*Picea* pollen yielded between 17 and 109 and *Pinus sylvestris* yielded from 4 to 119 in numbers. Numbers of *Larix* was 1 or 2. On the otherhand, *Betula* and *Alnus* decreased and *Salix* disappeard. Gramineae, Cyperaceae and herbs which were abundant in Zone I remarkablly decreased in this zone. However, fern such as *S. sibilica*, *Lycopodium*, Polypodiaceae and *Sphagnum* appeared. *Botryococcus* decreased. Trees and shrubs were abundant and amounted to 25~74 % in total. Total numbers from Zone II was the least in three zones (Fig.7).

Zone III (2-9 m in depth).—Numbers of *Picea*, *Pinus* and *Betula* decreased, and *Alnus* disappeared. Gramineae, Cyperaceae and herbs especially Caryophyllaceae increased again. Although *S. sibilica* increased, *Lycopodium* decreased. *Botrycoccus* decreased moreover. Non arboreal pollen and spores amounted to more than 90% in total. Numbers of pollen and spores slightly increased again (Fig.7)

Vegetation and Climate

The present vegetation around Oiyagosky Yal is characterized as tundra. Forest tundra

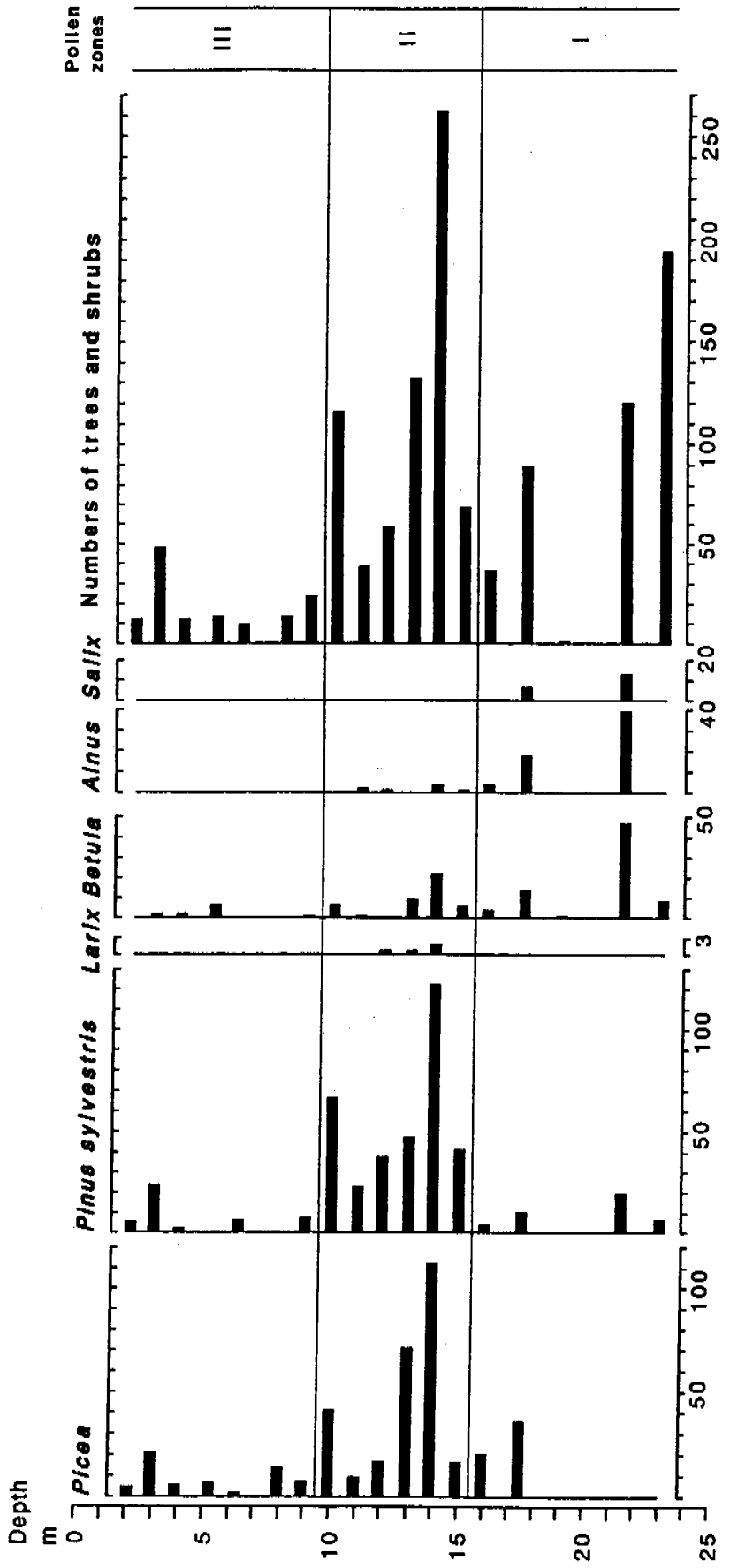

FIG. 3. Absolute pollen diagram of trees and shrubs from Oiyagosky Yal section.

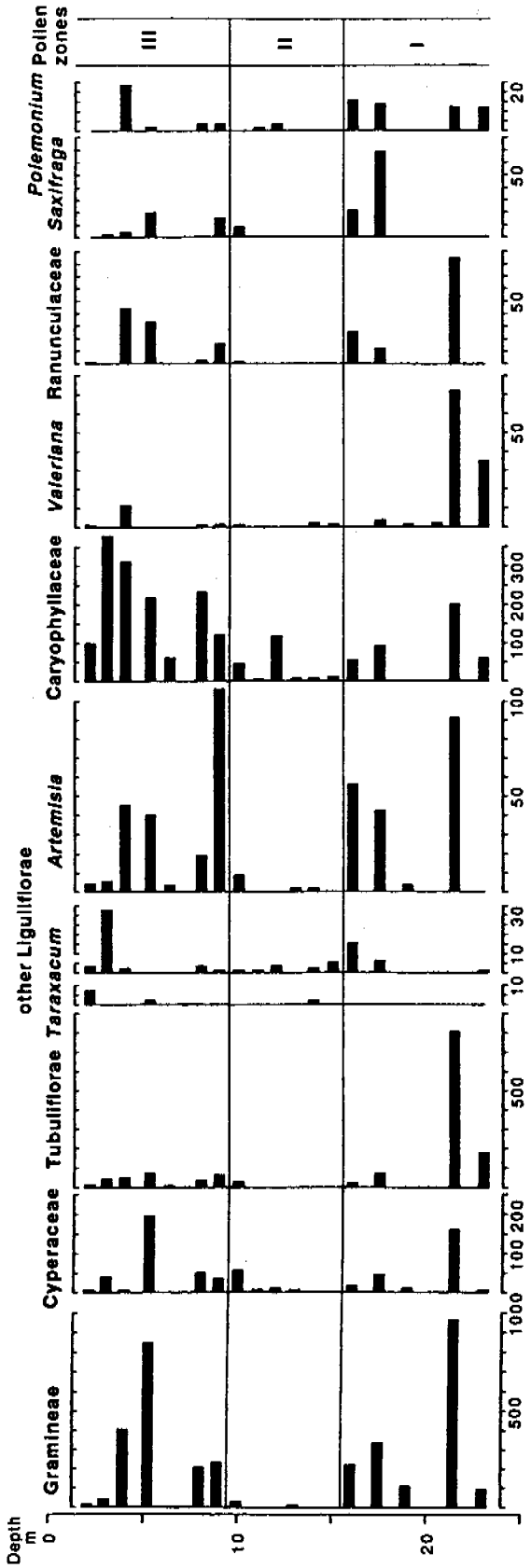

FIG. 4. Absolute pollen diagram of non arboreal pollen from Oiyagosky Yal section.

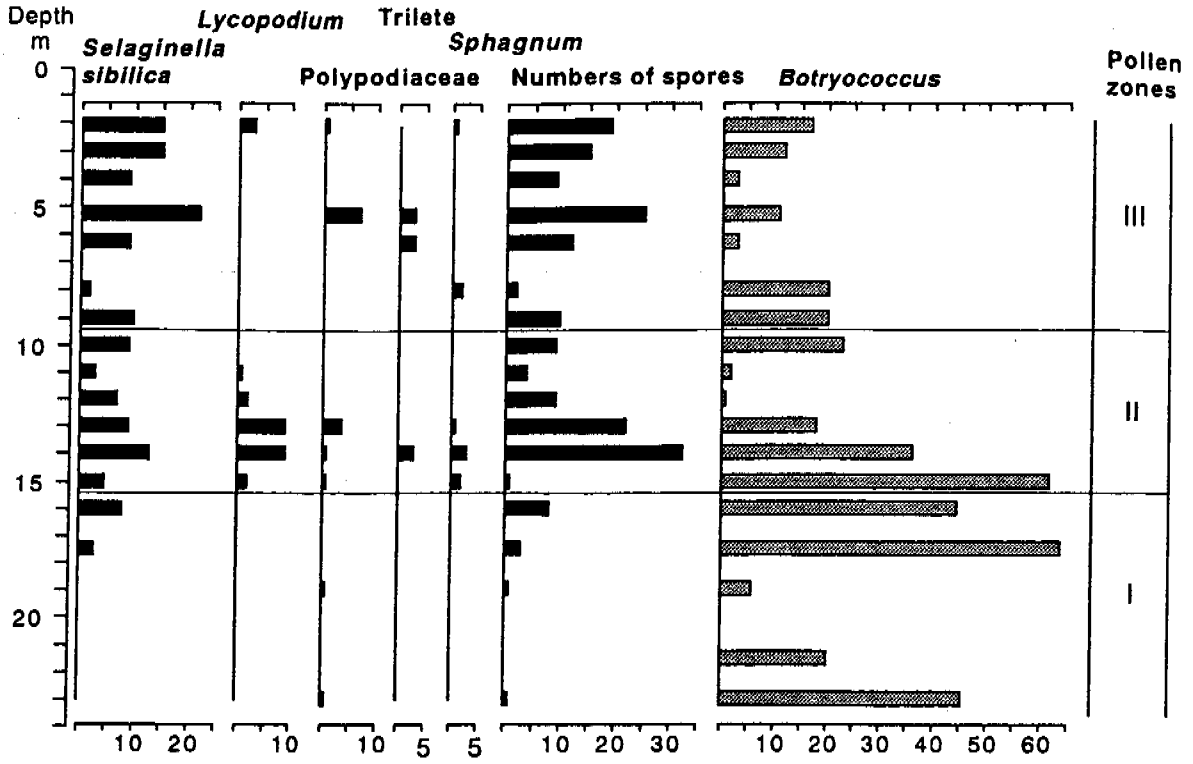

FIG. 5. Absolute spores diagram from Oiyagosky Yal section.

and taiga develop in the regions south of the tundra zone. Main component of forest tundra and taiga in east Siberia is *Larix* at present. Oiyagosky Yal is located approximately 300 km north of the northern limit of *Larix*, 1000 km northeast of the nearest northern limit of *Picea* and 1100 km north of the northern limit of *Pinus sylvestris* (Sukuryabin and Karavaev, 1991).

Vegetation reconstructed from pollen data during Zone I time was wet tundra mainly composed of grass, sedge and herbs coexisted with dwarf *Betula*, *Alnus* and *Salix*. Climate during the period was cold, however paludification progressed in summer. By Arkhipov (1984), Karginsky Interstadial was divided into three warming periods separated by two clod ages. Zone I time could be correlated with the cold age around 45 ky BP. In late stage of Zone I, *Picea* and *S. sibilica* began to grow in the region. *Picea* is distributed in southern regions of the taiga zone at present. *S. sibilica* grows on rock gravels in the alpine zone of Japan (Ooi, 1957). Appearance of *Picea* and *S. sibilica* shows an increasing trend of climatic warming and drying of wet tundra during the late stage of Zone I.

During the period of Zone II, *Picea* and *Pinus sylvestris* formed forest in Oiyagosky Yal region and/or in its vicinity. Although herbs decreased, fern such as *S. sibilica* and *Lycopodium* increased. Remarkable warming happened in the Zone II time. From very low percentages of *Larix* pollen it is suggested that *Larix* was not distributed around the region or its growing density was very low. As the reasons of very poor *Larix* abundance, next two possibilities are presumed. Distribution of vegetation zones during Karginsky Interstadial could be quite different from that of the present. Or the vegetation zone shifted towards north as a result of remarkable warming. Forest tundra and taiga of *Larix* could have migrated to the present continental shelf.

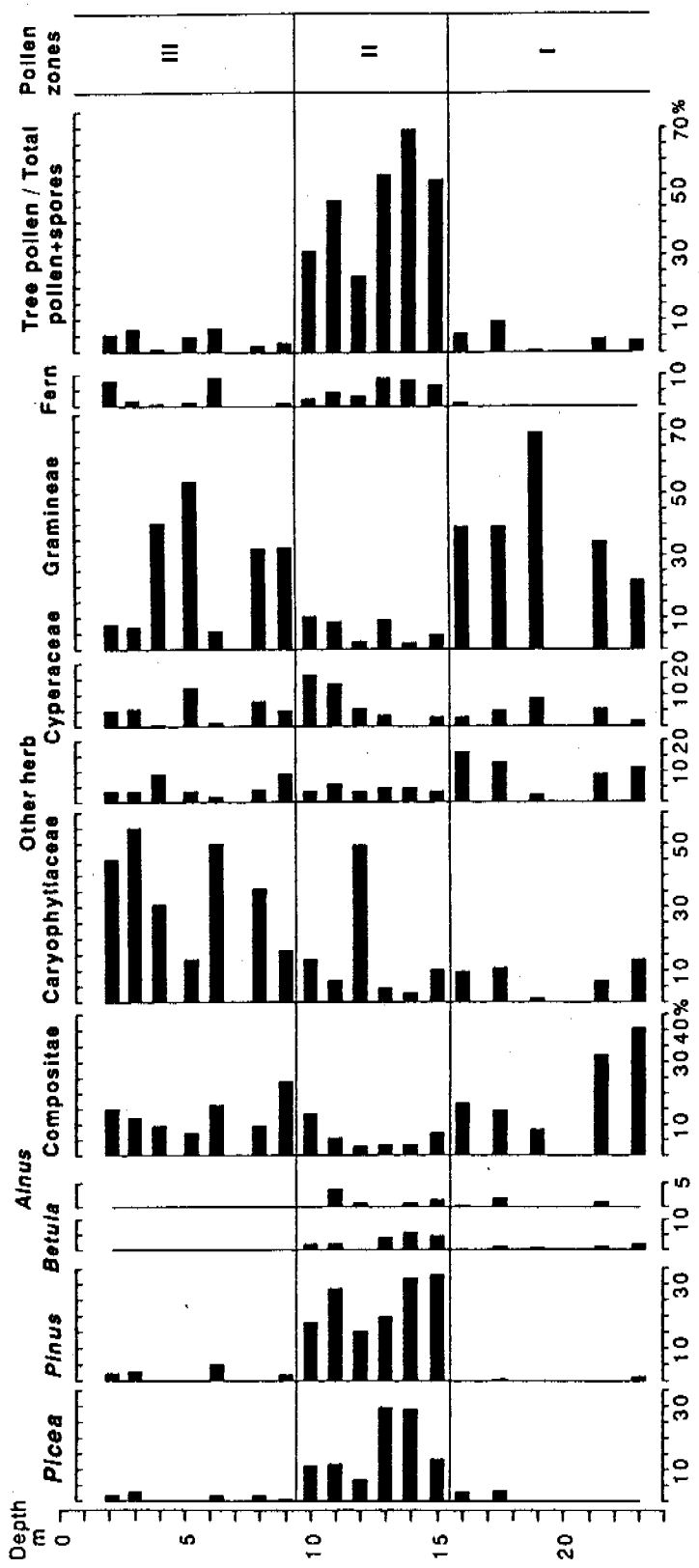

FIG. 6. Selected pollen diagram from Oiyagosky Yal section.

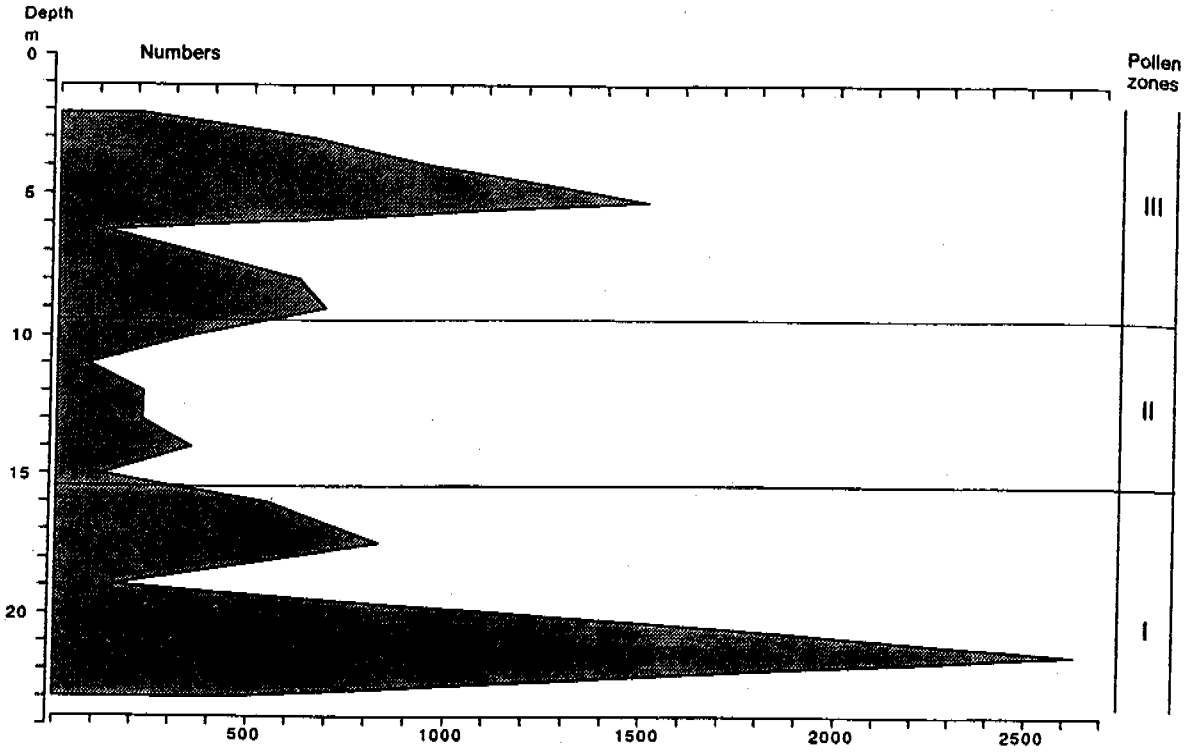

FIG. 7. Total numbers of pollen and spores per each dried five gram sample.

Vegetation during Karginsky Interstadial was very different from that of Mikulino Interstadial. In Mikulino Interstadial, shrub tundra or forest tundra developed in the Arctic coast and *Larix* taiga flourished in southern regions in vast scale. *Picea* was distributed in the regions further south than the *Larix* taiga zone (Grichuk,1984).

Zone II time of Oiyagosky Yal section could be correlated with a warm stage in Karginsky Interstadial which has its climax around slightly older than 40 ky BP (Arkhipov,1984). During the same period *Picea* pollen yielded 20–30 % at Baty–sala Basin. *Pinus sylvestris* was contained as small amounts. *Picea* trees miglated 500 km towards north in remarkable warming. Climate at that time was thought to be warmer than the present (Isayeva, 1984).

On the otherhand, Zone II could be correlated with Unit 2 of Duvanny Yal section which includes 40 ky BP date. Abundant pollen of tree (*Pinus pumila*) and shrubs (*Betula* and *Alnus*) in Unit 2 show climatic ameliolation (Giterman et al., 1979). Unit 2 does not include *Picea* pollen. *Picea* miglated from west to east accompanied by the climatic amelioration through the same migration route preferred by Takahashi (1994); however it could not reach to Duvanny Yal.

During Zone III time climate became cold and tundra developed again. Soil moisture condition was a little drier than that of Zone I. Although *Picea* and *Pinus* retreated to west and/or south, the forest zone shifted to slightly north than that of Zone I. Late stage of Zone I shifted to the maximum stage of Sartan Glacial.

Conclusion

By pollen analysis for 24 m thick pillar–shape sediments exposed at Oiyagosky Yal

section, east Siberian Arctic coast, vegetation and climate during accumulating period of Edoma was clarified as follows. 1) The sediments were divided into three pollen zones. In period of the lowest Zone I, there developed wet tundra mainly composed of sedge, grass and herbs coexisted shrubs. Climate was cold and paludification progressed in the summer season. Zone I time was correlated with a cold age around 45 ky BP in Karginsky Interstadial. 2) During Zone II time, *Picea* and *Pinus sylvestris* formed forest in Arctic coast and/or in a very near region. Remarkable warming occurred. *Larix* did not exist or its growing density was very low. This period was correlated to warming around 40 ky BP in Karginsky Interstadial. 3) Tundra vegetation recovered again in Zone III time. Climate became colder, and forest retreated to the south during the maximum stage of Sartan Glacial.

References

Arkhipov, S.A. 1984. Late Pleistocene Glaciation of Western siberia. in Late Quaternary Environments of the Soviet Union. Univ. of Minnesota Press, 13–19.

Fukuda, M. 1993. Occurrence of Ice–complex (Edoma) in Lena River Delta Region and Big Lhyavosky Island, High Arctic Eastern Siberia. in Proceedings of the Second Symposium on the Joint Siberian Permafrost Studies between Japan and Russia in 1993, 5–13.

Giterman, R.E., A.V. Sher, and J.V. Matthews, Jr. 1982. Comparison of the Development of Tundra–Steppe Environments in West and East Beringia: Pollen and Macrofossil Evidence from Key Sections. in Paleoecology of Beringia. Academic Press, 43–73.

Grichuk, V.P. 1984. Late Pleistocene Vegetation History. in Late Quaternary Environments of the Soviet Union. Univ. of Minnesota Press,155–178.

Isayeva, L.L. 1984. Late Pleistocene Glaciation of North–Central Siberia. in Late Quaternary Environments of the Soviet Union, Univ. of Minnesota Press, 21–30.

Nagaoka, D. 1993. Properties of Ice–complex Deposits in Eastern Siberia. in Proceedings of the Second Symposium on the Joint Siberian Permafrost Studies between Japan and Russia in 1993, 14–18.

Ooi, J. 1975. Flora of Japan. Shibundo, 244pp.

Sukuryabin, S.Z., and M.N. Karavaev. 1991. Green cover of Yakutia. Yakutsk Publ. Co., Yakutsk, 173 pp.

Takahashi, H. 1994. Phytogeography of vascular plants in Yakutia (Sakha). Proc. Jap. Soc. Pl. Tax.,10, 21–33.

Vegetation of model alas and ion composition of pond water of some alases in the basin of Lena River, eastern Siberia

FUSAYUKI KANDA[1], SHIGERU UEMURA[2], TATSUICHI TSUJII[3], HIDEHARU HONOKI[4], A.P. ISAEV[5], and R.V. DESYATKIN[5]

[1]*Department of Biology, Hokkaido University of Education, Kushiro 085 Japan*
Tel: +81-154-41-6161; Fax: +81-154-43-0855
[2]*Teshio Experimental Forest, Faculty of Agriculture, Hokkaido University, Horonobe 098-29 Japan*
[3]*Laboratory of Agro-Forestrial Ecology, Faculty of Agriculture, Hokkaido University, N9W9, Sapporo 060 Japan*
[4]*Toyama Science Museum, Nishinakanocho 1-8-31, Toyama 939 Japan*
[5]*Yakutsk Institute of Biology, Siberian Division, Russian Academy of Sciences, 41 Lenin Avenue, Yakutsk 677891, Republic of Sakha, Russia*

Introduction

The permafrost distributed at large areas of Siberia. The basin of Lena River near Yakutsk city in eastern Siberia is also included in the permafrost region of Siberia. There exist many alases that are the topographical structures found in the permafrost region of Siberia. Especially, on the right side of the basin of Lena River near Yakutsk city, there formed many alases with various types.

We investigated the vegetation of the Model Alas Experimental Field in the Alas station in Republic of Sakha, Russia in the summer of 1994. Ion composition of the water of some alases was also examined using ion-chromatography.

Study area

The vegetation of alas was investigated in the Model Alas Experimental Field in the Alas station of Yakutsk Institute of Biology located at about 60 km ENE of Yakutsk city. In this field some researches have been done by some groups between Japan and Russia in 1993. We set a line across the Model Alas from south to north through a small pond with 20 m in diameter in the center of the alas for the research of the vegetation of alas. The line is the same one for the soil survey that was carried out in 1993 by Matsuura et al. (1994).

In order to investigate the ion composition (Na^+, K^+, Ca^{2+}, Mg^{2+}, Cl^-, SO_4^{2-}, NO_3^-, NO_2^- and NH_4^+) of the water in the pond which lay in the center of alas, an ion-chromatography was used. The pH, conductivity, turbidity, DO, temperature and salinity were measured with an automatic water quality check machine.

Results and Discussion

The Model Alas was a wide circular grassland of about 300 m diameter surrounded with larch forest (*Larix cajanderi*) (Matsuura et al. 1994). There grew no young larch trees and other species of tall trees in the Model Alas. The vegetation of the alas changed discontinuously from the central pond to the edge of the alas like concentric circles.

There grew some water-plants in the central pond of the Model Alas, *Polygonum amphibidium, Lemna trisulca* and *Sporodela polyrhiza*, those are typical fresh-water species. In the northern belt the vegetation was divided into 12 different plant communities, while six communities in the southern belt (Table 1). This is due to the difference of depth of the soil

TABLE 1. Belt transects survey of plant communities in Model Alas in the basin of Lena River, eastern Siberia.

	Northern Belt												Southern Belt					
	12	11	10	9	8	7	6	5	4	3	2	1	1	2	3	4	5	6
Glyceria triflora												4,4	5,5					
Beckmannia syzigachne												1,1	1,1	4,4				
Scirpus pauciflorus											+	+						
Alopecurus arundinaceus									+	5,5	5,5	+		4,4	5,5	3,3		2,3
Polygonum amphibidum											3,3			4,4				
Lemna trisulca											4,4			1,1				
Sporodela polyrhiza											1,1							
Potentilla anserina							5,5	4,4	4,4	2,2					2,2			3,3
Puccinellia tenuiflora				3,3	+	5,5	2,2		5,5							4,4		
Agropyrum repens			1,2	1,1				4,4										
Agrostis sp.								3,3									5,5	
Polygonum sibiricum		1,1		3,3	5,5	1,1	+											+
Chenopodium viride					1,1	+												
Descurainia sophia						+												
Taraxacum ceratophorum			1,1	4,4														
Artemisia commutata	2,2	3,3	3,3															
Linaria acutiloba			+															
Veronica incana		+	+															
Lychnis sibirica	1,1		+															
Peucedanum baikalense			1,1															
Artemisia tanacetifolia	1,1	2,2																
Euphrasia jacutica		2,2																
Sanguisorba officinalis		1,1																
Thalictrum simplex		1,1																4,4
Galium verum	2,2	1,1																
Saussurea amara	1,1	1,1																
Poa pratense	1,2	3,3																
Poa sp.	2,3	+																1,1
Betula platyphylla	5,5																	
Larix cajanderii	1,1																	
Campanula langsdorffiana	+																	
Sedum purpurea	+																	
Vicia multicaulis	1,1																	
Convolvulus arvensis	+																	
Achillea cartilaginea	+																	
Calamagrostis neglecta															3,3			
Inula britannica															2,2			
Potentilla sibirica															1,1			
Ranunculus borealis																4,4		1,1
Lactuca sibirica																		3,3
Salix sp.																		1,1
Distance (m)	147	132	118	109	96	78	63	56	47	39	23	16	12	28	52	69	106	117
Water depth (cm)										3	40	50	60	40	5			
Total coverage (%)	75	90	85	98	90	100	100	100	100	100	90	65	90	80	100	100	100	100

active layer on northern and southern belts in the summer. It must be noted that *Potentilla anserina* is a halophilous plant. This may suggest that the vegetation is specific to the alases.

To know the nature of alas we collected water of the ponds in the center of some alases. Water quality was examined in relation to vegetation of the alases. Table 2 shows pH, conductivity, turbidity, DO, alkalinity, some cations and anions in the pond water of the alases. Most of the water samples showed significantly high values of Mg^{2+} and Ca^{2+} ions. Especially, water samples of A–1 was extremely salty. The strange ion condition seems to influence the characteristic vegetation of the alases.

TABLE 2. PH, conductivity, turbidity, DO, salinity and ion composition of the water of seven alases. Water samples of A–1 and A–2 were measured on July 27. The B–1 to B–5 were measured on July 28, 1994. The A–1 is the complex of many alases; A–2 is the Model Alas.

	A-1	A-2	B-1	B-2	B-3	B-4	B-5
pH	9.0	7.7	7.8	8.0	9.3	9.8	10.0
Conductivity ($\Omega^{-1} \cdot m^{-1}$)	2.00	0.57	0.31	0.32	0.53	0.34	0.29
Turbidity	10	10	0	10	60	130	30
DO (mg/l)	8.9	8.7	5.3	6.0	6.3	6.4	8.0
Temperature(℃)	18	20	18	18	18	18	18
SALT (%)	0.1	0	0	0	0	0	0
Alkalinity (meq/l)	19.00	6.67	3.60	3.42	4.94	4.41	3.41
Na^+ (mg/l)	322	34.8	17.8	9.31	35.0	23.0	13.3
K^+ (mg/l)	47.1	11.5	7.60	4.90	8.49	7.68	5.17
Ca^{2+} (mg/l)	8.03	36.1	35.0	34.3	51.8	19.9	25.0
Mg^{2+} (mg/l)	147	55.1	28.4	23.2	49.0	30.8	26.1
Cl^-(mg/l)	173	16.3	9.80	2.96	10.0	6.40	5.16
SO_4^{2-} (mg/l)	115	3.40	4.76	5.64	74.4	2.46	7.68
NO_3^- (mg/l)	2.99	0.23	15.23	0.16	2.42	0.23	0.17
NH_4^+ (mg/l)	0.00	5.12	10.77	0.85	2.63	0.23	0.17
NO_2^- (mg/l)	0.00	0.00	0.00	0.00	0.04	0.00	0.00

Reference

Matsuura, Y., M.S. Sanada, S. Ohta and R.V. Desyatkin. 1994. Carbon and nitrogen storage in soils developed on two different toposequencerian of the Lena River terrain. Proceedings of the Second Symposium on the Joint Siberian Permafrost Studies between Japan and Russia in 1993:177–182.

Forest succession in Aldan, eastern Siberia

S. UEMURA[1], F. KANDA[2], A.P. ISAEV[3], and T. TSUJII[4]

[1]*Teshio Experimental Forest, Faculty of Agriculture, Hokkaido University, Horonobe 098-29 Japan*
Tel: +81-1632-6-5211; Fax: +81-1632-6-5003
[2]*Biological Laboratory, Kushiro College, Hokkaido University of Education, Kushiro 085 Japan*
[3]*Yakutian Institute of Biology, Russian Academy of Sciences, Yakutsk 677891 Sakha, Russia*
[4]*Research Laboratory of Agro-Forestrial Ecology, Faculty of Agriculture,*
Hokkaido University, Sapporo 060 Japan

Abstract. In Aldan, eastern Siberia, located on the southern margin of continuous permafrost zone, wildfires have occurred very frequently, and the fire cycle of this region is about 60 years, which is one of the shortest periods in the circumpolar ecosystems. Unlike the spruce-dominated taiga in North America and northern Europe, larch trees predominate in the eastern part of the Siberian taiga, with occasional occurrence of spruce forest in the wet basin. The vertical structure of the forests showed that spruce forests were preceded by larch forest, indicating that frequent occurrence of fire may prevent the ecological succession from larch forest to spruce forest, and therefore, resulting the predominance of larch forest in the Siberian taiga. Mixed forests of larch and dwarf-pine were self renewable: they seemed independent of the normal course of ecological succession by dominating dry habitats where their competitors were not successful.

Introduction

Fires frequently occur in the taiga of the Northern Hemisphere and strongly control the floral makeup, vegetation structure, and biological productivity (Heinselman 1981, Wein and MacLean 1983). Unlike in the spruce-dominated taiga in North America and northern Europe, the Siberian taiga is predominated by larch, which is considered to occur in earlier stages of ecological succession. In the southern parts of the Siberian taiga area, larch forests predominate with occasional occurrence of spruce, which is shade tolerant and generally the climax species in this area. The effects of fires on vegetation are considered to be remarkably variable among different types of forests (Van Cleve and Viereck 1981), suggesting that the postfire vegetation of Siberian taiga may be dissimilar to that of Alaska-Canada or northern European taiga. Nevertheless, the effects of fire on vegetation have been little studied in the Siberian taiga to date, with only a few exceptions such as Shcherbakow (1979), Sofronov (1967) and Uemura et al. (1990). We surveyed postfire vegetation in southeastern Siberia, and hereby show some features of postfire succession and discuss why the taiga of this area is predominated by larch trees that are less tolerant to shade stress than spruce trees.

Study area

The study area was chosen in Aldan, the southernmost of Sakha Republic, Russia, and is a hilly zone of the Stanovoi Range. This region is situated on the southern margin of the continuous permafrost zone (Dyrness et al. 1986). The region has a typical continental climate, with relatively little precipitation (ca. 600 mm per year) and very cold winters (about -30°C average in January). The sites surveyed have deep, periglacially produced gravel that are covered with organic soil layer. Because of the existence of permafrost, underground of the forest sites is wet especially in shallow basins. These habitats are covered predominantly

by larch, *Larix cajanderi*, and spruce, *Picea obovata*, with spororadical birch, *Betula platyphylla*. On the other hand, ground surface of hillslopes has quite a thin soil layer and is relatively dry by rapid drainage and such habitats are dominated by mixed forests of larch and dwarf-pine, *Pinus pumila*. The frequent occurrence of wildfire is well known in this area: the fire cycle is about 60 years, which is similar to 50–100 years in Alaska and western Canada (Heinselman 1981, Van Cleve and Viereck 1981) but shorter than 100 years in Scandinavia (Zackrission 1977), 150–200 years in eastern Canada (Wein and MacLean 1983), and 120 years in northern China (Uemura et al. 1990).

Methods

From 22 to 26 July 1994, the vegetation survey was conducted in the three 20 x 20 m quadrats, which were set in larch forest located on a mesic gentle-slope of Yakokit, about 30 km north of Aldan (AL), in spruce forest on a humid basin of Nimyar, ca. 100 km south of Aldan (AS), and in mixed forest of larch and dwarf-pine on a dry hillslope near Aldan (AM). In each quadrat, all trees taller than 1.5 m were measured of trunk height and diameter at breast height (dbh). Trunk height of seedlings and saplings smaller than 1.5 m was measured in five 2 x 2 m subquadrats randomly chosen in each quadrat. For woody shrub and herbaceous understory including mosses and lichens, canopy coverage of each species was measured in the subquadrats.

Results

Size structure of tree populations.—Fig. 1 shows the size structure of trees in the three quadrats surveyed. Though the larch forest (AL) is primarily dominated by *Larix cajanderi*, the smaller classes lower than 6 m in height or less than 5 cm in dbh are overwhelmingly occupied by saplings of *Picea obovata*, that is, this forest seems to be replaced by spruce-dominated forest unless it has been disturbed by, for instance, wildfires or artificial cutting. In the spruce forest (AS), some tall trees of *Larix cajanderi* existed in the predominately spruce canopy, and some large dead trees of this species were found in the interior, suggesting that this spruce forest had been preceded by a larch forest.

Mixed forest of larch and dwarf-pine (AM) seemed to be self-renewable. Though there were some saplings of *Picea obovata*, it is estimated that they cannot become dominant over this forest because the habitat is too dry to grow for them. This forest is probably reestablished by the immigration of seeds of *Larix cajanderi* and *Pinus pumila* after deforestation even if wildfires destroy older forests. Birch species in this forest was a hybrid between *Betula platyphylla* and *Betula middendorffii* and its growth form was shrub with no erect stems.

Understory vegetation.—Understory vegetation of the three quadrats surveyed was tabulated in Table 1. Species richness in the understories of AL, AS and AM is 31, 54 and 19, respectively. The difference among these forests is mainly due to the abundance of herbaceous plants. The forest floor in AS seemed to be the most stable and was inhabited by many species including the following six dominant species: *Vaccinium uliginosum, Limnas stelleri, Saussurea parviflora, Polygonum viviparum, Aegopodium alpestre* and *Geranium albiflorum*, and the coverage of vascular plants was about 65% while the dominant species in AL were *Vaccinium vitis-idaea, Vaccinium uliginosum, Ledum palustre, Equisetum scirpoides* and the coverage was about 50%.

Not only the floor of spruce forest but also that of larch forest was densely covered by

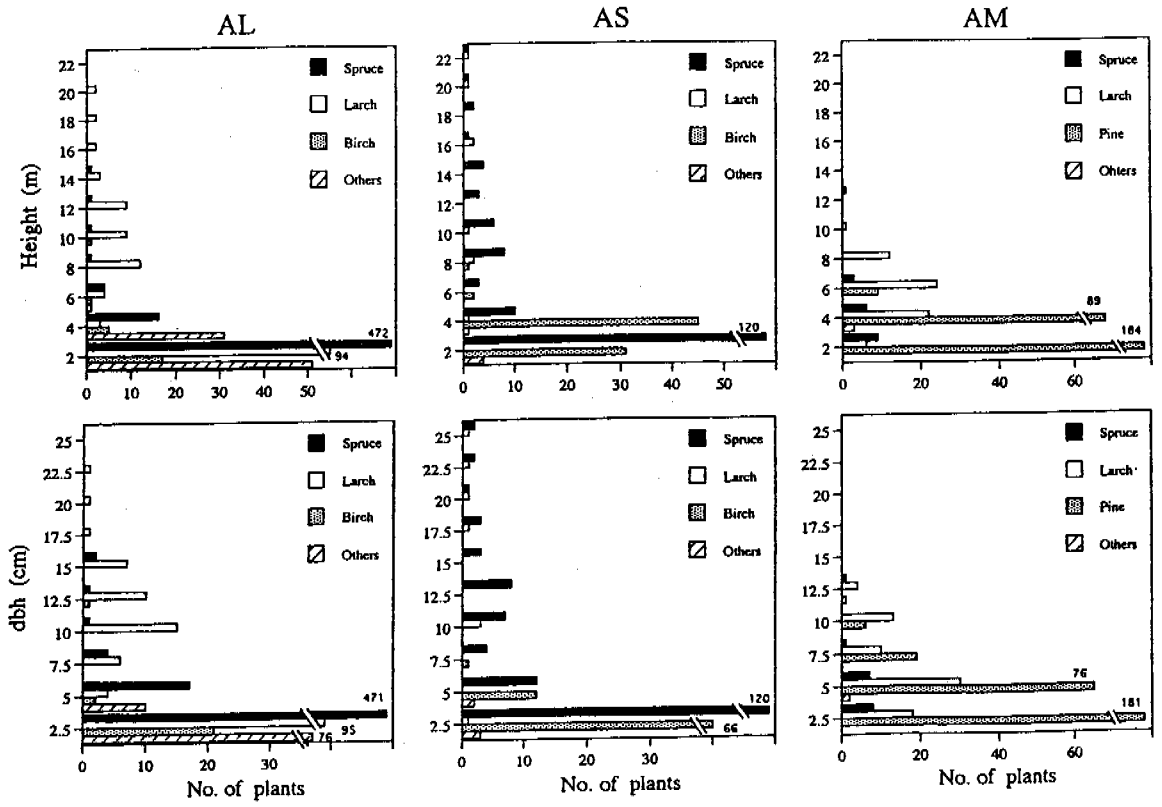

FIG. 1. Size structure of tree populations in larch forest (AL), spruce forest (AS) and mixed forest of larch and dwarf-pine (AM). The number of tree saplings smaller than 1.5 m was estimated by the real densities measured in the five subquadrats randomly chosen in each quadrat.

the carpet of feather mosses such as *Pleurozium schreberi*, *Hylocomium splendens* and *Aulacommium palustre*, that generally dominate the closed and long-term stable habitats. This suggests that, at least, the last deforestation by fire did not burn up the understory, probably because the understory was very wet by the melting water supplied from the permafrost underlaid. Despite the similar occurrence of lichen species in AS and AL, however, its coverage was quite low in AS. This seemed to be due to the existence of the thick organic soil layer in the spruce forest where more competitive herbaceous species are successful.

In the mixed larch and dwarf-pine forest, the floor was densely covered by thick lichen mat mainly composed of *Cladonia stellaris*, *Cladonia rangiferina* and *Cetraria repigata* but there was no herbaceous species only without *Carex vanheurckii*.

Discussion

Larix species generally show hardiness to low temperature; in particular, *Larix gmelinii*, *L. cajanderi* and *L. dahurica*, which predominate eastern Siberia possess trichome around the buds and are therefore very tolerant to frost and drought in midwinter. However, winter hardness is not sufficient to explain why larch dominates over spruce in this region of Siberian taiga, while the opposite condition exists in the Alaska-Canada taiga where the temperature frequently falls to -40°C or less in winter.

As described in Uemura et al. (1990), eastern Siberia is principally covered by a thick gravely layer that was repeatedly moved by freeze-thaw cycles of the periglacial period. Unlike the thick sandy-silt or peat layer extensively covering the Alaska-Canada taiga, the

TABLE 1. Understory vegetation surveyed by the method of Braun–Blanquet except for the trees taller than 1.5 m.

Forest stand	Larch forest (AL)					Spruce forest (AS)					Mixed forest (AM)				
Subquadrat No.	1	2	3	4	5	1	2	3	4	5	1	2	3	4	5
Picea obovata	2,1	2,2	2,2	2,2	2,2	1,1	1,1	2,1	1,1	3,3	1,1				
Larix cajanderi	1,1	+	2,2	+	1,1	1,1	+	1,1	+	1,1					
Corydalis paeonifolia	+	1,1		1,1			+								
Vaccinium vitis-idaea	2,2	3,3	1,2	4,4	2,2	1,1	+	+		1,1	1,1	2,3	1,2	1,1	+
Vaccinium uliginosum	3,3	1,1	3,3	2,2	2,2	1,1	2,2	2,2	5,5	4,4	3,3		4,4	1,1	3,3
Ledum palustre	1,1	4,4		3,3	2,2										
Carex sp.	+														
Pedicularis labradorica	+							+		+					
Equisetum scirpoides	+,2	+,2	1,2	1,1	+,2		+								
Potentilla sp.	+		1,1												
Ramschia obtusata	1,1						+	+		1,2					
Limnas stelleri	+	+	1,1	+	+	+,2	1,2	2,3	1,2	+,2					
Elymus interior?	+														
Pinus sibirica		+		2,1											
Arctous erythrocarpa		1,1	2,2												
*Betula platyphylla**			3,2				+				2,2	4,3		3,3	1,1
Equisetum arvense			+												
Goodyera repens			+		+										
Clematis sibirica			+												
Saussurea parviflora					+		1,1	1,1	+	2,2					
Pinus pumila									+				+	1,1	1,1
Zygadenus sibiricus						+	+			+					
Geranium albiflorum						1,2	3,3	+		1,1					
Aconitum ranuncloides						+	+	+		+					
Mitella nuda						1,2	+	+							
Pedicularis verticulata						1,1	+								
Polygonum viviparum						1,2	3,3	1,2	+,2	1,1					
Rosa davurica						+									
Pyrola minor						+									
Galium boreale						+,2		1,1	+	+					
Aegopodium alpestre						+	1,1	2,2	1,1	+,2					
Equisetum pratense						+		+	+						
Luzula parviflora						+	+			+					
Callianthemum isopyroides						+	+								
Carex vanheurckii						+	3,3	2,3					+,2		
Bromus pumpellianus						+		+	+						
Swertia obtusata						1,2									
Sanguisorba officinalis						+	+	1,1	+						
Trollius boreosibiricus						+	+			+					
Parnassia palustre							1,1								
Empetrum nigrum							1,1			1,1					
Juniperus sibirica							2,2								
Polemonium coeruleum							1,1			+					
Solidago virga-aurea							+								
Salix sp.								1,1							

TABLE 1. (CONTINUE)

Forest stand	Larch forest (AL)					Spruce forest (AS)					Mixed forest (AM)				
Subquadrat No.	1	2	3	4	5	1	2	3	4	5	1	2	3	4	5
Antenaria sp.								+							
Poa pratense								+		+					
Artemisia sp.								+							
Carex pediformis								1,2		1,1					
Aquilegia sp.										+					
Potentilla fruticosa										+					
Festuca rubra										+					
Vaccinium myrtillus											1,1		2,2	+	2,2
(Mosses)															
Pleurozium schreberi	4,4	2,2	4,4	4,4		3,3	2,2	1,1		1,1	1,1				1,1
Hylocomium splendens		4,4	1,2	1,1	3,3	1,1	2,2		4,4	5,5					
Aulacommium palustre	3,3	3,3	2,2	3,3	4,4	4,4	4,4	3,3	3,3	2,2			1,1		
Ptilidium sp.		+													
Pogonatum sp.					+						2,3	3,3		1,2	1,2
Dicranum polysetum								4,4	+	+	1,1	2,2	1,1		2,2
Ptilium crista-castrensis								1,1					+		
(Lichens)															
Cladonia stellaris	1,1	+	1,1	1,1							2,2	3,3	3,3	3,3	3,3
Cladonia rangiferina	2,2		1,1	2,2	1,2	1,1		1,1	+		3,3	2,3	2,2	2,2	3,3
Cladonia uncialis?		2,2	+					+							
Cetraria repigata	1,2	2,2	2,2	1,1	1,1	+		1,1	+	+	2,2	3,3	4,4		3,3
Peltigera aphthosa		1,1		1,1	+		+		+		1,1		+		+
Cladonia amaurocrea				+	+						+	+	1,1	+	+,2
Cladonia sp.								+							
Nephroma irripilytigra									+						
Peltigera sp.											+				
Stereocaulon sp.											3,3	2,2	3,3	4,4	3,3
No. of species	20	19	20	18	17	30	32	32	20	29	17	10	15	11	15
Total coverage (%)															
Vascular plants	40	50	50	80	25	30	70	60	85	75	50	70	80	50	40
Mosses and lichens	95	90	98	70	95	95	80	95	90	98	80	95	85	99	95

**In AM the hybrid of Betula platyphylla X Betula middendorffii*

gravely layer has low water-holding capacity and is always dry. This may prevent the expansion of spruce, which need more water than larch especially in spring. Moreover, spruce seem less tolerant to fires than larch, because the low branches of spruce trees conduct fire into the crown and have thinner bark than larch (Sakai 1973). Larch is less resinous than spruce and their leaves have higher water contents. Larch forest development seems to be a precursor for spruce forest: hence, the frequent occurrences of wildfires prevent the establishment of spruce forests more so than that of larch forests.

Both trees of larch and pine, which are usually intolerant to shade stress, are less competitive in fertile habitats (Zackrisson 1977, Bradshow and Browne 1987), indicating that the mixed larch dwarf-pine forest may develop toward spruce forest. However, the mixed forests are limited to only higher lands or very dry habitats where their competitors cannot grow, suggesting that the mixed forests are independent of the normal course of ecological succession: those habitats are repeatedly dominated by the mixed forests.

Literature cited

Bradshow, R.H.W., and P. Browne. 1987. Changing patterns in the post-glacial distribution of Pinus sylvestris in Ireland. J. Biogeogr. 14:237–248.

Dyrness, C.T., L.A., Viereck, and K., Van Cleve. 1986. Fire in taiga communities of Interior Alaska. In: Forest ecosystems in the Alaskan taiga. (ed. by L.A. Viereck), pp. 74–86. Springer-Verlag, New York.

Heinselman, M.L. 1981. Fire and succession in the conifer forests of northern North America. In: Forest succession, concept and application. (eds. by D.C. West, H.H. Shugart & D.B. Botkin), pp. 374–405. Springer-Verlag, New York.

Sakai, A. 1973. Ecological characteristics of forests in Yakutia Plain. Low Temp. Sci., B 31: 49–70.

Shcherbakow, I.P. 1979. Forest fires in the Yakut A.S.S.R. and effects on the forest environment. Nauka, Novosibirsk.

Sofronov, M.A. 1967. Forest fires in the mountains of southern Siberia. Nauka, Moscow.

Uemura, S., S. Tsuda, and S. Hasegawa. 1990. Effects of fire on the vegetation of Siberian taiga predominated by Larix dahurica. Can. J. For. Res. 20: 547–553.

Van Cleve, K., and L.A. Viereck. 1981. Forest succession in relation to nutrient cycling in the boreal forest of Alaska. In: Forest succession, concept and application. (eds. by D.C. West, H.H. Shugart & D.B. Botkin), pp. 185–211. Springer-Verlag, New York.

Wein, R.W., and D.A. MacLean. 1983. An overview of fire in northern ecosystems. In: The role of fire in northern circumpolar ecosystems. (eds. by R.W. Wein & D.A. MacLean), pp. 1–18. John Wiley & Sons, New York.

Zackrisson, O. 1977. Influence of forest fires on the North Swedish boreal forest. Oikos, 29: 22–32.

Analysis of age and size structures of larch forests in the transitional zone between taiga and tundra

AKIO TAKENAKA[1] and YASUO YAMAMURA[2]

[1]*National Institute for Environmental Studies, 16-2 Onogawa, Tsukuba 305 Japan*
Tel: +81-298-51-6111; Fax: +81-298-51-4732
[2]*Faculty of Science, Ibaraki University, Bunkyo, Mito 310 Japan*

Introduction

A large part of the higher latitude regions of Eurasia is covered by coniferous forests. In Siberia, the main tree components of the forests around their northern limit are larch trees such as *Larix gmelinii* and *L. sibirica*. Beyond the northern boarder of the forest is covered with tundra vegetation with grasses, herb and some shrubs predominating.

In the scenario of the global warming process due to the anthropogenic green house gasses, the higher latitude regions will suffer larger changes of climate. To predict how the climate change would affect the distribution pattern of the northern forests, information on the dynamics and maintenance mechanism of the forest at its boarder of distribution is indispensable.

To monitor the forest dynamics is a time and energy consuming work, especially for the forest which is not easy to access. In the present study, we tried to get a coarse view of the forest dynamics from the age and size structures and spatial distribution of the trees in the forest tundra in the transitional zone between taiga and tundra in the Siberian region.

Study area

In the summer of 1994, we visited two locations in the forest tundra. One was on the west bank of Lena river ca. 100 km west of Tiksi. The location of the site determined with GPS was 71°37'N and 125°32'E. The other one was in Taymir peninsula, ca. 100 km north of Noril'sk, and was located at 70°03'N and 87°36'E.

The site west of Tiksi (hereafter called Tiksi site) is a flat area near a small stream and some flat-top hills. The altitude was ca. 150 m a.s.l. The tree density of the forest diminishes from south to north, toward the tundra with no trees. The canopy of the forest is solely composed of *Larix gmelinii*. The forest floor was typical of the forest-tundra, dominated by sphagnums and herb and grass species with some shrubs of a few tens of cm high. Two belts of 10 m x 50 m were set, one (Belt-T1) a few hundred meters interior from the tree line and the other (Belt-T2), near the tree line. In both of the belts, most of the trees had old cones, but current-year cones were seldom found.

The site north of Noril'sk is near a large lake called Pyasino (hereafter we call this site Pyasino site). In this area with small lakes, marshes, and hills, patch-like stands of *Larix sibirica* trees are scattered in tundra. Dense shrub community composed of *Alnus, Betula* and *Salix* species was found abundant. Some of the patches of *L. sibirica* have the shrub layer and some do not. Like in Tiksi site, many trees had old cones, but new ones were rare.

Two belts of the same size as in Tiksi site were set, one (Belt-P1) on a slope facing a small pond and the other (Belt-P2), on top of a flat hill. The former had a dense layer of *Alnus*, while the other were lacking any shrub layer. The altitude of the study site was ca. 30 m a.s.l.

Methods

In the four belts (two in Tiksi site and another two in Pyasino site), all the larch trees were tagged and their locations in the belts were determined. After measuring the tree height, disk samples of the stem near the ground surface were collected for all the tagged trees. In Belt–T2, where the seedlings of small sizes were abundant, only seedlings found in 10 m x 20 m area within the belt were mapped and sampled. The seedlings were also collected in Belt–T1 from 10 m x 20 m area, but their locations were not determined. There was hardly any seedlings in the belts in Pyasino site.

The collected disk samples were used for the determination of the age of the tree. Binoculars were used for reading the samples because of the very thin annual rings. The accuracy of the reading was guaranteed by checking the patterns of ring widths among the trees from each belt.

Results and discussion

The spatial distribution pattern of the trees in the belts are shown in Fig. 1. There is an obvious tendency for aggregation of trees except in Belt–T1. The tendency was most

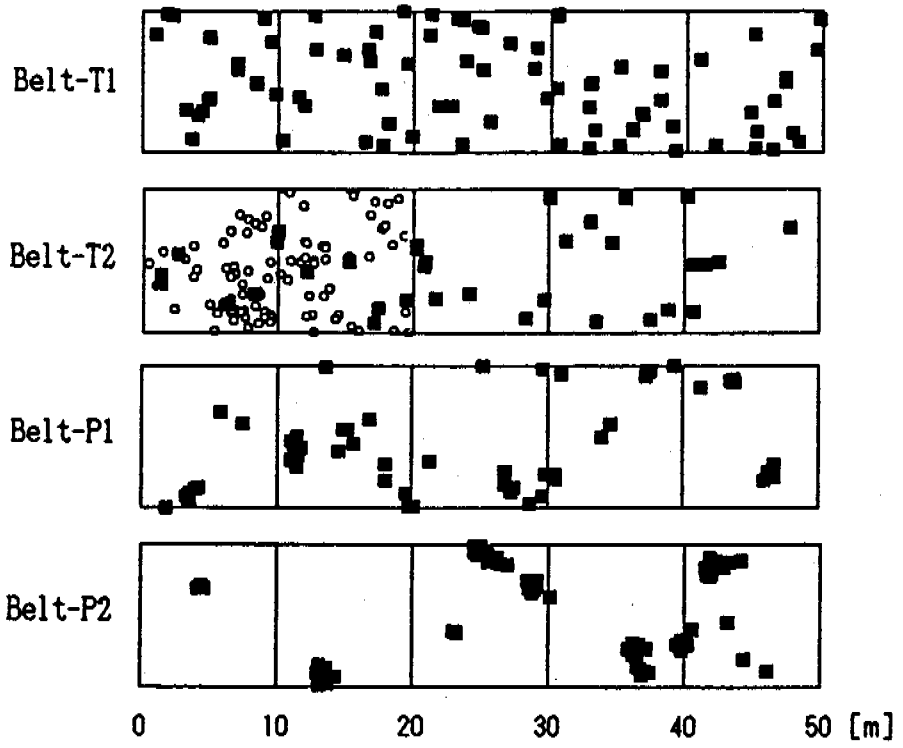

FIG. 1. Spatial distribution of larch trees in the study plots. The numbers of the plotted trees are 84 in Belt–T1, 35 in Belt–T2, 61 in Belt–P1, and 84 in Belt–P2. In the map for Belt–T2, locations of 88 short trees (< 1 m) in 10 m x 20 m area are plotted with open circles.

pronounced in Belt–P2. Some of the neighboring trunks were from one stump, but most of the aggregation was not due to such sprouting. This spatial pattern of the larch trees suggests patchy distribution of the habitat suitable for the tree establishment, even though we can not specify what factor was controlling the recruitment success of the larches.

The height of the forest canopy was around 5 or 6 m in Tiksi site, and a little taller in Pyasino site (Fig. 2). High abundance of short trees was observed in Tiksi site. High abundance of short trees even in Belt–N1 at the front facing tundra suggests vigorous regeneration of the forest. Whether the forest is expanding into the tundra area was not obvious. Some, but not many, of larch seedlings and saplings were found in the tundra outside of the forest tundra area.

Not all of the disk samples had been read for the age yet. Only data for trees in Belt–P1 and some in Belt–N1 are available and shown in Fig. 3. There is a distinct difference in the patterns of age distribution between the two belts. In Belt–P1, the distribution was symmetric and unimodal, being centered around 90–100 years. The age of the most of the trees are in the range of 50 to 150 years. No 'good year' or 'good decade' for tree regeneration can be recognized. In Tiksi site, on the other hand, the age distributions was much more scattered,

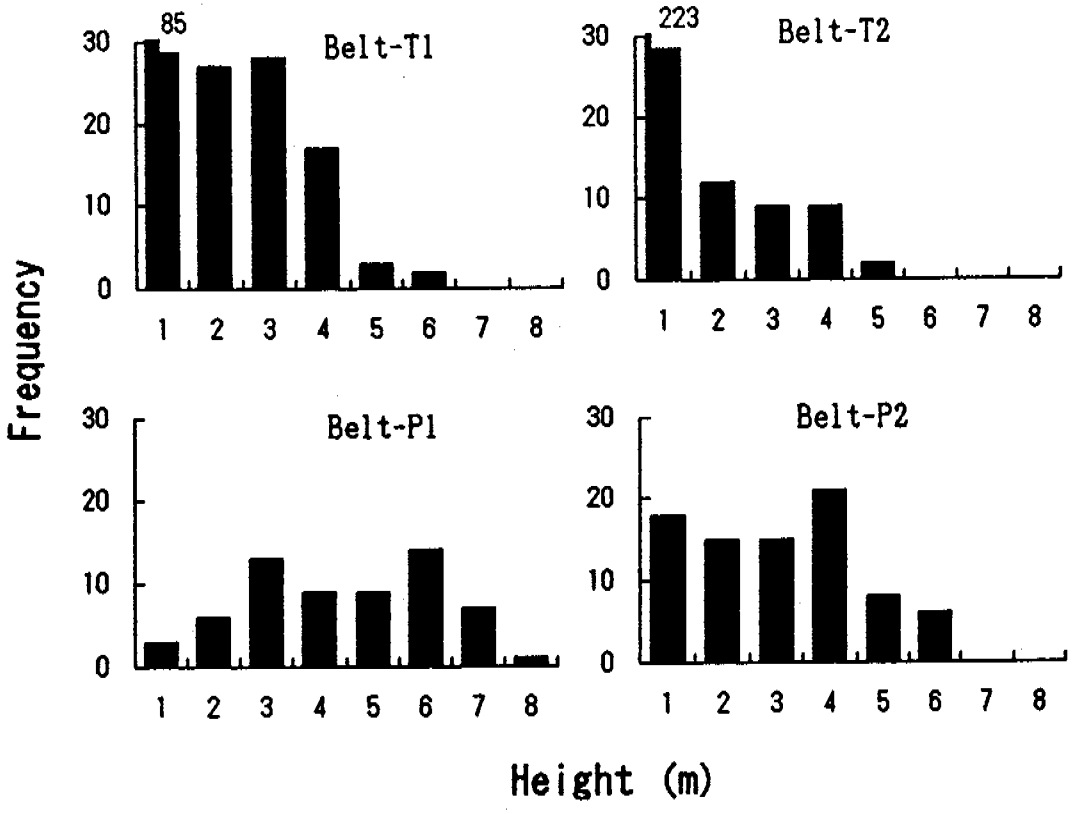

FIG. 2. Histograms of the height of the larch trees. In the belts in Tiksi site, then number of trees less than 1 m high were calculated by multiplying the number observed in 10 m x 20 m area by 2.5 (or, 50 m / 20 m).

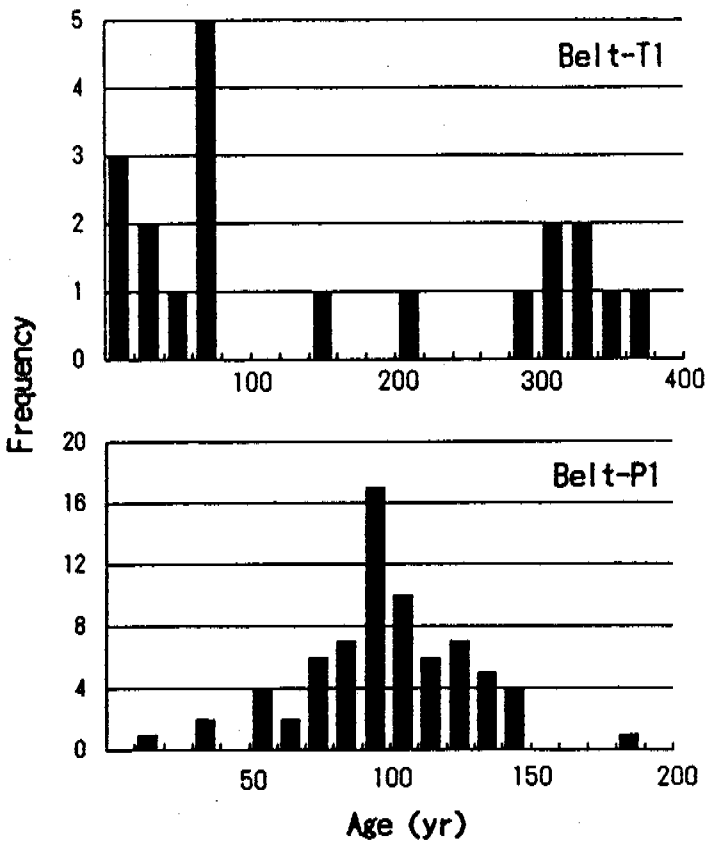

FIG. 3. Histograms of the age of the larch trees in Belt–T1 and Belt– P1. Only part of the data are shown for Belt–T1.

with a group of trees younger than 80 years, another group older than 300 years, and some in–between.

The age–height relationships did not differ between the two sites for the trees less than 100 years old (Fig. 4). In Pyasino site, some of the trees older than 100 years were higher than the younger ones, while there are a lot of old ones with less height. In Tiksi, where trees older than 300 years are not rare, the height remained less than 6 m regardless of age. The apparent limitation of the height growth in Tiksi site is likely to be due to the damage of the leader shoots, which was observed for many trees in Tiksi site. Further analysis of the height growth pattern is presented by Yamamura and Takenaka elsewhere in this issue.

The spatial distribution of the trees in Belt–P1 plotted with their ages (Fig. 5) gives some idea of the history of the forest. There are several clumps of the trees as stated earlier, but the ages of the trees were not clumped within each clump. There are a few tens or more years difference in the ages of the trees in each clump. There seems no distinct difference of tree age among the clumps. If the clumping of trees is a result of heterogeneity in suitability for tree establishment, the spatial pattern of the tree ages suggests that many suitable sites were created simultaneously (sometime around 120–150 years ago), and the condition remained suitable for several decades. Still, what was the condition which favored the new tree recruitment is not clear. Further observation is needed for determining the critical process and requirements of seedling establishment of larch trees in forest tundra regions.

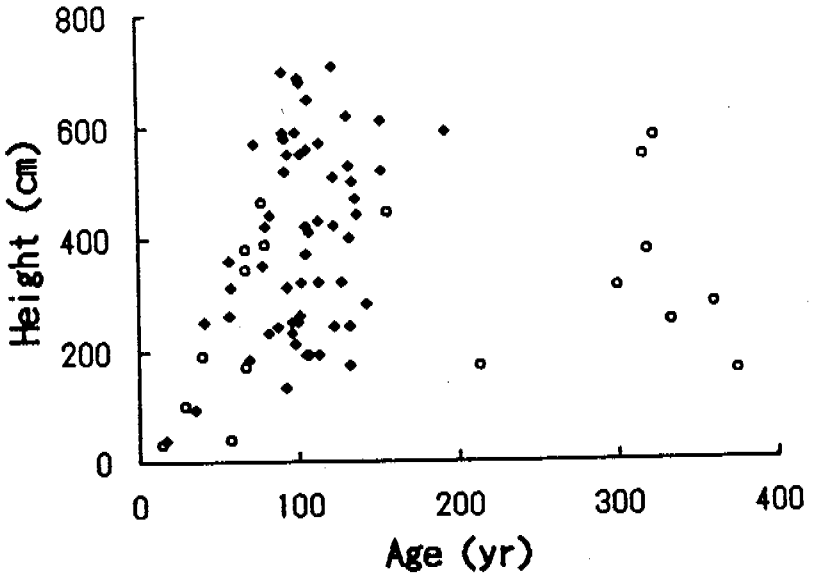

FIG. 4. Relationships between the height and age of larch trees. Closed circles, Belt-P1; open circles, Belt-T1.

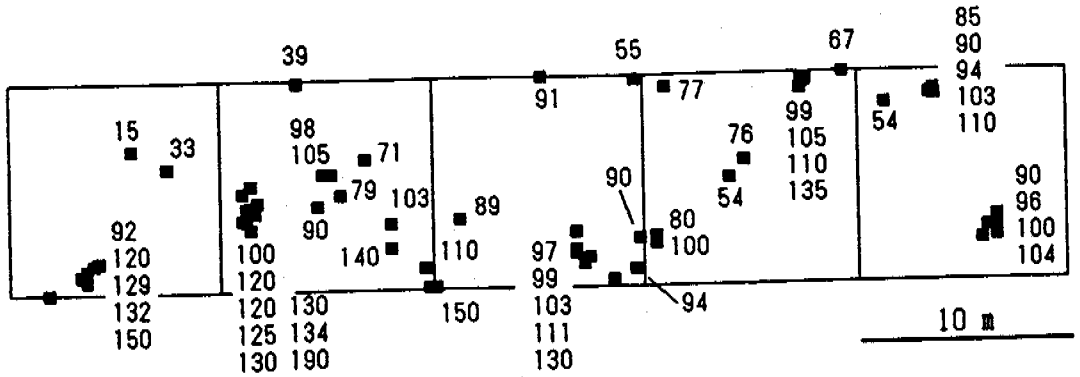

FIG. 5. Age of larch trees in Belt-P1.

Growth patterns of *Larix gmelinii* in the transitional zone between taiga and tundra

YASUO YAMAMURA[1], and AKIO TAKENAKA[2]

[1]*Faculty of Science, Ibaraki University, Mito 310 Japan*
Tel: +81-292-28-8386; Fax: +81-292-28-8404
[2]*National Institute for Environmental Studies, 16-2, Onogawa, Tsukuba 305 Japan*

Introduction

In the latitudinal timber-line growth of trees is severely limited by the extreme environmental conditions. Climatic change by the global warming is predicted to be more conspicuous in high latitude regions, and thus will affect plant growth considerably.

Larch is the only tree component in the transitional zone between taiga and tundra in Siberia. Its growth pattern recorded as annual rings is expected to be closely correlated with climatic fluctuation. Height growth will be frequently disturbed by severe physical conditions. Larch tree grows monopodially as an characteristic of conifers. Therefore injury of apical tissues must affect seriously on growth of whole plant. Frequency of such an injury seems to be related to snow depth and vertical distribution of wind speed, and consequently to tree height.

The present study was conducted to analyze growth patterns of dahurian larch (*Larix gmelinii*) in the northern limit of its distribution. Radial growth, height growth and volume growth of main trunk are examined by measuring annual rings. We ask the following questions; (1) Is there an apparent change pattern in the radial growth which is attributable to climatic fluctuations? (2) Are there any growth patterns associated with plant height?

Materials and Methods

Study site is an open forest stand on a foot of a plateau, located about 150 km west of Tiksi (71°37'N, 125°32'E). The altitude is about 150 m. *Larix gmelinii* is the only tree species. The stand is about 5 to 6 m high and does not have shrub layers. Sampling was carried out at two points; the edge and inside of the stand. Density of large trees was lower at the edge point. The two sampling points were several hundreds meters apart. At each point, five sample trees with straight trunk were selected from various size classes for the stem analysis. Several disks were collected from a trunk of each sample tree at an equal height interval.

Annual increments in each disk were measured with a micrometer in two opposite radii. The values of the annual increment were corrected by multiplying the ratio of mean radius of woody tissues in four directions and a radius in the direction of the measurement. Vertical section diagrams of woody tissues of the trunk were drawn with the radial growth data from disks at various heights. Tree height in past years was determined and annual volume increment was calculated using these diagrams.

Results and Discussion

Radial growth.—Annual increments and growth curves in basal disks were shown for all the sample trees (Fig. 1). Mean annual increment in each sample tree was from 0.2 to 0.4

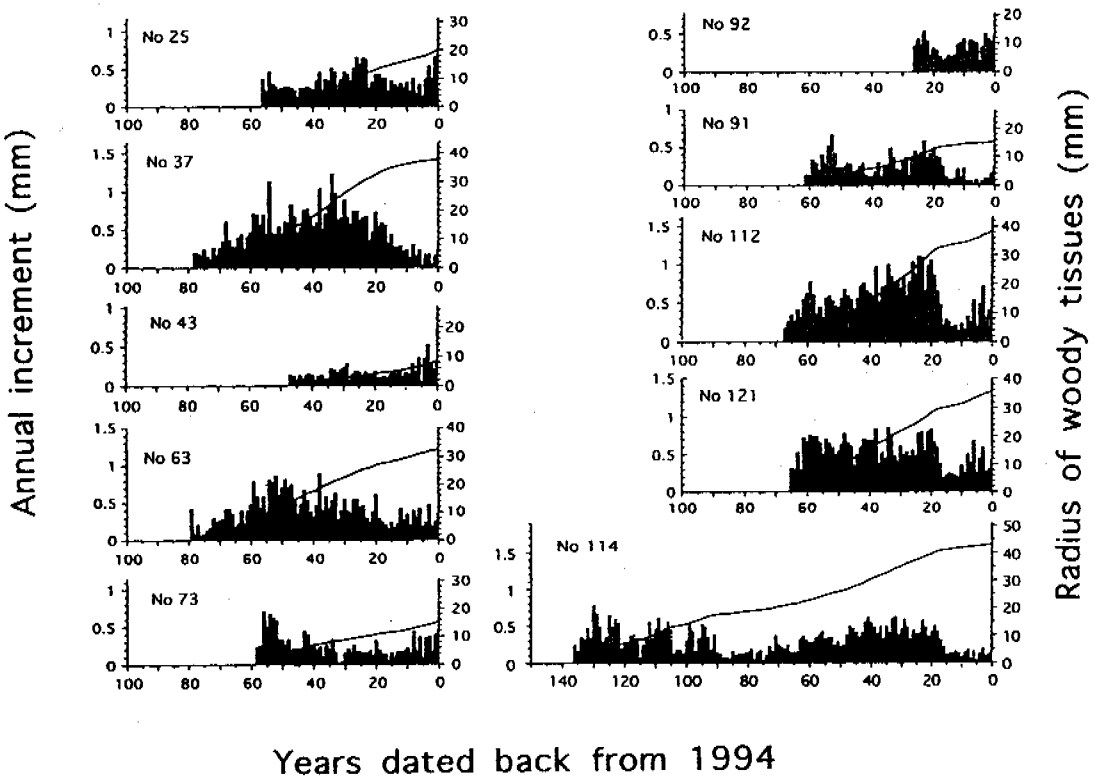

FIG. 1. Radial growth of individual sample trees in basal disks, collected at about 0.1 m high. Panels for each sample are arranged in each sampling point: Left, inside of the larch stand; Right, edge of the stand. Bars and a curve in each panel show annual increments in each year and a growth curve of mean radius of woody tissues, respectively.

mm yr^{-1}. Radial growth pattern was apparently synchronous among the sample trees. For example in 1989, 1985 and 1978, the growth was depressed in most of the sample trees. The pattern of the radial growth seems to reflect clearly climatic fluctuations. On the other hand the radial growth was apparently related to plant size. Sigmoid growth curves in larger trees indicate that their sizes are close to an upper limit.

There was a difference in the radial growth pattern between the sampling points. Annual increments were very little after 1978 in the samples from the stand edge point. This may be caused by human disturbances. There were many stumps being about 1 m high around the stand edge point. It is supposed that reindeer breeders had stayed here and cut larch trees during winter in the past. It is likely that such a disturbance changed micro-environment for the sample trees and depressed their growth.

Height growth.—Height growth was represented also by sigmoid-type curve, and depression of the growth at large size was more conspicuous than the radial growth (Fig. 2). Fig. 2 also shows that the growth of most sample trees was depressed temporarily when they were 1 to 2 m high. This suggests that apical parts of the plants are exposed more frequently to natural disturbances at that height.

Fig. 3 shows the relationship between the basal radius of trunk and tree height for each samples. Slope of the graph tends to decrease with growth of trees. This means that height growth is depressed more than radial growth in larger size. Conspicuous change in this relationship is found at 1 to 2 m and around 4 m in height. The slopes for sample trees from

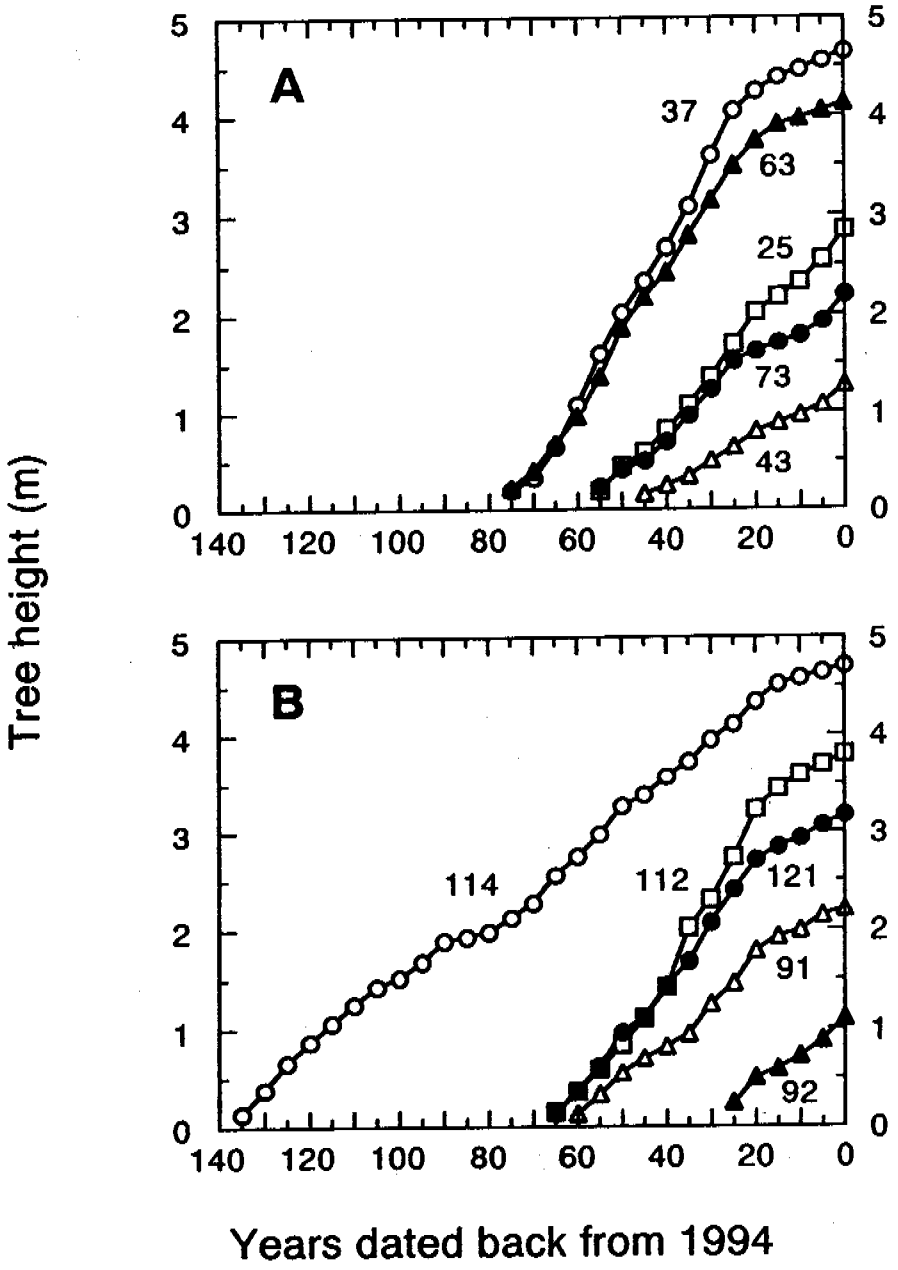

FIG. 2. Height growth curves of sample trees in each sampling point: A, inside of the larch stand; B, edge of the stand. Data are plotted at intervals of 5 years. Numerals in the figure show sample numbers.

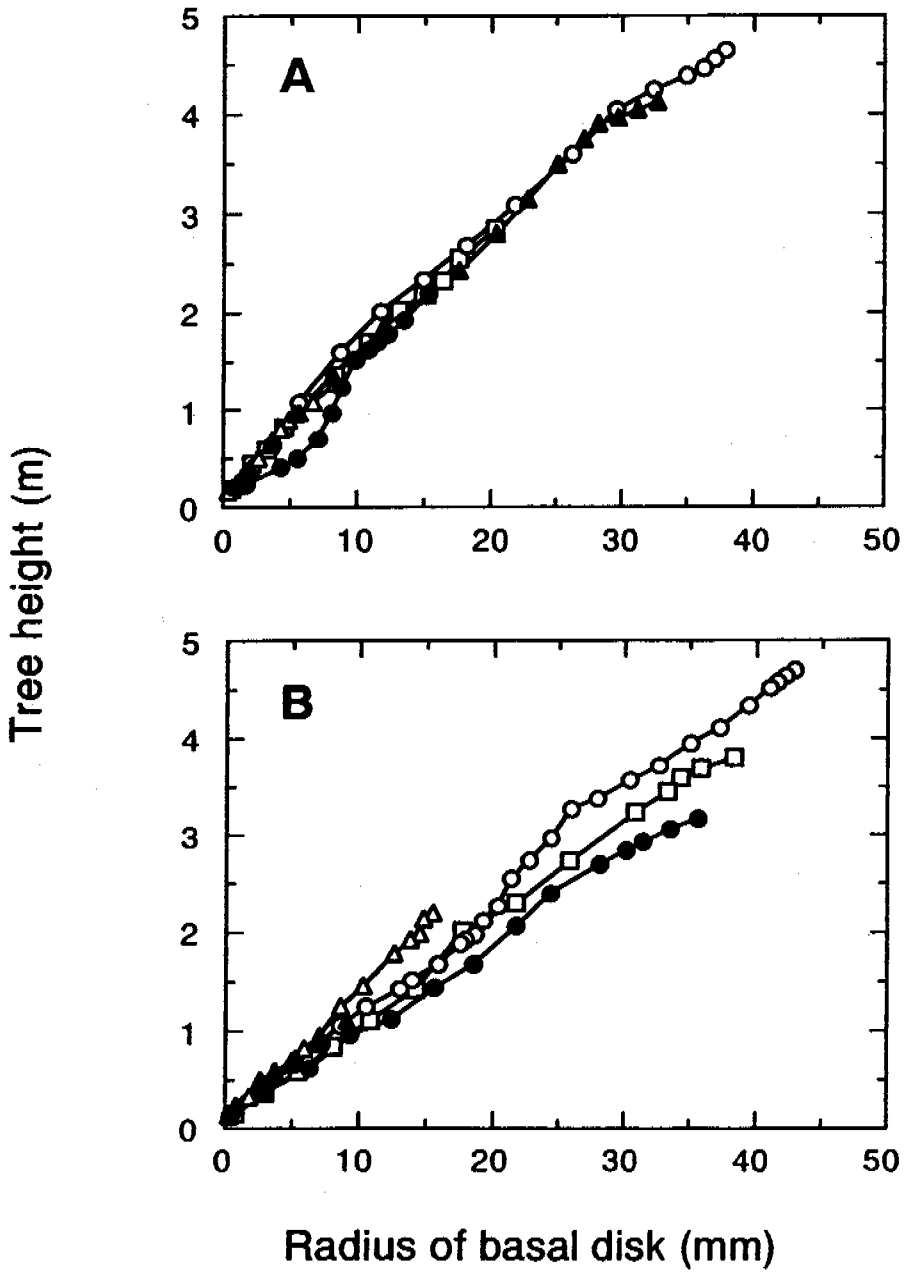

FIG. 3. Relationships between basal radius of woody tissues of a trunk and tree height in each sample tree. Sampling points are distinguished as Fig. 2. Data are plotted at intervals of 5 years.

the stand edge point were more gentle than those from the inside point. The condition for height growth will be more severe at the stand edge point.

Volume increment.—Annual volume increment, which represents annual wood production in a main trunk, increased rapidly during early decades and then became an approximately constant value in most sample trees (Fig. 4). Relationships between tree height and the

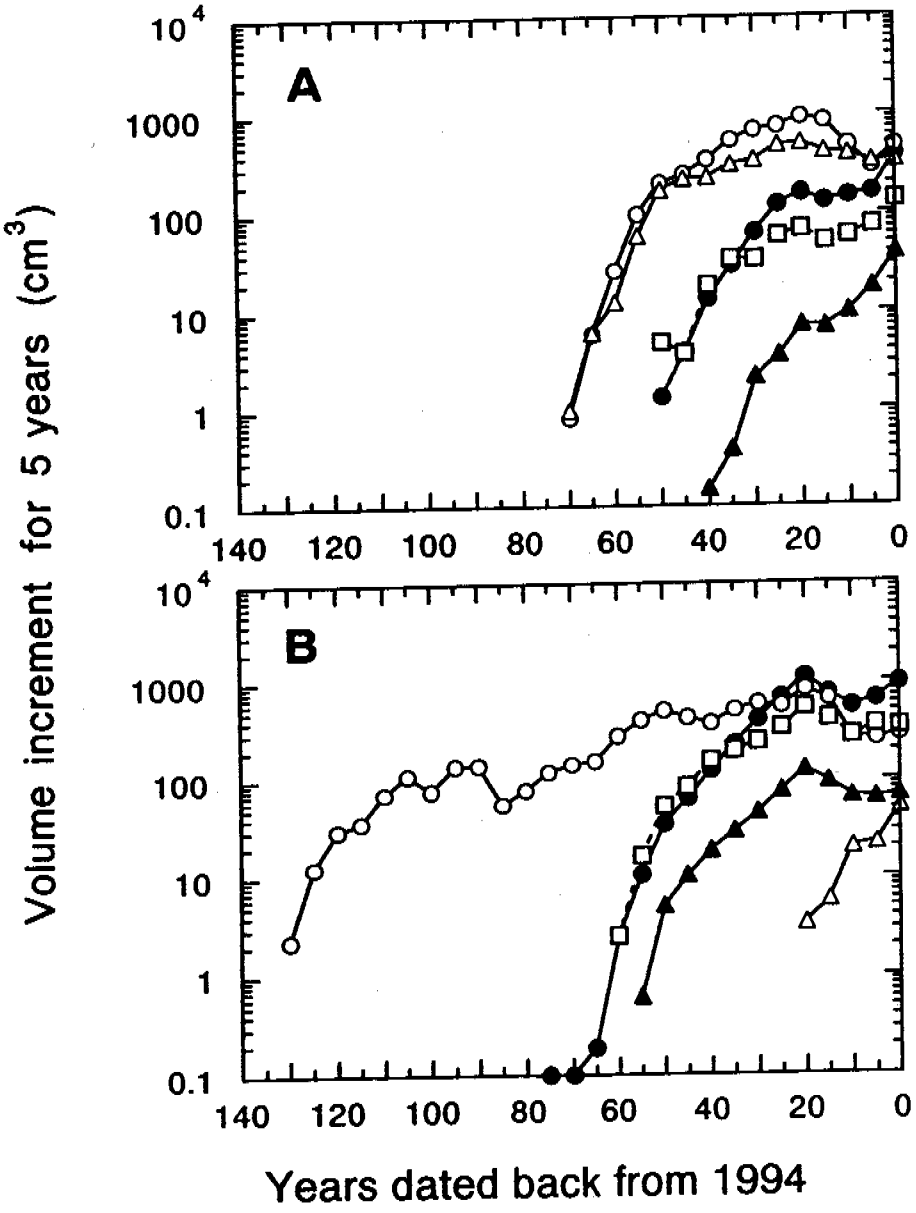

FIG. 4. Changes in wood volume increments in main trunk during life time for each sample tree. Accumulated values for 5 years are plotted. Sampling points are distinguished as in Fig. 2.

annual volume increment showed that the wood production increased little after the tree grew up to 2 m, and then decreased when it reached about 4 m (Fig. 5).

Tree form and the height of stumps indicated that snow depth was about 1 m or less in this open forest stand. The larch must be exposed to extremely low temperature and strong winds throughout long winter over the snow surface.

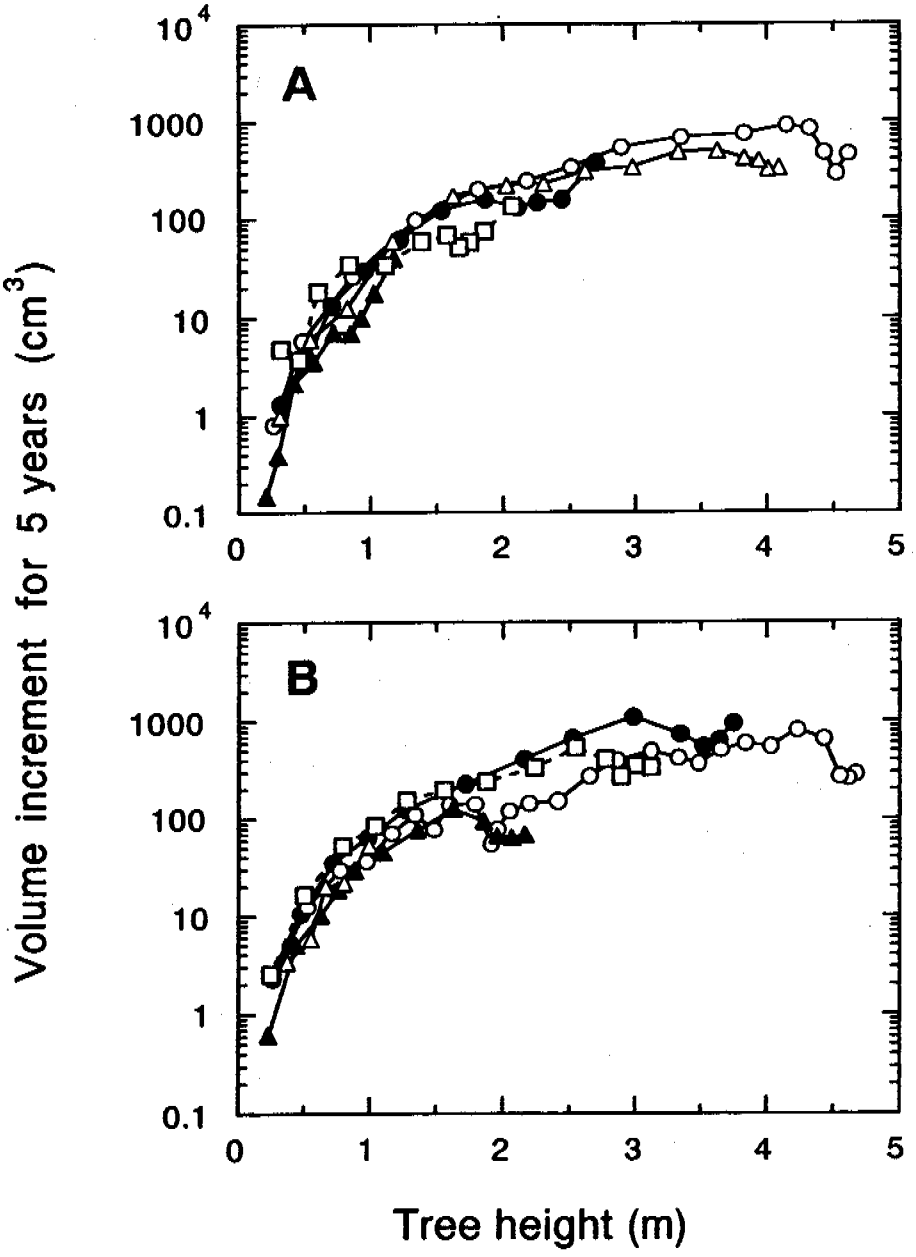

FIG. 5. Dependency of wood volume increments in main trunk on tree height. Accumulated values for 5 years are plotted. Sampling points are distinguished as in Fig. 2.

Synchronized cyclicity in growth shift events of northern circumpolar coniferous trees, with an analysis of the effect of anthropogenic tree cutting on tree growth at Kholuda Yurakh, Siberia

AKIRA OSAWA[1], DANIEL P. YEFREMOV[2], BORIS I. IVANOV[2], DAVID K. YAMAGUCHI[1], KUNIHIDE TAKAHASHI[1], and OWE MARTINSSON[3]

[1]*Forestry and Forest Products Research Institute, Hokkaido Research Center, 7 Hitsujigaoka, Toyohira, Sapporo 062 Japan; Tel: +81-11-851-4131; Fax: +81-11-851-4167*
[2]*Yakutian Institute of Biology, Russian Academy of Sciences, 41 Lenin Avenue, Yakutsk 677891, Russia*
[3]*Swedish University of Agricultural Sciences, S-90183 Umeå, Sweden*

Abstract. Examination of tree-ring data from coniferous trees of northern circumpolar regions revealed an approx. 40-year cycle of synchronized events of shifts in growth patterns. Stem core samples were obtained initially from five species and total of ~140 trees at six locations in nothern Asia, North America and Scandinavia. The wood samples were extracted with an increment borer and mounted on wooden strips for ring width measurement. We drew the u-w diagram for stem cross-sectional area growth of each tree, and estimated frequency of growth shift events for each locality for every ten years. Observation of the synchronized growth shifts at distant parts of northern circumpolar regions suggests that there may be cyclical changes of some environmental factors at common temporal and geographical scales. In addition, analysis of tree cutting history and growth patterns at Kholuda Yurakh suggested that tree growth is little affected by the anthropogenic tree cutting at a forest tundra in Siberia.

Introduction

A few-decade cycles of rapid-and-slow growth patterns in trees have been suggested for the conifers of western Russia (Kocharov 1990, Mazepa 1990) in relation to changes in solar activity. True causes are uncertain; however, such patterns should be examined closely for their potential effects on the analysis of tree rings with respect to the predicted rise in atmospheric CO_2 concentration and air temperature. The general trends of increasing temperature or tree growth must be separated from the inherent patterns of cyclicity, if any. This is particularly relevant for the circumpolar coniferous trees, because the effect of global warming is predicted to be most intense at the higher latitudes of northern hemisphere (Manabe and Stoufer 1980). The first author (Osawa 1992) reported a potential pattern of cyclicity in the growth shift events of coniferous trees in Canada, eastern Siberia, and Hokkaido in northern Japan. Here we present additional data supporting the previous claim, with possible exceptions. Potential mechanism of such cyclic patterns is also suggetsed.

Materials and methods

Stem cores were collected from coniferous trees growing in boreal forests of Canada, eastern Siberia, Scandinavia, and northern Japan. Black spruce (*Picea mariana*) cores were obtained at South Slave (61°N,128°W) along the south shore of Great Slave Lake in Northwest Territories, Canada; white spruce (*Picea glauca*) was sampled at Inuvik

(69°N,133°W) near the mouth of MacKenzie River, Northwest Territories, Canada; dahurian larch (*Larix gmelinii* or *L. cajanderi*) cores were collected at two locations in eastern Siberia, one at Spaskayapad (62°N,128°E), near Yakutsk, and the other at Kholuda Yurakh (72°N,125°E), west of Tiksi, Siberia; Scotch pine trees were sampled at Umeå, Sweden (64°N,20°E); aka-ezomatsu (*Picea glehnii*) cores were obtained at Hokkaido (43°N,142°E), Japan.

Two cores were collected from each stem with an increment borer, at waist height, and from opposite sides of a tree. The cores were brought to the laboratory, air dried, mounted on wooden strips, and sanded with succeedingly finer grains (up to #800) for preparation of the smooth surface. They were cross-dated with the list method (Yamaguchi 1991). The ring widths were then measured under a dissecting microscope to 0.01 mm accuracy. The ring patterns were analyzed with the aid of the $u-w$ diagram (Hozumi 1985) for estimating growth phases and their changes over time.

Ax-cut stumps and living trees with previous ax marks were present in the forest tundra at Kholuda Yurakh and its vicinity near the latitudinal tree line (Ishizuka et al. 1994). These are likely to have been caused by the reindeer herders of the Arctic coast who migrated southward during severe winters for shelter. We obtained disk samples of these trees, and estimated the times of anthropogenic cuttings utilizing ring-counting to the start of callus growth, and presence of traumatic resin canals (Swaine and Craighead 1924, Core et al. 1979, Yamaguchi 1993).

Results and discussion

A 30-40 year cycle of more frequent growth shift events are commonly observed at Hokkaido, South Slave, and Spaskayapad (Fig. 1). The cyclic patterns are also synchronized. For example, many trees changed growth patterns during 1920s, 1950s and 1980s in these regions separated by the Arctic Ocean or the Japan Sea. The cyclicity can be traced back to 1680s in *Picea glehnii* in Hokkaido. A similar cyclic pattern was found for *Pinus sylvestris* in Sweden (Fig. 1); however, the frequent growth shifts occurred ~10 years prior to those in Hokkaido, South Slave and Spaskayapad. On the other hand, the cyclicity was not clearly observed at Kholuda Yurakh and Inuvik. Difference of these two sites to the other localities is that trees at Kholuda Yurakh and Inuvik were growing on drier sites compared to the other sampling locations. The stumps at Kholuda Yurakh were estimated to have been cut with axes in 1656, 1696, 1735, and 1906. Average interval of the cuttings was ~80 years. There is no clear release or suppression of ring-width patterns following the harvests on trees that have been growing without the ax marks (Osawa et al. 1995). Therefore, we tentatively assume that the anthropogenic tree cutting had a minimum effect on the growth patterns of the surviving trees there.

Causes of the synchronized cyclicity in growth shifts of the trees are not clear; however, there is suggestive evidence that cyclic changes in regional hydrology may be related to the observed pattern. The water level of alas ecosystems, circular dipressions of a few hundred meters to several dozen kilometers in diameter that developed by melting of the permafrost, is believed to have been fluctuating with 30-40 year cycles in the Yakutsk region of Siberia (N.G. Solomonov, *personal communication*). The level was high ~1917 at the time of the Russian Revolution, and again ~1950. On the other hand, the water was low in mid 1930s and in late 1960s. The times of more frequent growth shifts corresponded with those of low water level. This implies a possibility that the regional hydrology has been fluctuating with 30-40 year intervals at large areas of the northern circumpolar zone, and this fluctuation is causing changes in the growth patterns of the conifer trees. Further examination of regional

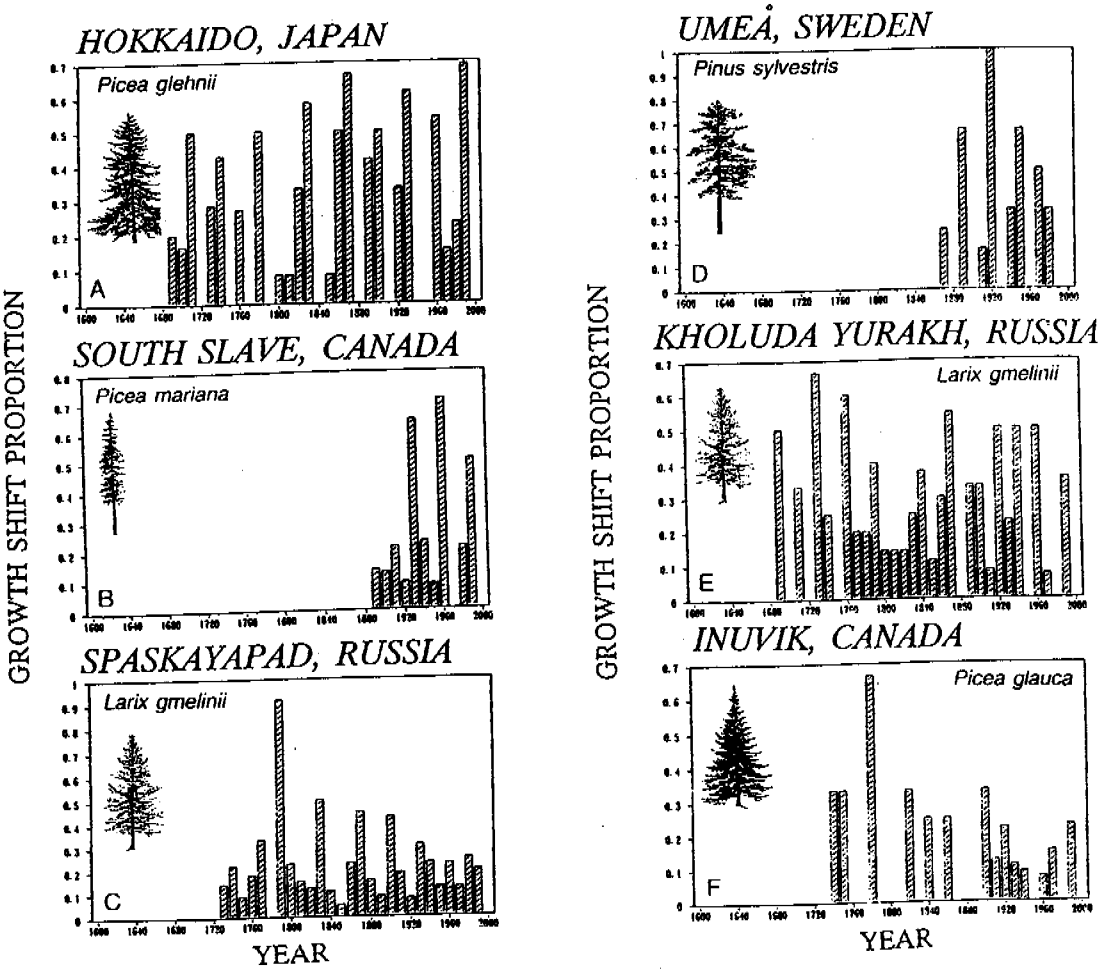

FIG. 1. Proportions of growth shift events for individual trees within tree populations over time. Five conifer species were sampled at six locations in the northern circumpolar regions. The growth shift proportion is shown for each decade, which is defined as the ratio of the number of trees in a population that changed growth patterns during a given ten-year period.

hydrology and the history of water level fluctuation is desired. Tree growth data from additional locations will also be useful for estimating generality of the synchronized cyclicity in growth patterns.

Acknowledgments

This project was supported in part by the Japan Environment Agency Grant for Integrated Global Environment Research. Similar content was delivered as an invited lecture at "the International Arctic Science Symposium" sponsored by the Science and Technology Agency of Japan, held on 12–13 January 1995 at Tsukuba Center for Institutes, Tsukuba, Japan.

Literature cited

Core, H.A., W.A. Côté, and A.C. Day. 1979. Wood structure and identification. 2nd ed.

Syracuse University Press, Syracuse.
Hozumi, K. 1985. Phase diagramatic approach to the analysis of growth curve using the $u-w$ diagram. Basic concepts. Botanical Magazine, Tokyo 98:239–250.
Ishizuka, M., S. Uemura, T. Tsujii, and K.A. Volotovsky. 1994. Vegetation of the boreal forest–tundra transition zone in the basin of Lena River. I. Forest stand structure. *In* G. Inoue ed. Proceedings of the second symposium on the joint Siberian permafrost studies between Japan and Russia in 1993. National Institute for Environmental Studies, Tsukuba, Japan.
Kocharov, G.E. 1990. Tree rings: A unique source of information on processes on the Earth and in Space. *In* E.R. Cook and L.A. Kairiukstis (eds.) Methods of Dendrochronology. Kluwer Academic Publishers, Dordrecht.
Manabe, S., and R.J. Stouffer. 1980. Sensitivity of global climate model to an increase of CO_2 concentration in the atmosphere. Journal of Geophysical Research 85:5529–5554.
Mazepa, V. 1990. Spectral approach and narrow band filtering for assessment of cyclic components and ecological prognoses. *In* E.R. Cook and L.A. Kairiukstis (eds.) Methods of Dendrochronology, Kluwer Academic Publishers, Dordrecht.
Osawa, A. 1992. A thirty–year cycle of growth shifts in northern circulpolar conifers. *In* Abstracts, Annual meeting of the Hokkaido Section of Ecological Society of Japan. December 19, 1992. Hokkaido University, Sapporo, Japan (*in Japanese*).
Osawa, A., D. Efremov, B.I. Ivanov, and D. K. Yamaguchi. 1995. Anthropogenic tree cutting and development of forest–tundra boundary at Kholuda Yurakh, Siberia: preliminary results. *In* Proceedings of "International Workshop on Asian and Pacific Dendrochronology" held on 3–6 March 1995 at Forestry and Forest Products Research Institute, Tsukuba, Japan (*in press*).
Swaine, J.M., and F.C. Craighead. 1924. A general account of the outbreaks, injury and associated insects. PP.3–27. *In* Studies on the spruce budworm (*Cocoecia fumiferana* Clem.). Canada, Department of Agriculture, Bulletin (new series) No. 37.
Yamaguchi, D.K. 1991. A simple method for cross–dating increment cores from living trees. Canadian Journal of Forest Research 21:414–416.
Yamaguchi, D.K. 1993. Tree–ring evidence for 1842–1843 eruptive activity at the Goat Rocks dome, Mount St. Helens, Washington. Bulletin of Volcanology 55:264–272.

Morphological variability of *Pyrola asarifolia* and *P. grandiflora* in Yakutia, eastern Siberia

HIDEKI TAKAHASHI

Botanic Garden, Faculty of Agriculture, Hokkaido University, N3W8 Sapporo 060 Japan
Tel: +81-11-221-0066; Fax: +81-11-221-0664

Introduction

The lowest state of floristic knowledge in Yakutia is noticed in the Aldan Mountains, the Verkhoyansk Mountains and the Cherskiy Mountains (Frodin, 1984). Regions botanically surveyed in the 1992, 1993 and 1994 summers in Yakutia were restricted in the lowlands except for the southern margin of the Verkhoyansk Mountains in the 1994 summer (Fig. 1). Further cooperative floristic study is needed especially in the hard-to-approach locations of the three mountains. Geographical distribution patterns are not determined for the Yakutian plant species having a taxonomic problem and such species are frequently found in the Aldan and Yana-Indigirka regions including the above-mentioned three mountains (see the case of

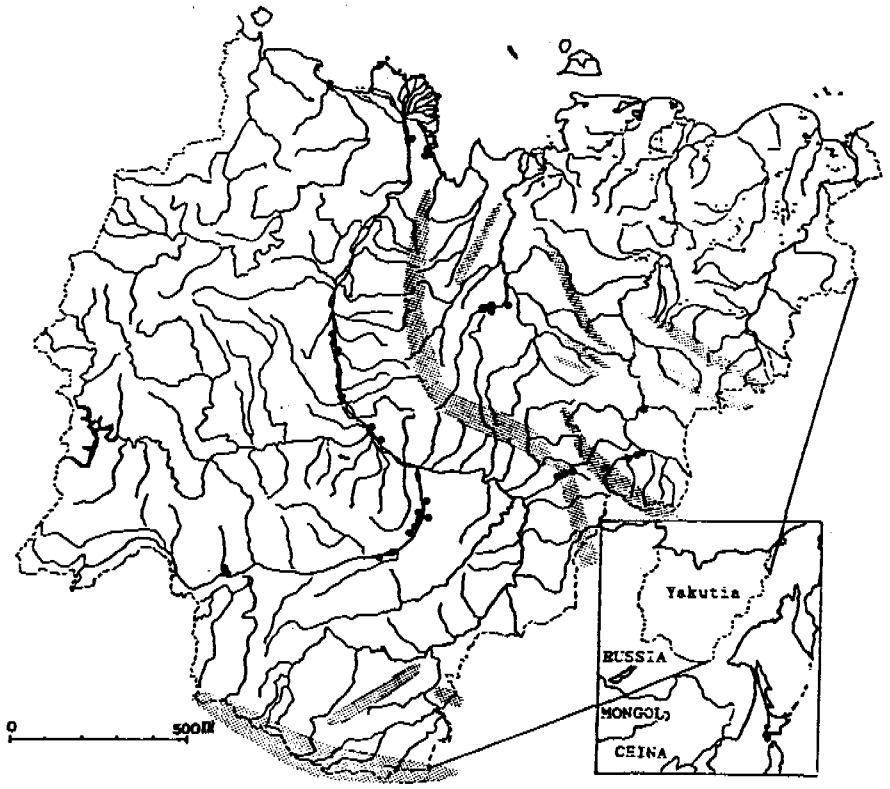

FIG. 1. Map showing the collection sites in Yakutia during the last three years (1992-1994).

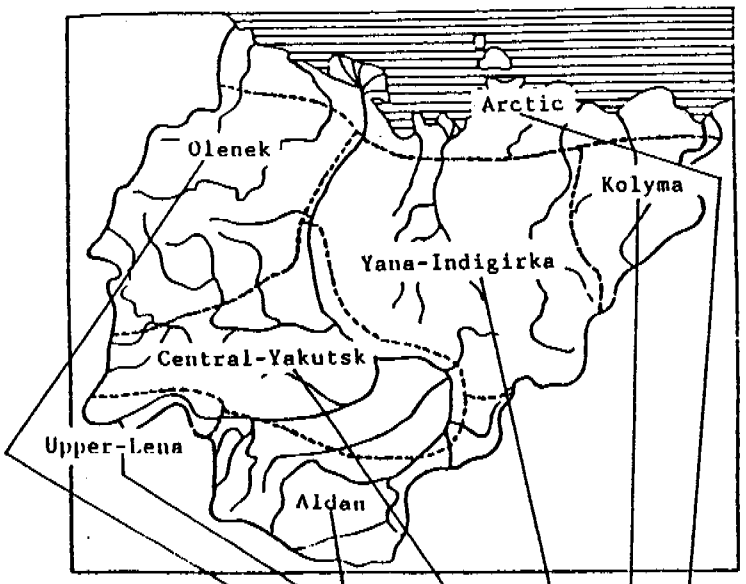

			[75] Al	[52] Ol	[46] Le	[60] Ya	[72] YI	[33] Ko	[41] Ar
Eur-As-Am	35	[39]	32	44	37	35	31	48	49
As	23	[26]	29	21	26	30	26	18	10
Eur-As	11	[12]	9	10	20	17	10	3	5
As-Am	9	[10]	5	6	4	5	11	18	17
Indet.	22	[25]	25	19	13	13	22	13	19
	100	[112]	100	100	100	100	100	100	100

FIG. 2. Proportion of geographical distribution patterns in Yakutian *Carex*. Figures in brackets indicate species numbers. Abbreviations: Eur, Europe; As, Asia; Am, America; Indet., Indeterminate.

the dominant genus *Carex* in Fig. 2). Therefore from the plant taxonomical and phytogeographical points of view, the most attractive place in Yakutia is the Aldan and Yana-Indigirka regions containing the Aldan, Verkhoyansk and Cherskiy Mountains.

Quantitative and serious comparison of the Yakutian plant species with those of the adjacent regions; northern China, the Far East, Korea and Japan is hoped. Based on this comparative study the exact taxonomic evaluation and the correct selection of the scientific names for the Yakutian plant species are possible.

General characteristics of the Yakutian flora were summarized (Takahashi, 1993, 1994a), and the taxonomic and phytogeographic notes on the Yakutian *Batrachium* and the other aquatic plants were reported (Takahashi, 1994b; Takahashi et al., 1994).

In this study the present author attempted to analyze the inter- and intra-specific quantitative morphological variability of *Pyrola asarifolia* and *P. grandiflora* in Yakutia. There are few distinctive characteristics available for the delimitation of species within species complexes in *Pyrola* (Haber, 1983). This is the case in *Pyrola asarifolia* and *P. grandiflora* in eastern Siberia.

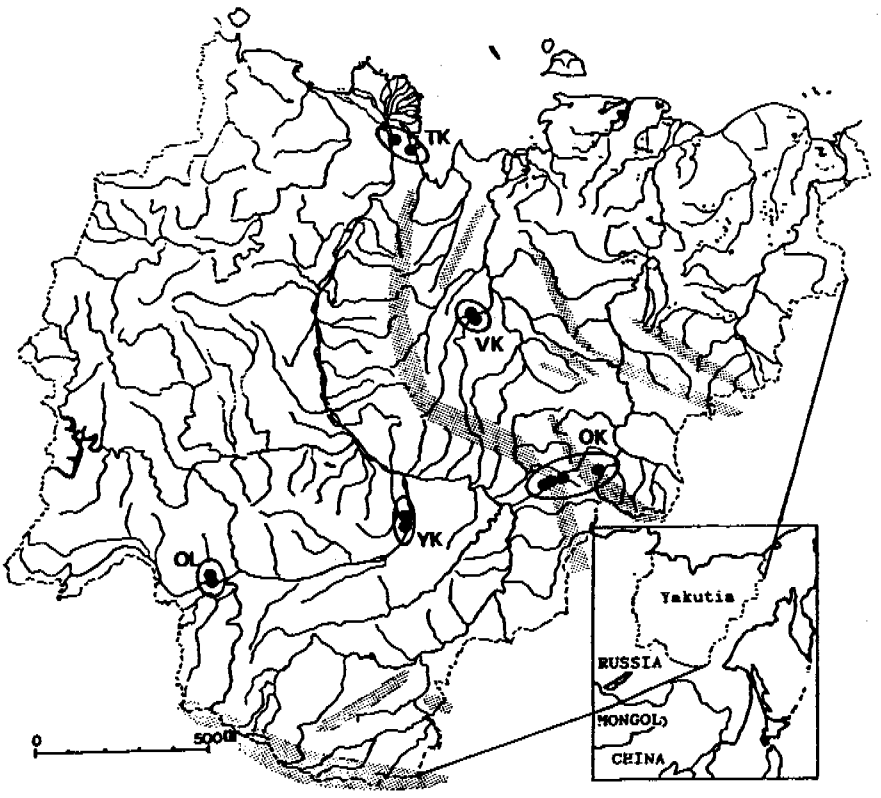

FIG. 3. Map showing the collection sites of *Pyrola asarifolia* and *P. grandiflora* in Yakutia.

Study sites and methods

Specimens of *Pyrola asarifolia* and *P. grandiflora* were collected from the five regions, twelve populations (Fig. 3). Measurements were made of 12 characters on a total of 338 individual plants. In this report the comparison of the mean value of each population was made. Multivariate analyses based on the values of individual plants will be conducted in the future.

Results and discussion

A total morphological characteristic in each population was shown in polygonal graphs of Fig. 4. Based on subtle differences in the spectrum of variation in such features as the size and form of leaf, bract, pedicel, sepal, anther and style, the southern eight populations of Oimyakon to Khandyga (OK), Yakutsk (YK), Olekminsk (OL) were determined as *Pyrola asarifolia*, and the northern four populations of Tiksi (TK) and Verkhoyansk (VK) were as *P. grandiflora*. The principal component analysis using the mean values of each population was conducted for estimating the overall similarity between the Yakutian populations of *Pyrola asarifolia* and *P. grandiflora* (Table 1 and Fig. 5). In conclusion, the low morphological differentiation between the two *Pyrola* species may reflect the lack of strong or long genetic isolation between them in eastern Siberia.

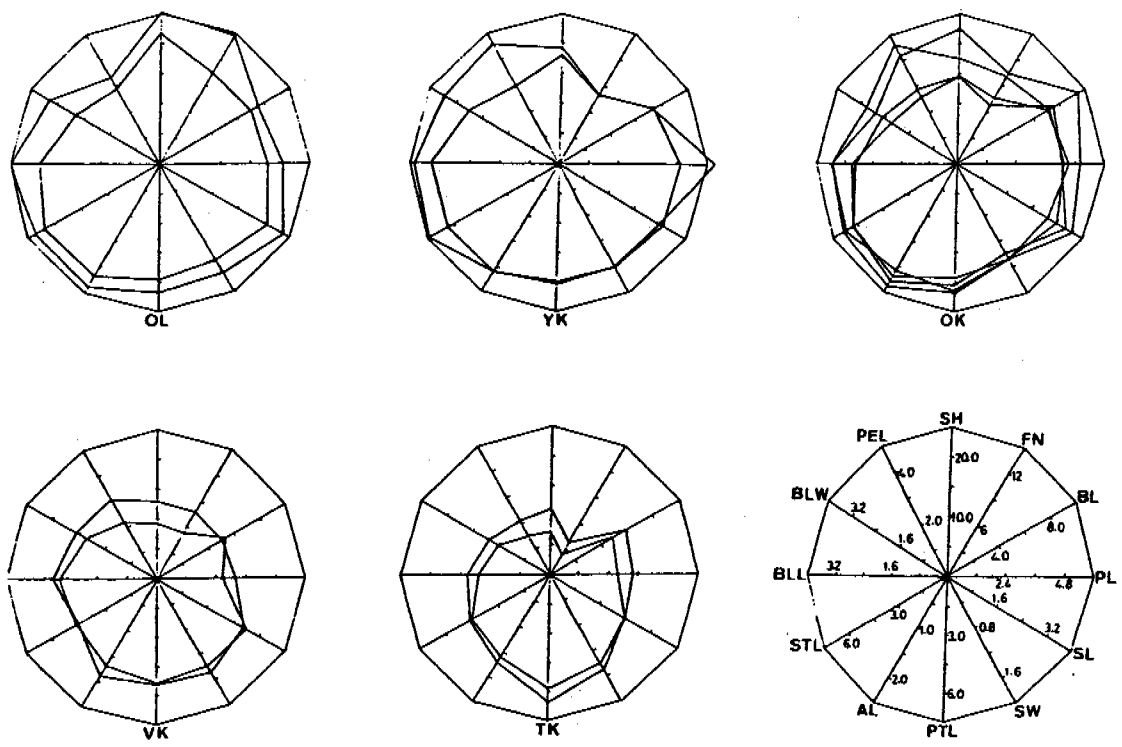

FIG. 4. Polygraphs showing variations in 12 morphological characters of twelve populations and five regions of *Pyrola asarifolia* and *P. grandiflora* in Yakutia. Abbreviations: SH, scape hight (cm); FN, flower numbers; BL, bract length (mm); PL, pedicel length (mm); SL, sepal length (mm); SW, sepal width (mm); PTL, petal length (mm); AL, anther length (mm); STL, style length (mm); BLL, leaf blade length (cm); BLW, leaf blade width (cm); PEL, petiole length (cm).

References

Frodin, D. G. 1984. Guide to standard floras of the world. Cambridge University Press, Cambridge.

Haber, E. 1983. Morphological variability and flavonol chemistry of the *Pyrola asarifolia* complex (Ericaceae) in North America. Syst. Bot. 8:277–298.

Takahashi, H. 1993. An analysis of spermatophytes flora of Sakha SSR (Yakutskaya), eastern Siberia. In M. Fukuda ed., Proceedings of first symposium on joint Siberian permafrost studies between Japan and Russia in 1992, pp. 82–86, Sapporo.

Takahashi, H. 1994a. Phytogeography of vascular plants in Yakutia (Sakha). Proc. Jap. Soc. Pl. Tax. 10(1):21–33. (in Japanese with English summary).

Takahashi, H. 1994b. Habitat and morphological features of *Ranunculus* subgenus *Batrachium* in central southern Yakutia. In G. Inoue ed., Proceedings of the second symposium on the joint Siberian permafrost studies between Japan and Russia in 1993, pp. 122–126, Tsukuba.

Takahashi, H., T. Sato, N. G. Solomonov and B. I. Ivanov. 1994. Phytogeographic notes on some aquatic plants in Yakutia, eastern Siberia. Acta Phytotax. Geobot. (in press).

TABLE 1. Results of principal component analysis of 12 characters for 12 populations of *Pyrola asarifolia* and *P. grandiflora*

Principal component No.	1	2	3
Cumulative variance (%)	74.0	83.1	89.2
Characters	Eigenvectors		
Scape height (SH)	0.32	0.02	-0.04
Number of flowers (FN)	0.30	-0.12	-0.17
Bract length (BL)	0.29	0.42	-0.08
Pedicel length (PL)	0.30	-0.06	0.15
Sepal length (SL)	0.30	0.19	-0.35
Sepal width (SW)	0.24	-0.36	0.48
Petal length (PTL)	0.17	0.59	0.67
Anther length (AL)	0.30	0.22	-0.34
Style length (STL)	0.32	0.06	-0.06
Blade length (BLL)	0.33	-0.18	-0.06
Blade width (BLW)	0.30	-0.42	0.09
Petiole length (PTL)	0.27	-0.17	0.09

FIG. 5. Principal component analysis of twelve morphological characters of twelve populations and five regions of *Pyrola asarifolia* and *P. grandiflora* in Yakutia.

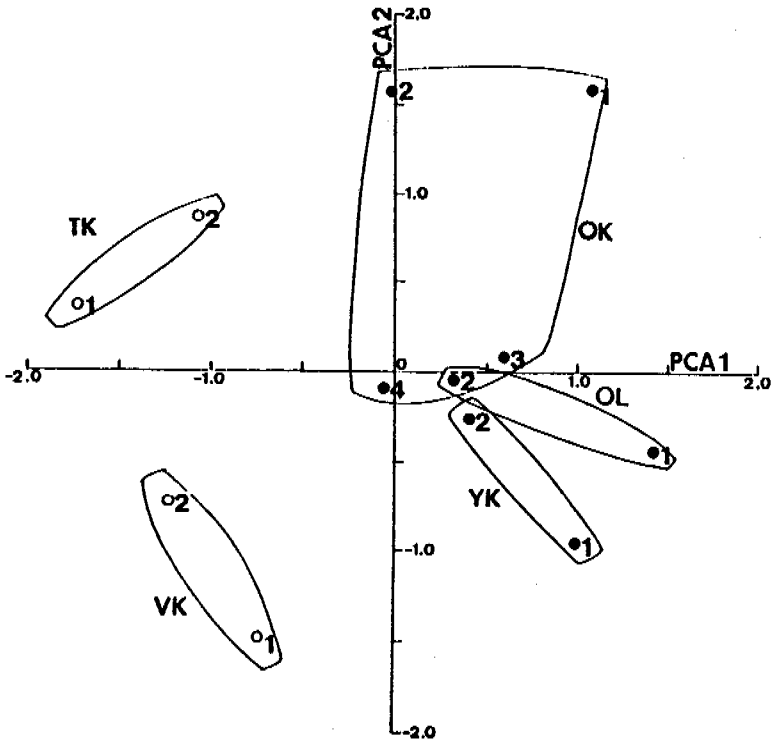

Biodiversity and vegetation patterns of arctic plants with scaling: a consideration from permafrost contributions in Siberia

TOSHIYUKI SATO and MASAMI FUKUDA

The Institute of Low Temperature Science, Hokkaido University, Sapporo 060 Japan
Tel: +81-11-706-5495; Fax: +81-11-706-7142

Abstract. Vegetation patterns in eastern Siberia are considered from a view point of permafrost contributions to vegetation cover in Siberia where has less precipitation and severe coldness. Many small herbs coexist in a small scale but a few trees disperse in a large scale. Tundra regions around Tiksi have higher phytodiversity (ca. 30 spp.) than that of taiga and cool temperate regions (ca. 15–20 spp.) in the small scales (1–8 m^2); however, a higher total number of species is recorded in temperate regions (50–70 spp.) than that of tundra and taiga regions (ca. 40 spp. in a scale of 1 ha). Floristic heterogeneity in tundra might be cased by the moderate

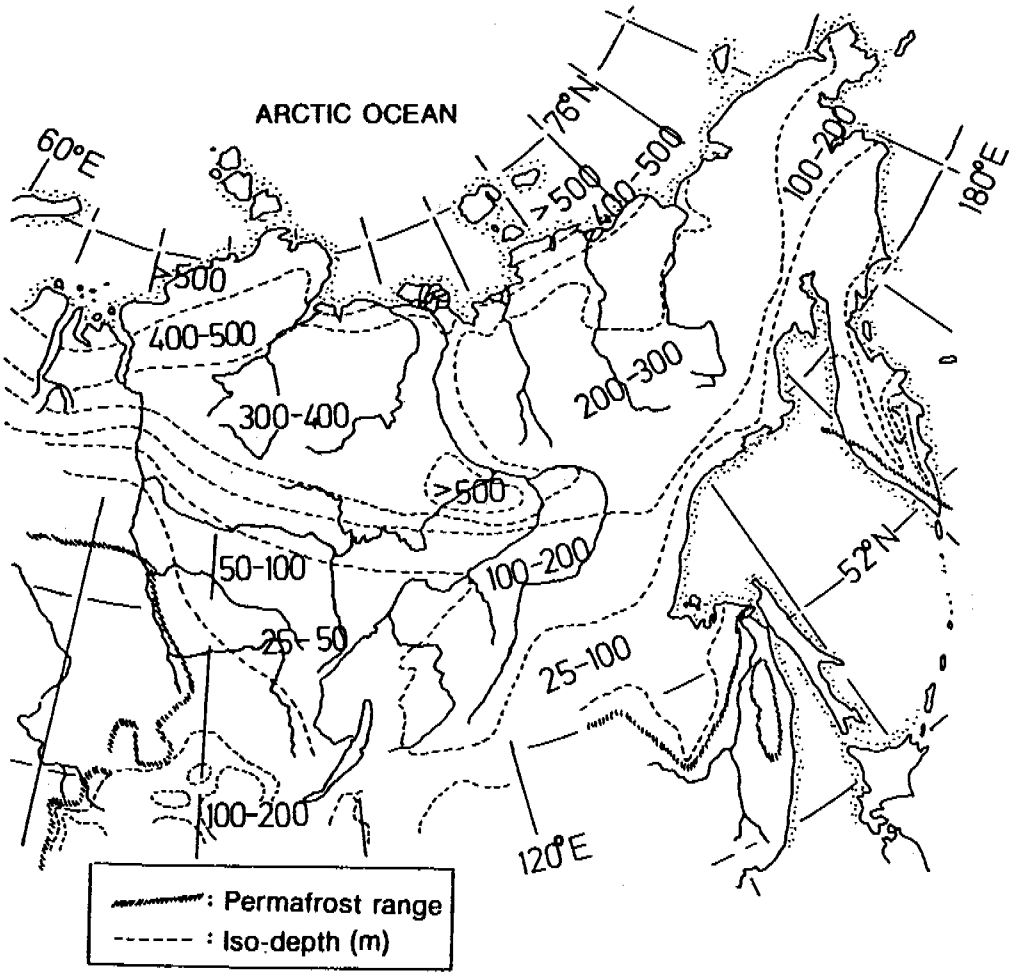

FIG. 1. Brief distribution map of iso-depth of permafrost in eastern Siberia (redrawn after Velichiko, 1985).

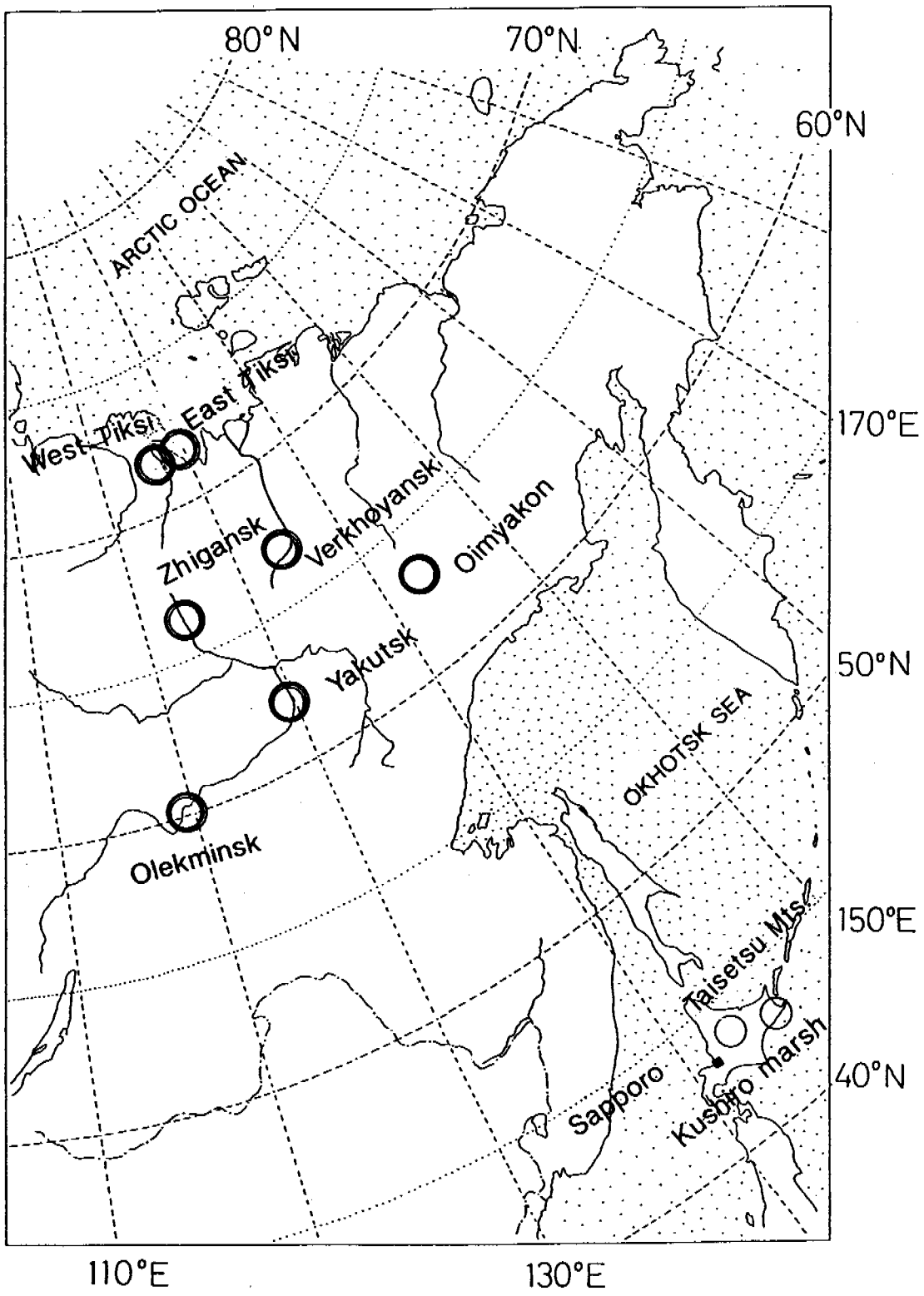

FIG. 2. Survey localities in eastern Siberia during 1992–1994 summers. Locations correspond to Table 1 represented by main vegetation types and genera with number of species.

disturbance of seasonal freeze–thaw cycles in micro-scales (0.5–5 m) of sorting patterns. Physiognomical observations showed some micro vegetation changes associated with polygones in tundra (5–500 m), change from *Larix* forest to steppe at hill slopes (500–50000 m) in transition regions. Another vegetation change from forest to alas was found in taiga regions around Yakutsk (1–10 km). Total annual precipitation in tundra and taiga regions have only 200–250 mm which is almost the same as that of desert regions in central Asia. Permafrost and seasonal melting in Siberia must contribute to the presence of vegetation cover by the seasonal ground melting and water supply (spring flooding) by river systems that drain toward the Arctic Ocean.

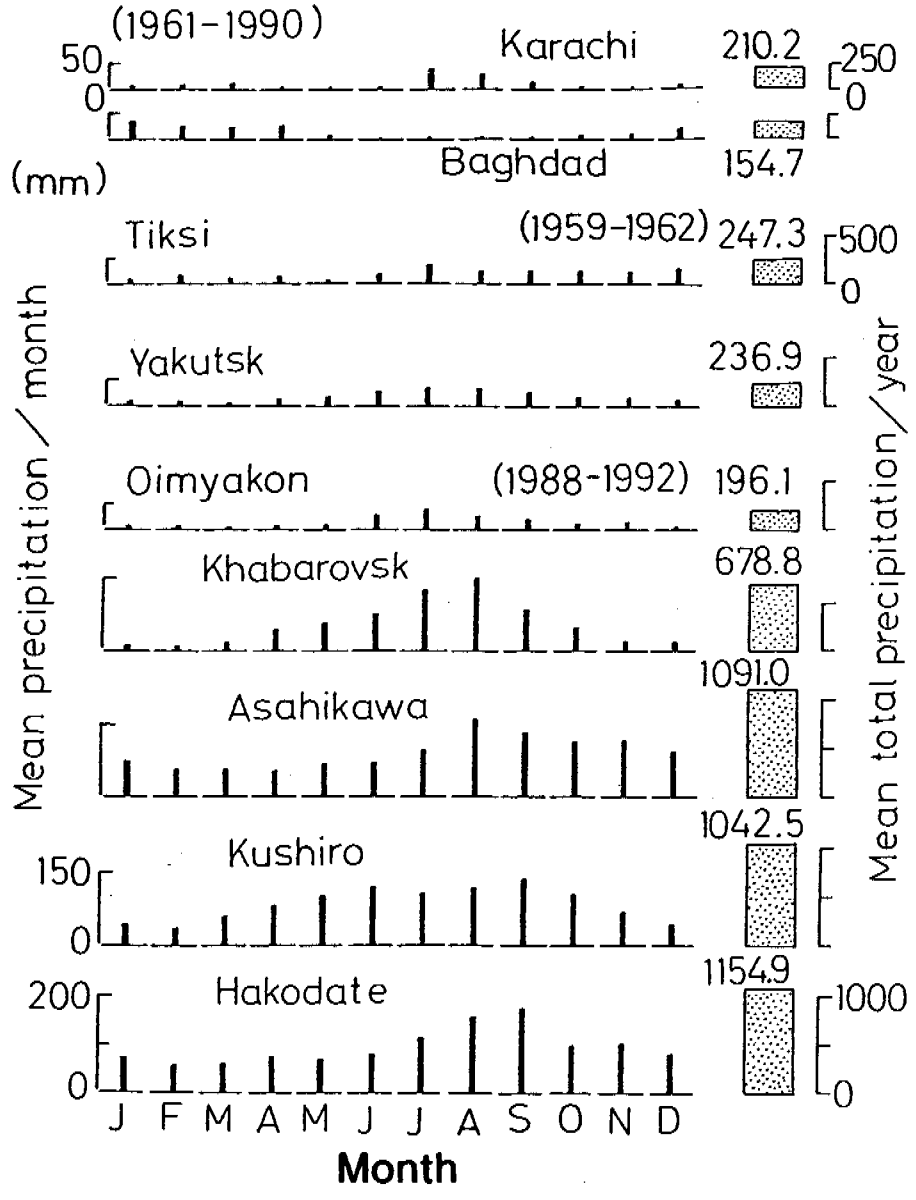

FIG. 3. Amount of monthly and annual precipitations in several locations in Siberia, Central Asia and northernmost Japan.

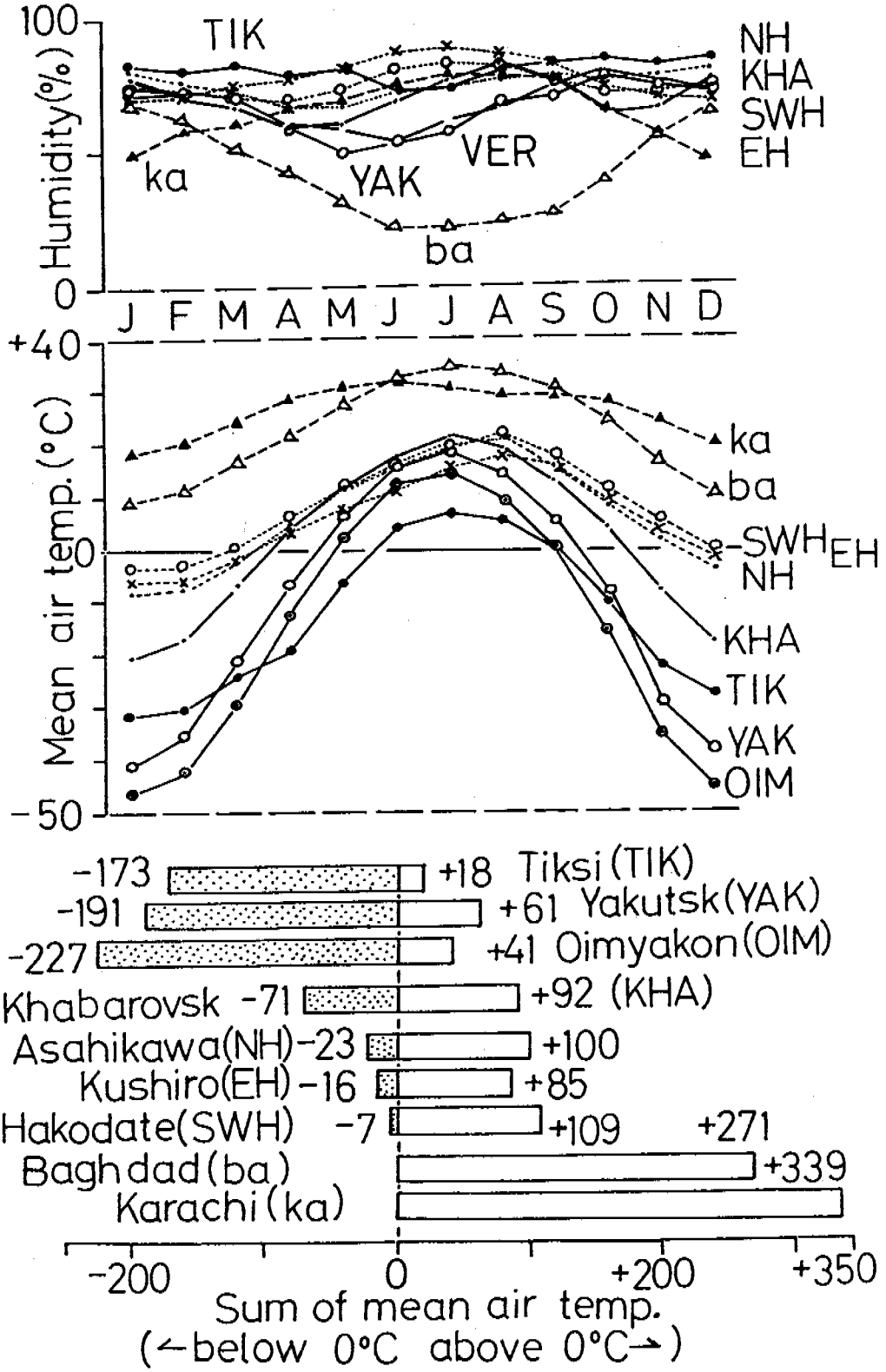

FIG. 4. Some meteorological data of eastern Siberia, central Asia and northernmost Japan. Monthly mean humidity (top), monthly mean air temperature (center) and sum of below- and above-freezing monthly mean air temperatures (bottom) are shown.

TABLE 1. Frequency of main genera per research site with respect to vegetation zone in Siberia. Numbers show frequency of the genus among sites. Numbers in the brackets show range in number of species per genus per site. These genera and species are found at least in each vegetation zone; however, not all genera and species were identified. Family of Gramineae consists of some unknown genera. Genera are ordered from the higher frequency.

<Tundra: 12 sites in East Tiksi>		
Gramineae 11(1-6),	*Luzula* 11(1-3),	*Polygonum* 11(1-2),
Salix 10(1-4),	*Saxifraga* 10(1-5),	*Carex* 8(1-9),
Pedicularis 8(1-3),	*Dryas* 8(1),	*Minuartia* 7(1-3),
Draba 7(1-3),	*Cassiope* 7(1),	*Artemisia* 6(1-2),
Hierochloe 6(1-2),	*Lloydia* 6(1),	*Festuca* 6(1),
Rhodiola 5(1),	*Potentilla* 5(1-2),	*Lagotis* 5(1),
Aster 5(1),	*Brassica* 5(1),	*Stellaria* 4(1-2),
Juncus 4(1-2),	*Erigeron* 4(1),	*Vaccinium* 4(1-2),
Diapensia 4(1),	*Poa* 3(1-2),	*Anemone* 3(1),
Cerastium 3(1),	*Eriophorum* 3(1),	*Arabis* 3(1),
Novosieversia 3(1)		
<Transition from taiga to tundra: 5 sites in West Tiksi>		
Polygonum 5(1-3),	*Salix* 5(1-2),	Gramineae 5(2-7),
Pedicularis 5(1-2),	*Luzula* 4(1-2),	*Dryas* 4(1),
Equisetum 4(1-2),	*Rhododendron* 4(1),	*Larix* 4(1),
Cassiope 3(1),	*Arctous* 3(1),	*Carex* 2(1-3)
Alnus 3(1)	*Vaccinium* 2(1-2),	*Saxifraga* 2(1),
Lagotis 2(1),	*Rubus* 2(1)	
<Transition from taiga to alpine tundra: 5 sites in Oimyakon>		
Betula 4(1-2),	*Polygonum* 3(1),	*Vaccinium* 3(1-2),
Carex 3(2-3),	*Salix* 3(1-3),	Gramineae 2(2-6),
Ledum 2(1),	*Eriophorum* 2(1),	*Aconitum* 2(1),
Cerastium 2(1),	*Brassica* 2(1),	*Rubus* 2(1),
Viola 2(1),	*Taraxacum* 2(1),	*Stellaria* 2(1),
Potentilla 2(1),	*Galium* 2(1)	
<Mosaic steppe in taiga: 13 sites in Verkhoyansk>		
Graminea 13(2-6),	*Potentilla* 11(1-3),	*Pulsatilla* 9(1),
Stellaria 7(1),	*Galium* 6(1-2),	*Veronica* 5(1),
Carex 4(1-3),	*Poa* 4(1-2),	*Aster* 4(1),
Brassica 4(1),	*Achillea* 4(1),	*Salix* 3(1-3),
Ranunclus 3(1-3),	*Selaginella* 3(1),	*Thalictrum* 3(1),
Euphorbia 3(1)		
<Taiga: 19 sites in Zhigansk, Yakutsk and Olekminsk>		
Gramineae 18(1-5),	*Rosa* 9(1),	*Artemisia* 8(1-2),
Equisetum 8(1),	*Carex* 8(1),	*Vaccinium* 8(1-2),
Salix 6(1),	*Linaria* 5(1),	*Vicia* 5(1-2),
Larix 5(1),	*Astragalus* 5(1),	*Potentilla* 5(1-3),
Sanguisorba 5(1),	*Achillea* 5(1-2),	*Galium* 5(1-3),
Thalictrum 5(1),	*Aster* 4(1-2),	*Plantago* 4(1-2)
Geranium 4(1-2),	*Poa* 4(1),	*Alnus* 4(1),
Epilobium 4(1),	*Linnaeus* 4(1),	*Viola* 4(1),
Scorzonera 4(1)		

TABLE 2. Possible factors associated with vegetation patterns with scaling in eastern Siberia and temperate and tropics. A star (*) indicates a high permafrost contribution to vegetation patterns.

Vegetation types (scales, m)	Habitat heterogeneity		Possible factors	Phyto-diversity
Tundra				
(0.05-5)	Stone size & soil	*	River and Ocean	+++
(5-500)	Sortted pattern & polygon	*	Seasonal melting	+
(500-50000)	Hill, marsh and seashow		Permafrost	-
(50000-)	River system		Permafrost depth	---

(TABLE 2, CONTINUED)

Transition				
(0.05-5)	Rock size & stream		Soil stability	+
(5-500)	Taiga and steppe	*	Permafrost depth	++
(500-50000)	Alpine tundra & taiga	*	Seasonal flooding	+
(50000-)	Mossaic		Topography	--
Taiga				
(0.05-5)	Forest floor & open		Light & Soil	-
(5-500)	Forest type & Alace		Flooding & Melting	+
(500-50000)	Fire, Steppe	*	Seasonal melting	++
(50000-)	Dry & human activity	*	Melting & Salt	+
Temperate forest				
(0.05-5)	Litter & soil		Light competition	+
(5-500)	Seasonal		Hierarchy	++
(500-50000)	River		Humidity	+++
(50000-)	Mountain		River system	+
Tropical forest				
(0.05-5)	Litter cover		Herbivory	-
(5-500)	Tree size		Light competition	+
(500-50000)	Hill & valley		Precipitation	+++
(50000-)	River system		Solar energy	+++

Star (*) indicatea a high permafrost contribution to vegetation patterns.

Flora and life form similarities among localities in northeastern Siberia, with respect to adaptive radiation and convergence for coexistence

TOSHIYUKI SATO

The Institute of Low Temperature Science, Hokkaido University, Sapporo 060 Japan
Tel: +81-11-706-5495; Fax: +81-11-706-7142

Abstract. Vegetation and floristic characteristics represented by proportions of number of species among different life (growth) forms and species composition as a function of the number of species within a genus were surveyed in some locations in eastern Siberia. These proportions were compared among tundra and taiga in Siberia and temperate forest in the northernmost Japan. Mean number of species was higher in the cool temperate (north Hokkaido) and tundra (near Tiksi) as 45–50 spp./ca. 1ha than those of taiga and transition sites as 35–40 spp. The highest proportion of herbs (>90 %) was found in tundra near Tiksi and about 70 % of the herbs was found in taiga, transition and temperate forests. The proportion of number of species with more than two species per genus was gradually

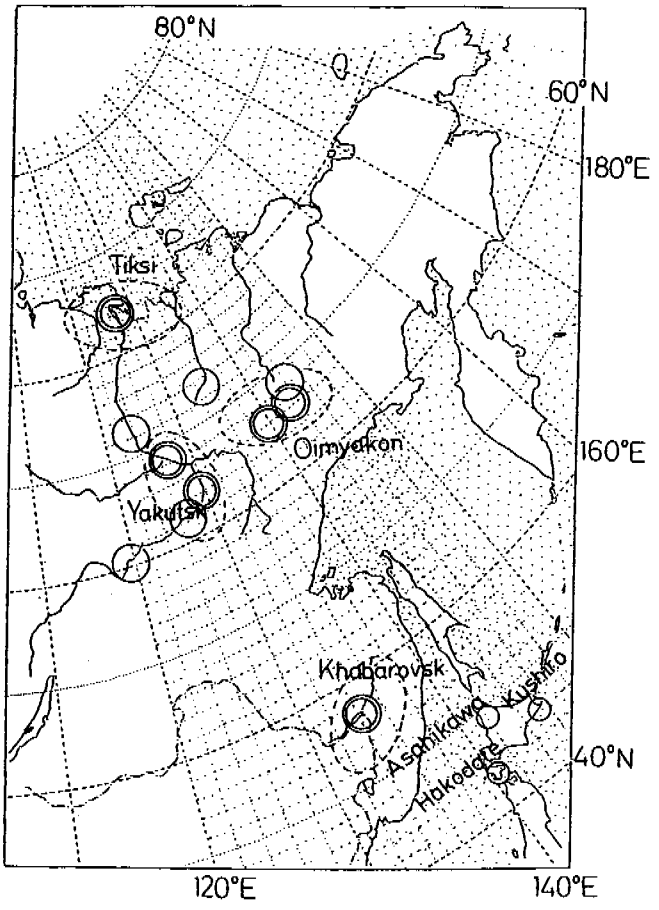

FIG. 1. Research sites in eastern Siberia and northernmost Japan.

decreasing with increasing latitudes from temperate forest, taiga, and tundra. The higher number of species in a middle scale (per ca. 1ha) was found in cool temerate regions in Hokkaido and tundra than those of taiga. Floristic diversity in tundra might be characterized by the higher proportion of coexistence of the species with the same genus than those of the temperate regions.

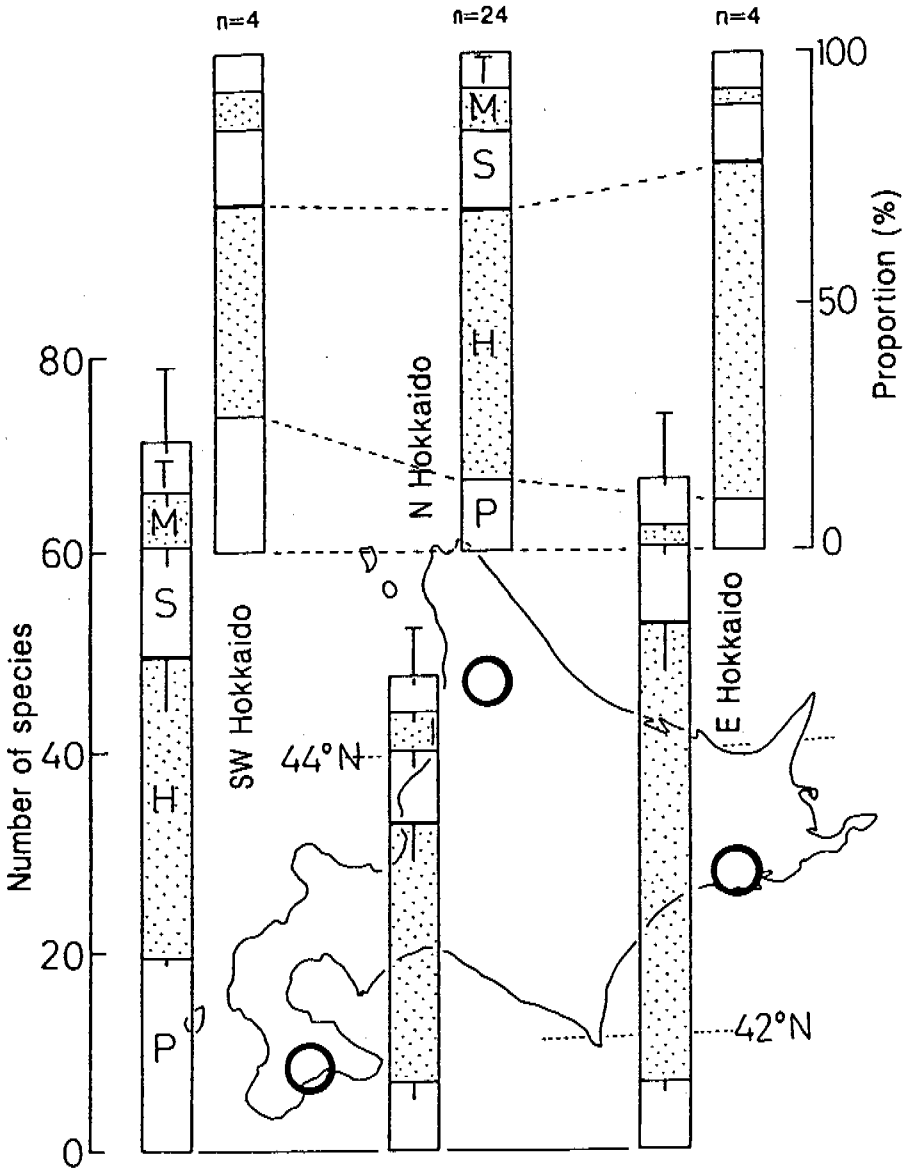

FIG. 2. Distributions of number of species and its proportion among different life forms of plants in northernmost Japan. Locations are as follows: Hakodate (SW Hokkaido), Horokanai near Asahikawa (N Hokkaido) and Kushiro (E Hokkaido). Life forms are as follows: pteridophyts (P), herbs (H), small trees (S), middle trees (M) and tall trees (T).

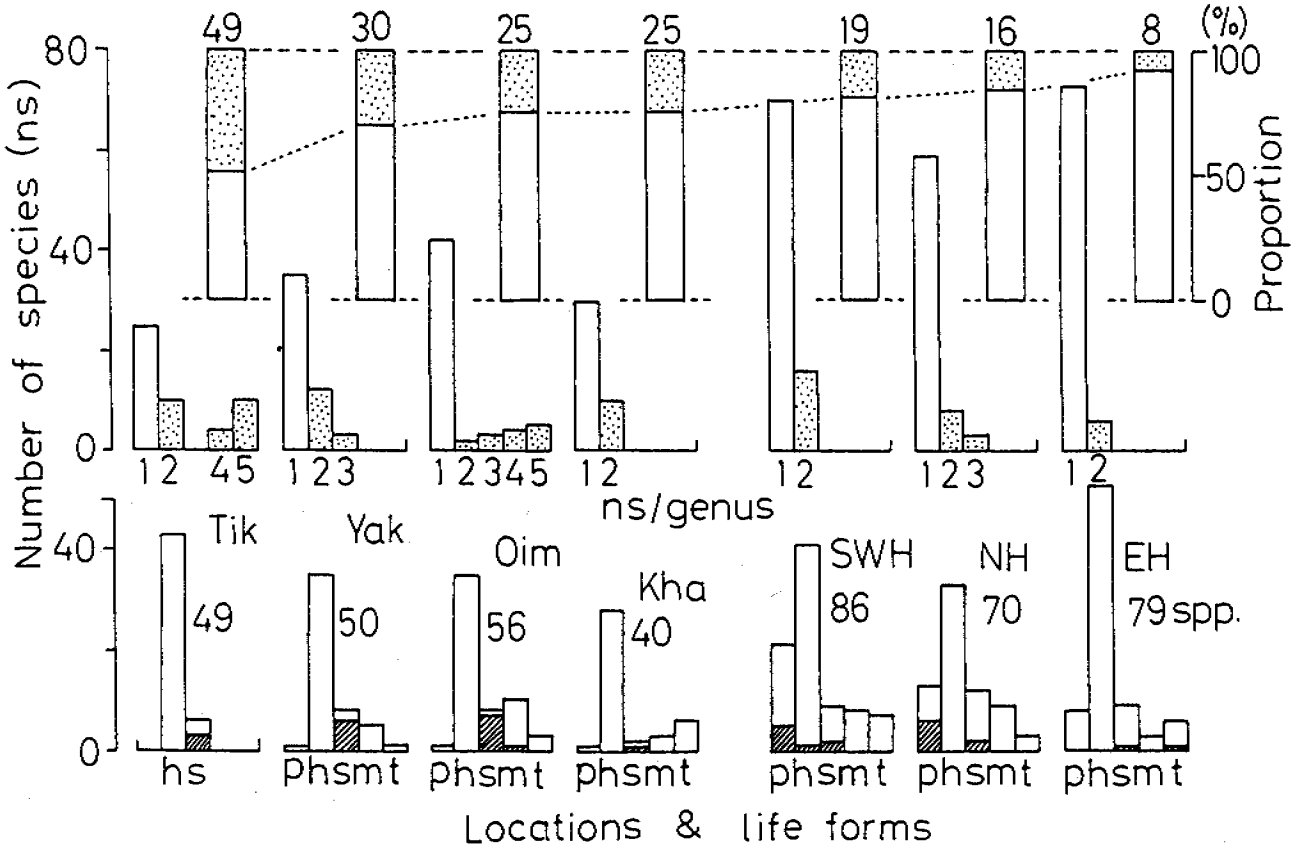

FIG. 3. Frequencies of number of species as functions of life forms and number of species per genus and its proportion on selected populations in Siberia and northernmost Japan. Dotted bars indicate species with more than 2 species per site. Dashed bars incicate evergreen species. Life forms are as follows: pteridophytes (p), herb (h), small trees (s), middle trees (m) and tall trees (t). Locations are as follows: Tiksi (Tik), Yakutsuk (Yak), Oimyakon (Oim), Khavarovsk (Kha), Hakodate (SWH, south-western Hokkaido), Horokanai near Asahikawa (NH, north-Hokkaido) and Kushiro (EH, east Hokkaido).

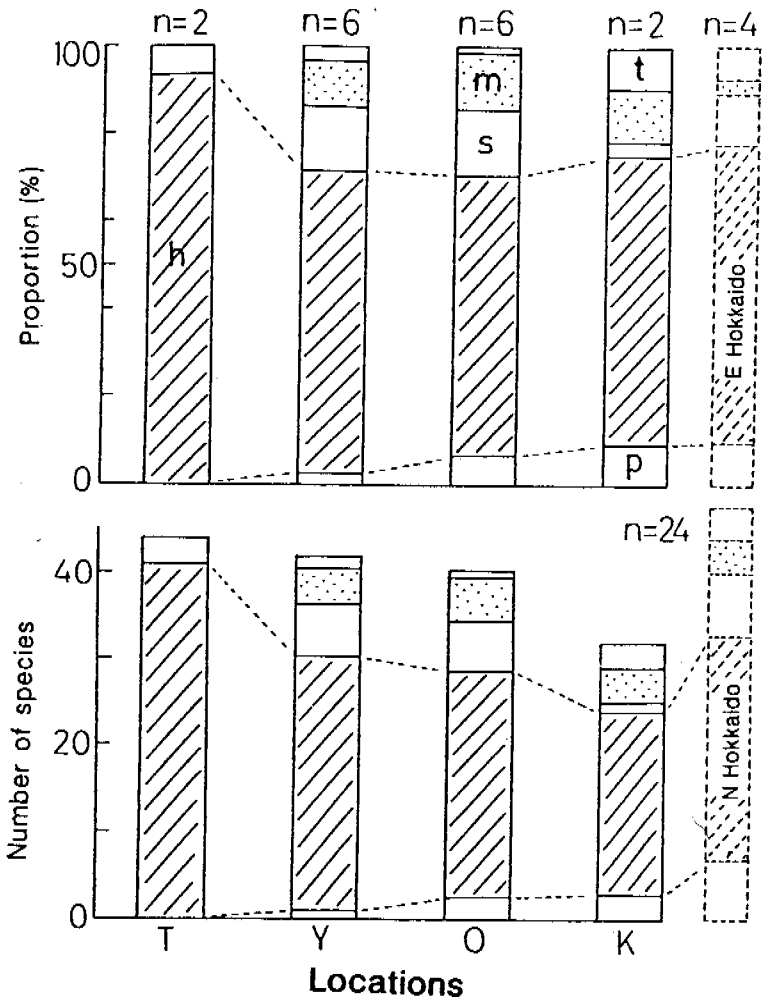

FIG. 4. Distributions of number of species and its proportion among different life forms of plants in Siberia. Locations are as follows: Tiksi (T), Yakutsk (Y), Oimyakon (O) and Khabarovsk (K). Life forms are: pteridophytes (p), herbs of seed plants (h), small trees (s), middle trees (m) and tall trees (t).

Biodiversity in drosophilid communities of cool-temperate and boreal birch forests: a special reference to the vertical distribution within forest

MASANORI J. TODA[1] and NIKOLAI N. VINOKUROV[2]

[1]*Institute of Low Temperature Science, Hokkaido University N19W8 Sapporo 060 Japan*
Tel: +81-11-706-6887; Fax: +81-11-706-7142
[2]*Yakutsk Institute of Biology, Siberian Branch of the Russian Academy of Sciences, 41 Lenin Avenue, Yakutsk 677891 Russia*

Introduction

Continuous forest vegetation stretches over the longest distance on the earth from tropical rain forest in South-East Asia to taiga in East Siberia through relatively humid areas along the easternmost periphery of Eurasian Continent. In general, the species diversity decreases from south to north along this green belt. Pianka (1978) reviewed ten hypothetical mechanisms for determination of species diversity in a community. The spatial heterogeneity of habitat is one of such mechanisms. Structurally complex habitats usually support more species than homogeneous ones do, offering a variety of different microhabitats. The structure of forest stratification affects animal communities living there. Multi-layered forests contain more species of birds than simple-layered ones (Cox and Moore, 1993), or the bird species diversity (measured by Shannon-Weaver index) is correlated with the foliage height diversity (MacArthur and MacArthur, 1961). Toda (1992) demonstrated that there was a significant positive correlation between the foliage height diversity and the degree of vertical habitat segregation among drosophilid species within a cool-temperate deciduous forest.

This study covers the northernmost part of the Asia-Siberian green belt. To compare the biodiversity of drosophilid community between cool-temperate and boreal regions, the vertical distribution patterns of drosophilids were investigated in birch forests. In boreal regions, coniferous trees are generally predominant, but birches are also rather common, broad-leaved trees, along with willows and poplars. The foliage height profile is quite different between coniferous and broad-leaved forests. The surveyed forests were similar in general appearance, though different from each other in birch tree species. The viewpoints of this study are twofold: 1) Does the biodiversity change differently between different drosophilid guilds? 2) What environmental factors cause the changes, if observed, in biodiversity and structure of drosophilid community?

Methods

Collecting flies.—Surveys were made at the following four localities: Inuvik (68°N, 134°W), northern Canada; Spaskayapad (63°N, 129°E) *ca.* 30 km north of Yakutsk, East Siberia; Koryukozan and Misumai in the suburbs of Sapporo (43°N, 141°E), northern Japan. Four 'retainer'-type I traps (Toda 1977) with fermenting bananas or malt baits (Lakovaara et al. 1969) were set at different heights from the canopy to the ground in a birch forest. The top trap corresponded to the upper canopy layer, the second to the lower canopy, the third to the shrub layer, and the fourth to the ground. The upper two traps were suspended by a rope hung from a bough in the crown of a birch tree, and the lower two were tied to the trunk of the same tree. Trapped flies were collected one to two weeks later after setting. The

detailed procedure is given below for each locality.

Inuvik: In a birch, *Betula papyrifera*, forest with tree tops ca. 15 m high, situated ca. 20 to 30 km south of the northern limit of subarctic forest; trap heights, 10.5, 5.5, 1, and 0.1 m; from 31 July to 8 August, 1980 (1 sampling period); using banana as bait.

Spaskayapad: In a birch forest consisting of *B. platyphylla* and *B. alba* with tree tops ca. 15 m high, near the station of Spaskayapad Experiment Forest, situated in the huge taiga of East Siberia; trap heights, 11, 6, 1, and 0.1 m; from 28 June to 11 July, 1994 (1 sampling period); using malt as bait.

Koryukozan: In a secondary forest dominated by *B. platyphylla* with tree tops ca. 12 m high, neighboring a coniferous and broad-leaved mixed forest, at ca. 600 m above sea level; trap heights, 9.5, 4.5, 1.5, and 0.2 m; sampling and renewing baits at weekly intervals during 19 August to 2 September, 1977 (2 sampling periods); using banana as bait.

Misumai: In a birch, *B. platyphylla*, grove with tree tops *ca.* 12 m high, *ca.* 100 m remote from a natural broad-leaved forest, at *ca.* 300 m above sea level; trap heights, 9, 5, 1, and 0.1 m; sampling and renewing baits at weekly intervals during 30 June to 3 August, 1977 (4 sampling periods); using banana as bait.

Data analysis.—The following measures with respect to the biodiversity of drosophilid community were calculated for each sampling period. If the data for 2 or 4 sampling periods were available, means and standard deviations were calculated for each locality.

1) The total number of individuals collected: N

2) The total number of species collected: S

3) The total diversity measured by Shannon–Weaver index:

$$H'_T = -\sum_{i=1}^{S} \frac{N_i}{N} \ln \frac{N_i}{N} \qquad (1)$$

where N_i is the total number of individuals of species i.

4) The equitability measured by Pielou's J':

$$J' = \frac{H'_T}{H'_{max}} = \frac{H'_T}{\ln S} \qquad (2)$$

5) The degree of vertical habitat segregation among drosophilid species: This was evaluated by a method of niche dimensionality analysis (Lumme et al., 1979). Intercategory diversity (H'_{inter}), that is, the diversity due to differences among four trap samples, is equal to the total diversity (H'_T) minus intracategory diversity (H'_{intra}), that is, the average diversity within samples. Weighting H'_{intra} by the total number of individuals collected at each trap, H'_{inter} was calculated by the following formula:

$$H'_{inter} = H'_T - \sum_{j=1}^{c} \frac{N_j H'_j}{N} \qquad (3)$$

where N_j is the total number of individuals collected at trap j, H'_j is the Shannon–Weaver diversity for trap sample j, and c is the number of traps (in this case c = 4). When used as a measure of the degree of vertical habitat segregation, H'_{inter} was expressed as a percentage of H'_T.

The average height of fly catch was calculated for each species by the following formula:

$$\hat{h}_i = \sum_{j=1}^{c} \frac{h_j N_{ij}}{N_i} \qquad (4)$$

where h_j is the height of trap j, and N_{ij} is the number of individuals of species i collected at trap j.

Results

Diversity measures.—The four drosophilid communities in birch forests of boreal and cool-temperate regions were compared for various measures connected with the biodiversity (Table 1). The total number of individuals collected during a sampling period tended to be more in boreal forests than in cool-temperate forests. However, this measure usually varies to a great magnitude due to weather and seasonal conditions and many other factors. The total numbers of species collected during a sampling period were surprisingly the same (8 spp.) between the two boreal forests in northern Canada and East Siberia. About 1.7 to 1.8 times more species were collected in the cool-temperate forests. The total diversity, the equitability, and the degree of vertical habitat segregation decreased with increasing latitude.

Guild structure.—The vertical distributions of component species are shown in Fig. 1 for the two boreal communities. The component species showed species-specific distribution patterns, and the patterns were quite stable in some species common to both communities, e.g., *Chymomyza costata, Drosophila rellima,* and *D. transversa*. The layer corresponding to the height at which the most number of individuals were collected was regarded as the main living space for each species. In Inuvik, three groups dwelling at different layers were recognized: LC) *Amiota quadrata* living at the lower canopy layer, S) *Ch. costata, D. athabasca, D. neotestacea, Ch. aldrichii,* and *D. rellima* at the shrub layer, and G) *D. transversa,* and *D. montana* at the ground layer. In Spaskayapad, four groups were recognized: UC) *Cacoxenus kaszabi* at the upper canopy layer, LC) *Ch. costata,* S) *D. bifasciata, D. testacea, D. rellima, Hirtodrosophila subarctica,* and *D. funebris,* and G) *D.*

TABLE 1. Measurements of diversities in drosophilid communities inhabiting cool-temperate and boreal birch forests. All measures were calculated for each sampling period. As for the communities at Misumai and Koryukozan, in which the data for four or two sampling periods were available, means per sampling period and standard deviations were calculated.

Locality	Misumai		Koryukozan		Spaskayapad	Inuvik
Latitude	43°N		43°N		63°N	66°N
Number of sampling periods	4		2		1	1
	Mean	s.d.	Mean	s.d.		
Total number of individuals	111.5	26.4	187.5	17.5	162	266
Total number of species	13.8	0.4	14.5	1.5	8	8
Todal diversity	2.110	0.079	1.908	0.219	1.394	1.028
Equitability	0.805	0.027	0.713	0.054	0.670	0.494
Inter-trap diversity	0.358	0.037	0.382	0.154	0.163	0.086
% to total diversity	16.98	1.52	21.21	10.52	11.65	8.40

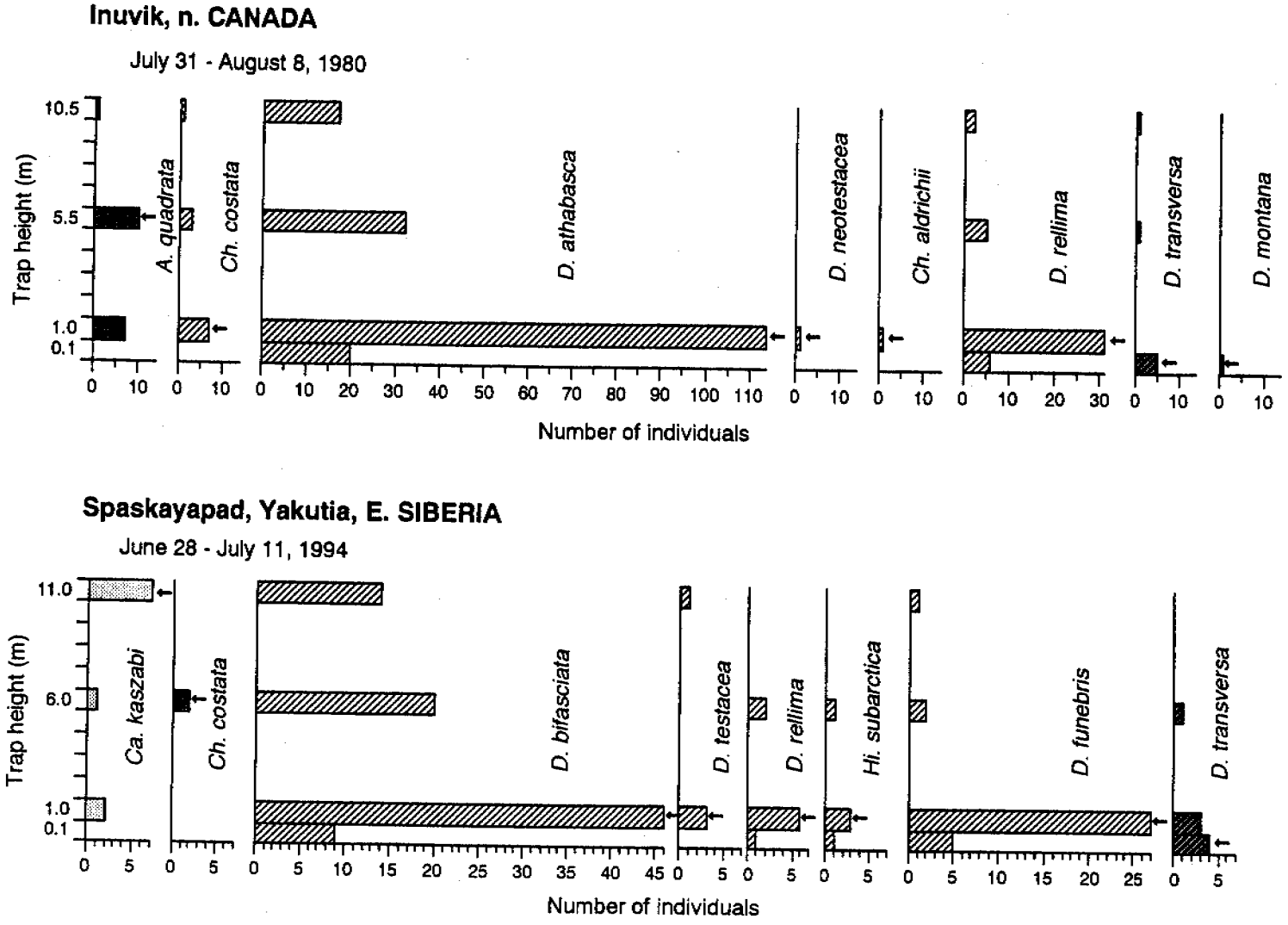

FIG. 1. Vertical distributions of component species of drosophilid communities in birch forests at Inuvik, northern Canada, and Spaskayapad, East Siberia. The component species are classified into four groups (shown with different hatchings) centering at different layers (shown with arrows).

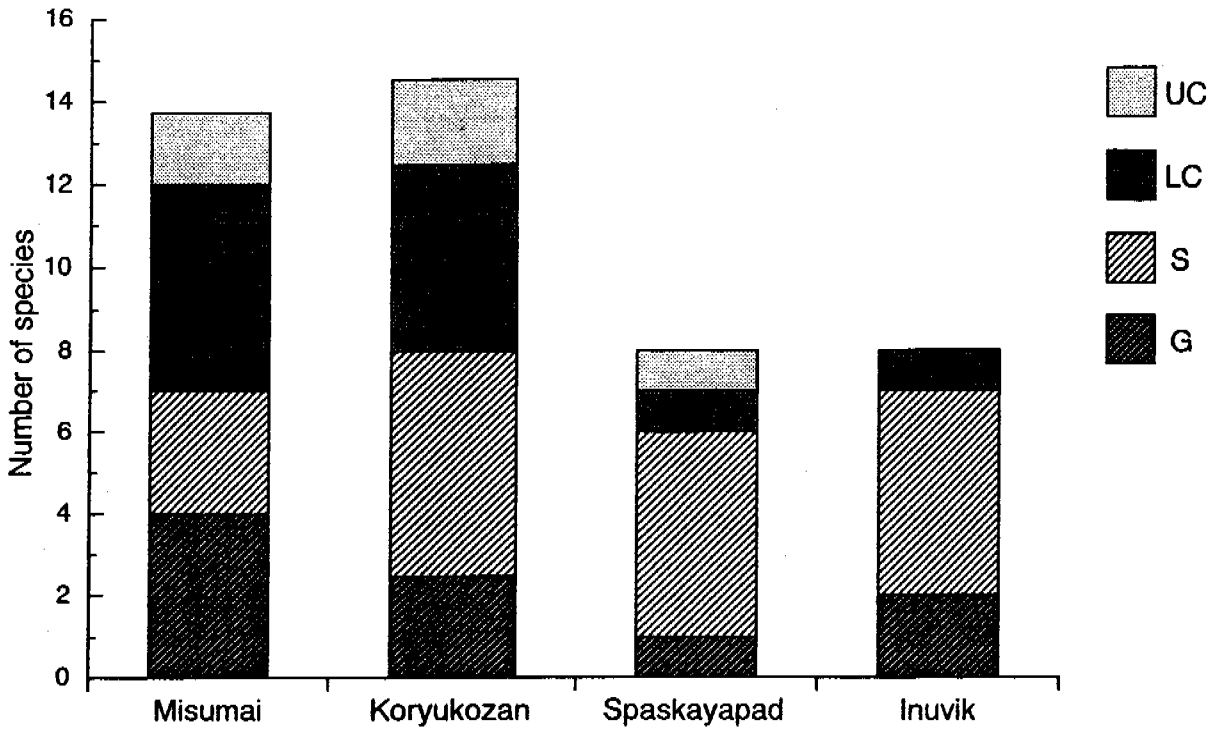

FIG. 2. Numbers of species of four groups (UC: distributed mainly at the upper canopy, LC: at the lower canopy, S: at the shrub layer, and G: at the ground layer) in four drosophilid communities inhabiting cool-temperate (Misumai and Koryukozan) or boreal (Spaskayapad and Inuvik) birch forests. Numbers of species are means per one sampling period for Misumai and Koryukozan communities.

transversa. In Fig. 2 numbers of species of the four groups are compared among the four communities. It is obvious that the decrease in the total number of species from cool-temperate forests to boreal ones was due to the decrease in number of species living at the canopy layer. The number of species living at the forest floor layer was almost constant throughout cool-temperate to boreal forests.

Toda (1984) defined a guild of drosophilid flies as 'a group of species having nearly identical food habits and habitat preferences.' To compare the guild structure and to estimate ecological equivalents between different local communities, natural principal food is indicated for each component species in Fig. 3, along with the average height of fly capture. The information on food habits was based on data actually obtained in the study areas or on literature (Kimura et al., 1977; Shorrocks, 1982; etc.). All the species collected throughout the survey period are shown for every community, and the average height was calculated on the basis of data summed up for the whole period. Two types of food habits, tree sap feeders and fungus feeders, dominated in boreal birch forests. Tree sap feeders usually inhabited higher layers than fungus feeders, though many of them were distributed mainly at the shrub layer in boreal forests. Therefore, the drosophilid communities in boreal birch forests are regarded as consisting principally of two guilds: 'tree sap feeder' (T)-'canopy dweller' (C) and 'fungus feeder' (M)-'floor dweller' (F). These two guilds were major components of drosophilid communities also in cool-temperate forests, although there were other minor components such as 'fruit feeder'-'floor dweller', 'tree sap feeder'-'floor dweller', 'herbage feeder'-'floor dweller', and occasional immigrants from other habitats. The number of component species decreased from cool-temperate forests to boreal ones in both guilds,

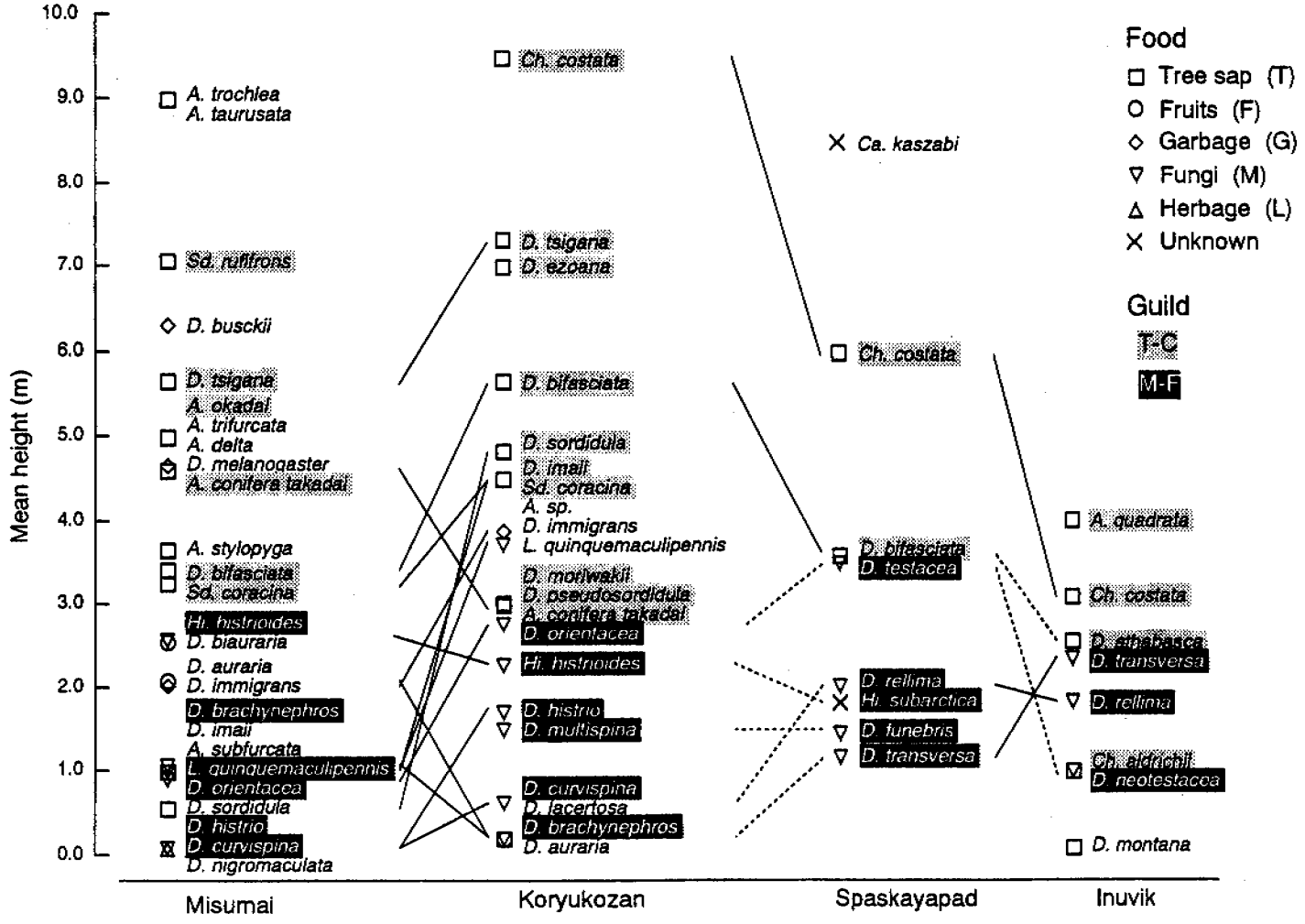

FIG. 3. The average distribution heights and the pricipal foods of component species in four drosophilid communities, with indication of two major guilds (T–C: 'tree sap feeder'–'canopy dweller', M–F: 'fungus feeder'–'floor dweller') and changes in the distribution height between conspecific populations (solid lines) and between supposed ecological equivalents (broken lines).

especially in the T–C guild.

Considering the ecological nature and the phylogenetic relationship, some pairs of species are regarded as ecological equivalents between different local communities. *Drosophila orientacea* in Hokkaido, *D. testacea* in Eurasian Continent, and *D. neotestacea* in North America are very close relatives, which are all dependent on fungi as principal food but are distributed allopatrically (Grimaldi et al., 1992). Mycophagous *D. brachynephros* and *D. curvispina* of the *quinaria* species–group in cool–temperate forests of Hokkaido seem to be equivalent to *D. transversa* and *D. rellima* of the same species–group in boreal forests of East Siberia and northern Canada, respectively. *Drosophila funebris* is a wild species in East Siberia, but is distributed in Hokkaido as a domestic species. The corresponding niche in nature may be occupied by another species, *D. multispina*, of the same species–group in Hokkaido. Although food habits of *Hi. subarctica* are still unknown, *Hi. histrioides* may be its equivalent. *Drosophila bifasciata* and *D. athabasca* of the *obscura* species–group were most dominant and showed very similar vertical distribution patterns in the boreal birch forests of East Siberia and northern Canada, respectively (Fig. 1). These two species are certainly ecological equivalents. Changes in the average height of fly capture are indicated in Fig. 3 for some species occurring commonly at different localities, e.g., *Ch. costata* and *D. bifasciata*, or between the pairs of ecological equivalents estimated above. The average height decreased remarkably in the members of the T–C guild with increasing latitude, while it did not in the members of the M–F guild.

Discussion

All the measures, except for the total number of individuals collected, with respect to the biodiversity decreased with increasing latitude in drosophilid communities of cool–temperate and boreal birch forests. This means that the structure of drosophilid community becomes simpler at higher latitudes. In particular, the decrease in the degree of vertical habitat segregation among component species implies the simple–layered structure of drosophilid community in boreal forests.

The composition of functional groups or guilds in drosophilid community is depauperated in boreal forests in comparison with cool–temperate forests. Although the T–C and M–F guilds are major components in both forests, some minor components such as fruit feeders are completely lacking from boreal forests. The lack of fruit feeders from boreal drosophilid communities is not attributed to the absence of fruits there but to the discrepancy in phenology between fruiting plants and drosophilids. In fact, plenty of various berries are produced in autumn in boreal regions. However, most drosophilid species, except for domestic ones, enter the diapause much prior to the real winter arrival (Lumme and Lakovaara, 1983) and do not use the rich amount of berries as breeding resources. In addition to the lack of some minor guilds, drosophilid communities in boreal birch forests are further depauperated by decreasing numbers of component species of the T–C and M–F guilds. This decrease is more prominent in the T–C guild than in the M–F guild.

Distribution heights of the T–C members are remarkably lowered, almost down to the shrub layer, in boreal forests. However, such changes are not seen in the M–F members.

In conclusion, all the features mentioned above point to the following: Drosophilid living space is almost limited to the floor layer in boreal forests, and this contraction of living space causes the decrease in biodiversity mainly of 'tree sap feeder'–'canopy dweller' guild.

This change in drosophilid communities from cool–temperate to boreal birch forests seems to be related to some differences in vegetation structure between the two forests. It has been empirically recognized that the tree architecture varies latitudinally not only at the

community level but also even in the same tree species: boreal forests are dominated by trees with apically pointed, deep, conical crowns (conifers), whereas temperate forests consist mostly of trees with apically round, shallow, spherical crowns (broad-leaved trees). In consequence, the upper surface of forest canopy is highly rugged in boreal coniferous forests, while it is more continuously waved in temperate broad-leaved forests. Sprugel (1989) interpreted the close association either between needle leaves and evergreenness or between broad leaves and deciduousness in cool-temperate to boreal forests as a strategy to maximize the net production of the whole crown in an individual tree, considering the relationship between leaf orientation, crown architecture, cost for having leaves, photosynthetic rates, and ambient temperatures in active season. His interpretation is as follows: Small, needle-shaped leaves can readily be displayed in a pattern that disperses the incoming light over a larger number of leaves. This strategy is most effective for trees that retain their leaves for several years and develop a deep crown with many layers of leaves (evergreen coniferous trees), in which light passing through the first few layers is captured by the leaves deeper in the crown. Since low temperatures reduce photosynthesis more in light-saturated leaves than in un-saturated leaves, mechanisms that minimize saturation are especially important for trees that may carry out substantial photosynthesis at low temperatures. This explains the predominance of evergreen conifers in boreal forests, although deciduous, needle-leaved larches dominate in vast areas of East Siberia due to exceptionally severe winter conditions under the extreme continentality of the climate there. This explanation may be partly applicable to the latitudinal variation in crown architecture of birch trees. In fact, canopies of the birch forests surveyed at Inuvik and Spaskayapad were not completely closed, due to deep, pseudo-conical crowns of individual trees. Thus, the almost single-layered structure of drosophilid communities in boreal birch forests may be attributed to the virtual absence of continuous canopy layer as a distinct microhabitat for drosophilids.

Acknowledgments

We wish to express our hearty thanks to the following persons for their great help in this study: The Director, Prof. N.G. Solomonov, Dr. B.I. Ivanov, Dr. T.K. Maximov, and other staff members of the Yakutsk Institute of Biology. We thank also Dr. H. Watabe, Hokkaido University of Education, for his help in the field work at Yakutsk. This work was partly carried out in "The Joint Siberian Permafrost Studies between Japan and Russia" conducted by Prof. M. Fukuda of Hokkaido University, which was supported by Grants-in-Aid for Overseas Scientific Study from the Ministry of Education, Science, and Culture of Japan (No. 04041014).

References

Cox, C.B., and P.D. Moore. 1993. Biogeography: An Ecological and Evolutionary Approach (5th ed.). 326 pp. Blackwell, Oxford.

Grimaldi, D., A.C. James, and J. Jaenike. 1992. Systematics and modes of reproductive isolation in the Holarctic *Drosophila testacea* species group (Diptera: Drosophilidae). Ann. Entomol. Soc. Am., 85:671-685.

Kimura, M.T., M.J. Toda, K. Beppu, and H. Watabe. 1977. Breeding sites of drosophilid flies in Sapporo, northern Japan, with supplementary notes on adult feeding habits. Kontyu, 45: 571-582.

Lakovaara, S., W. Hackman, and K. Vepsalainen. 1969. A malt bait in trapping drosophilids. Drosophila Inform. Serv., 44:123.

Lumme, J., and S. Lakovaara. 1983. Seasonality and diapause in drosophilids. In Ashburner, M., Carson, H.L. and Thompson Jr., J.N. (eds.), The Genetics and Biology of Drosophila, 3c. pp. 171–220. Academic Press, London.

Lumme, J., S. Lakovaara, O. Muona, and O. Jarvinen. 1979. Structure of a boreal community of drosophilids (Diptera). Aquila Ser. Zool., 20:65–73.

MacArthur, R.H., and J. MacArthur. 1961. On bird species diversity. Ecology, 42:594–598.

Pianka, E.R. 1978. Evolutionary Ecology (2nd ed.). Harper and Row, New York.

Shorrocks, B. 1982. The breeding sites of temperate woodland Drosophila. In Ashburner, M., Carson, H.L. and Thompson Jr., J.N. (eds.), The Genetics and Biology of Drosophila, 3b. pp. 385–428. Academic Press, London.

Sprugel, D.G. 1989. The relationship of evergreenness, crown architecture, and leaf size. Am. Nat., 133:465–479.

Toda, M.J. 1977. Two new 'retainer' bait traps. Drosophila Inform. Serv., 52: 180.

Toda, M.J. 1984. Guild structure and its comparison between two local drosophilid communites. Physiol. Ecol. Jpn., 21:131–172.

Toda, M.J. 1992. Three–dimensional dispersion of drosophilid flies in a cool temperate forest of northern Japan. Ecol. Res., 7:283–295.

A comparative study on drosophilid faunas of east Siberia and neighboring regions

HIDE-AKI WATABE[1], MASANORI J. TODA[2], NIKOLAI N. VINOKUROV[3], and VASILY S. SIDORENKO[4]

[1]*Biological Laboratory, Hokkaido University of Education, Ainosato 5-3-1, Sapporo 002 Japan*
Tel: +81-11-778-8811; Fax: +81-11-778-8822
[2]*Institute of Low Temperature Science, Hokkaido University, N19W8, Sapporo 060 Japan*
[3]*Laboratory of Entomology, Yakutsk Institute of Biology, Yakutsk, Yakutia 677891 Russia*
[4]*Laboratory of Entomology, Institute of Biology and Pedology, Vladivostok 690022 Russia*

Introduction

High latitudes of the Holarctic Region are very important for considering biogeographical relationships between Eurasia and North America and for studying adaptations of insects to an extremely cold climate, but our knowledge on the drosophilid fauna of Siberia has been quite limited. Since 1992, we have been engaged in a joint study of Siberian drosophilids. Here, we report the drosophilid fauna of Yakutia, comparing it with those of neighboring regions.

We wish to express our hearty thanks to the following persons for their great help in this study: Prof. N.G. Solomonov, Dr. B.I. Ivanov, Dr. T.K. Maximov, and Dr. A.I. Averensky of the Yakutsk Institute of Biology.

Study areas and collection methods

The faunal survey was made in tundra and taiga regions (Fig. 1), from late June to mid August for three years, 1992 to 1994. Fly collections were made by traps baited with fermenting malt (Lakovaara et al. 1969) and by net sweeping on herbaceous plants and mushrooms.

Results and discussion

Thirty-six drosophilid species including five undetermined ones were obtained (see Appendix). In tundra and alpine tundra, we did not obtain any drosophilid species, except for a well-known domestic species, *Drosophila melanogaster* collected in a heated fruit shop of Tiksi (No.1 in Fig. 1). A limited number of species, usually less than 10 species, were collected in two districts within the Arctic Circle (Nos. 2, 3), and in Tomponskij (Nos. 6, 7) and Oimyakonskij districts (Nos. 8, 9). The drosophilid fauna was relatively rich in the further south: 24 spp. in Yakutsk and 17 spp. in Olekminsk. Three species, *Chymomyza costata, D. rellima,* and *D. transversa* were common at many places in East Siberia. *Drosophilla funebris*, a cosmopolitan species usually dwelling in and near human habitations, was rather common also in natural forests in East Siberia.

In addition to the 36 species collected by ourselves, six species, *Stegana hypoleuca, D. kuntzei, D. histrio, Scaptonmyza graminum, Sc. baechlii,* and *Sc. flava*, have been collected in East Siberia (Hackman 1959, Wheeler 1981, etc.). In consequence, a total of 42 species have been so far recorded from this region.

The drosophilid fauna of East Siberia was compared with those of six neighboring regions, based on the following data sources: northern Japan (148 spp.; Okada 1988, Toda unpubl.), northeastern China (94 spp.; Watabe et al. 1993, Toda unpubl.), Russian Far East

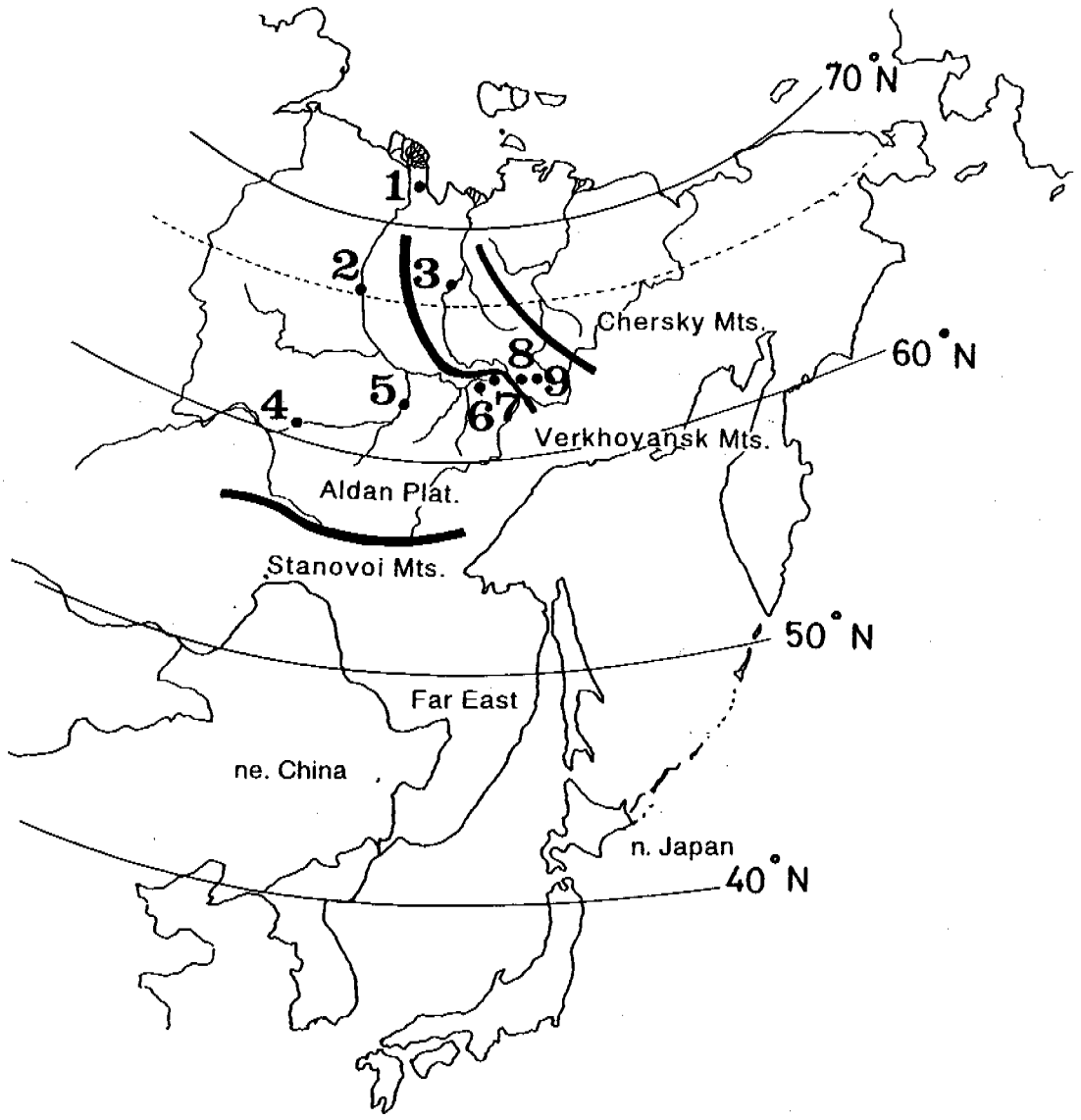

FIG. 1. Map of eastern Eurasia showing the collection sites in Yakutia, East Siberia. 1: Tiksi in Bulubskij District, 2: Zhigansk, 3: Verkhoyansk, 4: Olekminsk, 5: Yakutsk, 6: Rosomakha in Tomponskij District, 7: Geological Station in Tomponskij District, 8: Agayakan in Oimyakonskij District, 9: Tomtor in Oimyakonskij District.

(114 spp.; Sidorenko 1990a, b, 1993, etc.), Central Asia (44 spp.; Maca 1988, 1992; Watabe et al. 1993), northern Europe (61 spp.; Bachli and Rocha-Pite 1981, 1982), and northern parts of North America (25 spp.; Wheeler and Throckmorton 1964; Toda 1984). Faunal similarity between two regions was evaluated by Jaccard's coefficient of similarity (Udvardy 1969): $S = c/(a+b-c)$, where c is the number of species common to both regions and a or b is the number of species occurring in each region. The similarity matrix resulting from pairwise calculations was then subjected to a cluster analysis.

Three regions, Russian Far East (abbreviated RFE in Fig. 2), northeastern China (NEC),

and northern Japan (NJP), constituted a compact group in the dendrogram. On the other hand, East Siberia (ESB) showed a much closer similarity in the species composition with Central Asia (CAS) and northern Europe (NEU) than with the three regions of eastern Eurasia or northern North America (NNA).

The drosophilid faunas of the three regions in eastern Eurasia (NJP, NEC, RFE) are rich in number of species, consisting primarily of species adapted to cool-temperate deciduous forests in this area and including some Sino-Japanese elements distributed mainly in warm-temperate evergreen broad-leaved forests from southern Japan to southern China (Watabe et al. 1993). On the other hand, the drosophilid fauna of East Siberia almost lacks these elements, instead consisting of a number of Palearctic or Holarctic elements adapted to boreal forests and a few others distributed in rather arid areas in Central Asia. There is a large "waterfall" of the species diversity between the Far East and East Siberia. Mountain ranges such as Aldan Plateau and Verkhoyansk Mountains lie south and east of Yakutia. Eastern Asiatic elements of drosophilids may be strongly restricted to expand their ranges northward by these distribution barriers.

References

Bachli, G., and M.T.R., Rocha-Pite. 1981. Drosophilidae of the Palearctic region. In Ashburner, M., Carson, H.L., and Thompson Jr., J.N. (eds.), The Genetics and Biology of Drosophila, 3a:167-196. Academic Press, London.

Bachli, G., and M.T.R., Rocha-Pite. 1982. Annotated bibliography of Palearctic species of Drosophilidae (Diptera). Beitr. Ent., Berlin 32 (2s):303-392.

Hackman, W. 1959. On the genus Scaptomyza Hardy (Diptera, Drosophilidae), with descriptions of new species from various parts of the world. Act. Zool. Fenn., 97:1-73.

Lakovaara, S., W. Hackman, and K. Vepsalainen. 1969. A malt bait in trapping drosophilids. DIS 44: 128.

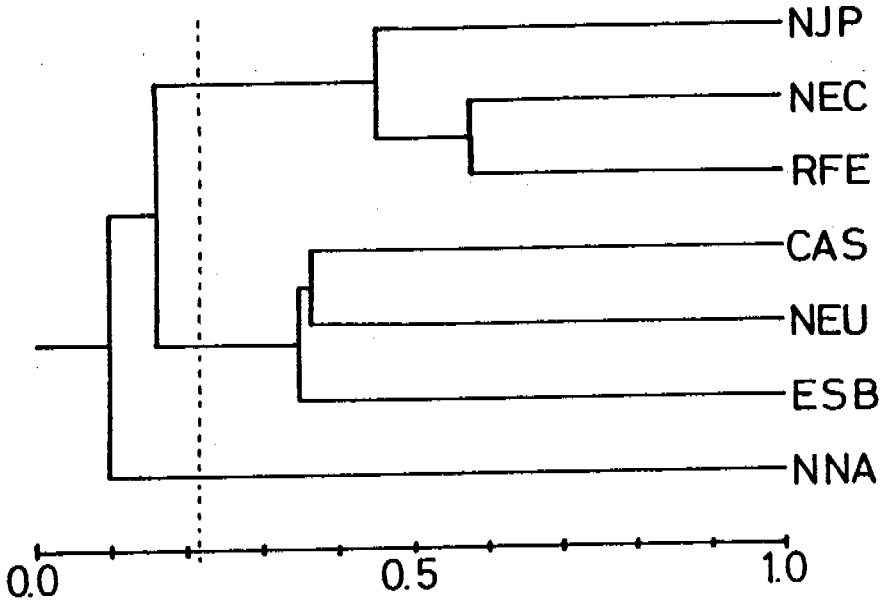

FIG. 2. Comparison of drosophilid faunas of East Siberia and neighboring regions, based on the Jaccard's coefficient of similarity.

Maca, J. 1988. Drosophilidae (Diptera) of Soviet Middle Asia. Annot. Zool. bot., 185:1–16.
Maca, J. 1992. Addition to the fauna of Drosophilidae, Camillidae, Curtonotidae, and Campichoetidae (Diptera) of Soviet Middle Asia. Ibid., 210:1–8.
Okada, T. 1988. Selected Papers by Dr. Toyohi Okada (ed. by Dr. K. Suzuki). iii+412 pp. The Association of the Memorial Issue of Dr. Toyohi Okada, Toyama, Japan.
Sidorenko, V.S. 1990. A new species of the genus Domomyża Rondani (Diptera, Drosophilidae) from the Soviet Far East. G. it. Ent., 5:129–131.
Sidorenko, V.S. 1993a. On two species of Drosophilidae (Diptera) described by Dr. T. Okada from Russia Far East. Mitt. Schweiz. Entom. Gesell., 66:75–79.
Sidorenko, V.S. 1993b. Tribe Drosophilini of the Asian part of the USSR. Zeit. fur Entom., 14:253–268.
Toda, M.J. 1984. The northernmost subarctic Drosophilidae. DIS 60:193–194.
Udvardy, M.D.F. 1969. Dynamic Zoogeography with Special Reference to Land Animals. 445 pp. Van Nostrand Reinhold, New York.
Watabe, H., Y. Hu, and M.J. Toda. 1993. Drosophilid fauna of Liaoning Province, Northeast China. J. Hokkaido Univ. of Education (Sec. IIB), 44:1–13 (In Japanese with English summary).
Wheeler, M.R., and L.H. Throckmorton. 1984. Notes on Alaskan Drosophilidae (Diptera), with the description of a new species. Bull. Brooklyn Ent. Soc., 55:134–147.

APPENDIX. A list of drosophilid flies collected in Yakutia, East Siberia, from 1992 to 1994. TKS,Tiksi; ZGS, Zhigansk; VHY, Verkhoyansk; OLK, Olekminsk; YKT, Yakutsk; RSM, Rosomakha; GLS, Geological Station; AGY, Agayakan; TMT, Tomtor.

Districts	TKS	ZGS	VHY	OLK	YKT	RSM	GLS	AGY	TMT
(Number in Fig. 1)	1	2	3	4	5	6	7	8	9
Genus *Leucophenga* Mik									
1. *Le. quinquemaculipennis* Okada					+	+			
Genus *Cacoxenus* Loew									
2. *C. kaszabi* (Okada)					+		+		
Genus *Gitona* Meigen									
3. *G. distigma* Bezzi					+				
Genus *Amiota* Loew									
4. *A. subtusradiata* Duda					+				
5. *A. sp.*,like *conifera takadai*				+	+			+	
Genus *Scaptodrosophila* (Duda)									
6. *Sd. rufifrons* (Loew)					+				
Genus *Chymomyza* Czerny									
7. *Ch. caudatula* Oldenberg					+				
8. *Ch. costata* (Zetterstedt)		+	+	+	+	+	+	+	
9. *Ch. fuscimana* (Zetterstedt)					+	+	+	+	
10. *Ch. distincta* (Egger)				+					
Genus *Hirtodrosophila* (Duda)									
11. *Hi. subarctica* (Hackman)		+	+		+	+	+		
Genus *Drosophila* Fallen									
12. *D. alpina* Burla		+	+			+	+		
13. *D. bifasciata* Pomini				+	+	+			
14. *D. melanogaster* Meigen	+				+				

APPENDIX (CONTINUED)

15. *D. busckii* Coquillett				+					
16. *D. funebris* (Fabricius)		+	+	+		+			
17. *D. ezoana* Takada & Okada	+	+			+	+			
18. *D. littoralis* Meigen	+		+						
19. *D. lummei* Hackman	+			+					
20. *D. montana* Patterson & Wheller						+	+		
21. *D. immigrans* Sturtevant				+					
22. *D. rellima* Wheeler		+		+	+	+	+	+	
23. *D. phalerata* Meigen			+						
24. *D. transversa* Fallen	+	+	+	+	+		+		
25. *D. testacea* von Roser			+	+					
26. *D. sp.*, like *makinoi*					+				
Genus *Lordiphosa* (Basden)									
27. *Lo. hexasticha* (Papp)			+	+					
Genus *Scaptomyza* Hardy									
28. *Sc. okadai* Hackman			+						
29. *Sc. trochanterata* Collin			+	+					
30. *Sc. unipunctum unipunctum* (Zetterstead)			+						
31. *Sc. sp. 1*, like *unipunctum*			+	+	+	+	+		
32. *Sc. consimilis* Hackman							+		
33. *Sc. sp. SB1*, like *graminum*				+					
34. *Sc. montana* Wheeler			+				+		
35. *Sc. polygonia* Okada			+						
36. *Sc. pallida* (Zetterstedt)			+	+			+		
Total spp.	1	7	7	17	24	11	10	10	1